Analysis of the Herbicide Glyphosate and related Organophosphonates in Seawater

–

Overcoming Salt-Matrix-Induced Limitations

Kumulative Dissertation

zur Erlangung des akademischen Grades

doctor rerum naturalium (Dr. rer. nat.)

der Mathematisch-Naturwissenschaftlichen Fakultät

der Universität Rostock

vorgelegt von

Marisa Andrea Wirth

geb. am 01. August 1992 in Hamburg

Rostock, November 2020

https://doi.org/10.18453/rosdok_id00003030

This thesis was produced between November 2017 and November 2020 under supervision from Prof. Dr. Detlef E. Schulz-Bull in the working group "Organic Trace Substances" at the Leibniz Institute for Baltic Sea Research Warnemünde and within the scope of the Leibniz ScienceCampus Phosphorus Research Rostock.

Gutachter:

1. Gutachter
   Prof. Dr. Detlef E. Schulz-Bull
   Leibniz-Institut für Ostseeforschung Warnemünde

2. Gutachter
   Prof. Dr. Ellery D. Ingall
   Georgia Institute of Technology, USA

3. Gutachter
   Prof. Dr. Arne Körtzinger
   GEOMAR Helmholtz-Zentrum für Ozeanforschung Kiel

Datum der Einreichung: 09. November 2020

Datum der Verteidigung: 20. April 2021

Table of Contents

Contributions to the Manuscripts

Publication 1:

Title: Electrodialysis as a sample processing tool for bulk organic matter and target pollutant analysis of seawater

Authors: **Wirth, Marisa A.**; Sievers, Moritz; Habedank, Friederike; Kragl, Udo; Schulz-Bull, Detlef E.; Kanwischer, Marion

Journal: Marine Chemistry, 217, 103719

Year: 2019

Marisa A. Wirth conceptualized the manuscript. Experimental work and data analysis were performed by Marisa A. Wirth, together with Moritz Sievers and Friederike Habedank. The manuscript was written by Marisa A. Wirth and reviewed by all authors.

The overall contribution of Marisa A. Wirth to this manuscript was approximately 85 %.

Publication 2:

Title: The challenge of detecting the herbicide glyphosate and its metabolite AMPA in seawater – Method development and application in the Baltic Sea

Authors: **Wirth, Marisa A.**; Schulz-Bull, Detlef E.; Kanwischer, Marion

Journal: Chemosphere, 262, 128327

Year: 2021

Marisa A. Wirth conceptualized the manuscript, conducted the experimental work and analyzed the data. The manuscript was written by Marisa A. Wirth and reviewed by all authors.

The overall contribution of Marisa A. Wirth to this manuscript was approximately 95 %.

Publication 3:

Title: Methodological aspects of methylphosphonic acid analysis: Determination in river and coastal water samples

Authors: Lohrer, Constantin; Cwierz, Paul P.; **Wirth, Marisa A.**; Schulz-Bull, Detlef E.; Kanwischer, Marion

Journal: Talanta, 211, 120724

Year: 2020

Marisa A. Wirth performed the electrodialysis experiments together with Paul P. Cwierz and contributed to data analysis as well as writing and reviewing of the manuscript.

The overall contribution of Marisa A. Wirth to this manuscript was approximately 10 %.

Publication 4:

Title: Leaching and degradation of (13)C2-(15)N-glyphosate in field lysimeters

Authors: Gros, Peter; Meissner, Ralf; **Wirth, Marisa A.**; Kanwischer, Marion; Rupp, Holger; Schulz-Bull, Detlef E.; Leinweber, Peter

Journal: Environmental Monitoring and Assessment, 192(2), 127

Year: 2020

Marisa A. Wirth performed the analysis of glyphosate and AMPA in leachates and soil extracts, which required the development of specialized methods. Furthermore, Marisa A. Wirth contributed to data analysis as well as writing and reviewing of the manuscript.

The overall contribution of Marisa A. Wirth to this manuscript was approximately 15 %.

Publication 5:

Title: A Glyphosate Pulse to Brackish Long-Term Microcosms Has a Greater Impact on the Microbial Diversity and Abundance of Planktonic Than of Biofilm Assemblages

Authors: Janßen, René; Skeff, Wael; Werner, Johannes; **Wirth, Marisa A.**; Kreikemeyer, Bernd; Schulz-Bull, Detlef E.; Labrenz, Matthias

Journal: Frontiers in Marine Sciences, 6(758)

Year: 2019

Marisa A. Wirth performed the analysis of glyphosate, AMPA and sarcosine, which required the development of specialized methods. Furthermore, Marisa A. Wirth contributed to data analysis as well as writing and reviewing of the manuscript.

The overall contribution of Marisa A. Wirth to this manuscript was approximately 5 %.

Zusammenfassung

Die Bestimmung polarer Organophosphonate wie dem weltweit genutzten Herbizid Glyphosat, dessen Metabolit Aminomethylphosphonsäure (AMPA) oder der natürlich vorkommenden Methylphosphonsäure (MPn) in Meerwasser ist nötig, um ihre Bedeutung als marine Schadstoffe bzw. in biogeochemischen Prozessen verstehen zu können. Die Anreicherung und Detektion dieser organischen Spurenstoffe in Meerwasser kann allerdings erheblich durch Salzmatrixeffekte gestört oder sogar verhindert werden.

In der vorliegenden Dissertation wurden Salzmatrixeffekte bei der Analyse von Glyphosat, AMPA und MPn untersucht und Verfahren entwickelt, diese zu minimieren. Speziell wurde Meerwasserentsalzung mittels Elektrodialyse (ED) zur Reduktion von Matrixeffekten getestet.

Mit ED konnte die Trennung von organischen Analyten und Salzionen in Meerwasser erreicht werden. Somit stellt ED ein geeignetes Verfahren zur Isolierung von Zielsubstanzen und gelöstem organischen Material aus Meerwasser dar. Darüber hinaus ermöglicht Entsalzung mit ED die anschließende Festphasenextraktion (SPE) von Organophosphonaten mit Ionenaustauscherharzen. Es konnte allerdings für Glyphosat und AMPA ein analytisch besser geeignetes und zudem kostengünstigeres Verfahren mit einem molekular geprägten Polymer als SPE-Material entwickelt werden.

Auch die instrumentelle Analyse der Organophosphonate konnte durch Matrixabtrennung mit ED und SPE verbessert werden. Während der LC-MS/MS bzw. GC-MS/MS Messungen lagen ein einheitliches chromatographisches Verhalten und niedrige Matrixeffekte bei der Detektion vor.

Mit den entwickelten Methoden konnten Glyphosat und AMPA in der Ostsee bestimmt werden, was den ersten Nachweis dieser Komponenten in Meerwasser darstellt. Die gemessenen Konzentrationen lagen zwischen 0.4 und 1.4 ng/L. Die regionalen Konzentrationsunterschiede implizierten eine bevorzugte Metabolisierung von AMPA gegenüber Glyphosat und eine mögliche Persistenz von Glyphosat in der marinen Umwelt.

In weiteren Untersuchungen wurden eine geringe Auswaschung von Glyphosat und AMPA aus Boden und ein unwahrscheinlicher Effekt gegenwärtiger Glyphosat-Umweltkonzentrationen auf die mikrobielle Gemeinschaft der Ostsee ermittelt.

Abstract

The determination of polar organophosphonates like the globally used herbicide glyphosate, its metabolite aminomethylphosphonic acid (AMPA) and the naturally occurring methylphosphonic acid (MPn) in seawater is necessary to elucidate their roles as marine pollutants or in marine biogeochemical processes. However, the enrichment and detection of these organic trace compounds in seawater can be significantly hampered or even prevented through salt-matrix-induced interferences.

The present thesis investigated salt-matrix effects that occur during the analysis of glyphosate, AMPA and MPn as well as measures to minimize them. Especially, seawater desalination with electrodialysis (ED) was tested for the reduction of salt matrix interferences.

ED was shown to be suitable for the separation of organic compounds and salt ions in seawater, making it a promising tool for the isolation of target compounds and dissolved organic matter. Moreover, sample desalination with ED enabled the subsequent solid phase extraction (SPE) of organophosphonates with ion exchange resins. Nonetheless, in case of glyphosate and AMPA, a more analytically feasible as well as cheaper approach with a salt-insensitive molecularly imprinted polymer as SPE material was developed.

The instrumental analysis of organophosphonates could also be improved through salt matrix separation with ED and SPE. During LC-MS/MS and GC-MS/MS analysis, uniform chromatographic behavior and low matrix effects during analyte detection were present.

With the developed methods, glyphosate and AMPA could be detected in the Baltic Sea, which is the first report on the occurrence of these compounds in seawater. The determined concentrations were between 0.4 and 1.4 ng/L. The regional concentration patterns suggested preferential metabolization of AMPA compared to glyphosate and possible persistence of glyphosate in the marine environment.

In additional experiments, leaching of glyphosate and AMPA through soil was determined to be a negligible transport mechanism of these compounds into the aquatic environment. Furthermore, an effect of current environmental glyphosate levels on the Baltic Sea microbial community was deemed unlikely.

Acknowledgement

Ich bedanke mich bei meinem Doktorvater Prof. Dr. Detlef E. Schulz-Bull für die Möglichkeit, meine Promotion unter seiner Betreuung anfertigen zu können, für das in mich gesetzte Vertrauen, für seine fachlichen Ratschläge und für die vielen Freiheiten, die mir bei der Gestaltung meiner Arbeit gelassen wurden.

Bei meiner Betreuerin Dr. Marion Kanwischer bedanke ich mich für ihre Unterstützung in jeder Phase meiner Promotion, für ihr offenes Ohr und für die vielen fachlichen Gespräche mit wertvollen Hinweisen, Denkanstößen und Vorschlägen.

Dem Leibniz Wissenschaftscampus Phosphorforschung Rostock danke ich für die Finanzierung der von mir bearbeiteten Projekte.

Den weiteren Mitgliedern meines Thesis Komitees, Prof. Dr. Udo Kragl, Prof. Dr. Gregor Rehder und Dr. Angela Vogts danke ich für die fachliche Begleitung meiner Promotion, für ihr Interesse an meinem Thema und für die produktiven Komitee-Sitzungen.

Ich bedanke mich bei allen MitautorInnen der Publikationen, die Teil dieser kumulativen Dissertation sind, besonders bei Peter Gros, Friederike Habedank, René Janßen, Constantin Lohrer und Moritz Sievers, für ihre Mitarbeit an meinen Projekten bzw. für die Möglichkeit an der Durchführung ihrer Forschungsprojekte mitwirken zu dürfen.

Weiterhin bedanke ich mich bei allen MitarbeiterInnen des IOW, die mich in der Umsetzung meines Promotionsprojektes in Form von Probennahmen, Bereitstellung von Material, Hilfe bei Laborarbeiten oder Durchführung von Analysen unterstützt haben. Besonders genannt seien hier: Dr. Olaf Dellwig, Ines Hand, Jenny Jeschek, Irina Goldschmidt, Nadine Hollmann, Christoph Kamper, Anne Köhler, Lars Kreuzer, Astrid Lerz, Birgit Sadkowiak, Andrea Tschakste sowie die Besatzungen der IOW Forschungsschiffe.

Besonderer Dank gilt außerdem meinen MentorInnen, die meine Forschungspraktika und Abschlussarbeiten im Rahmen meines Studiums betreut haben. Sie haben mich geprägt, mir viel beigebracht und mich zu der Wissenschaftlerin gemacht, die ich heute bin. Vielen Dank an Dr. Gunnar Gerdts, Dr. Uta Passow, Dr. Sebastian Primpke, Dr. Christopher Rüger und Dr. Martin Sklorz.

Ich bedanke mich bei meinen KollegInnen am IOW und den Mitgliedern der AG Organische Spurenstoffe für die angenehme Arbeitsatmosphäre und die vielen bereichernden fachlichen und nicht fachlichen Gespräche und Aktivitäten. Besonders genannt seien hier: Paul P. Cwierz, Carina Deich, Dr. Kathrin Fisch, Malte Pallentin, Janika Reineccius und Lisa Rönspieß.

Zuletzt gilt auch ein besonderer Dank meinem Lebenspartner Felix Unglaube, meinen Eltern Dr. Hans Wirth und Marion Beckmann-Wirth sowie meiner Familie und meinen Freunden, besonders Erik Jacobs, Felix Leidner, Isabel Nitsch und Alexander Wotzka, die mich immer unterstützt und somit maßgeblich zum Gelingen meiner Dissertation beigetragen haben.

Vielen Dank!

List of Abbreviations

AMPA	aminomethylphosphonic acid
DOC	dissolved organic carbon
DOM	dissolved organic matter
DON	dissolved organic nitrogen
DOP	dissolved organic phosphorus
ECHA	European Chemicals Agency
ED	electrodialysis
EDTA	ethylenediaminetetraacetic acid
ESI	electrospray ionization
FLD	fluorescence detection
FMOC	fluorenylmethoxycarbonyl
GC	gas chromatography
IARC	International Agency for Research on Cancer
IER	ion exchange resin
IS	internal standard
ICP-OES	inductively coupled plasma optical emission spectroscopy
LC	liquid chromatography
LOD	limit of detection
LOQ	limit of quantification
log K_{ow}	*n*-octanol water partition coefficient
MIP	molecularly imprinted polymer
MOF	metal organic framework
MPn	methylphosphonic acid
MS/MS	tandem mass spectrometry
MW	molecular weight
r_{eff}	effective ion radius
RO	reverse osmosis
S	salinity
SPE	solid phase extraction
WWTP	wastewater treatment plant

List of Figures

List of Tables

1 Motivation and Aims

The world's oceans are vast and complex ecosystems around which many unresolved scientific questions and unexplained phenomena revolve. Furthermore, the marine environment is increasingly affected by anthropogenic stressors such as climate change, traffic, tourism and pollution (Steffen et al., 2011). Especially the long-term effects and interdependencies of the various stressors are largely unknown and difficult to determine. Therefore, it is of great scientific, societal and governmental interest to conduct environmental analyses in seawater to understand naturally occurring processes as well as the causes and effects of marine anthropogenic stress.

A large branch within the field of seawater analysis is the measurement of dissolved organic substances of natural as well as anthropogenic origin. This can be conducted in the form of target analysis, i.e., the detection of single compounds, or bulk analysis, i.e., the measurement of the entirety of all molecules with a joint physical, chemical or biological property. Common techniques for target analysis are liquid (LC) or gas chromatography (GC) coupled to a suitable detector, e.g., tandem mass spectrometry (MS/MS) (Hühnerfuss and Kallenborn, 1992; Magi and Di Carro, 2018). Bulk analysis methods are, for example, the determination of dissolved organic carbon, nitrogen or phosphorus or the structural analysis of dissolved organic matter (DOM) with spectroscopic or spectrometric techniques (Minor et al., 2014; Mopper et al., 2007).

Due to the sheer size of the world's oceans, organic molecules are usually present at comparatively low concentrations, because of dilution effects. Hence, enrichment steps are required during sample preparation in order to increase analyte concentrations to instrumentally detectable levels (Hühnerfuss and Kallenborn, 1992; Repeta, 2015). Moreover, the elevated salt content of seawater needs to be considered during its analysis. While the salinity (S) of freshwater is usually below 1, the world's oceans and seas have a salinity of ~35. Areas in which freshwater and saltwater are mixed, leading to intermediate salinities, are classified as brackish. For example, the brackish Baltic Sea has a salinity gradient from $S \approx 2$ in the eastern part to $S \approx 15$ in the western part (Kniebusch et al., 2019).

The large amount of dissolved salt matrix ions in seawater can complicate the analysis of organic compounds. In general, polar and small molecules that are physiochemically similar to salt ions are especially prone to salt matrix interferences. Members of this

compound group are, for example, metabolites from biological processes (Ternon et al., 2018), organophosphonates (Singh et al., 2015; Skeff et al., 2016), perfluorinated compounds (van Leeuwen et al., 2009; Wille et al., 2010) or halomethane sulfonic acids (Zahn et al., 2019). Moreover, other analysis procedures like the investigation of bulk DOM can also be affected by matrix ions (Green et al., 2014; Minor et al., 2014).

Several different sample preparation steps can be hampered by salt ions. The preconcentration of analytes through rotary evaporation or lyophilization of seawater is often inapplicable, since salt concentrations outweigh analyte concentrations by several orders of magnitude (Minor et al., 2014; Repeta, 2015). In this case, the inevitable simultaneous concentration of the salt matrix prevents, for example, successful instrumental analysis of bulk DOM, which requires relatively pure isolates (Green et al., 2014). Alternative enrichment procedures such as solid phase extraction (SPE) can also be aggravated when polar analytes, e.g., organophosphonates, and matrix components compete for binding sites on the solid phase (Corbera et al., 2005; Singh et al., 2015).

Moreover, the instrumental analysis of organic compounds can be affected by the salt matrix. LC-MS/MS with atmospheric pressure ionization, e.g., electrospray ionization (ESI) is extremely prone to matrix effects (Panuwet et al., 2016; Trufelli et al., 2011). The co-elution of analytes and salt matrix components can lead to ion suppression or enhancement (Boulard et al., 2018; Gosetti et al., 2010; Jimenez-Skrzypek et al., 2020; Kock-Schulmeyer et al., 2019; Skeff et al., 2016; van Leeuwen et al., 2009; Zahn et al., 2019). Furthermore, matrix components can affect the chromatographic behavior of analytes, for example, through the formation of adducts or complexes between analytes and matrix components, resulting in altered retention times or the occurrence of several peaks for the same analyte (Fang et al., 2015; Skeff et al., 2016).

The consequences of the described salt matrix effects can be erroneous reports of analyte concentrations, low overall method sensitivity or even the complete prevention of analyte enrichment or detection. Hence, specially designed methodological approaches are required to properly address and potentially circumvent such effects.

The overall aim of this thesis was the development of strategies to overcome salt matrix limitations during the analysis of organic compounds in seawater. In this context, the desalination technique of electrodialysis (ED) was investigated as a seawater processing tool, since it enables the separation of organic analytes from the salt matrix (Chambers et al., 2016; Vetter et al., 2007). In this thesis, the ED process was to be characterized in

terms of salt matrix removal and organic compound retention. Moreover, it was to be investigated whether seawater desalination with ED can facilitate subsequent sample processing and analysis procedures. This was done in the context of bulk as well as target analysis [Publication 1: Wirth et al. (2019)].

Furthermore, within this thesis, specific analysis procedures for two target analytes from the group of organophosphonates, which are especially prone to salt matrix effects, were to be adapted towards seawater. The globally used herbicide glyphosate (*N*-[phosphonomethyl]glycine) and its metabolite AMPA (aminomethylphosphonic acid) are suspected to be relevant marine pollutants (Skeff et al., 2015; Tsui and Chu, 2003); however, methods for their quantitation in seawater are currently lacking. In this thesis, suitable sample preparation and instrumental analysis procedures for glyphosate and AMPA in seawater were to be developed, characterized with regard to their salt matrix sensitivity and applied to the analysis of environmental seawater samples. The applicability of ED in these analysis procedures was to be evaluated, as well [Publication 2: Wirth et al. (2021)].

The developed ED analysis concepts were to be further used during the analysis of methylphosphonic acid (MPn) in seawater [Publication 3: Lohrer et al. (2020)]. This naturally occurring organophosphonate has also not been previously quantified in the marine environment due to a lack of suitable, salt-matrix-insensitive methods.

Finally, the developed methodology for glyphosate and AMPA analysis was used in two additional experiments. The first study investigated the environmental transport and degradation of glyphosate in a lysimeter experiment [Publication 4: Gros et al. (2020)]. The second study analyzed the effect of glyphosate on a brackish microbial community in a microcosm experiment [Publication 5: Janßen et al. (2019)].

2 Introduction

2.1 The Herbicide Glyphosate

2.1.1 General Information

Glyphosate was first sythesized in 1950 by swiss chemist Henri Martin. Since its introduction as a broadband herbicide under the name Roundup® by the U.S. company Monsanto in 1974, glyphosate quickly gained popularity and is currently among the globally most applied herbicides (Duke and Powles, 2008; Richmond, 2018). For example, in 2014, the global application of glyphosate was estimated to be 825 800 tons, out of which 90 % were agricultural use and 10 % were non-agricultural use, e.g., in urban areas or on railroad tracks (Benbrook, 2016). In agriculture, glyphosate-based herbicides are mainly applied during the cultivation of soybeans, corn, grains and sugar beets (Benbrook, 2016). The main application periods are before sowing and after harvest (Steinmann et al., 2012). Glyphosate's mode of action is based on the blocking of the shikimate pathway, which is present in all plants (Giesy et al., 2000). Through the inhibition of the enzyme 5-enolpyruvylshikimate-3-phosphate synthase, the synthesis of essential aromatic amino acids is prevented (Steinrücken and Amrhein, 1980).

2.1.2 Environmental Transport, Degradation and Occurrence

Glyphosate is strongly bound in soils, because its polar functional groups and amphoteric character enable the formation of diverse bonds to minerals as well as organic molecules present in soil (Borggaard and Gimsing, 2008; Gros et al., 2017). Hence, its potential for leaching from the application site is often stated to be low. Despite this, the herbicide is transported in the environment and has often been detected in aquatic systems (Battaglin et al., 2014; Coupe et al., 2012; Huntscha et al., 2018; Skeff et al., 2015). Spray drift or precipitation-induced surface runoff can directly introduce glyphosate into surface waters (Battaglin et al., 2005; Payne et al., 1990; Yang et al., 2015). Additionally, the herbicide can be indirectly introduced into the aquatic environment from the air. It can reach the atmosphere *via* spray drift or wind erosion, i.e., the transport of particle-bound compounds into the atmosphere (Chang et al., 2011; Silva et al., 2018). The relative importance of different transport processes is largely controlled by the environmental conditions, e.g., soil type, precipitation and wind frequency as well

as intensity (Silva et al., 2018). Finally, the surfactants added to glyphosate-based herbicide formulations have been proven to increase glyphosate mobility in the environment and, thus, facilitate its distribution (Grant et al., 2011; Katagi, 2008).

In the environment, glyphosate can be subject to different kinds of degradation such as biodegradation by microorganisms, photodegradation or hydrolysis (Lund-Hoie and Friestad, 1986; Mallat and Barcelo, 1998; Rueppel et al., 1977; Tang et al., 2019). Among these, biodegradation is widely agreed to be the dominant occurring process. Two main glyphosate degradation pathways have been described (Figure 1): either C-N bond cleavage leading to AMPA and glyoxylic acid, or C-P bond cleavage resulting in sarcosine and phosphate (Borggaard and Gimsing, 2008; Giesy et al., 2000; Jacob et al., 1988; Kishore and Jacob, 1997). The degradation products can be further converted to NH_4^+, PO_4^{3-} H_2O and CO_2.

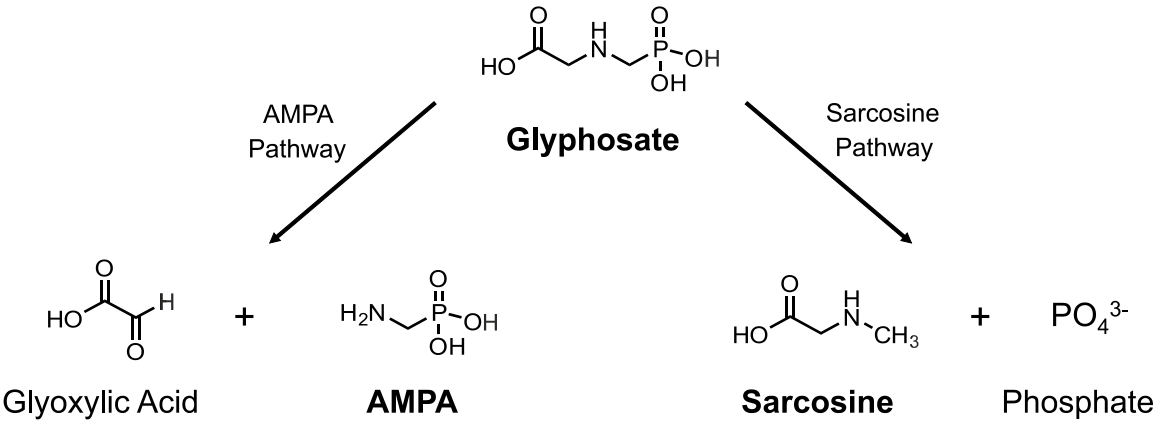

Figure 1 Main biodegradation mechanisms of glyphosate.

It is currently unclear which glyphosate degradation pathway predominately occurs in the environment. Nonetheless, most studies consider AMPA as the main metabolite (Borggaard and Gimsing, 2008). This is presumably owed to the fact that glyphosate and AMPA can be easily co-analyzed (see section 2.2), while a separate method would be required to measure sarcosine. Hence, investigations on the environmental transport, degradation or occurrence of glyphosate usually only consider its metabolization to AMPA.

Biodegradation of glyphosate to AMPA can occur in soil as well as in the aquatic environment. In soil, glyphosate half-lives of 2 to 215 days have been described, while AMPA is considered to be more stable, with half-lives between 60 and 240 days (Bergstrom et al., 2011; Giesy et al., 2000; Grunewald et al., 2001). In the aquatic

environment, glyphosate half-lives have been reported for freshwater (7 to > 70 days) as well as seawater (47 to 267 days) (Giesy et al., 2000; Mercurio et al., 2014). Studies of specific AMPA biodegradation rates in environmental water are currently lacking.

Many investigations on the occurrence of glyphosate in aquatic systems, e.g., streams, canals, rivers and lakes have been carried out across the globe (Battaglin et al., 2005; Coupe et al., 2012; Skeff et al., 2015). In these studies, the metabolite AMPA is usually analyzed alongside glyphosate. In this context, it is important to note that AMPA can also originate from the degradation of other industrial phosphonates (Jaworska et al., 2002; Nowack, 2003). Hence, AMPA that is detected in the environment must not necessarily have originated from glyphosate degradation, especially in proximity to urban areas or industrial sites.

Most studies on the occurrence of glyphosate and AMPA in the aquatic environment present data from Europe, North- and South America or Australia, while studies from Asia and Africa are scarce (Aparicio et al., 2013; Battaglin et al., 2014; Huntscha et al., 2018; Okada et al., 2020). Reported concentrations vary substantially from low ng/L levels to peak values in the mg/L range, depending on the study area. Glyphosate and AMPA have also been detected in rivers and estuaries discharging into seas and oceans, which proves that both compounds are transported into the marine environment (Ramirez et al., 2014; Ruiz-Toledo et al., 2014; Skeff et al., 2015). Nonetheless, data on the concentrations of glyphosate and AMPA in seawater have not been published, yet.

2.1.3 Toxicity

The toxicity and potential carcinogenicity of glyphosate and glyphosate-based-herbicides are a topic of intense debate (Tarazona et al., 2017). The International Agency for Research on Cancer (IARC) classified glyphosate as probably carcinogenic in 2015 (IARC, 2015). In contrast, the committee for risk assessment of the European Chemicals Agency (ECHA) emphasized in 2017 that there is not sufficient scientific evidence for carcinogenic, mutagenic or reprotoxic properties of glyphosate (ECHA, 2017). Glyphosate is, however, classified as toxic to aquatic organisms. Several adverse effects of the herbicide, such as acute toxicity or changes in gene expression and community structure have been reported (Folmar et al., 1979; Stachowski-Haberkorn et al., 2008; Tsui and Chu, 2003; Vera et al., 2010). Interestingly, marine organsims were found to be considerably more sensitive to glyphosate than freshwater organsims (Tsui and Chu,

2003). Furthermore, formulated products containing surfactants and other additives were often found to be more toxic than glyphosate alone. However, the concentrations applied in many studies were in the µg/L or mg/L range, which is higher than most determined environmental concentrations. Hence, the acute toxicity of glyphosate to aquatic organisms appears to be comparatively low under environmentally relevant conditions but the long term effects of chronic pollution with the herbicide are currently not known.

2.2 Analysis Methods for Glyphosate and AMPA in Environmental Water

Both glyphosate and AMPA are analytically challenging compounds due to their high polarity, high water solubility and amphoteric character (Table S1). Hence, specialized methods are required for their analysis in environmental water samples.

2.2.1 Derivatization and Instrumental Analysis

Nowadays, the most common techniques for the instrumental analysis of organic target compounds are LC-MS/MS and GC-MS/MS. Analytes are chromatographically separated from one another and from matrix components on GC- or LC-columns and selectively detected with MS-instruments. However, the low vapor pressure of glyphosate and AMPA makes them unsuitable for GC-separation. Moreover, their high polarity prevents separation on commonly used reversed-phase LC-columns. Therefore, derivatization procedures are often applied, which convert glyphosate and AMPA into derivatives that are more suitable for GC-MS/MS or LC-MS/MS analysis (Arkan and Molnár-Perl, 2015). Presumably the most widespread approach is the conversion of glyphosate and AMPA with fluorenylmethoxycarbonyl-chloride (FMOC-Cl) in borate-buffered solution (Gill et al., 2016; Valle et al., 2018). The obtained FMOC-derivatives are less polar and, thus, suitable for reversed-phase LC-columns. Moreover, the FMOC moiety contains a chromophore that makes the derivatives accessible to fluorescence detection (FLD) as an alternative to MS. Several methods that base on FMOC-derivatization coupled to LC-FLD or LC-ESI-MS/MS have been published for glyphosate and AMPA analysis. Detection limits (LODs) between 0.05 and 1 µg/L are common (Demonte et al., 2018; Hidalgo et al., 2004; Ramirez et al., 2014; Wang et al., 2016) and some methods even reach LODs between 10 and 50 ng/L (Gauch et al., 1989; Le Fur et al., 2000; Montiel-León et al., 2019; Skeff et al., 2015). The use of FLD has

been largely displaced by MS-techniques, which are more selective and sensitive. Moreover, MS-based detection enables the use of isotopically labeled analogues of glyphosate and AMPA as internal standards. These molecules have identical properties but deviating masses from the analytes, which allows their separate detection with MS/MS. Through this, certain identification of the analytes is facilitated and matrix effects as well as analyte losses during sample preparation can be compensated.

2.2.2 SPE Techniques for Preconcentration and Matrix Cleanup

For successful measurement of glyphosate and AMPA in the aquatic environment, the applied methodology needs to be sufficiently sensitive to enable trace-level detection of the analytes, and selective enough to be applicable in environmental water matrices. Therefore, enrichment and/or cleanup steps to increase analyte concentrations and achieve matrix separation are usually necessary.

Preconcentration with rotary evaporation or lyophilization is possible but time-consuming and inevitably co-concentrates matrix components (Küsters and Gerhartz, 2010; Ramirez et al., 2014). The generally widespread extraction with organic solvents is not applicable for glyphosate and AMPA, since their high polarity and high water solubility causes them to remain in the water phase. A more suitable enrichment approach is the use of solid phase extraction (SPE). This technique bases on the binding of target analytes to a solid material and subsequent elution with suitable solvents. A concentration increase of the analytes is achieved when the sample volume is larger than the elution volume.

Many different SPE materials have been used to enrich glyphosate and AMPA (Rigobello-Masini et al., 2019). The employed techniques can be divided into pre- and post-derivatization methods, during which the original compounds or the derivatives thereof are bound on the SPE material (Table 1).

Table 1 Selected examples of SPE procedures for glyphosate and AMPA.

Reference	Material	Matrix	Analysis Method	LOD	
				Glyphosate	AMPA
Pre-Derivatization SPE with Ion Exchange Resins					
Borjesson and Torstensson (2000)	Chelex 100/ AG1-X8	Groundwater	GC-MS	50 ng/L	50 ng/L
Corbera et al. (2006)	Amberlite IRA 900 Cl	River Water	LC-MS/MS	100 ng/L	300 ng/L
Mallat and Barcelo (1998)	Amberlite IRA 410	Ground- and River Water	LC-FLD	20 ng/L	-
Patsias et al. (2001)	PRP-X100	Ground- and River Water	LC-MS	20 ng/L	100 ng/L
Royer et al. (2000)	Chelex 100/ AG1-X8	Mineral Water	GC-MS/MS	25 ng/L	25 ng/L
Pre-Derivatization SPE with Tailored Materials					
Claude et al. (2017)	Affinimip Glyphosate	Mineral-, Ground- and Seawater	LC-MS/MS	10 ng/L	10 ng/L
Pan et al. (2019)	Synthesized MOF	River Water	LC-MS	10 ng/L	30 ng/L
Puzio et al. (2014)	Synthesized MIP	Mineral Water	LC-MS	50 ng/L	50 ng/L
Post-Derivatization SPE with C_{18}-based sorbents					
Hanke et al. (2008)	Strata-X	River-, Lake and Groundwater	LC-MS/MS	0.2 ng/L	0.2 ng/L
Ibanez et al. (2005)	Oasis HLB	Ground- and Surface Water	LC-MS/MS	5 ng/L	5 ng/L
Poiger et al. (2017)	Gemini-NX C_{18}	River Water	LC-MS/MS	5 ng/L	5 ng/L
Sanchís et al. (2012)	C_{18} EC	Groundwater	LC-MS/MS	3 ng/L	3 ng/L
Toss et al. (2017)	Strata-X	Surface Water	LC-MS/MS	200 ng/L	200 ng/L

Pre-derivatization SPE is usually conducted with strong anion exchange resins (IERs), which are able to bind the highly polar analytes, but are also prone to matrix interferences (Corbera et al., 2006). In recent years, the use of tailored materials with selective binding sites for target compounds has become increasingly popular, as these sorbents are often less sensitive towards matrix components (Ansari and Karimi, 2017). Metal organic frameworks (MOFs) as well as molecularly imprinted polymers (MIPs) for pre-derivatization SPE of glyphosate and AMPA have been developed (Claude et al., 2017; Pan et al., 2019; Puzio et al., 2014). Post-derivatization SPE after reaction with FMOC-Cl is usually conducted with C_{18}-based materials. This approach is generally associated with low matrix sensitivity, but has the important disadvantage of producing high amounts of special waste when conducted on a larger scale (Hanke et al., 2008).

By employing SPE enrichment steps, method LODs can be lowered compared to direct instrumental analysis techniques. Values in the range of 3 – 50 ng/L are common and even sub-ng/L LODs have been reported (Table 1).

The main purpose of the above described SPE procedures is the preconcentration of glyphosate and AMPA before instrumental analysis. Nonetheless, SPE can also serve as a purification procedure since interferences with deviating physiochemical properties will be separated from the analytes. At the same time, compounds with similar characteristics might be co-concentrated. There are also literature examples in which SPE has not been used for glyphosate and AMPA enrichment but solely for sample cleanup and the removal of polar or nonpolar matrix components (Küsters and Gerhartz, 2010; Mörtl et al., 2013; Patsias et al., 2001; Puzio et al., 2014; Sancho et al., 1996).

2.3 Salt Matrix Sensitivity during Glyphosate and AMPA Analysis

The physiochemical properties of glyphosate and AMPA render these organophosphonates extremely prone to salt matrix interferences (Table S1). Due to their low molecular weight and polar functional groups, they possess high water solubility and a low log K_{ow}. As a result, they are charged at circumneutral pH and behave similarly to salt matrix ions.

When aiming for glyphosate and AMPA analysis in seawater, SPE preconcentration is required. As described above, IERs are common materials for this task. However, they can be highly sensitive to even small amounts of salt in water samples. SPE recoveries

have been reported to decrease, often below 10 %, even in drinking water, groundwater or river water of a salinity below 1 (Corbera et al., 2005; Jiang and Lucy, 2007; Küsters and Gerhartz, 2010; Patsias et al., 2001). These effects result from the competition of analytes and salt ions for binding sites on the IERs, which hampers the SPE enrichment. Hence, the applicability of IERs in seawater samples without previous desalination steps is highly questionable. Salt-matrix sensitivity is, however, not limited to IERs, but has also been described to occur to a lesser extent when using C_{18} sorbents or tailored MIPs (Hanke et al., 2008; Puzio et al., 2014). At the same time, a MIP is currently the only published material for glyphosate and AMPA SPE that has been described as insensitive to matrix ions and applicable to seawater samples (Claude et al., 2017).

Apart from the SPE procedures, the instrumental analysis of glyphosate and AMPA can also be affected by salt matrices. In the 1990s, a state-of-the-art method used direct injection onto an LC cation exchange column coupled to FLD for analyte detection. The presence of salts in the aqueous samples was reported to damage the LC-column, making routine analysis impossible (Abdullah et al., 1995; Mallat and Barcelo, 1998). Furthermore, a seawater matrix strongly influences the chromatographic behavior of glyphosate-FMOC, for which LC-retention time shifts of several minutes have been reported (Skeff et al., 2016; Wang et al., 2016). This finding was attributed to the formation of glyphosate-metal-complexes with deviating chromatographic behavior (Skeff et al., 2016). Finally, strong matrix effects that resulted in signal enhancement for glyphosate and signal suppression for AMPA as well as an increased signal-to-noise ratio have been reported for both FLD and MS/MS detection of glyphosate-FMOC and AMPA-FMOC (Skeff et al., 2016; Wang et al., 2016).

The various described salt-matrix-induced effects that occur during sample preparation and instrumental analysis of glyphosate and AMPA highlight the necessity for specialized approaches to enable their detection in seawater.

2.4 Electrodialysis

Electrodialysis (ED) can be used to reduce the salinity of seawater samples. The technique is based on the migration of charged compounds, e.g., sea salt ions, through ion exchange membranes positioned in an electric field (Rapp, 2006; Sillanpää and Shestakova, 2017; Strathmann, 2010). In an ED cell, *n* pairs of anion and cation exchange membranes are positioned alternatingly between two electrodes. Typical membranes consist of a polymeric matrix to which charged functional groups are bound, e.g., $R\text{-}SO_3^-$ or $R\text{-}COO^-$ for cation-selective membranes and R_4N^+ or R_4P^+ for anion-selective membranes. Laboratory scale cells contain ~ 10 pairs but cells with up to 300 pairs are possible. The membranes are separated by 0.5 – 1.0 mm thick spacers, enabling the passage of water between them.

During the ED process, three solutions are circulated in the system: the diluate solution, from which ions are removed, the concentrate solution, which receives the removed ions, and the electrode rinse solution, which transports formed hydrogen and oxygen gas away from the electrodes (Figure 2). The diluate represents the to-be-desalted sample. Diluate and concentrate are circulated through the alternating interspaces between the membranes while the electrode rinse solution is circulated between the outermost membranes and the electrodes.

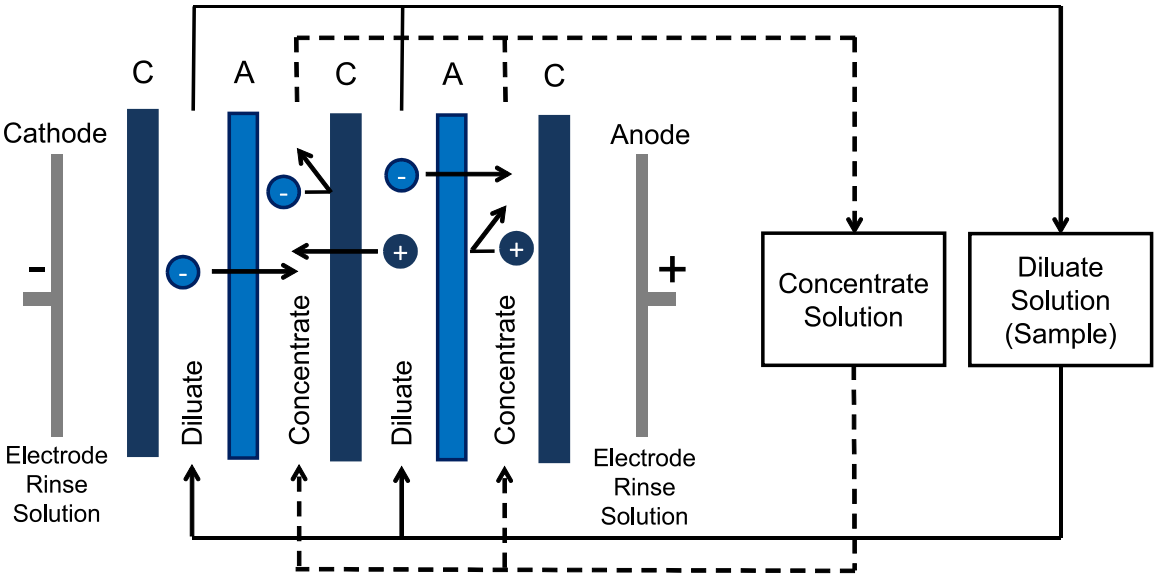

Figure 2 Schematic of an electrodialysis system [modified from: Rapp (2006)]. C = cation exchange membrane, A = anion exchange membrane.

An ED system is operated in batch mode, meaning that the solutions are circulated between the ED cell and storage tanks, until the goal salinity of the diluate is reached. Desalination of the diluate is achieved because the applied electric field causes the migration of ions towards the respectively charged electrodes. Since anions can only transfer trough the anion exchange membranes and cations can only pass the cation exchange membranes, ions are alternatingly removed from and concentrated in the interspaces (Figure 2).

ED has a wide field of applications ranging from industrial processes to wastewater treatment and seawater desalination for drinking water production (Bagastyo et al., 2017; Strathmann, 2010; Xu et al., 2018). It has also been recognized as a promising sample processing tool in environmental analytical chemistry. In this context, ED has mainly been used for the isolation of bulk DOM from seawater (Vetter et al., 2007; Young and Ingall, 2010). The characterization of DOM with spectroscopic or spectrometric techniques requires relatively pure isolates. Hence, when seawater is analyzed, the separation of DOM and salt matrix is vital to avoid the co-concentration of matrix components. Several techniques for this task exist but the combination of ED for DOM isolation and reverse osmosis (RO) for isolate concentration currently represents the state-of-the-art method. ED-RO has the smallest isolation bias and achieves the highest DOM recoveries (40 – 95 %) compared to other methods like ultrafiltration (20 – 78 %) or SPE (10 – 65 %) (Chambers et al., 2016; Dittmar et al., 2008; Minor et al., 2014; Walker et al., 2011). The applicability of ED and ED-RO for DOM isolation before instrumental characterization has been demonstrated with samples from various parts of the world's oceans (Chen et al., 2014; Helms et al., 2015; Koprivnjak et al., 2009; Mao et al., 2012).

As described above, the achieved recovery of the to-be-analyzed compounds after ED is a decisive criterion for its potential integration into analytical methods. Investigations on the recovery of single compounds and, thus, information about influence factors thereon, are scarce. A small selection of target compounds has been investigated in two studies, which determined that both the molecular weight, i.e. the size, and the charge of a molecule affect the ED-recovery (Bell et al., 2017; Chambers et al., 2016). Despite these initial investigations, the integration of ED into target analysis methods for specific compounds is yet to be described.

3 Methodological Approach

3.1 Sample Processing with Electrodialysis

The ED experiments were conducted with a custom-made laboratory scale system (Figure S1). After the establishment of a standard operation protocol, several experiments characterizing different aspects of sample processing were conducted [Publication 1: Wirth et al. (2019)]. The general approach was always similar (Figure 3). Coastal Baltic Sea water samples were desalinated from their respective initial salinity (S ≈ 9-11) down to a residual salinity of 0.1. Subsamples were taken at specific goal salinities. By analyzing the subsamples for the parameter in question, its development throughout the desalination process could be determined. The aspects that were investigated were (1) the removal of the salt matrix, (2) the retention of bulk organic matter in the form of dissolved organic C, N and P (DOC, DON and DOP) and (3) the retention of several hundred organic target analytes.

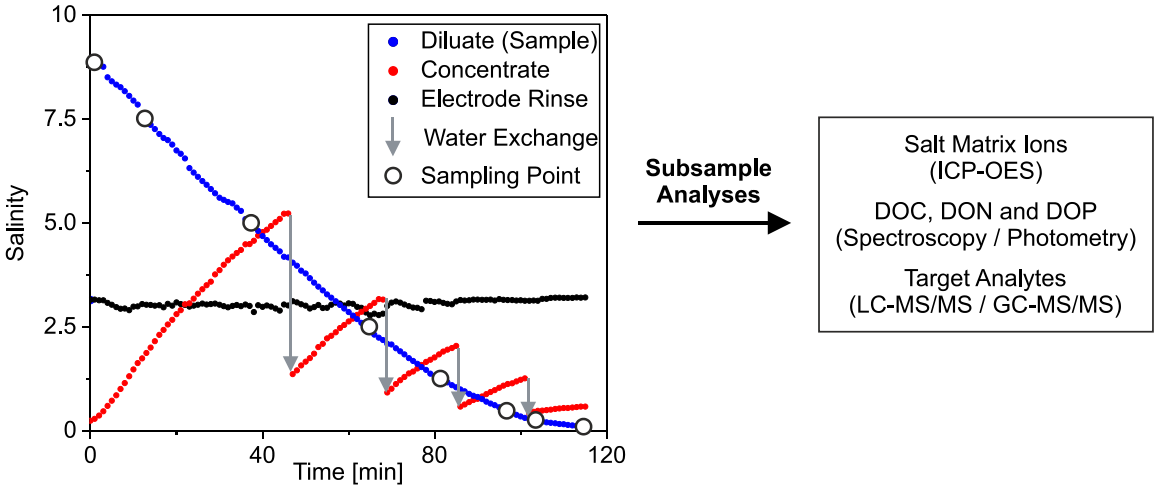

Figure 3 Scheme of electrodialysis experiments: Salt ions are removed from seawater samples (blue) and received by the concentrate solution (red). Part of the concentrate is regularly replaced by pure water to maintain a concentration gradient. Subsamples are collected at specific goal salinities and analyzed for matrix ions, bulk organic matter and/or target analytes.

The coupling of ED to target analysis of the organophosphonates glyphosate, AMPA and methylphosphonic acid was tested by investigating the effect of sample desalination on subsequent SPE and instrumental detection [Publication 2: Wirth et al. (2021), Publication 3: Lohrer et al. (2020)].

3.2 Analysis of Glyphosate and AMPA

Generally, glyphosate and AMPA were analyzed with LC-ESI-MS/MS after derivatization with FMOC-Cl based on a previously developed method (Skeff et al., 2015). Their isotopically labeled counterparts 1,2-$^{13}C_2$-^{15}N-glyphosate and ^{13}C-^{15}N-AMPA were used as internal standards (IS). The basic procedure remained the same for all conducted analyses; however, utilized sample volumes and required sample processing steps were adjusted for the respective area of application. Two main analysis pipelines were developed and validated (Figure 4). The small-scale method with 1 mL sample volume was used for ED experiments [Publication 1: Wirth et al. (2019)] and the additional experiments on glyphosate transport and effects in the environment [Publication 4: Gros et al. (2020), Publication 5: Janßen et al. (2019)]. The small-scale method with 5 mL sample volume as well as the large-scale method were used for seawater analyses [Publication 2: Wirth et al. (2021)].

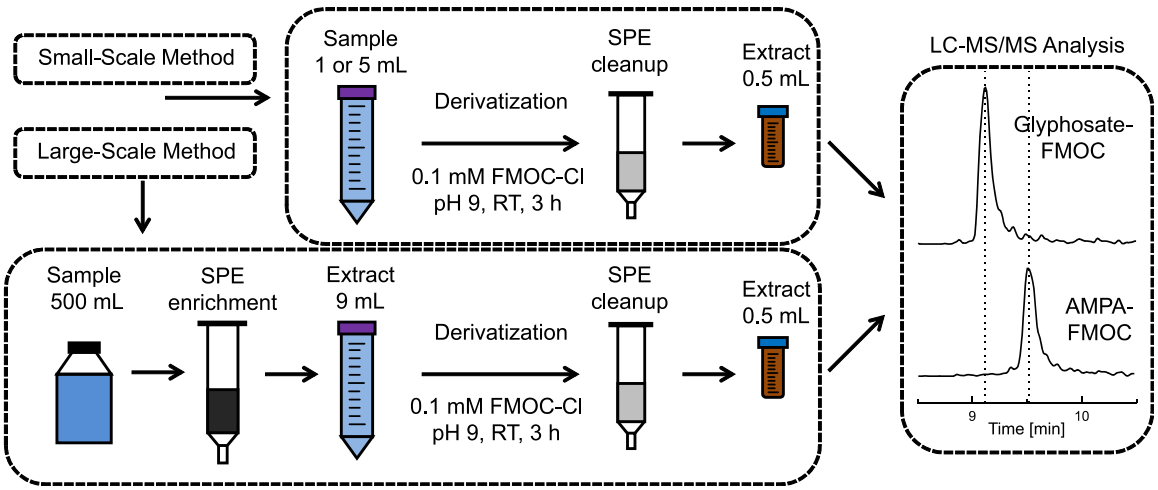

Figure 4 Sample processing protocols for the analysis of glyphosate and AMPA: The small-scale method includes direct FMOC-derivatization followed by SPE cleanup and LC-MS/MS analysis. The large-scale method contains an additional SPE enrichment step before FMOC-derivatization.

The SPE enrichment of glyphosate and AMPA from seawater (large-scale method) was tested with three different materials: the ion exchange resins *Chromabond® PS-OH⁻* and *Amberlite® IRA 900 Cl*, and the molecularly imprinted polymer *Affinimip® Glyphosate*. First, the respective procedures were tested in ultrapure water. Afterwards, they were evaluated in view of their salt matrix sensitivity. For this, coastal seawater was processed with ED and the subsamples collected at specific residual salinities were spiked with the analytes and used for SPE recovery experiments. Based on these results, *Affinimip® Glyphosate* was selected as the SPE material for preconcentration.

Subsequently, derivatization, SPE cleanup and LC-MS/MS measurement were performed. These steps were identical for the small-scale and the large-scale method. The small-scale method simply represents a more straightforward approach with direct derivatization of samples without elaborate SPE preconcentration. The SPE cleanup step with *Chromabond® C_{18} hydra* columns was conducted for removal of matrix components and excess derivatization agent as well as for analyte enrichment. The salt sensitivity of this SPE cleanup and the subsequent LC-MS/MS analysis was also tested with seawater of different salinity, which was obtained through ED, as described above for the large-scale method.

The applicability of the developed methods was tested with environmental seawater samples. The small-scale method was tested with samples from the Warnow Estuary in Mecklenburg Western Pomerania, Germany and the large-scale method was applied to samples from the Western Baltic Sea.

4 Results and Discussion

4.1 Recovery of Target Compounds during Electrodialysis (Publication 1)

Electrodialysis (ED) has been previously used for the isolation of bulk DOM from seawater, but has not been implemented into target analysis methods for single compounds, yet. In order to determine for which molecules ED might be a suitable sample processing tool, the recovery of individual compounds during sample desalination with ED was evaluated. Organic molecules with various physiochemical properties as well as matrix ions were considered.

In this thesis, two mechanisms of compound removal from samples during ED were derived: First, molecules can pass through the ion exchange membranes and into the concentrate solution in the ED cell. Second, they can adsorb to surfaces within the system, i.e. tank walls, tubing or the ion exchange membranes. A competitive process occurs for compounds that are prone to the same loss mechanism. Nonetheless, both removal processes occur simultaneously.

Molecules that are susceptible to loss from the sample *via* ion exchange membrane passage are predominantly small, mobile and charged. The majority of salt matrix ions in seawater hold these properties. Hence, most matrix ions were usually removed to below 1 % of their initial concentration at the final salinity S = 0.1 [see Figure 1 in Wirth et al. (2019)]. The removal speed depended on ion size (effective ion radius, r_{eff}) and charge. The higher the charge and the smaller r_{eff}, the faster the removal was. For comparatively small ions, recoveries mainly decreased in the early stage of the ED process, while recoveries of bulkier or single-charged ions mainly decreased in the late stage of the ED process (Figure 5).

Hydrophilic target compounds that are often charged and of low molecular weight (i.e., size) were also predominately lost *via* membrane passage. The final recovery of these molecules at S = 0.1 was determined by their log K_{ow}. Final recovery decreased linearly with decreasing log K_{ow} (range from -4 to +1), i.e. with increasing hydrophilicity [see Figure 3 in Wirth et al. (2019)]. Twice charged molecules had lower recoveries than single charged ones. Since the investigated organic target molecules are larger and, thus, less mobile than most matrix components, these compounds only passed the ion

exchange membranes in the late stage of the ED process when the supply of mobile matrix ions was already lowered. Hence, the recovery curves of the molecules in question also displayed increasing loss towards the end of the ED process (Figure 5).

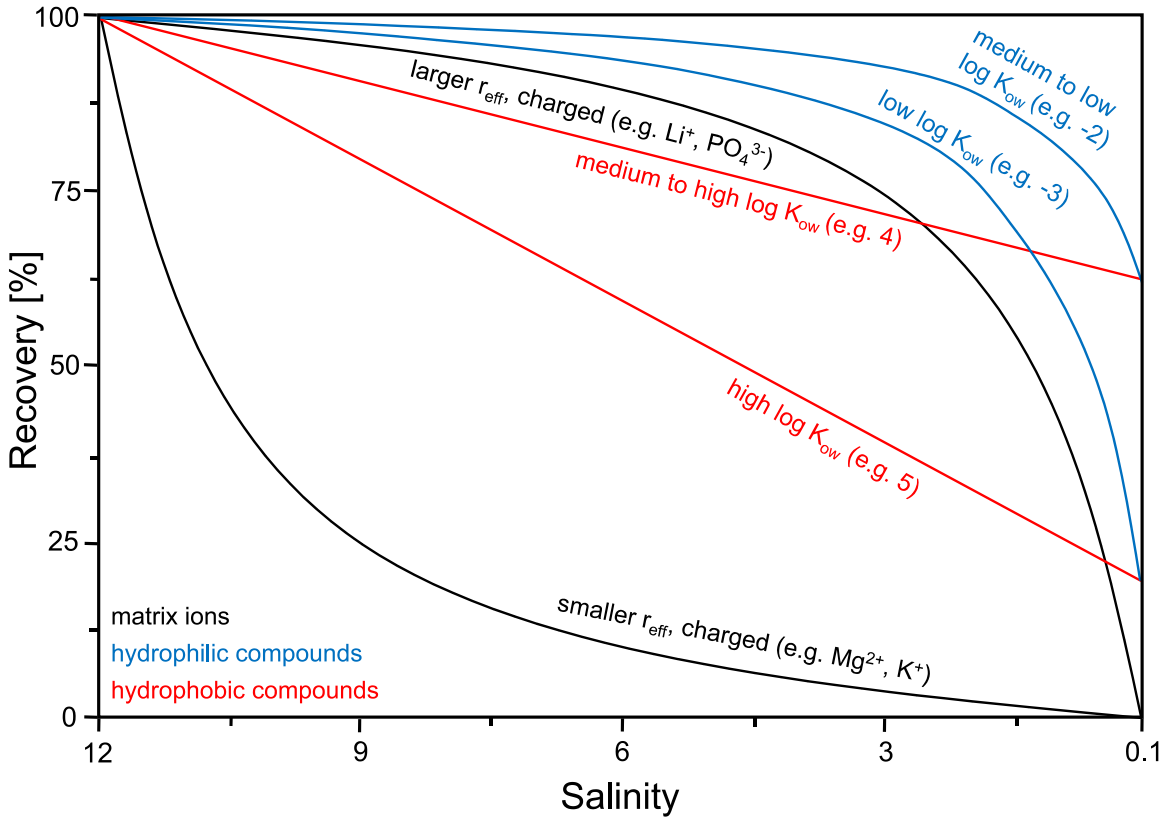

Figure 5 Schematic of recovery curves of compounds with different physiochemical properties during electrodialysis.

Hydrophobic target compounds were susceptible to the second loss mechanism: system wall adsorption. The surfaces of the utilized ED system were made out of plastics, which mainly attract nonpolar compounds. As for the hydrophilic compounds, the final recovery of these molecules at S = 0.1 was determined by their log K_{ow}. Final recovery decreased linearly with increasing log K_{ow} (range from +1 to +6), i.e. with increasing hydrophobicity [see Figure 3 in Wirth et al. (2019)]. As the speed of surface adsorption is dependent on the surface area of the adsorbent and the concentration of the adsorbing compound in solution, the respective recovery curves showed an exponential recovery decrease with time [see Figure 4b in Wirth et al. (2019)]. During the ED process, salinity also decreases exponentially with time (Figure 3), resulting in a linear decrease of the recovery of hydrophobic compounds with decreasing salinity (Figure 5). Due to these dependencies, molecules of medium log K_{ow} (range -1 to +3) are especially favorable for

retention in the ED system, as they are susceptible to neither of the described loss mechanisms, resulting in consistently high recoveries above 80 % [see Figure 3 in Wirth et al. (2019)].

Previous assessments of hydrophilic target compound recoveries have been conducted during ED and ED/RO. Bell et al. (2017) investigated the ED/RO recovery of six target analytes in the molecular weight (MW) range of 169 to 3360 Da and found a positive linear relationship between recovery and log (MW). Similarly, Chambers et al. (2016) determined a high ED recovery of 98 % for vitamin B_{12} (MW = 1355 Da). For the herein investigated compounds, no dependency of recoveries on MW was found [see Figure 3 in Wirth et al. (2019)]; however, the considered MW-range for hydrophilic compounds, was rather narrow (96 – 248 Da) compared to Bell et al. (2017), which explains this finding. In contrast, the herein determined dependency of recoveries on molecule charge was confirmed by Chambers et al. (2016), who found lowered recovery for the charged EDTA (68 %) compared to the neutral glucose molecule (90 %). Bell et al. (2017) reported no effect of the mass-to-charge ratio on recoveries; however, most of their investigated molecules had high MW that was presumably above membrane size cutoff, resulting in their retention despite their charge. Their two smallest tested compounds, glyphosate (169 Da) and glucose-6-phosphate (260 Da) are both twice negatively charged at ED operating pH and showed lowered recoveries of 50 and 57 %, respectively.

In summary, the achieved recovery of target compounds during ED as well as the course of the recovery during the desalination process is determined by the compounds' physiochemical properties. Increased size as well as decreased charge promote the retention of hydrophilic molecules. Nonetheless, small molecules can be retained as long as they are neutrally charged (no electric field influence) and larger molecules can be retained despite their charge (membrane size cutoff). Overall, ED processing is suitable for hydrophilic compounds of low log K_{ow} because they are retained throughout the majority of the desalination procedure. This finding is convenient, as these molecules are especially prone to salt matrix interferences during their analysis. In contrast, hydrophobic compounds of high log K_{ow} are less suitable for ED processing, as their loss from samples already occurs in the early stage of the desalination procedure. However, hydrophobic compounds are generally less prone to salt matrix interferences, making sample desalination unnecessary in most cases.

4.2 Overcoming Salt Matrix Effects during Seawater Analysis

Within this thesis, four different salt matrix effects that can occur during the analysis of organic compounds in seawater were covered (Figure 6). Conceivable resolutions for each effect were introduced and evaluated on the basis of existing literature reports. The central tool in these investigations was electrodialysis. It was used for the characterization of salt matrix effects and was integrated into methodological approaches to overcome them.

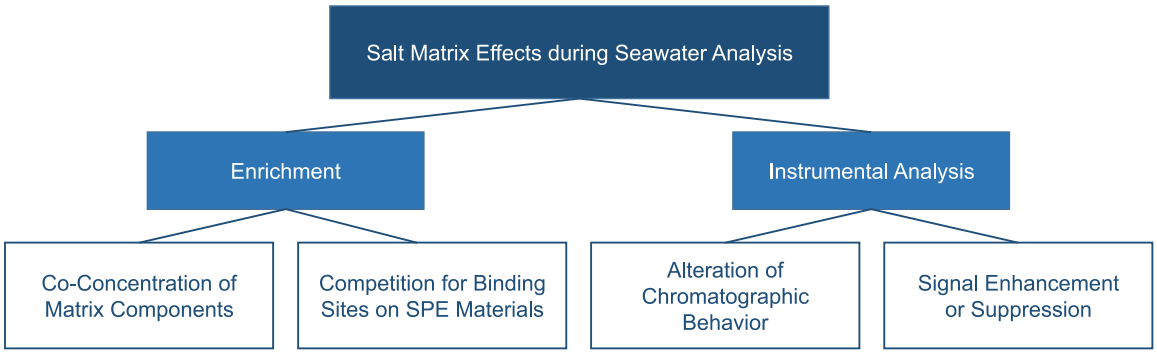

Figure 6 Considered salt matrix effects during organic compound analysis in seawater.

4.2.1 Co-Concentration of Matrix Components (Publication 1)

When aiming for the structural characterization of DOM from seawater, it is vital to separate the sample material from the salt matrix before analysis because relatively pure isolates are required and salt concentrations outweigh DOM concentrations by several orders of magnitude (Minor et al., 2014; Repeta, 2015). Therefore, isolation techniques that do not co-concentrate matrix components are required. The main criteria to judge the suitability of different techniques are the obtained recovery of DOM and the integrity of the isolates, i.e. whether they are representative of the source material.

In this thesis, ED was evaluated with regard to these factors. In order to obtain an overview that is as holistic as possible, the retention of all three main dissolved organic sum parameters, DOC, DON and DOP, was analyzed. At S = 0.1, the respective average recoveries of DOC, DON and DOP were 44, 53 and 89 % [see Figure 2 in Wirth et al. (2019)]. Overall, these results are comparable to reported values in the literature. For DOC, the herein achieved recoveries are rather low. Similar recoveries of 40 and 46 % were only reported by Chen et al. (2014) for samples from the North Atlantic Ocean,

while other authors mainly found values in the range of 50 to 80 % (Figure 7). DON recoveries have not yet been specifically reported but have been stated to be similar to DOC recoveries (Chambers et al., 2016; Green et al., 2014), which was confirmed by the experiments conducted within this thesis. By contrast, the herein achieved DOP recoveries were significantly higher than for DOC and DON, but very similar to previously reported literature values, indicating that the favorable retention of DOP might not be an exclusive trait of the herein used ED system.

Since DOC and DON recoveries were in the same range, the calculated C/N ratios only changed moderately between the samples (14.7 ± 1.4) and the isolates (12.1 ± 0.7). This indicates that the sample isolates were representative of the source material in terms of carbon and nitrogen content. Due to the elevated DOP recoveries, C/P ratios decreased from 268.6 ± 11.4 in the original samples to 131.1 ± 4.9 in the isolates, which underlines the apparent isolation bias towards P-containing compounds during ED.

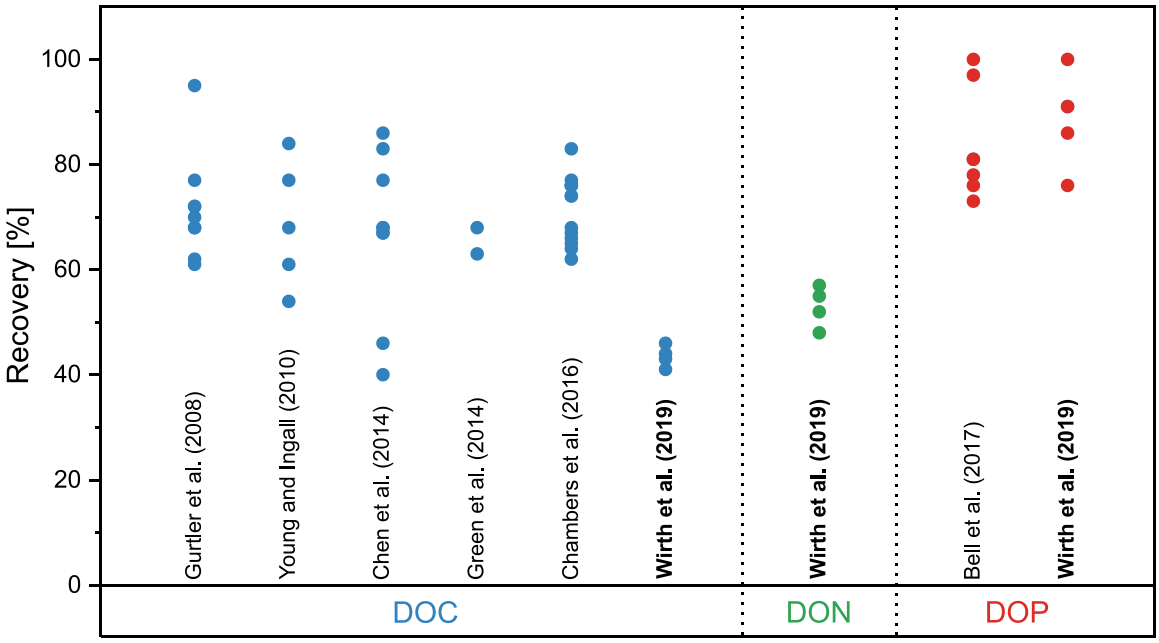

Figure 7 Comparison of DOM recoveries after ED or ED/RO between different literature reports and this thesis. Each data point represents the reported recovery of one sample at the respective final salinity.

In order to further understand the discrepancies between DOC, DON and DOP behavior in the ED system, knowledge obtained from investigating compound-specific recoveries can be used (see section 4.1). The recorded recovery curves indicate dominant

loss mechanisms for molecules belonging to each compound class and can help to derive compounds from each DOM-group that are particularly prone to loss during ED.

DOP was retained throughout the majority of the ED process. Loss only occurred below S = 2 [see Figure 2 in Wirth et al. (2019)]. Apparently, only a fraction of comparatively small and charged compounds was lost via ion exchange membrane passage. Most molecules in DOP must, hence, either be uncharged or larger than the membrane size cutoff. Furthermore, the DOP fraction was presumably composed of rather hydrophilic compounds, as system wall adsorption did not seem to occur. Molecules from the DOP pool that meet the above criteria are, e.g., polyphosphates, adenosine-triphosphate (ATP), nucleotides or ribonucleic acid (RNA) (Bell et al., 2017). The small, charged compounds that can pass the ED membranes could, for example, be small phosphate esters or phosphonates (Young and Ingall, 2010).

DOC and DON recoveries decreased throughout the entire desalination process, indicating that both derived loss mechanisms occurred [see Figure 2 in Wirth et al. (2019)]. Especially for DON, compound loss *via* wall adsorption took place in the first half of the ED process. The corresponding compounds are presumably part of the high molecular weight, rather hydrophobic fraction of DOM, which has undergone little structural characterization so far (Hertkorn et al. 2008; Repeta, 2015). The increased loss of DOC and DON at low residual salinity suggests that membrane passage of small, charged molecules, e.g. amino acids, occurred, as well.

To conclude, the herein conducted evaluation of ED for DOM isolation confirmed its suitability for the task. Separation of DOM and salt matrix was achieved and satisfactory DOM recoveries that are comparable to literature values were obtained (Figure 7). Consistent with previous studies, isolates showed high integrity regarding carbon and nitrogen content but an isolation bias towards phosphorus-containing compounds was present (Bell et al., 2017; Chambers et al., 2016; Green et al., 2014; Koprivnjak et al., 2009). This highlights that the isolation bias of ED might be lower compared to SPE or ultrafiltration techniques but it is, nonetheless, present, as compounds with specific physiochemical properties were preferentially lost from the seawater samples.

4.2.2 Competition for Binding Sites on SPE Materials (Publication 2 and 3)

SPE of Glyphosate and AMPA (Publication 2)

Solid Phase extraction (SPE) of target compounds from seawater can be necessary to preconcentrate analytes before instrumental analysis (Fisch et al., 2017; Kock-Schulmeyer et al., 2019). The main criterion to evaluate the applicability of an SPE step towards specific compounds or matrices is the achieved analyte recovery, which strongly influences the sensitivity and the detection capacity of the entire analysis method.

In this thesis, SPE was used to enrich the herbicide glyphosate and its metabolite AMPA from seawater, in order to obtain instrumentally detectable concentrations. Both compounds have physiochemical properties that make them highly susceptible to salt matrix interferences (Table S1). Hence, their extraction from seawater can be hampered when analytes and salt ions compete for binding sites on the SPE material. The most common materials used for pre-derivatization SPE of glyphosate and AMPA are ion exchange resins (IERs) but molecularly imprinted polymers (MIPs) have also gained popularity in recent years (Claude et al., 2017; Corbera et al., 2005; Jiang and Lucy, 2007; Patsias et al., 2001; Puzio et al., 2014). Both described sorbent types were evaluated in this thesis.

When used in pure water, IERs as well MIPs mostly achieve high recoveries for glyphosate and AMPA (Figure 8). With the herein utilized first IER, *Amberlite® IRA 900 Cl*, recoveries for glyphosate and AMPA were 89 and 77 % while the second IER, *Chromabond® PS OH*$^-$, gave 62 and 35 % recovery, respectively. The applied MIP *Affinimip® Glyphosate* enabled glyphosate and AMPA recoveries of 86 and 68 %. Overall, these values compare well to previously published data and confirm the applicability of all sorbents (Figure 8). However, if the SPE of glyphosate and AMPA is conducted in different types of natural water instead of pure water, almost all previously conducted studies reported decreases in analyte recovery, which are sometimes substantial, i.e. < 10 % (Figure 8). When samples of different salinity were evaluated, the recovery decreases were always more substantial at higher salinity (Corbera et al., 2005). The sensitivity towards matrix components was more prominent for IERs than for MIPs, which were, nonetheless, negatively affected in most cases. The salt sensitivity of the herein used sorbents was tested with untreated and desalted seawater of different residual salinity that was obtained through electrodialysis [Figure 8, and Figure 1 in Wirth et al.

(2021)]. Both tested IERs proved to be very salt-matrix-sensitive, as no glyphosate and AMPA could be recovered from the original sample. Only when the sample salinity was reduced below S = 1, SPE with the IERs was possible. At a residual salinity of S = 0.1, recoveries were similar to those obtained in pure water.

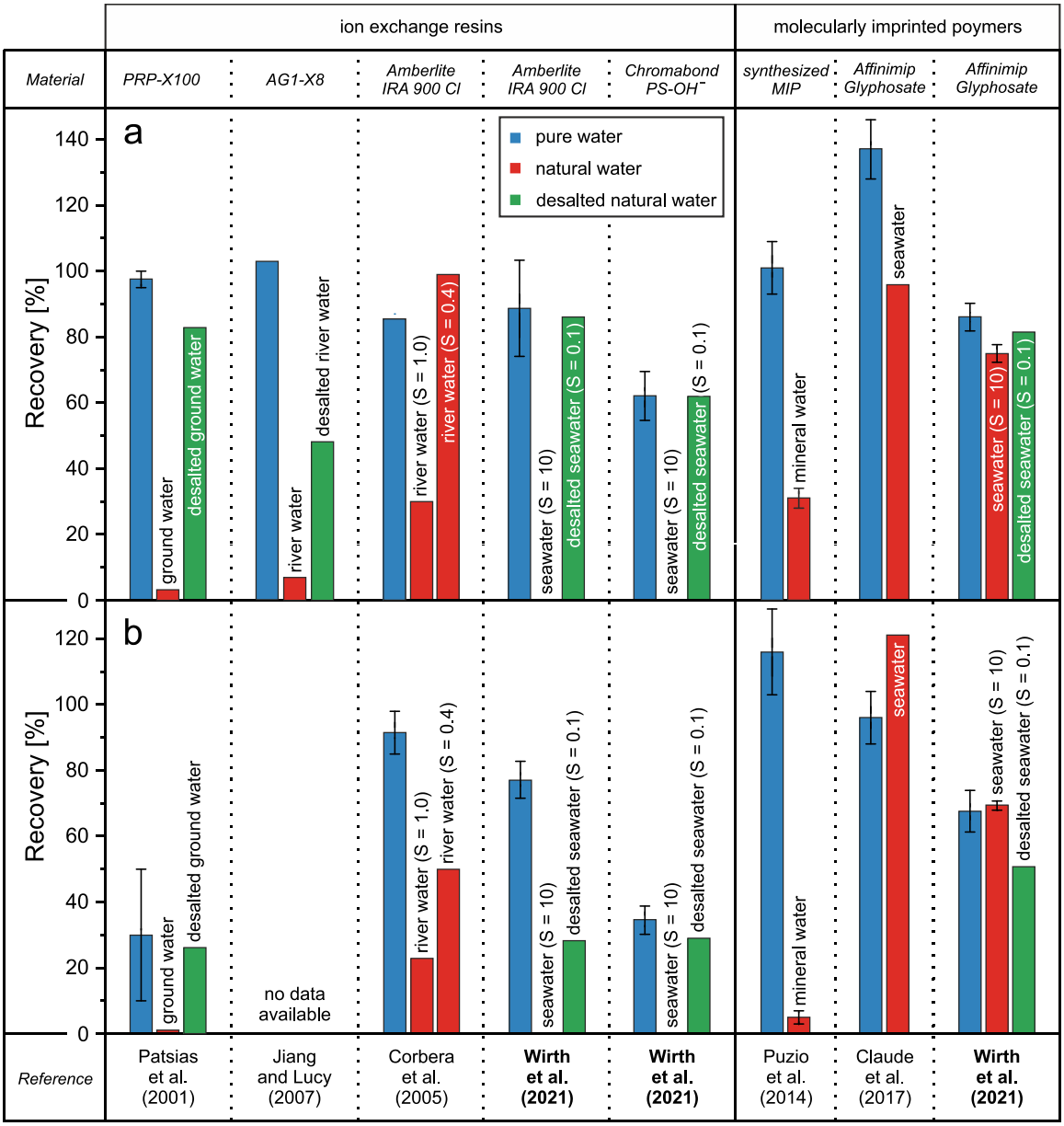

Figure 8 Comparison of achieved SPE recoveries in pure water, natural water and desalted natural water for glyphosate (a) and AMPA (b) between different literature reports and this thesis (sample salinity is given, when available).

Previous studies have employed desalination steps with mixed ion exchangers that bind salt ions but not glyphosate and AMPA (Jiang and Lucy, 2007; Patsias et al., 2001). This approach could improve recoveries in river and ground water but could rarely compensate for the salt-matrix-induced decrease (Figure 8). Thus, its applicability to seawater, which has much higher salinity, is questionable. More promising is the use of MIPs, as the herein tested MIP enabled similar recoveries in untreated seawater and in pure water and was, thus, barely sensitive to salt ions.

In summary, IERs were confirmed to be highly susceptible to salt matrix interferences and can, therefore, only be used for SPE of glyphosate and AMPA from seawater when further sample treatment, e.g., sample desalination, is applied (see section 4.3 for further discussion). In contrast, MIPs can be used for direct analyte preconcentration from seawater since their highly selective molecular recognition sites enable glyphosate and AMPA extraction in the presence of salts.

SPE of Methylphosphonic Acid (Publication 3)

Comparable findings regarding the salt-sensitivity of SPE materials were found by Lohrer et al. (2020) for methylphosphonic acid (MPn). This organophosphonate is structurally and physiochemically similar to glyphosate and AMPA (Table S1). The SPE of MPn from water samples is necessary, because its subsequent derivatization for GC-MS/MS analysis requires a water-free environment. The utilized material was the weak IER *Strata-X-AW*, which enabled the recovery of 110 % MPn in pure water. In contrast, in artificial seawater with S = 8, a recovery decrease to approx. 4 % was found [see Figure 3 in Lohrer et al. (2020)]. Moreover, when testing the procedure in river water with S = 0.3, decreased recoveries compared to pure water were observed as well [see Figure 4 in Lohrer et al. (2020)].

Hence, salt matrix ions significantly hampered the developed method for MPn analysis in environmental water, making it only applicable to samples of low salinity. However, MPn is suspected to play a role in the resolution of the marine methane paradox, making its quantitation in seawater desirable (McGrath et al., 2013; Metcalf et al., 2012). Therefore, the analysis concept of sample desalination with ED before IER-SPE that was developed for glyphosate and AMPA within this thesis was tested for MPn analysis in seawater, as well. This contribution to Lohrer et al. (2020) will be discussed in section 4.3.

4.2.3 Alteration of Chromatographic Behavior (Publication 2)

When conducting instrumental analyses with chromatographic techniques, the chromatographic behavior of target compounds should be as consistent as possible and ideally not affected by matrix components to assure reliable analyte quantitation.

The chromatographic separation of glyphosate has been reported to be impacted by the presence of a salt matrix by two studies that performed direct injection into an LC-MS/MS or LC-FLD system after FMOC-derivatization (Skeff et al., 2016; Wang et al., 2016). In both cases, retention time shifts of several minutes for glyphosate-FMOC in saltwater compared to pure water were observed. This was attributed to the formation of complexes with divalent cations, resulting in changed interactions with the stationary phase of the LC-column. Different effects were observed for individual ions. The presence of Cu^{2+}, Co^{2+}, Zn^{2+} and Mn^{2+} entirely prevented glyphosate-FMOC detection, while Ca^{2+} and Mg^{2+} only caused the aforementioned retention time shift. Moreover, the effect was found to be concentration dependent, resulting in different retention times depending on the ion concentrations, even yielding two peaks in an intermediate concentration range (Skeff et al., 2016). Such variable interactions significantly complicate the detection of glyphosate-FMOC in a saline matrix.

In this thesis, an SPE cleanup step with the revered phase material *Chromabond® C_{18} hydra* was introduced prior to LC-MS/MS analysis in order to separate the FMOC-derivatives from the salt matrix and the excess derivatization agent. When comparing the obtained retention times for glyphosate-FMOC and AMPA-FMOC at different salinities, it was found that no shifts occurred in the tested range of S = 0 – 10 (Table S2). This indicates that the employed separation procedure prevented the previously described matrix effects and resulted in uniform chromatographic behavior of the analytes, which greatly facilitated the instrumental analysis.

4.2.4 Signal Enhancement or Suppression (Publication 1, 2 and 3)

LC-MS/MS with atmospheric pressure ionization techniques is highly susceptible to matrix effects in the form of ion suppression or enhancement (Panuwet et al., 2016; Trufelli et al., 2011). Such effects often arise from the co-elution of analytes and matrix components or from the formation of complexes between the two (Boulard et al., 2018; Gosetti et al., 2010; Skeff et al., 2016). GC-MS/MS is generally less prone to such matrix effects but reports of signal enhancement or suppression exist nonetheless (Erney et al.,

1993; Silvestro et al., 2013). Salt matrix ions have mainly been reported to have suppressing effects on target analyte signals (Jimenez-Skrzypek et al., 2020; Kock-Schulmeyer et al., 2019; van Leeuwen et al., 2009).

In this thesis, it was investigated whether a reduction of the sample salinity with ED can enhance the LC-MS/MS and/or GCMS/MS signals of target analytes. In all investigated cases, sample extraction steps were performed before instrumental analysis, meaning that the observed effects are presumably owed to a combination of two factors: (1) the lower residual salt content in the instrumentally measured extracts and (2) increased recoveries of the extraction steps at reduced salinity.

When comparing the obtained LC-MS/MS and GC-MS/MS signals of target analytes in ED-processed seawater (S = 0.1) to those in untreated seawater, significant signal enhancement could be found for glyphosate and AMPA (Wirth et al., 2021), for MPn (Lohrer et al., 2020) and for 21 target compounds that were investigated during the initial ED characterization (Wirth et al., 2019) (Figure 9). Increase factors for the latter were between 25 and 620 %. The IS-Signal of MPn even increased by 820 % [see also Figure 5c in Lohrer et al. (2020)]. The effect was less prone for glyphosate and AMPA and increase factors were only 13 and 34 %, respectively. These findings show that separation of salt ions and analytes through ED can clearly increase the sensitivity and detection capacity of target analysis methods.

The above described signal enhancement due to sample desalination was least pronounced for glyphosate and AMPA because the conducted SPE cleanup step after FMOC-derivatization (Figure 4) was specifically introduced for matrix separation and to limit salt effects on the LC-MS/MS analysis (also see section 4.2.3). The suitability of the SPE cleanup for this task was tested by calculating remaining matrix effects after cleanup at different salinities (Equation S1 and S2). The absolute effects were of low to moderate suppressing nature for both analytes and decreased with decreasing salinity [see Figure 2a in Wirth et al. (2021)]. Strongest signal suppression of -14.6 and -22.3 % for glyphosate and AMPA was found in untreated seawater (S = 10). Nonetheless, these results represent an important reduction in matrix effects compared to previously used direct injection techniques. Skeff et al. (2016) reported a strong dependency of LC-MS/MS signals on the sample salinity. For glyphosate-FMOC, they found signal increases of up to +181 % at S = 2-10 compared to pure water while signals were increasingly suppressed at higher salinities (e.g. +36 % at S = 30). For AMPA-FMOC,

signal suppression of up to -38% was observed in the entire considered range of S = 2-30. An increased LC-FLD signal of +48 % for glyphosate-FMOC in seawater was also reported by Wang et al. (2016). Therefore, the comparatively low absolute matrix effects that were still present after the herein performed SPE cleanup were deemed negligible, enabling sample analysis without desalination through ED. Furthermore, any remaining matrix effects could be corrected through the use of isotopically labeled compounds as internal standards, as all effective matrix effects were below 5 % [see Figure 2b in Wirth et al. (2021)]. Since analytes and IS behave alike during sample processing and instrumental analysis, weighting of their signals compensates for remaining matrix effects, as long as the effects do not prevent analyte detection entirely.

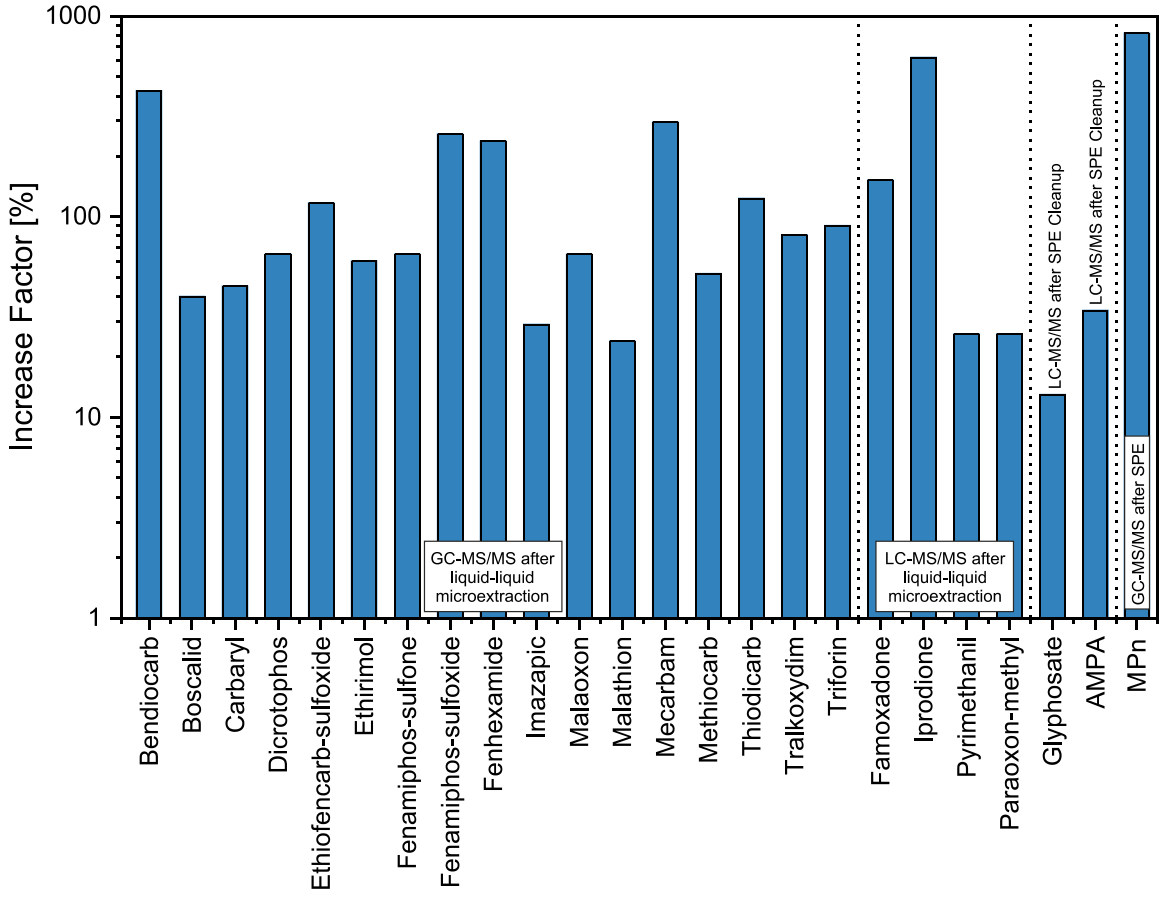

Figure 9 Increase factors of target analyte signals in ED-desalted seawater of S = 0.1 compared to untreated seawater of S = 9-11.

4.3 Suitability of Electrodialysis for Coupling to Target Analysis in View of Methodic and Economic Aspects (Publication 1, 2 and 3)

As shown in the previous section 4.2, electrodialysis can be successfully applied during the sample preparation of glyphosate and AMPA. Salinity reduction with ED can enable the subsequent SPE with ion exchange resins, which is hampered in seawater due to competition of salt ions and analytes for binding sites on the SPE material.

A basic requirement for possible coupling of ED to other sample processing steps is sufficient recovery of the analytes during the desalination procedure. Glyphosate and AMPA show typical recovery curves for hydrophilic target compounds. They are retained in the early stage of the ED process and show increasing loss rates at lower residual salinities [see Figure 4a in Wirth et al. (2019)]. Hence, their achieved ED recovery is highly dependent on the chosen residual salinity, i.e., the end of the desalination procedure. Since ED recovery decreases with decreasing salinity, but SPE recovery on IERs increases with decreasing salinity, the selected final salinity will always be a compromise between these two factors. The ideal residual sample salinity is, thus, dependent on the target analyte as well as on the subsequent sample preparation steps and needs to be individually determined.

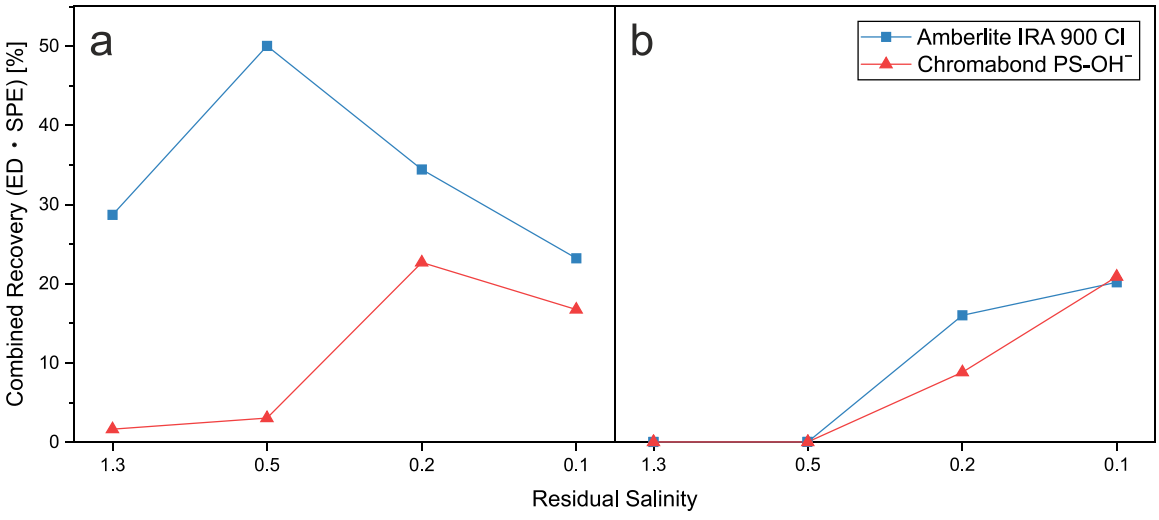

Figure 10 Calculated combined (i.e., multiplied) recoveries of glyphosate (a) and AMPA (b) after electrodialysis and solid phase extraction with two different ion exchange resins at different residual sample salinities.

For glyphosate and AMPA, the maximized combined recovery differs between the analytes and the utilized IERs (Figure 10). Since, on the one hand, the twice charged glyphosate has lower ED recoveries than the singly charged AMPA, and on the other hand, SPE recoveries on IERs are generally higher for glyphosate than for AMPA, the maximized combined recovery for AMPA lies at residual salinity S = 0.1, while maximum glyphosate recovery is obtained at S = 0.5 or 0.2, depending on the IER. This highlights that even the combined analysis of two target analytes requires compromises when selecting ED sample processing parameters.

Overall, the combined SPE and ED recoveries of glyphosate and especially of AMPA are relatively low, meaning that the coupling of the two procedures would result in high analyte losses and, thus, low method sensitivity. Hence, direct SPE with a salt-insensitive molecularly imprinted polymer, which enables higher analyte recoveries, seems to be the analytically favorable approach in this case. Nonetheless, the two procedures do not only vary in the achieved recoveries but also in cost and work load. To determine which approach is more economically feasible, costs for the processing of 10 samples were estimated for both procedures (Table 2).

The SPE material costs for the MIP *Affinimip® Glyphosate* are substantially higher than, for example, for the IER *Amberlite® IRA 900 Cl*. Expenses for consumables and chemicals were similar in both cases. However, sample processing with ED is elaborate, which resulted in more than thrice as many necessary working hours when using ED and IER-SPE. The additional personnel costs outweigh the cheaper SPE material by far, making sample processing with ED and subsequent IER-SPE more than twice as expensive as direct MIP-SPE. In conclusion, direct preconcentration of glyphosate and AMPA with the MIP does not only achieve higher analyte recoveries, but is also more economically feasible, making it the preferable method over IER-SPE combined with ED.

Of course, tailored MIPs that enable salt-insensitive SPE are not available for every target analyte. In case of methylphosphonic acid, whose analysis in seawater was to be enabled in Lohrer et al. (2020), desalination with ED before IER-SPE was the only option that presented itself [Publication 3]. The recovery curve of MPn during ED is highly similar to those of glyphosate and AMPA, with high retention in the early stage of the process and increasing loss rates at lower residual salinity [see Figure 5a in Lohrer et al. (2020)]. The required residual salinity for successful MPn quantitation was

investigated by processing a coastal seawater sample with ED and analyzing subsamples of different salinity for MPn content [see Figure 5b in Lohrer et al. (2020)]. Consistent with laboratory experiments, no MPn could be recovered from the original sample (S = 10.4) due to salt interference with the IER-SPE procedure. However, interestingly, MPn could already be measured at a comparatively high residual salinity of 5.6. Upon further desalination, determined concentrations decreased due to ED membrane passage of MPn. The recorded recovery curve was highly comparable to previous spiking experiments [see Figure 5a,b in Lohrer et al. (2020)].

Table 2 Sample processing costs for 10 samples with different conceivable methods for the analysis of glyphosate, AMPA and methylphosphonic acid. Costs for the SPE materials, consumables and chemicals were calculated based on the materials used in the publications (Lohrer et al., 2020; Wirth et al., 2021). Personnel costs for a scientist were calculated from the required working hours.

	Glyphosate and AMPA		**Methylphosphonic Acid**	
	MIP-SPE without ED	**IER-SPE with ED**	**ED without IS**	**ED with IS**
SPE Material	107.91 €	2.30 €	325.64 €	65.13 €
Consumables	70.33 €	84.61 €	52.76 €	21.23 €
Chemicals	10.00 €	13.15 €	63.18 €	314.81 €
Working Hours	20 hours	68 hours	94 hours	64 hours
Personnel	375.00 €	1275.00 €	1762.50 €	1200.00 €
Sum	**563.24 €**	**1375.06 €**	**2204.08 €**	**1601.17 €**

Based on these results, two possibilities for MPn quantitation in seawater were derived. On the one hand, ED subsamples of different residual salinity could be analyzed for MPn content and its concentration in the original seawater sample could be estimated through exponential extrapolation of the recorded loss curve. This first approach was successfully used to estimate the MPn concentration in a Baltic Sea coastal sample [see Figure 5b in

Lohrer et al. (2020)]. On the other hand, the isotopically labeled MPn internal standard could be added prior to ED, which would compensate for compound loss during ED and require the analysis of only one subsample of sufficiently low salinity.

This second approach would lead to more accurate results since extrapolation is not considered to be a reliable quantitation method. However, high amounts of expensive labeled MPn would be required in this case, as the minimal volume for sample processing with the herein utilized ED system is 3 L. In order to determine whether the additional IS makes this approach less economically feasible, the costs for processing 10 samples with both possible procedures were estimated (Table 2). In case of the first approach, the analysis of 5 subsamples of different residual salinity was assumed for each of the 10 samples. The required processing of 50 samples after ED with the first method ("ED without IS") compared to just 10 samples with the second method ("ED with IS") resulted in higher SPE material and consumable costs for the former. In contrast, the chemical costs were higher for the second method due to the aforementioned large amount of required IS. Both methods are generally elaborate due to the required ED-step but several additional working hours are necessary for the processing of 50 samples instead of 10. The resulting elevated personnel costs for the first approach outweigh the higher chemical costs for the second approach. To conclude, the addition of the MPn IS before ED would not only enable more accurate quantitation of MPn in seawater, but is also the more economically feasible approach.

In summary, electrodialysis was shown to be suitable for coupling to target compound analyses. Its main drawback is currently the high workload, which makes it expensive and prevents a high sample throughput. A possibility to circumvent this factor would be system downscaling in order to achieve lower required sample volumes and, thus, faster sample processing.

4.4 Analysis of Glyphosate and AMPA in Environmental Seawater

4.4.1 Method Development and Validation (Publication 2)

After the evaluation of salt matrix effects that occur during the analysis of glyphosate and AMPA in seawater and after choosing appropriate solutions, suitable analysis pipelines were developed and validated. Since the introduced SPE cleanup step alone enabled the LC-MS/MS analysis of both compounds without salt matrix interferences,

two different methods were set up: a fast, small-scale method that uses 5 mL samples for direct derivatization before SPE cleanup, and a more elaborate, large-scale method that includes MIP-SPE preconcentration of 500 mL samples before derivatization (Figure 4).

Both methods were validated in ultrapure water and environmental seawater and showed significant linearity and satisfactory accuracy and precision (RSD% and RE% < 12 % in all cases) [see Table 2 in Wirth et al. (2021)]. The small-scale method achieved an LOQ of 10 and 15 ng/L for glyphosate and AMPA. The obtained LOQs were comparable to similar published methods that utilized small-scale SPE of derivatized samples before instrumental analysis (Ibanez et al., 2005; Poiger et al., 2017; Sanchís et al., 2012). For example, Sanchís et al. (2012) used online-SPE of 4 mL water samples and achieved an LOQ of 9.6 ng/L for both glyphosate and AMPA.

With the added preconcentration step, the LOQs of the large-scale method were lowered to 0.17 and 0.31 ng/L for glyphosate and AMPA. Methods for glyphosate and AMPA analysis in the sub-ng/L range are currently scarce. Only Hanke et al. (2008) achieved LOQs of 0.7 and 0.8 ng/L for glyphosate and AMPA by performing a large-scale SPE-step after FMOC-derivatization. Compared to this approach, the herein introduced MIP-SPE procedure is more environmentally friendly, as it does not produce comparatively large amounts of special waste from performing the derivatization reaction in a large sample volume (200 mL in that case).

The different sensitivity levels achieved by the two developed methods define their respective areas of application. The small-scale method is suitable for coastal regions or areas with high levels of pollution, while the large-scale method can be used in areas with lower analyte concentrations, i.e., stations further offshore or distant from potential analyte sources.

4.4.2 Method Application in the Baltic Sea (Publication 2)

The applicability of both developed methods was shown by analyzing a set of environmental samples with each method. The small-scale method was applied to thirteen surface water samples from the Warnow Estuary in Mecklenburg Western Pomerania, Germany, which discharges into the Baltic Sea (Figure 11). Glyphosate and AMPA were detected in most samples in a concentration range of < LOD to 28 ng/L for glyphosate and < LOD to 208 ng/L for AMPA [see Table S3 and Figure 3 in Wirth et al. (2021)]. Analyte concentrations were generally found to decrease towards the Baltic Sea

due to dilution of river water with comparatively high analyte concentrations with Baltic Sea water [see Figure 4 in Wirth et al. (2021)]. Furthermore, evidence for analyte degradation along the flow path was found. Lastly, the wastewater treatment plant (WWTP), which discharges into the estuary was recognized as an important point source of glyphosate, and especially of AMPA, to the estuary. Measured concentrations near the WWTP outlet were 106 and 2633 ng/L for glyphosate and AMPA, respectively. Nonetheless, these large amounts of AMPA presumably originate at least partially from alternative sources like degradation of industrial phosphonates and not exclusively from glyphosate degradation (Jaworska et al., 2002; Nowack, 2003).

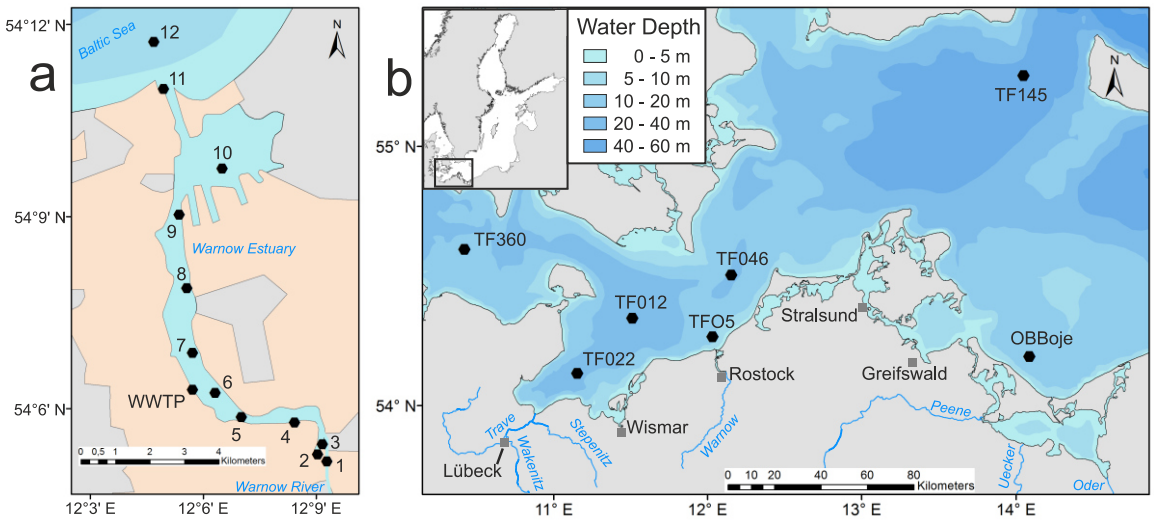

Figure 11 Seawater sampling stations for glyphosate and AMPA in the Warnow Estuary (a) and the Western Baltic Sea (b).

The large-scale method was used to analyze seven surface water samples collected in the Western Baltic Sea (Figure 11). Glyphosate and AMPA were detected in all analyzed samples, especially at stations close to estuaries [see Table S4 and Figure 5 in Wirth et al. (2021)]. The determined glyphosate concentrations were relatively constant between most stations (0.42 - 0.49 ng/L), with an exception of 1.22 ng/L in the Bight of Lübeck, close to the mouth of the river Trave. Highest AMPA concentrations were found close to the Trave, Oder and Warnow Estuary (0.88, 1.42 and 0.97 ng/L, respectively). At stations further offshore, AMPA levels were below the LOQ of 0.31 ng/L. The findings indicate riverine discharge as an important source of glyphosate and AMPA to the marine environment.

To the best of the author's knowledge, the conducted measurements of glyphosate and AMPA in this thesis are the first report on their occurrence in seawater. Previous studies have performed measurements of both compounds in rivers, streams or canals close to the coast but none have expanded their sampling beyond the shore (Aparicio et al., 2013; Masiol et al., 2018; Peruzzo et al., 2008; Ramirez et al., 2014; Skeff et al., 2015). Hence, comparative data for glyphosate and AMPA in the marine environment are currently lacking. The herein determined analyte concentrations in the Warnow Estuary rather compare to the lower previously reported environmental concentrations of glyphosate and AMPA in Europe (Coupe et al., 2012; Huntscha et al., 2018; Masiol et al., 2018; Poiger et al., 2017), showing that the Warnow River is subject to comparatively low levels of pollution. This finding was previously confirmed by Skeff et al. (2015), who measured glyphosate and AMPA levels in the Warnow River that compare well to the herein determined values.

4.5 Environmental Transport, Degradation and Effects of Glyphosate and AMPA (Publication 4 and 5)

The analysis of seawater samples from the Warnow Estuary implied that glyphosate and AMPA are introduced into the aquatic environment from agricultural as well as urban areas. Presumable introduction pathways of both compounds into surface water are precipitation-induced surface runoff, spray drift, discharge from point sources or atmospheric transport through wind (Battaglin et al., 2005; Chang et al., 2011; Payne et al., 1990; Peruzzo et al., 2008; Silva et al., 2018). In contrast, the leaching potential of glyphosate and AMPA through soil is generally considered to be low (Battaglin et al., 2014).

Aspects of the transport and degradation of glyphosate and AMPA in soil were investigated in a lysimeter experiment by Gros et al. (2020). Contributions to this study in the form of glyphosate and AMPA analyses were performed within this thesis [Publication 4]. Maize-cultivated lysimeters were treated with labeled $^{13}C_2$-^{15}N-glyphosate and its degradation and distribution through soil, water and plants was monitored for one hydrological year. No $^{13}C_2$-^{15}N-glyphosate or ^{15}N-AMPA was detected in leachates or subsoil extracts despite high amounts of precipitation, suggesting that vertical transport through the soil column did not occur. In contrast, both compounds could be detected in topsoil extracts, even one year after glyphosate application. This indicates that $^{13}C_2$-^{15}N-glyphosate was strongly bound in the topsoil layer, where

biodegradation to ^{15}N-AMPA took place. The experiment confirmed previous findings of strong glyphosate binding to soil (Borggaard and Gimsing, 2008; Gros et al., 2017), biodegradation to AMPA in soil (Bergstrom et al., 2011; Borggaard and Gimsing, 2008; Tang et al., 2019) and unlikely leaching of glyphosate through the soil column (Battaglin et al., 2014). The results underline that the occurrence of glyphosate and AMPA in the aquatic environment must, thus, mainly be owed to the other above described transport mechanisms.

Biodegradation of glyphosate occurs not only in soil but also in the aquatic environment (Giesy et al., 2000). Evidence for this process in the form of changing AMPA-to-glyphosate ratios (Battaglin et al., 2005) was also found during the herein conducted analysis of environmental samples from the Warnow Estuary and the Western Baltic Sea (Figure 12, Table S3, Table S4).

A more specific investigation into the degradation of glyphosate by a Baltic Sea microbial community and the effect of the herbicide on community structure has been conducted by Janßen et al. (2019). Contributions to this study in the form of glyphosate, AMPA and sarcosine analyses were performed within this thesis [Publication 5]. Microorganisms from the Baltic Sea were incubated in microcosms and subjected to a glyphosate pulse. The measured decrease in glyphosate concentrations together with the occurrence of low concentrations of AMPA and enhanced biomass production confirmed utilization of both compounds by the microbial community. In contrast, no evidence for degradation to the second possible metabolite sarcosine could be found.

AMPA concentrations during the experiment were consistently low (< 1 % of glyphosate concentration), an observation that was also made by Mercurio et al. (2014) in their investigations on glyphosate degradation in seawater. The findings from both experiments point towards preferential metabolization of AMPA compared to glyphosate in seawater. Implications for this phenomenon, which contrasts previously determined degradation patterns in soil (Aparicio et al., 2013; Grunewald et al., 2001), have also been derived from the herein measured environmental concentrations of glyphosate and AMPA (Figure 12, Table S3, Table S4). From station 1 to 7 in the Warnow Estuary, AMPA-to-glyphosate ratios consistently increased, indicating biodegradation of glyphosate to AMPA along the flow path. This trend reversed under increasingly marine conditions and ratios consistently decreased from station 8 to 11 in the Warnow Estuary. This pattern continued into the Baltic Sea and ratios decreased further towards coastal

and offshore stations. The faster decrease of AMPA concentrations compared to glyphosate concentrations, which caused the observed ratio trend, implies more rapid removal of AMPA from marine surface water compared to glyphosate. Elevated biodegradation rates of AMPA are a conceivable explanation for this phenomenon; however, other removal mechanisms, e.g., association with particulate matter could also contribute to the observation.

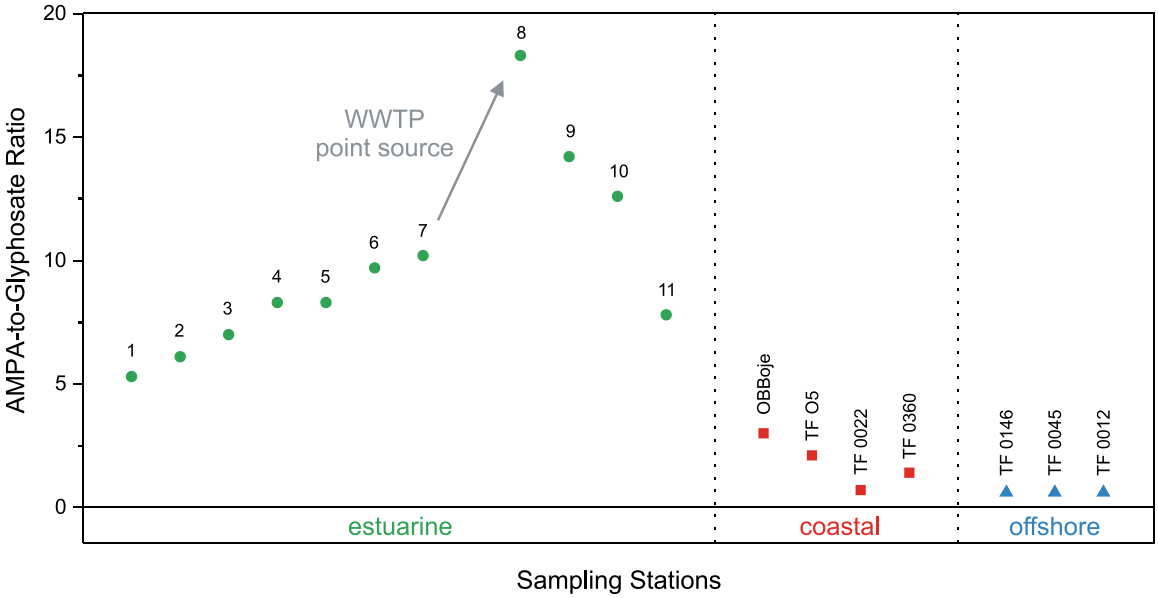

Figure 12 Differences in calculated AMPA-to-glyphosate ratios between sampled estuarine, coastal and offshore stations in the Warnow Estuary and the Western Baltic Sea (see Figure 11 for station locations).

In the microcosm experiment (Janßen et al., 2019), glyphosate was detectable throughout the entire experimental period of 71 days. Hence, it was concluded that low concentrations of glyphosate might persist in seawater, which was also suggested by Mercurio et al. (2014). The relatively constant low levels of glyphosate that were determined at different coastal and offshore stations in the Baltic Sea support this hypothesis (Table S4).

The presence of glyphosate in the microcosm experiment also had an effect on the microbial community structure (Janßen et al., 2019). This reaction of the microorganisms to the herbicide mainly occurred within the first 22 days of the experimental period, when glyphosate concentrations were above 5 µM, i.e., 854 µg/L. The herein determined environmental glyphosate concentrations in the Baltic Sea are in the low ng/L range (Wirth et al., 2021), which is several orders of magnitude lower. This indicates that

microbial communities in the Baltic Sea are unlikely to be directly affected by the herbicide under current conditions. Nonetheless, the possible long-term effects of a chronic low-level pollution with glyphosate are as of yet unknown.

5 Summary and Outlook

This thesis addresses salt-matrix-induced difficulties that arise during the analysis of polar organic trace compounds in seawater. The main focus was the determination of the herbicide glyphosate and its metabolite AMPA in the marine environment, as their hydrophilic character makes these compounds highly susceptible to salt interferences. In addition, an existing analysis procedure for the structurally similar, naturally occurring organophosphonate methylphosphonic acid was adapted towards seawater.

Several different salt matrix effects that occur during sample preparation or instrumental analysis of the analytes as well as possible measures to minimize them were investigated. For this, the desalination technique of electrodialysis was applied to seawater and its potential for the reduction of salt matrix effects was tested.

Electrodialysis was shown to be suitable for the separation of organic compounds and salt ions in seawater, making it a promising tool for the isolation of dissolved organic matter or target compounds. However, partial loss of compounds was found to occur *via* passage of the ED membranes or adsorption to system walls based on analyte physiochemical properties.

The herein analyzed small and charged organophosphonates were sufficiently retained throughout the majority of the ED process but passed through the ED membranes at low residual salinity. Nonetheless, it was shown that seawater desalination with ED can enable the subsequent solid phase extraction of glyphosate, AMPA and methylphosphonic acid with ion exchange resins, which is impossible in untreated seawater due to competition of salt ions and analytes for binding sites on the SPE material. However, especially for glyphosate and AMPA, this approach is associated with high analyte losses and the use of a salt-insensitive molecularly imprinted polymer for their SPE was shown to be more analytically as well as economically feasible. Since a similar material was not available for methylphosphonic acid, the coupling of ED and IER-SPE was necessary in its case. Currently, the main drawbacks of this approach are the high workload and high analysis costs. Therefore, downscaling of the ED system to reduce the required sample volume should be considered in future work in order to enable higher sample throughput and reduced workload and costs.

In addition to sample preparation techniques, the instrumental analysis of organophosphonates could also be improved through salt matrix separation with ED or SPE. Matrix independent measurements were achieved by assuring uniform chromatographic behavior and low matrix effects during LC-MS/MS and GC-MS/MS analysis. Any remaining interferences could be corrected through the use of isotopically labeled internal standards.

Based on the investigations of salt matrix effects, suitable analysis pipelines for glyphosate, AMPA and methylphosphonic acid in seawater were derived. The analysis of methylphosphonic acid in seawater was only conducted with an exemplary sample to prove the applicability of the concept. The analysis of marine water samples with the herein suggested approach should be the subject of future work in order to investigate the role of methylphosphonic acid in the marine environment and in the possible resolution of the methane paradox.

Furthermore, with the herein developed methods, glyphosate and AMPA could be successfully detected in samples from the Baltic Sea. Determined concentrations were between 0.4 and 1.4 ng/L. To the best of the author's knowledge, these data are the first report on the occurrence of glyphosate and AMPA in seawater. The regional concentration patterns suggested preferential metabolization of AMPA compared to glyphosate and possible persistence of glyphosate in the marine environment. However, experiments that investigate these implications in detail will be necessary in the future.

Finally, the developed methods for glyphosate and AMPA analysis were used to contribute to additional experiments on the environmental transport, degradation and effects of glyphosate and AMPA. First, a lysimeter study confirmed unlikely leaching of the analytes through soil and, thus, indicated other transport mechanisms, e.g., surface runoff, for glyphosate and AMPA into the aquatic environment. Secondly, a microcosm experiment indicated that current glyphosate concentrations in the Baltic Sea are unlikely to directly affect the pelagic microbial community. Nonetheless, the possible long-term effects of a chronic pollution with glyphosate are as of yet unknown and should be subject of future studies.

Moreover, since glyphosate has a strong affinity towards particulate matter, the herein developed methods should be expanded from the dissolved to the particulate phase in order to enable investigations of the environmental concentrations, transport and effects of particle-bound glyphosate.

References

Abdullah, M.P., Daud, J., Hong, K.S., Yew, C.H., 1995. Improved method for the determination of glyphosate in water. J. Chromatogr. A, 697: 363-369.

Ansari, S., Karimi, M., 2017. Novel developments and trends of analytical methods for drug analysis in biological and environmental samples by molecularly imprinted polymers. TrAC Trend. Anal. Chem., 89: 146-162.

Aparicio, V.C., De Geronimo, E., Marino, D., Primost, J., Carriquiriborde, P., Costa, J.L., 2013. Environmental fate of glyphosate and aminomethylphosphonic acid in surface waters and soil of agricultural basins. Chemosphere, 93(9): 1866-1873.

Arkan, T., Molnár-Perl, I., 2015. The role of derivatization techniques in the analysis of glyphosate and aminomethyl-phosphonic acid by chromatography. Microchem. J., 121: 99-106.

Bagastyo, A.Y., Anggrainy, A.D., Nindita, C.S., Warmadewanthi, 2017. Electrodialytic removal of fluoride and calcium ions to recover phosphate from fertilizer industry wastewater. Sustain. Environ. Res., 27(5): 230-237.

Battaglin, W.A., Kolpin, D.W., Scribner, E.A., Kuivila, K.M., Sandstrom, M.W., 2005. Glyphosate, other herbicides, and transformation products in Midwestern streams, 2002. J. Am. Water Resour. As.: 323-332.

Battaglin, W.A., Meyer, M.T., Kuivila, K.M., Dietze, J.E., 2014. Glyphosate and Its Degradation Product AMPA Occur Frequently and Widely in U.S. Soils, Surface Water, Groundwater, and Precipitation. J. Am. Water Resour. As., 50: 275-290.

Bell, D.W., Pellechia, P., Chambers, L.R., Longo, A.F., McCabe, K.M., Ingall, E., Benitez-Nelson, C.R., 2017. Isolation and molecular characterization of dissolved organic phosphorus using electrodialysis-reverse osmosis and solution 31 P-NMR. Limnol. Oceanogr. Meth., 15(5): 436-452.

Benbrook, C.M., 2016. Trends in glyphosate herbicide use in the United States and globally. Environ. Sci. Eur., 28(1).

Bergstrom, L., Borjesson, E., Stenstrom, J., 2011. Laboratory and lysimeter studies of glyphosate and aminomethylphosphonic acid in a sand and a clay soil. J. Environ. Qual., 40(1): 98-108.

Borggaard, O.K., Gimsing, A.L., 2008. Fate of glyphosate in soil and the possibility of leaching to ground and surface waters: a review. Pest. Manag. Sci., 64(4): 441-456.

Borjesson, E., Torstensson, L., 2000. New methods for determination of glyphosate and (aminomethyl)phosphonic acid in water and soil. J. Chromatogr. A, 886: 207-216.

Boulard, L., Dierkes, G., Ternes, T., 2018. Utilization of large volume zwitterionic hydrophilic interaction liquid chromatography for the analysis of polar pharmaceuticals in aqueous environmental samples: Benefits and limitations. J. Chromatogr. A, 1535: 27-43.

Chambers, L.R., Ingall, E.D., Saad, E.M., Longo, A.F., Takeuchi, M., Tang, Y., Benitez-Nelson, C., Haley, S.T., Dyhrman, S.T., Brandes, J., Stubbins, A., 2016. Enhanced Dissolved Organic Matter Recovery from Saltwater Samples with Electrodialysis. Aquat. Geochem., 22(5-6): 555-572.

Chang, F.C., Simcik, M.F., Capel, P.D., 2011. Occurrence and fate of the herbicide glyphosate and its degradate aminomethylphosphonic acid in the atmosphere. Environ. Toxicol. Chem., 30(3): 548-555.

Chen, H., Stubbins, A., Perdue, E.M., Green, N.W., Helms, J.R., Mopper, K., Hatcher, P.G., 2014. Ultrahigh resolution mass spectrometric differentiation of dissolved

organic matter isolated by coupled reverse osmosis-electrodialysis from various major oceanic water masses. Mar. Chem., 164: 48-59.

Claude, B., Berho, C., Bayoudh, S., Amalric, L., Coisy, E., Nehme, R., Morin, P., 2017. Preliminary recovery study of a commercial molecularly imprinted polymer for the extraction of glyphosate and AMPA in different environmental waters using MS. Environ. Sci. Pollut. Res. Int., 24(13): 12293-12300.

Corbera, M., Hidalgo, M., Salvadó, V., 2006. Extraction and Preconcentration of the Herbicide Glyphosate and its Metabolite AMPA Using Anion-Exchange Solid Phases. Microchim. Acta, 153(3-4): 203-209.

Corbera, M., Hidalgo, M., Salvadó, V., Wieczorek, P.P., 2005. Determination of glyphosate and aminomethylphosphonic acid in natural water using the capillary electrophoresis combined with enrichment step. Anal. Chim. Acta, 540(1): 3-7.

Coupe, R.H., Kalkhoff, S.J., Capel, P.D., Gregoire, C., 2012. Fate and transport of glyphosate and aminomethylphosphonic acid in surface waters of agricultural basins. Pest. Manag. Sci., 68(1): 16-30.

Demonte, L.D., Michlig, N., Gaggiotti, M., Adam, C.G., Beldomenico, H.R., Repetti, M.R., 2018. Determination of glyphosate, AMPA and glufosinate in dairy farm water from Argentina using a simplified UHPLC-MS/MS method. Sci. Total Environ., 645: 34-43.

Dittmar, T., Koch, B., Hertkorn, N., Kattner, G., 2008. A simple and efficient method for the solid-phase extraction of dissolved organic matter (SPE-DOM) from seawater. Limnol. Oceanogr. Meth., 6: 230-235.

Duke, S.O., Powles, S.B., 2008. Glyphosate: a once-in-a-century herbicide. Pest. Manag. Sci., 64(4): 319-325.

ECHA, 2017. ECHA/PR/17/06: Glyphosate not classified as a carcinogen by ECHA, Helsinki.

Erney, D.R., Gillespie, A.M., Gilvydis, D.M., Poole, C.F., 1993. Explanation of the matrix-induced chromatographic response enhancement of organophosphorus pesticides during open tubular column gas chromatography with splitless or hot on-column injection and flame photometric detection. J. Chromatogr., 638: 57-63.

Fang, N., Yu, S., Ronis, M.J., Badger, T.M., 2015. Matrix effects break the LC behavior rule for analytes in LC-MS/MS analysis of biological samples. Exp. Biol. Med., 240(4): 488-497.

Fisch, K., Waniek, J.J., Schulz-Bull, D.E., 2017. Occurrence of pharmaceuticals and UV-filters in riverine run-offs and waters of the German Baltic Sea. Mar. Pollut. Bull., 124(1): 388-399.

Folmar, L.C., Sanders, H.O., Julin, A.M., 1979. Toxicity of the herbicide glyphosate and several of its formulations to fish and aquatic invertebrates. Arch. Environm. Contain. Toxicol., 8: 269-278.

Gauch, R., Leuenberger, U., Miiller, U., 1989. Bestimmung des Herbicids Glyphosat und dessen Hauptmetabolit Aminomethylphosphons iure (AMPA) in Trinkwasser mit Hilfe der HPLC. Z. Lebensm. Unters. Forsch., 188: 36-38.

Giesy, J.P., Dobson, S., Solomon, K.R., 2000. Ecotoxicological Risk Assessment for Roundup Herbicide. Rev. Environ. Contam. Toxicol., 167: 35-120.

Gill, J.P.K., Sethi, N., Mohan, A., 2016. Analysis of the glyphosate herbicide in water, soil and food using derivatising agents. Environ. Chem. Lett., 15(1): 85-100.

Gosetti, F., Mazzucco, E., Zampieri, D., Gennaro, M.C., 2010. Signal suppression/enhancement in high-performance liquid chromatography tandem mass spectrometry. J. Chromatogr. A, 1217(25): 3929-3937.

Grant, S., Mortimer, M., Stevenson, G., Malcom, D., Gaus, C., 2011. Facilitated Transport of Dioxins in Soil Following Unintentional Release of Pesticide-Surfactant Formulations. Environ. Sci. Technol., 45: 406-411.

Green, N.W., Perdue, E.M., Aiken, G.R., Butler, K.D., Chen, H., Dittmar, T., Niggemann, J., Stubbins, A., 2014. An intercomparison of three methods for the large-scale isolation of oceanic dissolved organic matter. Mar. Chem., 161: 14-19.

Gros, P., Ahmed, A., Kuhn, O., Leinweber, P., 2017. Glyphosate binding in soil as revealed by sorption experiments and quantum-chemical modeling. Sci. Total Environ., 586: 527-535.

Gros, P., Meissner, R., Wirth, M.A., Kanwischer, M., Rupp, H., Schulz-Bull, D.E., Leinweber, P., 2020. Leaching and degradation of (13)C2-(15)N-glyphosate in field lysimeters. Environ. Monit. Assess., 192(2): 127.

Grunewald, K., Schmidt, W., Unger, C., Hanschmann, G., 2001. Behavior of glyphosate and aminomethylphosphonic acid (AMPA) in soils and water of reservoir Radeburg II catchment (Saxony/Germany). J. Plant Nutr. Soil Sci. , 164: 65-70.

Gurtler, B.K., Vetter, T.A., Perdue, E.M., Ingall, E., Koprivnjak, J.F., Pfromm, P.H., 2008. Combining reverse osmosis and pulsed electrical current electrodialysis for improved recovery of dissolved organic matter from seawater. J. Membrane Sci., 323(2): 328-336.

Hanke, I., Singer, H., Hollender, J., 2008. Ultratrace-level determination of glyphosate, aminomethylphosphonic acid and glufosinate in natural waters by solid-phase extraction followed by liquid chromatography-tandem mass spectrometry: performance tuning of derivatization, enrichment and detection. Anal. Bioanal. Chem., 391(6): 2265-2276.

Helms, J.R., Mao, J., Chen, H., Perdue, E.M., Green, N.W., Hatcher, P.G., Mopper, K., Stubbins, A., 2015. Spectroscopic characterization of oceanic dissolved organic matter isolated by reverse osmosis coupled with electrodialysis. Mar. Chem., 177: 278-287.

Hidalgo, C., Rios, C., Hidalgo, M., Salvado, V., Sancho, J.V., Hernandez, F., 2004. Improved coupled-column liquid chromatographic method for the determination of glyphosate and aminomethylphosphonic acid residues in environmental waters. J. Chromatogr. A., 1035(1): 153-157.

Hühnerfuss, H., Kallenborn, R., 1992. Chromatographic separation of marine organic pollutants. J. Chromatogr., 580: 191-214.

Huntscha, S., Stravs, M.A., Buhlmann, A., Ahrens, C.H., Frey, J.E., Pomati, F., Hollender, J., Buerge, I.J., Balmer, M.E., Poiger T., 2018. Seasonal Dynamics of Glyphosate and AMPA in Lake Greifensee: Rapid Microbial Degradation in the Epilimnion During Summer. Environ. Sci. Technol., 52(8): 4641-4649.

IARC, 2015. IARC Monographs Volume 112: evaluation of five organophosphate insecticides and herbicides, International Agency for Research on Cancer.

Ibanez, M., Pozo, O.J., Sancho, J.V., Lopez, F.J., Hernandez, F., 2005. Residue determination of glyphosate, glufosinate and aminomethylphosphonic acid in water and soil samples by liquid chromatography coupled to electrospray tandem mass spectrometry. J. Chromatogr. A., 1081(2): 145-155.

Jacob, G.S., Garbow, J.R., Hallas, L.E., Kimack, N.M., Kishore, G.M., Schaeffer, J., 1988. Metabolism of Glyphosate in Pseudomonas sp. Strain LBr. Appl. Environ. Microbiol., 54(12): 2953-2958.

Janßen, R., Skeff, W., Werner, J., Wirth, M.A., Kreikemeyer, B., Schulz-Bull, D., Labrenz M., 2019. A Glyphosate Pulse to Brackish Long-Term Microcosms Has

a Greater Impact on the Microbial Diversity and Abundance of Planktonic Than of Biofilm Assemblages. Front. Mar. Sci., 6.

Jaworska, J., Van Genderen-Takken, H., Hanstveit, A., van de Plassche, E., Feijtel, T., 2002. Environmental risk assessment of phosphonates, used in domestic laundry and cleaning agents in the Netherlands. Chemosphere, 47: 655-665.

Jiang, J., Lucy, C.A., 2007. Determination of glyphosate using off-line ion exchange preconcentration and capillary electrophoresis-laser induced fluorescence detection. Talanta, 72(1): 113-118.

Jimenez-Skrzypek, G., Gonzalez-Salamo, J., Varela-Martinez, D.A., Gonzalez-Curbelo, M.A., Hernandez-Borges, J., 2020. Analysis of phthalic acid esters in sea water and sea sand using polymer-coated magnetic nanoparticles as extraction sorbent. J. Chromatogr. A, 1611: 460620.

Katagi, T., 2008. Surfactant Effects on Environmental Behavior of Pesticides. In: D.M. Whitacre (Editor), Reviews of Environmental Contamination and Toxicology. Springer Verlag, New York, pp. 71-177.

Kishore, G.M., Jacob, G.S., 1997. Degradation of Glyphosate by Pseudomonas sp. PG2982 via a Sarcosine Intermediate. Appl. Environ. Microbiol., 54(12): 12164-12168.

Kniebusch, M., Meier, H.E.M., Radtke, H., 2019. Changing Salinity Gradients in the Baltic Sea As a Consequence of Altered Freshwater Budgets. Geophys. Res. Let., 46(16): 9739-9747.

Kock-Schulmeyer, M., Postigo, C., Farre, M., Barcelo, D., Lopez de Alda, M., 2019. Medium to highly polar pesticides in seawater: Analysis and fate in coastal areas of Catalonia (NE Spain). Chemosphere, 215: 515-523.

Koprivnjak, J.F., Pfromm, P.H., Ingall, E., Vetter, T.A., Schmitt-Kopplin, P., Hertkorn, N., Frommberger, M., Knicker, H., Perdue, E.M., 2009. Chemical and spectroscopic characterization of marine dissolved organic matter isolated using coupled reverse osmosis–electrodialysis. Geochim. Cosmochim. Acta, 73(14): 4215-4231.

Küsters, M., Gerhartz, M., 2010. Enrichment and low-level determination of glyphosate, aminomethylphosphonic acid and glufosinate in drinking water after cleanup by cation exchange resin. J. Sep. Sci., 33: 1139-1146.

Le Fur, E., Colin, R., Charrêteur, C., Dufau, C., Péron, J.J., 2000. Determination of glyphosate herbicide and aminomethylphosphonic acid in natural waters by liquid chromatography using pre-column fluorogenic labeling. Part I: Direct determination at the 0.1 μg/L level using FMOC. Analusis, 28(9): 813-818.

Lohrer, C., Cwierz, P.P., Wirth, M.A., Schulz-Bull, D.E., Kanwischer, M., 2020. Methodological aspects of methylphosphonic acid analysis: Determination in river and coastal water samples. Talanta, 211: 120724.

Lund-Hoie, K., Friestad, H.O., 1986. Photodegradation of the Herbicide Glyphosate in Water. Bull. Environ. Contam. Toxicol., 36: 723-729.

Magi, E., Di Carro, M., 2018. Marine environment pollution: The contribution of mass spectrometry to the study of seawater. Mass. Spectrom. Rev., 37(4): 492-512.

Mallat, E., Barcelo, D., 1998. Analysis and degradation study of glyphosate and of aminomethylphosphonic acid in natural waters by means of polymeric and ion exchange solid-phase extraction columns followed by ion chromatography–post-column derivatization with fluorescence detection. J. Chromatogr. A, 823: 129-136.

Mao, J., Kong, X., Schmidt-Rohr, K., Pignatello, J.J., Perdue, E.M., 2012. Advanced solid-state NMR characterization of marine dissolved organic matter isolated

using the coupled reverse osmosis/electrodialysis method. Environ. Sci. Technol., 46(11): 5806-5814.

Masiol, M., Gianni, B., Prete, M., 2018. Herbicides in river water across the northeastern Italy: occurrence and spatial patterns of glyphosate, aminomethylphosphonic acid, and glufosinate ammonium. Environ .Sci. Pollut. Res. Int., 25(24): 24368-24378.

McGrath, J.W., Chin, J.P., Quinn, J.P., 2013. Organophosphonates revealed: new insights into the microbial metabolism of ancient molecules. Nat. Rev. Microbiol., 11(6): 412-419.

Mercurio, P., Flores, F., Mueller, J.F., Carter, S., Negri, A.P., 2014. Glyphosate persistence in seawater. Mar. Pollut. Bull., 85(2): 385-390.

Metcalf, W.W., Griffin, B.M., Cicchillo, R.M., Gao, J., Janga, S.C., Cooke, H.A., Circello, B.T., Evans, B.S., Martens-Habbena, W., Stahl, D.A., van der Dook, W.A., 2012. Synthesis of Methylphosphonic Acid by Marine Microbes: A Source for Methane in the Aerobic Ocean. Science, 337: 1104-1107.

Minor, E.C., Swenson, M.M., Mattson, B.M., Oyler, A.R., 2014. Structural characterization of dissolved organic matter: a review of current techniques for isolation and analysis. Environ. Sci.: Proc. Imp., 16(9): 2064-2079.

Montiel-León, J.M., Munoz, G., Duy, S.V., Do, D.T., Vaudreuil, M.-A., Goeury, K., Guillemette, F., Amyot, M., Sauvé, S., 2019. Widespread occurrence and spatial distribution of glyphosate, atrazine, 2 and neonicotinoids pesticides in the St. Lawrence and tributary rivers. Environ. Pollut., 250: 29-39.

Mopper, K., Stubbins, A., Ritchie, J.D., Bialk, H.M., Hatcher, P.G., 2007. Advanced Instrumental Approaches for Characterization of Marine Dissolved Organic Matter: Extraction Techniques, Mass Spectrometry, and Nuclear Magnetic Resonance Spectroscopy. Chem. Rev., 107: 419-442.

Mörtl, M., Németh, G., Jurascek, J., Darvas, B., Kamp, L., Rubio, F., Székács, A., 2013. Determination of glyphosate residues in Hungarian water samples by immunoassay. Microchem. J., 107: 143-151.

Nowack, B., 2003. Environmental chemistry of phosphonates. Wat. Res., 37(11): 2533-2546.

Okada, E., Allinson, M., Barral, M.P., Clarke, B., Allinson, G., 2020. Glyphosate and aminomethylphosphonic acid (AMPA) are commonly found in urban streams and wetlands of Melbourne, Australia. Water Res., 168: 115139.

Pan, S., Chen, X., Li, X., Jin, M., 2019. Nonderivatization method for determination of glyphosate, glufosinate, bialaphos, and their main metabolites in environmental waters based on magnetic metal-organic framework pretreatment. J. Sep. Sci., 42(5): 1045-1050.

Panuwet, P., Hunter, R.E. Jr., D'Souza, P.E., Chen, X., Radford, S.A., Cohen, J.R., Marder, M.E., Kartavenka, K., Ryan, P.B., Barr, D.B., 2016. Biological Matrix Effects in Quantitative Tandem Mass Spectrometry-Based Analytical Methods: Advancing Biomonitoring. Crit. Rev. Anal. Chem., 46(2): 93-105.

Patsias, J., Papadopoulou, A., Papadopoulou-Mourkidou, E., 2001. Automated trace level determination of glyphosate and aminomethyl phosphonic acid in water by on-line anion-exchange solid-phase extraction followed by cation-exchange liquid chromatography and post-column derivatization. J. Chromatogr. A, 932: 83-90.

Payne, N.J., Feng, J.C., Reynolds, P.E., 1990. Off-target Deposits and Buffer Zones Required around Water for Aerial Glyphosate Applications. Pestic. Sci, 30: 183-198.

Peruzzo, P.J., Porta, A.A., Ronco, A.E., 2008. Levels of glyphosate in surface waters, sediments and soils associated with direct sowing soybean cultivation in north pampasic region of Argentina. Environ. Pollut., 156(1): 61-66.

Poiger, T., Buerge, I.J., Balmer, M.E., Bächli, A., Müller, M.D., 2017. Occurrence of the herbicide glyphosate and its metabolite AMPA in surface waters in Switzerland determined with on-line solid phase extraction LC-MS/MS. Environ. Sci. Pollut. Res., 24: 1588-1596.

Puzio, K., Claude, B., Amalric, L., Berho, C., Grellet, E., Bayoudh, S., Nehme, R., Morin, P., 2014. Molecularly imprinted polymer dedicated to the extraction of glyphosate in natural waters. J. Chromatogr. A, 1361: 1-8.

Ramirez, C.E., Bellmund, S., Gardinali, P.R., 2014. A simple method for routine monitoring of glyphosate and its main metabolite in surface waters using lyophilization and LC-FLD+MS/MS. Case study: canals with influence on Biscayne National Park. Sci. Total Environ., 496: 389-401.

Rapp, H.-J., 2006. Elektrodialyse. In: K. Ohlrogge and K. Ebert (Editors), Membranen: Grundlagen, Verfahren und industrielle Anwendungen. Wiley VCH Verlag GmbH & Co. KGaA, Weinheim, pp. 429-452.

Repeta, D.J., 2015. Chemical Characterization and Cycling of Dissolved Organic Matter. In: D.A. Hansell and C.A. Carlson (Editors), Biogeochemistry of Marine Dissolved Organic Matter. Elsevier, pp. 21-63.

Richmond, M.E., 2018. Glyphosate: A review of its global use, environmental impact, and potential health effects on humans and other species. J. Environ. Stud. Sci., 8: 416-434.

Rigobello-Masini, M., Pereira, E.A.O., Abate, G., Masini, J.C., 2019. Solid-Phase Extraction of Glyphosate in the Analyses of Environmental, Plant, and Food Samples. Chromatographia, 82(8): 1121-1138.

Royer, A., Beguin, S., Tabet, J.C., Hulot, S., Reding, M.A., Communal, M.Y., 2000. Determination of Glyphosate and Aminomethylphosphonic Acid Residues in Water by Gas Chromatography with Tandem Mass Spectrometry after Exchange Ion Resin Purification and Derivatization. Application on Vegetable Matrixes. Anal. Chem., 72: 3826-3832.

Rueppel, M.L., Brightwell, B.B., Schaefer, J., Marvel, J.T., 1977. Metabolism and Degradation of Glyphosate in Soil and Water. J. Agric. Food Chem., 25(3): 517-528.

Ruiz-Toledo, J., Castro, R., Rivero-Perez, N., Bello-Mendoza, R., Sanchez, D., 2014. Occurrence of glyphosate in water bodies derived from intensive agriculture in a tropical region of southern Mexico. Bull. Environ. Contam. Toxicol., 93(3): 289-293.

Sanchís, J., Kantiani, L., Llorca, M., Rubio, F., Ginebreda, A., Fraile, J., Garrido, T., Farré, M., 2012. Determination of glyphosate in groundwater samples using an ultrasensitive immunoassay and confirmation by on-line solid-phase extraction followed by liquid chromatography coupled to tandem mass spectrometry. Anal. Bioanal. Chem., 402: 2335-2345.

Sancho, J.V., Hernandez, F., Lopez, F.J., Hogendoorn, E.A., Dijkman, E., van Zoomen, P., 1996. Rapid determination of glufosinate, glyphosate and aminomethylphosphonic acid in environmental water samples using precolumn fluorogenic labeling and coupled-column liquid chromatography. J. Chromatogr. A, 737: 75-83.

Sillanpää, M., Shestakova, M., 2017. Electrochemical Water Treatment Methods. Elsevier Butterworth-Heinemann.

Silva, V., Montanarella, L., Jones, A., Fernandez-Ugalde, O., Mol, H.G.J., Ritsema, C.J., Geissen V., 2018. Distribution of glyphosate and aminomethylphosphonic acid (AMPA) in agricultural topsoils of the European Union. Sci. Total Environ., 621: 1352-1359.

Silvestro, L., Tarcomnicu, I., Rizea, S., 2013. Matrix Effects in Mass Spectrometry Combined with Separation Methods — Comparison HPLC, GC and Discussion on Methods to Control these Effects. In: A. Varela Coelho and C. De Matos Ferraz Franco (Editors), Tandem Mass Spectrometry - Molecular Characterization. IntechOpen, pp. 33-37.

Singh, V., Chinthakindi, S., Purohit, A.K., Pardasani, D., Tak, V., Dubey, D.K., 2015. Single vial sample preparation of markers of nerve agents by dispersive solid-phase extraction using magnetic strong anion exchange resins. J. Chromatogr. A, 1395: 48-56.

Skeff, W., Neumann, C., Schulz-Bull, D.E., 2015. Glyphosate and AMPA in the estuaries of the Baltic Sea method optimization and field study. Mar. Pollut. Bull., 100(1): 577-585.

Skeff, W., Recknagel, C., Schulz-Bull, D.E., 2016. The influence of salt matrices on the reversed-phase liquid chromatography behavior and electrospray ionization tandem mass spectrometry detection of glyphosate, glufosinate, aminomethylphosphonic acid and 2-aminoethylphosphonic acid in water. J. Chromatogr. A, 1475: 64-73.

Stachowski-Haberkorn, S., Becker, B., Marie, D., Haberkorn, H., Coroller, L., de la Broise D., 2008. Impact of Roundup on the marine microbial community, as shown by an in situ microcosm experiment. Aquat. Toxicol., 89(4): 232-241.

Steffen, W., Persson, A., Deutsch, L., Zalasiewicz, J., Williams, M., Richardson, K., Crumley, C., Crutzen, P., Folke, C., Gordon, L., Molina, M., Ramanathan, V., Rockstrom, J., Scheffer, M., Schellnhuber, H.J., Svedin, U., 2011. The anthropocene: from global change to planetary stewardship. Ambio, 40(7): 739-761.

Steinmann, H.H., Dickeduisberg, M., Theuvsen, L., 2012. Uses and benefits of glyphosate in German arable farming. Crop Prot., 42: 164-169.

Steinrücken, H.C., Amrhein, N., 1980. The herbicide glyphosate is a potent inhibitor of 5-enolpyruvylshikimic acid-3-phosphate synthase. Biochem. Biophys. Res. Comm., 94(4): 1207-1212.

Strathmann, H., 2010. Electrodialysis, a mature technology with a multitude of new applications. Desalination, 264(3): 268-288.

Tang, F.H.M., Jeffries, T.C., Vervoort, R.W., Conoley, C., Coleman, N.V., Maggi, F., 2019. Microcosm experiments and kinetic modeling of glyphosate biodegradation in soils and sediments. Sci. Total Environ., 658: 105-115.

Tarazona, J.V., Court-Marques, D., Tiramani, M., Reich, H., Pfeil, R., Istace, F., Crivellente, F., 2017. Glyphosate toxicity and carcinogenicity: a review of the scientific basis of the European Union assessment and its differences with IARC. Arch. Toxicol., 91(8): 2723-2743.

Ternon, E., Wang, Y., Coyne, K.J., 2018. Small Polar Molecules: A Challenge in Marine Chemical Ecology. Molecules, 24(1).

Toss, V., Leito, I., Yurchenko, S., Freiberg, R., Kruve, A., 2017. Determination of glyphosate in surface water with high organic matter content. Environ. Sci. Pollut. Res. Int., 24(9): 7880-7888.

Trufelli, H., Palma, P., Famiglini, G., Cappiello, A., 2011. An overview of matrix effects in liquid chromatography mass spectrometry. Mass. Spectrom. Rev., 30: 491-509.

Tsui, M.T.K., Chu, L.M., 2003. Aquatic toxicity of glyphosate-based formulations: comparison between different organisms and the effects of environmental factors. Chemosphere, 52(7): 1189-1197.

Valle, A.L., Mello, F.C.C., Alves-Balvedi, R.P., Rodrigues, L.P., Goulart, L.R., 2018. Glyphosate detection: methods, needs and challenges. Environ. Chem. Lett., 17(1): 291-317.

van Leeuwen, S.P., Swart, C.P., van der Veen, I., de Boer, J., 2009. Significant improvements in the analysis of perfluorinated compounds in water and fish: results from an interlaboratory method evaluation study. J. Chromatogr. A, 1216(3): 401-409.

Vera, M.S., Lagomarsino, L., Sylvester, M., Perez, G.L., Rodriguez, P., Mugni, H., Sinistro, R., Ferraro, M., Bonetto, C., Zagarese, H., Pizarro, H., 2010. New evidences of Roundup (glyphosate formulation) impact on the periphyton community and the water quality of freshwater ecosystems. Ecotoxicology, 19(4): 710-721.

Vetter, T., Perdue, E., Ingall, E., Koprivnjak, J., Pfromm, P., 2007. Combining reverse osmosis and electrodialysis for more complete recovery of dissolved organic matter from seawater. Separ. Purif. Technol., 56(3): 383-387.

Walker, B.D., Beaupré, S.R., Guilderson, T.P., Druffel, E.R.M., McCarthy, M.D., 2011. Large-volume ultrafiltration for the study of radiocarbon signatures and size vs. age relationships in marine dissolved organic matter. Geochim. Cosmochim. Acta, 75(18): 5187-5202.

Wang, S., Liu, B., Yuan, D., Ma, J., 2016. A simple method for the determination of glyphosate and aminomethylphosphonic acid in seawater matrix with high performance liquid chromatography and fluorescence detection. Talanta, 161: 700-706.

Wille, K., Vanden Bussche, J., Noppe, H., De Wulf, E., Van Caeter, P., Janssen, C.R., De Brabander, H.F., Vanhaecke, L., 2010. A validated analytical method for the determination of perfluorinated compounds in surface-, sea- and sewagewater using liquid chromatography coupled to time-of-flight mass spectrometry. J. Chromatogr. A, 1217(43): 6616-6622.

Wirth, M.A., Schulz-Bull, D.E., Kanwischer, M., 2021. The challenge of detecting the herbicide glyphosate and its metabolite AMPA in seawater – Method development and application in the Baltic Sea. Chemosphere, 262: 128327.

Wirth, M.A., Sievers, M., Habedank, F., Kragl, U., Schulz-Bull, D.E., Kanwischer, M., 2019. Electrodialysis as a sample processing tool for bulk organic matter and target pollutant analysis of seawater. Mar. Chem., 217: 103719.

Xu, D., Li, Y., Yin, L., Ji, Y., Niu, J., Yu, Y., 2018. Electrochemical removal of nitrate in industrial wastewater. Front. Env. Sci. Eng., 12(1).

Yang, X., Wang, F., Bento, C.P.M., Xue, S., Gai, L., van Dam, R., Mol, H., Ritsema, C.J., Geissen, V., 2015. Short-term transport of glyphosate with erosion in Chinese loess soil--a flume experiment. Sci. Total Environ., 512-513: 406-414.

Young, C.L., Ingall, E.D., 2010. Marine Dissolved Organic Phosphorus Composition: Insights from Samples Recovered Using Combined Electrodialysis/Reverse Osmosis. Aquat. Geochem., 16(4): 563-574.

Zahn, D., Meusinger, R., Fromel, T., Knepper, T.P., 2019. Halomethanesulfonic Acids-A New Class of Polar Disinfection Byproducts: Standard Synthesis, Occurrence, and Indirect Assessment of Mitigation Options. Environ. Sci. Technol., 53(15): 8994-9002.

Appendix

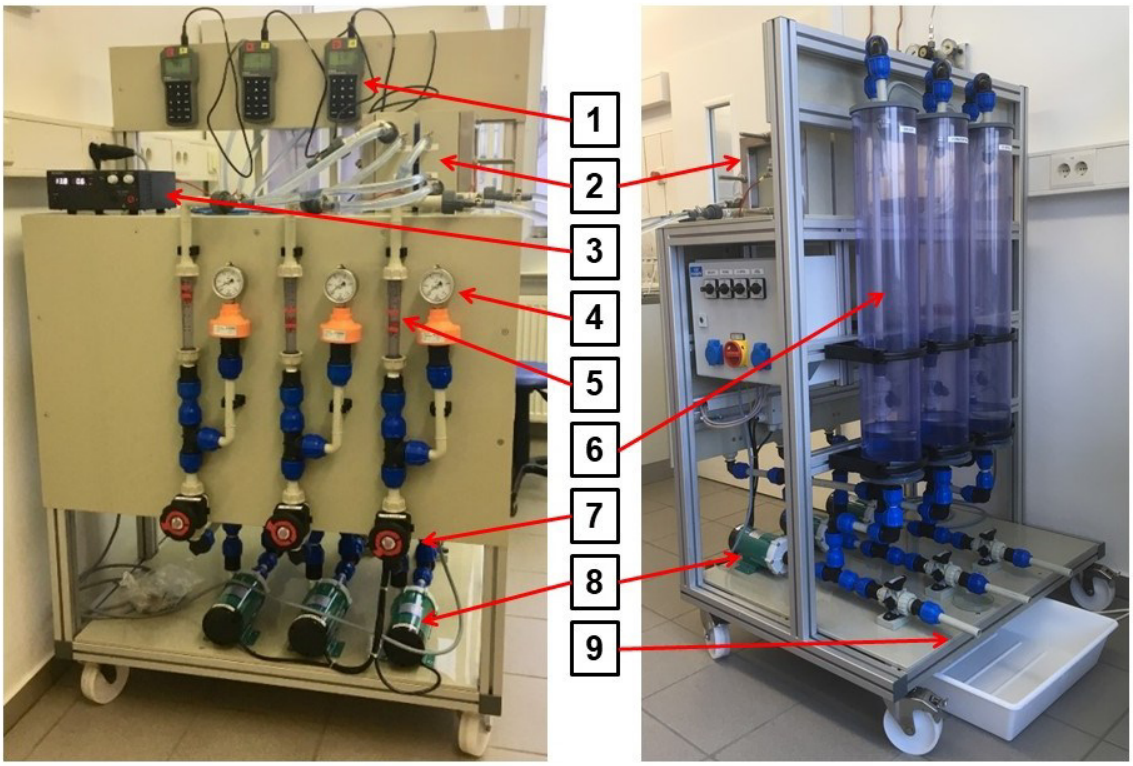

Figure S1 Photographs of the utilized electrodialysis system. 1: conductivity meter, 2: electrodialysis cell, 3: laboratory power supply, 4: barometer, 5: flowmeter, 6: tanks for diluate, concentrate and electrode rinse (left to right), 7: diaphragm valve, 8: magnetic centrifugal pumps, 9: outlet for sampling and draining (reproduced from the Supplementary Material of Publication 1).

Table S1 Physiochemical properties of glyphosate, AMPA and methylphosphonic acid (MPn).

Parameter	Glyphosate	AMPA	MPn
Molecular Formula	$C_3H_8NO_5P$	CH_6NO_3P	CH_5O_3P
Structural Formula	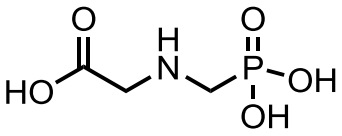	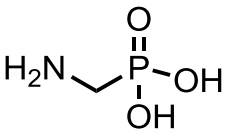	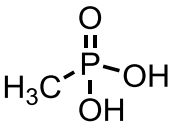
Molecular Weight	169.07 g/mol	111.04 g/mol	96.06 g/mol
Water Solubility	10 g/L	50 g/L	20 g/L
log K_{OW}	-3.40	-1.43	-2.02
Dissociation Constants	pKa_1 2.0 pKa_2 2.6 pKa_3 5.6 pKa_4 10.6	pKa_1 1.8 pKa_2 5.4 pKa_3 10.0	pKa_1 2.1 pKa_2 7.3
Main Charge at pH 7	-2	-1	-1
Structural Formula at pH 7	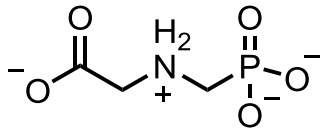	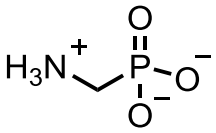	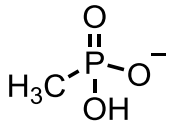

Table S2 LC-retention times of glyphosate and AMPA after sample derivatization at different salinities and subsequent SPE cleanup. Errors represent standard deviations from triplicate experiments. (reproduced from the Supplementary Material of Publication 2).

Sample Salinity	Retention Time [min]	
	Glyphosate	**AMPA**
10	9.04 ± 0.012	9.45 ± 0.007
6	9.06 ± 0.005	9.46 ± 0.006
3	9.04 ± 0.007	9.45 ± 0.002
0.5	9.04 ± 0.008	9.45 ± 0.004
0.2	9.04 ± 0.007	9.45 ± 0.007
0.1	9.03 ± 0.000	9.45 ± 0.002
ultrapure water	9.03 ± 0.005	9.44 ± 0.005

Table S3 List of sampling stations in the Warnow Estuary (reproduced from the Supplementary Material of Publication 2). Samples were collected in September 2019.

Station	Lat.	Long.	T in °C	Salinity	Glyphosate [ng/L]	AMPA [ng/L]	$R_{A/G}$
1	54.0833	12.1553	15.3	4.64	26.0	137.0	5.3
2	54.0852	12.1513	15.1	1.69	28.0	171.5	6.1
3	54.0878	12.1536	15.2	2.17	26.1	181.5	7.0
4	54.0938	12.1417	15.4	9.94	13.8	114.9	8.3
5	54.0958	12.1183	15.7	13.43	13.4	111.3	8.3
6	54.1024	12.1071	15.5	11.66	11.2	108.2	9.7
7	54.1131	12.0979	15.6	12.47	11.3	115.6	10.2
8	54.1300	12.0966	15.7	12.77	11.4	208.2	18.3
9	54.1492	12.0947	15.8	13.34	13.4	189.7	14.2
10	54.1607	12.1146	15.7	14.59	<LOQ	100.6	12.6
11	54.1821	12.0901	15.4	16.38	<LOQ	62.1	7.8
12	54.1945	12.0868	15.6	16.26	<LOD	<LOD	-
WWTP	54.1035	12.0972	17.3	9.82	105.9	2633.5	24.9

Lat. Latitude

Long. Longitude

T Temperature

$R_{A/G}$ AMPA-to-Glyphosate Ratio

$$R_{A/G} = \frac{c_{AMPA}}{c_{Glyphosate}}$$

*Ratios were only calculated when both analytes were > LOD. When analytes were < LOQ, the mean value between LOD and LOQ was used as an approximation.

Table S4 List of sampling stations in the Western Baltic Sea (reproduced from the Supplementary Material of Publication 2). Samples were collected in July 2019.

Station	Lat.	Long.	T in °C	Salinity	Glyphosate [ng/L]	AMPA [ng/L]	$R_{A/G}$
Stations close to the coast							
OB Boje	54.0844	14.1497	20.6	7.74	0.47	1.42	3.0
TF O5	54.2317	12.0750	16.1	10.95	0.47	0.97	2.1
TF 022	54.1100	11.1750	20.3	11.28	1.22	0.88	0.7
TF 360	54.6000	10.4500	21.3	13.05	0.43	0.61	1.4
Stations further offshore							
TF 012	54.3150	11.5500	18.9	9.11	0.42	<LOQ	0.6
TF 046	54.4667	12.2167	19.5	7.99	0.49	<LOQ	0.6
TF 145	55.1667	14.2500	19.7	7.82	0.44	<LOQ	0.6

Lat. Latitude

Long. Longitude

T Temperature

$R_{A/G}$ AMPA-to-Glyphosate Ratio

$$R_{A/G} = \frac{c_{AMPA}}{c_{Glyphosate}}$$

*Ratios were only calculated when both analytes were > LOD. When analytes were < LOQ, the mean value between LOD and LOQ was used as an approximation.

Equations

- Absolute Matrix Effect

$$ME_{abs}\ (\%) = 100 \cdot \left(\frac{M_A}{S_A} - 1\right) \qquad \text{(Equation S1)}$$

M_A	peak area of target analyte in water of different salinity
S_A	peak area of target analyte in ultrapure water

- Effective Matrix Effect

$$ME_{eff}(\%) = 100 \cdot \left(\frac{\frac{M_A}{M_{IS}}}{\frac{S_A}{S_{IS}}} - 1\right) \qquad \text{(Equation S2)}$$

M_A	peak area of target analyte in water of different salinity
S_A	peak area of target analyte in ultrapure water
M_{IS}	peak area of internal standard in water of different salinity
S_{IS}	peak area of internal standard in ultrapure water

Publication 1

Electrodialysis as a sample processing tool for bulk organic matter and target pollutant analysis of seawater

by

Marisa A. Wirth, Moritz Sievers, Friederike Habedank, Udo Kragl, Detlef E. Schulz-Bull, Marion Kanwischer

Marine Chemistry

Year 2019, Volume 217, Page 103719 ff.

DOI: 10.1016/j.marchem.2019.103719

Marine Chemistry 217 (2019) 103719

Contents lists available at ScienceDirect

Marine Chemistry

journal homepage: www.elsevier.com/locate/marchem

Electrodialysis as a sample processing tool for bulk organic matter and target pollutant analysis of seawater

M.A. Wirth[a,*], M. Sievers[a], F. Habedank[b], U. Kragl[c,d], D.E. Schulz-Bull[a], M. Kanwischer[a]

[a] Leibniz Institute for Baltic Sea Research Warnemünde, Department of Marine Chemistry, Seestraße 15, 18119 Rostock, Germany
[b] State Office for Agriculture, Food Safety and Fisheries Rostock, Thierfelderstraße 18, 18059 Rostock, Germany
[c] University of Rostock, Institute of Chemistry, Albert-Einstein-Str. 3a, 18059 Rostock, Germany
[d] Faculty for Interdisciplinary Research, Department Life, Light & Matter, University of Rostock, 18051 Rostock, Germany

ARTICLE INFO

Keywords:
Electrodialysis
Seawater analysis
Salt matrix
Natural organic matter
Pesticides

ABSTRACT

Electrodialysis (ED) is an advancing seawater sample processing tool that enables the separation of analytes from the often interfering salt matrix. In this study, we present the evaluation of a laboratory scale ED system for both dissolved organic matter (DOM) and target pollutant analysis of seawater.

The developed sample processing protocol yields reproducible data and was found to be robust towards moderate changes in sample composition. At the final salinity of 0.1, the average recovery of DOM in the form of dissolved organic carbon, nitrogen and phosphorus (DOC, DON and DOP) was 44, 53 and 89%, respectively. DOM loss occurred mainly in the late stage of the ED process.

When investigating specific ED processing parameters, it was discovered that the initial sample salinity does not influence DOM recovery. The final salinity, by contrast, is a dominant influence factor on DOM recovery. Furthermore, DOC and DOP recoveries could be improved by 8% by refining the electrical current in the ED cell. Surprisingly, adjustments of the sample pH did not lead to any improvements in DOM recovery.

The experiments with target analytes showed that the recovery of individual molecules is determined by their *n*-octanol water partition coefficients $\log K_{ow}$. High recoveries > 80% were achieved for compounds with medium $\log K_{ow}$ of −1 to 3. Hydrophobic compounds with $\log K_{ow} > 3$ were lost through surface adsorption to the system walls and tubing. Small, polar and charged compounds with $\log K_{ow} < -1$ are prone to loss via ED membrane passage, which occurred predominantly in the late stage of the ED process. Consequently, sample processing with ED was deemed beneficial for the LC-MS or GC–MS analysis of polar target compounds, because they are often difficult to enrich from seawater. Furthermore, during LC-MS or GC–MS analyses, matrix-dependent ion suppression was reduced in ED isolates, giving rise to increased signal responses of 25 to 620%, which resulted in improved instrumental sensitivity.

1. Introduction

Dissolved organic compounds in the marine environment constitute a complex pool of matter that is continuously influenced and transformed through terrestrial and atmospheric interactions as well as biogeochemical cycling (Moran et al., 2016; Ridgwell and Arndt, 2015). In the past decades, there have been numerous versatile efforts to characterize this dissolved organic matter (DOM) pool (Minor et al., 2014; Mopper et al., 2007; Nebbioso and Piccolo, 2013; Repeta, 2015; Seidel et al., 2017), since it is vital for our understanding of dynamics and drivers of biogeochemical processes and their interrelationships on different spatial and temporal scales. Moreover, in the era of rapidly increasing world population and industrialization, research on the anthropogenic influence on marine DOM brought on by climate change and pollution becomes increasingly important (Porcal et al., 2009; Remucal, 2014; Wenk et al., 2011; Zhuang and Yang, 2018).

DOM can be characterized trough a multitude of different approaches that range from comprehensive to selective techniques. An overview of the DOM characteristics can be gained by analyzing the bulk elemental composition in the form of dissolved organic carbon (DOC), nitrogen (DON) and phosphorus (DOP) (Hansell et al., 2009; Letscher et al., 2013; McGill, 1964) or carbon and nitrogen isotope signatures (Sanderman et al., 2009). The molecular characterization of DOM can be carried out by investigating functional group abundances, e.g. with nuclear magnetic resonance (NMR) or Fourier transform infrared- (FTIR) spectroscopy (Abdulla et al., 2010; Helms et al., 2015),

* Corresponding author.
E-mail address: marisa.wirth@io-warnemuende.de (M.A. Wirth).

https://doi.org/10.1016/j.marchem.2019.103719
Received 27 May 2019; Received in revised form 9 September 2019; Accepted 14 September 2019
Available online 31 October 2019

compound class distributions, e.g. with high resolution mass spectrometry (HRMS) (Chen et al., 2014), or the concentrations of single target compounds (amino acids, sugars, lipids etc.) (Kaiser and Benner, 2012; Meyers-Schulte and Hedges, 1986; Panagiotopoulos et al., 2013; Wakeham et al., 2003; Yamashita and Tanoue, 2003). Traditionally, compounds of anthropogenic origin, e.g. pollutants, are not considered during DOM analysis; however, they have become part of the natural DOM pool and are usually analyzed with the same target methodological approaches as natural compounds.

To date, the bulk elemental composition of DOM (DOC, DON and DOP) has been subject to several studies carried out across the globe (Hansell et al., 2009; Hansell et al., 2012; Karl and Björkman, 2015; Letscher et al., 2013; McGill, 1964; Sipler and Bronk, 2015). Molecular characterization of DOM has been less comprehensive, which is mainly owed to its complexity and the large number of individual compounds within the DOM pool (Hertkorn et al., 2008). Nonetheless, as a result of promising analytical advances, for example in the fields of HRMS (Helms et al., 2015; Seidel et al., 2017), NMR- (Mao et al., 2012; Young and Ingall, 2010), FTIR (Abdulla et al., 2010; Sleighter et al., 2008) or UV/VIS (Helms et al., 2008; Macdonald and Minor, 2013) spectroscopy, it was recently estimated that 60–70% of DOM has undergone some form of structural characterization (Repeta, 2015).

When aiming for a molecular characterization of DOM, researchers are faced with the task of isolating and concentrating DOM, to make it accessible to the respective analysis techniques. The separation from the salt matrix present in seawater usually poses the major challenge, since salt concentrations outweigh DOM concentrations by several orders of magnitude (Minor et al., 2014; Repeta, 2015). For spectroscopic or spectrometric analysis, salt removal is necessary, because relatively pure DOM isolates are required for a successful analysis. Several different techniques for DOM isolation have been introduced; however, they usually induce an isolation bias (Repeta, 2015). Solid phase extraction (SPE) recovers all components of DOM that can be adsorbed to the employed sorbent. This usually is the hydrophobic fraction of DOM (Dittmar et al., 2008; Li et al., 2017; Wünsch et al., 2018). Common sorbents are based on octadecyl-bonded silica (C-18), cross-linked polystyrene (XAD) or styrene-divinylbenzene (PPL) (Mopper et al., 2007). Ultrafiltration recovers all DOM components larger than the pore size of the utilized membrane. Therefore, DOM isolates obtained via ultrafiltration usually contain the high molecular weight fraction of DOM (Panagiotopoulos et al., 2013; Walker et al., 2011). However, some low molecular weight compounds can also be recovered through adsorption to the membrane, which is commonly made of cellulose or polysulone (Repeta, 2015).

A relatively novel approach for the isolation of DOM is the use of electrodialysis (ED) (Gurtler et al., 2008; Sillanpää and Shestakova, 2017; Vetter et al., 2007). An ED cell consists of alternatingly positioned anion- and cation exchange membranes between a set of electrodes. The sample (diluate) and a receiving solution (concentrate) are circulated through the alternating interspaces between the membranes. An electric field is applied perpendicular to the membrane surfaces, which causes salt ions in the diluate to be transported through the membranes and into the concentrate. A third solution (electrode rinse) is circulated along the electrodes to carry off oxygen and hydrogen gas formed due to water splitting at the electrodes.

ED is commonly used in drinking water production and industrial processes (Sillanpää and Shestakova, 2017), but it has only found limited application in environmental sciences, so far. ED was first used for the isolation of DOM coupled to a reverse osmosis (RO) unit (Bell et al., 2017; Gurtler et al., 2008; Vetter et al., 2007). With this technique, DOM can be simultaneously isolated and concentrated with recoveries ranging from 40 up to 95% (Chambers et al., 2016). ED/RO isolates of DOM were shown to usually be representative of the source material and highly suitable for analysis with NMR or HRMS techniques (Bell et al., 2017; Chen et al., 2014; Koprivnjak et al., 2009; Young and Ingall, 2010). This highlights that the isolation bias of ED/RO is greatly reduced in comparison to SPE or ultrafiltration techniques. Nonetheless, both the loss of hydrophobic DOM compounds due adsorption to membranes or system walls and the loss of hydrophilic compounds due to membrane passage at lowered salt concentrations were shown to occur during ED/RO (Bell et al., 2017; Chambers et al., 2016; Koprivnjak et al., 2009; Vetter et al., 2007). Chambers et al. (2016) showed that ED can also be used on a smaller scale without an RO unit. They concentrated DOM from ED-processed samples with lyophilization.

In addition to its benefits in bulk analysis, we hypothesized that ED could also be useful for target analysis of compounds in the marine environment. Such compounds are often analyzed with liquid or gas chromatography coupled to tandem mass spectrometry (LC-MS/MS or GC–MS/MS) (Bjorklund et al., 2016; Habedank et al., 2017; Koponen et al., 2015; Skeff et al., 2015). However, since the concentration of many target analytes in seawater lies well below instrumental limits of detection (LOD), analyte enrichment is required. For polar compounds, SPE is commonly used in this step (Fisch et al., 2017; Hanke et al., 2008; Svahn and Björklund, 2019). However, the salt matrix in seawater can also significantly hinder the SPE enrichment of polar target analytes due to competition of salt and analytes for binding sites on the solid phase (Corbera et al., 2005; Lohrer et al., 2019).

The aim of the current study was to evaluate a newly set up laboratory scale electrodialysis system as a pre-processing tool for bulk and target analysis of seawater. The removal of the salt matrix in the form of many major seawater ions was examined. Moreover, the recovery of DOM in the form of DOC, DON and DOP was investigated. The influence of initial salinity, supplied current and sample pH on recoveries was tested. Finally, the retention of many different target compounds, mainly pesticides, covering a broad range of $\log K_{ow}$ values was investigated in order to assess the suitability of ED for coupling to target analyses with LC-MS/MS and GC–MS/MS.

2. Material and methods

2.1. Chemicals

Purified water (18.2 MΩ) was obtained through a MilliQ IQ 7000 system from Merck Millipore (Schwalbach, Germany). Artificial sea salt (Tropic Marin Sea Salt Classic) was purchased from Tropic Marin AG (Hünenberg, Switzerland). Sodium sulphate and sodium hydroxide were obtained from Merck (Darmstadt, Germany). 5 M NaOH was prepared with MilliQ water. Hydrochloric acid (Normapur, 32% and Titrinorm, 5 M) was purchased from VWR (Darmstadt, Germany). The 32% HCl was used to prepare pH 2 HCl with MilliQ water.

2.2. Electrodialysis system

The herein used ED system was constructed by Deukum GmbH (Frickenhausen, Germany). Photographs of the system are provided in the Supplement (Fig. S1). The ED cell contains a type 100 quadro membrane stack with 10 cell pairs of anion and cation exchange membranes with an effective membrane surface of 1000 cm^2. The system is further equipped with 10 L polyethylene tanks for diluate (sample), concentrate and electrode rinse solutions. The solutions are circulated in the system with magnetic centrifugal pumps (Iwaki MD-30RZM from Iwaki Europe GmbH, Willich, Germany). The minimal volume required for stable circulation is 1.5 L. The required electric current is provided by a laboratory power supply (Voltcraft DPPS-32-15 from Conrad Electronic SE, Hirschau, Germany). The conductivity in diluate, concentrate and electrode rinse was monitored with portable conductivity and temperature probes (HI98192 from Hanna Instruments, Vöhringen, Germany). Since conductivity is temperature dependent and the sample temperature usually rose around 5 °C during an ED run, the probes were set to compensate for temperature change with a reference temperature of 25 °C. The pH in the diluate was

measured with an inoLab720 pH probe from WTW (Weilheim, Germany), which also corrects for temperature change with a reference temperature of 25 °C. The conductivity and pH probes were calibrated weekly.

2.3. System operation

If not in use, the ED system was filled with MilliQ water. To prevent growth in the system, all exposed tanks and tubing were covered with UV-tight foil during storage. To conduct an ED run, the tanks were filled with the required solutions. The concentrate was a 0.2 g/L salt solution prepared with artificial sea salt in MilliQ water. The electrode rinse was a 5 g/L Na_2SO_4 solution prepared in MilliQ water. During an ED run, the diluate and concentrate were circulated in the system at a flow rate of 50 L/h, while the electrode rinse was circulated at 125 L/h. To assure that the pressure difference between the channels never exceeded the tolerable 0.2 bar difference specified by the manufacturer, the volumes of diluate and concentrate were identical. The electrode rinse volume was always 10 L.

Desalination of the diluate is achieved through the electric field provided by the laboratory power supply. It was operated in the constant current mode. Over the course of the ED run, the current was adjusted so that it never exceeded 80% of the limiting current. Above the limiting current, the ED process becomes diffusion limited, since the transport of ions into the boundary layer is then slower compared to the ion transport through the ED membranes (Káňavová and Machuča, 2014; Lee et al., 2006). Water splitting at the membrane surfaces follows, leading to pH changes and potential damage to the system. The limiting current for the herein used ED system was previously determined following the method from Cowan and Brown (1959). At low salinity, the limiting current can be difficult to determine (Chambers et al., 2016). Therefore, the current was set to the minimally adjustable value of 0.1 A below a diluate conductivity of 0.5 mS/cm. Despite this, the diluate pH usually started to decrease below a diluate conductivity of 1 mS/cm due to exceeding of the limiting current. It was found that this decrease became substantial below 0.2 mS/cm. As a consequence, sample processing was not carried out below this point and 0.2 mS/cm was chosen as the lowest possible end point for ED experiments.

During an ED run, the diluate conductivity decreases and the concentrate conductivity increases. On order to maintain the concentration gradient along the membrane stack, ~80% of the concentrate (dependent on the total concentrate volume) was replaced with MilliQ water, whenever concentrate conductivity was 2 mS/cm above diluate conductivity (Chambers et al., 2016). Since the diluate volume decreased when samples were taken, the total concentrate volume was also adjusted during these concentrate exchanges to assure similar volumes in both channels.

2.4. Standard sample processing protocol

For sample processing, the system was carefully cleaned and conditioned before the ED run. The sample processing and cleaning protocols were developed based on Chambers et al. (2016) and Bell et al. (2017). All three channels first received a 5 min rinse with 2 L MilliQ water. Afterwards, the diluate channel was rinsed with 2 L of pH 2 HCl for at least 5 min. The channel was then flushed with MilliQ water until neutral pH was obtained. To save time, this pre-cleaning was usually done the night before sample processing. Directly before sample processing, all three channels received a 5 min rinse with 2 L of MilliQ water. The diluate channel was rinsed two more times with the same procedure. The third rinse solution from the diluate channel was sampled after circulation to obtain blank samples. Blanks were analyzed for the same parameters measured during the ED run (e.g. DOC, DON, DOP or target analytes). Finally, the system was conditioned with 2 L of the sample that was to be processed. The sample was circulated in the diluate channel for 7 min (entire volume circulated thrice).

Afterwards, the tanks were filled with the solutions for the ED run. The diluate volume was set so that after all samples were taken, the volume was still > 3 L. This resulted in initial volumes of 6–8 L. The concentrate volume was chosen accordingly. The solutions were circulated in the system until the entire sample volume was circulated thrice (e.g. 21 min for 6 L sample). Before the electric current was switched on, “start” samples were taken. The sample in the diluate channel was then processed from its initial conductivity (~15–20 mS/cm) down to a final conductivity of 0.2 mS/cm (see above for details on system operation and settings). Conductivity and temperature in all three channels as well as pH in the diluate channel were continuously monitored. Subsamples from the diluate tank were taken at conductivities of 15, 10, 5, 2.5, 1, 0.5 and 0.2 mS/cm (“end”). At 25 °C, this corresponds to salinities (S) of 8.7, 5.6, 2.7, 1.3, 0.5, 0.2 and 0.1. After the “end” subsamples were taken, the current was switched off, the solutions were drained from the system and their final volume was measured.

For the post-cleaning procedure, all three channels were rinsed three times with 2 L of MilliQ water for 5 min. Occasionally, the first rinse from the diluate channel was sampled as well to check for remaining organic matter. Finally, the diluate channel was again rinsed with 2 L of pH 2 HCl for at least 5 min and afterwards flushed with MilliQ water until neutral pH was obtained.

If not stated otherwise, subsamples taken during the ED run were stored frozen at −20 °C until analysis.

2.5. Environmental sampling

Coastal seawater for the ED experiments was collected from the Baltic Sea in Heiligendamm in Mecklenburg-Western Pomerania, Germany (54°08′46.7″N, 11°50′36.1″E) between March and September 2018 to test the system on samples with different characteristics. Surface water samples were taken at the head of the pier, which extends ~160 m into the sea. Water temperature and conductivity/salinity were simultaneously measured at the surface. The samples were collected in pre-cleaned 10 or 20 L polyethylene canisters (Hünersdorff GmbH, Ludwigsburg, Germany). An overview of all collected samples and their use is given in Table S1.

Samples were transported to the lab, filtered over precombusted GF/F filters (Ø 47 mm, 0.7 µm; Whatman GmbH, Dassel, Germany) and stored at 4 °C in the dark. The samples were processed with the ED system within the following three days.

2.6. Bulk and target analysis of subsamples

Detailed information on the analysis of bulk organic matter (DOC, DON, DOP), inorganic seawater ions (major metal ions, phosphate, sulphate, nitrate, nitrite, silicate) and target analytes is provided in the Supplement (Tables S2, S3, S4, S6).

2.7. Quality assurance

To assure that the ED system is free of contamination, blank samples were taken before each run. Reproducibility of the ED process was assessed though the triplicate processing of a single sample.

During all bulk and target analyses, blanks and control standards were run alongside the samples. Moreover, an appropriate number of replicates were conducted for each measured parameter (Table S2).

2.8. Data treatment

The sample volume was found to decrease by ~0.2–0.4 L during an ED run due to transport of small amounts of water through the membranes. From visual observations, it was found that this occurred predominately in the first half of the ED run. Consequently, the theoretical sample volume was corrected based on the following equation, which

assumes that water loss occurs twice as fast in the first half of the ED run compared to second half:

if $t_i < t_{tot}/2$:

$$V_{cor,i} = V_{theo,i} - t_i \cdot \frac{V_{lost} \cdot 2/3}{t_{tot}/2} \quad (1)$$

if $t_i > t_{tot}/2$:

$$V_{cor,i} = V_{theo,i} - V_{lost} \cdot 2/3 - (t_i - t_{tot}/2) \cdot \frac{V_{lost} \cdot 1/3}{t_{tot}/2} \quad (2)$$

with t_i = time at point i [min], t_{tot} = total runtime [min], $V_{cor,i}$ = corrected sample volume at point i [L], $V_{theo,i}$ = theoretical sample volume at point i [L] and V_{lost} = total sample volume lost during the run [L].

Recoveries of bulk organic matter or target analytes were calculated using the determined concentrations and the sample volume, which was corrected for water loss and subsample removal:

$$Rec_i\ [\%] = \frac{c_i \cdot (V_{cor,i} + \sum_{n=1}^{i-1} V_{sam,n})}{c_1 \cdot V_{cor,1}} \cdot 100 \quad (3)$$

with c_i = concentration at point i [mol/L or g/L], $V_{cor,i}$ = corrected sample volume at point i [L], $V_{sam,n}$ = volume of subsample taken at point n [L], c_1 = initial concentration [mol/L or g/L], $V_{cor,1}$ = initial sample volume [L].

No blanks were subtracted for the calculation of the recovery, because blank values for all utilized data were below the limit of quantification (LOQ). All data and calculated recoveries are presented as average ± standard deviation of the conducted replicates.

3. Results

3.1. Removal of the inorganic seawater matrix

For a comprehensive understanding of the utilized electrodialysis system, the removal of the inorganic seawater matrix was analyzed. For this, ED was conducted and subsamples were analyzed for a selection of inorganic seawater ions (n = 4, Fig. 1, Tables S1, S6).

The initial concentrations of the analyzed matrix components showed variation below 20%, except for phosphate, whose concentration in surface water varied between 0.03 and 0.43 µmol/L depending on the season (Table S2).

At the final salinity (S) of 0.1, the majority of analyzed components were removed to below 1% of their initial concentration (Fig. 1). This finding was independent of the chosen ED settings (e.g. initial salinity, pH, supplied current; data not shown). However, the recovery curves differed among the individual matrix components. Removal of the analyzed metal ions was determined, on the one hand, by their charge and, on the other hand, by their size. Hence, twice charged ions were eliminated faster than those of single charge. For ions of the same charge, the higher the effective ion radius $r_{eff,aq}$ (Nightingale, 1959), the faster the loss from the seawater samples.

The bulkier phosphate and sulphate (measured as sulphur) ions were generally removed slower than the analyzed metal ions. The majority of phosphate was not lost until S < 2. Among the considered matrix components, silicon, which is present in seawater mainly in the form of silicic acid (Brzezinski and Nelson, 1986), is the only component that showed minimal loss during ED processing.

3.2. Recovery of bulk organic matter

The retention of bulk organic matter in the form of DOC, DON and DOP was investigated by processing several Baltic Sea water samples with the electrodialysis system (n = 4, Table S1). In comparison with previously investigated sites (Bell et al., 2017; Chambers et al., 2016; Chen et al., 2014; Young and Ingall, 2010), the brackish Baltic Sea has lower salinity and higher organic matter content. The investigated sampling station in Heiligendamm can be highly variable in terms of

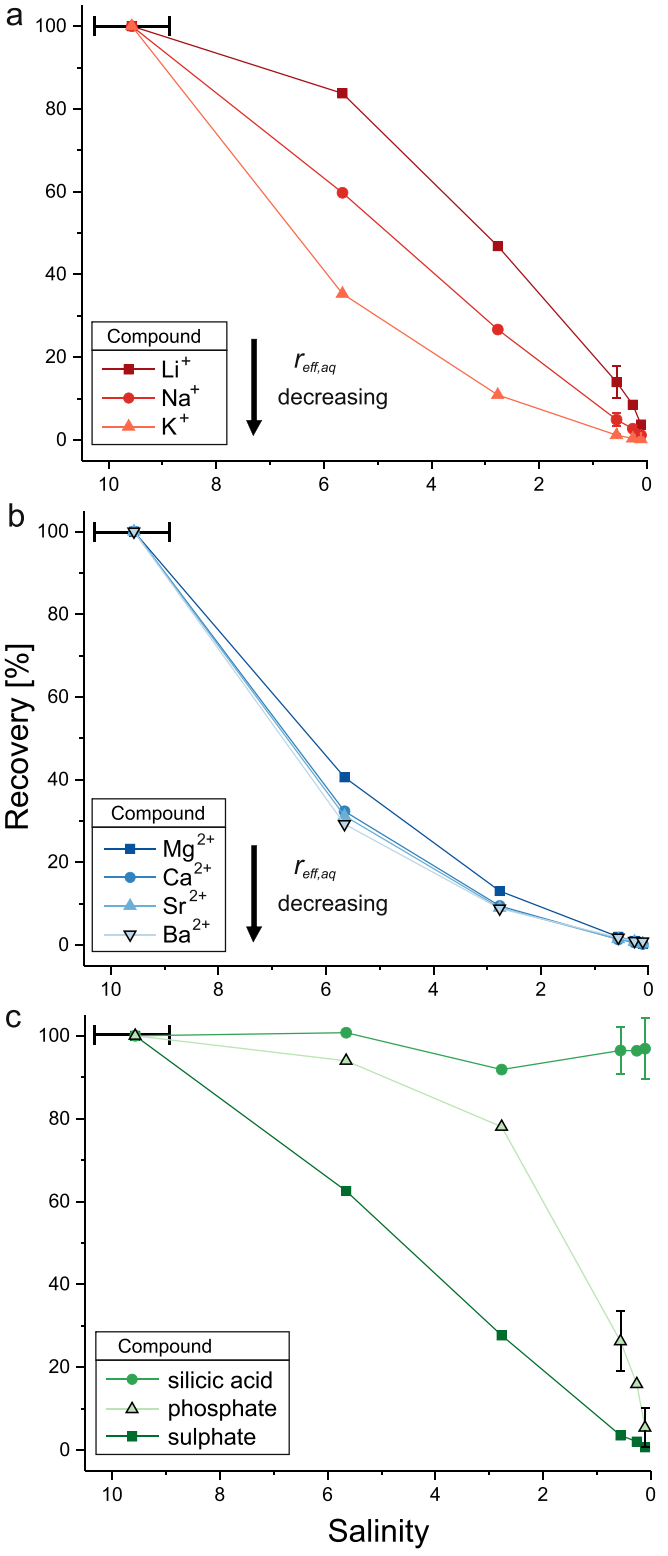

Fig. 1. Recovery of the analyzed inorganic seawater matrix components during ED (n = 4). Many vertical error bars are too small to be visible. The depicted initial salinity is the average initial salinity. The bold horizontal error bar shows the range of initial salinities of the processed samples. (a) Single positively charged metal ions, (b) twice positively charged metal ions and (c) sulphate (measured as S), phosphate and silicic acid (measured as Si).

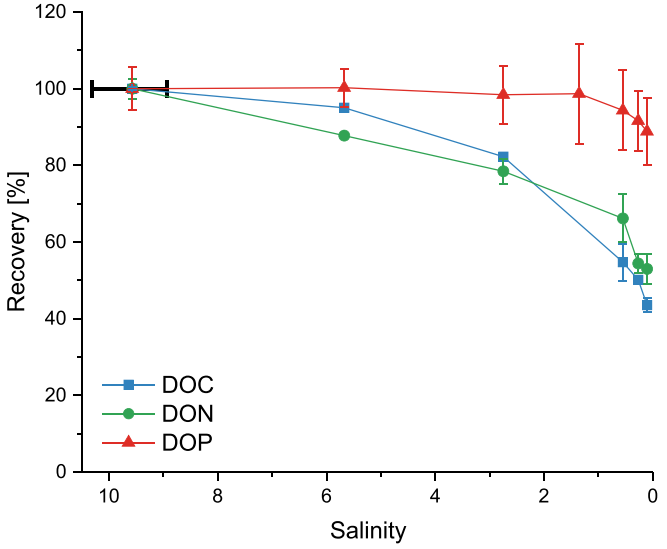

Fig. 2. Average recoveries of DOC, DON and DOP during desalination of Baltic Sea water samples (n = 4). The depicted initial salinity is the average initial salinity. The bold horizontal error bar shows the range of initial salinities of the processed samples.

salinity (S = 8–20) as well as nutrient and DOM concentration, dependent on the season and weather conditions (Naumann et al., 2018).

In our samples, the initial DOM concentrations were 326.7 ± 9.9, 19.2 ± 1.5 and 0.48 ± 0.02 µmol/L for DOC, DON and DOP, respectively. Bulk organic matter loss occurred mainly in the late stage of the ED process, with the loss rate increasing with decreasing salinity (Fig. 2). At S = 2.7, average recoveries were still 82, 78 and 98% for DOC, DON and DOP; however, at S = 0.1, average recoveries decreased to 44, 53 and 89%, respectively.

Overall, DOC and DON recoveries were similar. Therefore, the C/N ratios of the samples only changed moderately, from 14.7 ± 1.4 at the start to 12.1 ± 0.7 at the end of the ED process. This indicates that processed samples were representative of the source water in terms of organic carbon and nitrogen content, as was found by previously conducted studies (Chambers et al., 2016; Green et al., 2014). However, an isolation bias towards phosphorus-containing molecules was apparently present in our samples, as is evident from the much higher DOP recoveries (Fig. 2). In our experiments, DOP was only lost from the samples below S = 2. As a result, the C/P ratios of the samples decreased substantially, from 268.6 ± 11.4 (start) to 131.3 ± 4.9 (end). When conducting comparative measurements of DOC and DOP recoveries in an ED/RO system, Bell et al. (2017) also found differences between the two parameters. Possible reasons for the discrepancies are discussed below.

The reproducibility of ED experiments was investigated via (1) the triplicate processing of the same sample and (2) comparisons between different samples. The triplicate investigation of DOC, DON and DOP recovery showed good reproducibility, with RSDs of 6.3, 7.2 and 8.8%, respectively. The variation between different samples was also low, with 1.9, 3.9 and 8.7% RSD for DOC, DON and DOP, respectively. This indicates that the selected ED processing protocol is robust towards moderate changes in sample composition.

3.3. Influence of ED processing parameters on the recovery of DOM

In order to test how bulk organic matter recovery can be improved, the influence of discrete electrodialysis processing parameters was investigated, i.e. the initial salinity of the water sample, the supplied current and the sample pH. For these experiments, an aliquot of a Baltic Sea water sample was first processed according to the standard processing protocol. Afterwards, the remaining aliquot(s) were processed with the influence parameter in question changed (Table S1).

The effect of the initial salinity of the water sample on the recovery of bulk organic matter was analyzed by artificially increasing the salinity of the sample from 8.8 to 13.1 through the addition of artificial sea salt. The experimental data showed that the bulk organic matter recovery at a particular salinity is identical, regardless of the initial salinity of the sample (Table 1b). This indicates that the initial salinity is irrelevant for the achieved final recovery. This finding is supported by the fact that our DOM recoveries from brackish water (S = 9–12) were in the same range as recoveries achieved from coastal water (S = 18–28) (Bell et al., 2017) or open ocean saltwater (S = 35) (Chambers et al., 2016; Chen et al., 2014). The final sample salinity after ED-processing, by contrast, seems to be a dominant influence factor (Table 1), because DOM loss occurred predominately in the late stage of the ED process. This implies that care must be taken when comparing DOM recoveries from different studies, because the final salinities sometimes vary substantially (Bell et al., 2017; Chambers et al., 2016; Gurtler et al., 2008; Vetter et al., 2007).

Table 1
Recovery of bulk organic matter during various ED experiments with Baltic Sea water. Recoveries are shown for two discrete salinities (S = 0.5 and 0.1), which were sampled during the same respective ED experiment. DOP data for the "supplied current" and "sample pH" experiments are not shown, because they did not meet the set quality control standards (see Supplement for details). However, since DOP recoveries were generally high, a repetition of the experiments was abstained from.

Experiment		Salinity	Recovery [%]		
			DOC	DON	DOP
a) Reproducibility	Replicate 1	0.1	45.6 ± 0.5	48.0 ± 3.2	86.8 ± 10.7
	Replicate 2		45.8 ± 0.6	55.4 ± 1.9	103.6 ± 4.0
	Replicate 3		40.9 ± 0.5	52.2 ± 0.3	94.9 ± 1.8
b) Initial salinity	S_{start} 8.8	0.5	57.1 ± 0.1	64.2 ± 3.3	97.3 ± 1.3
	S_{start} 13.1		55.7 ± 0.3	62.3 ± 0.7	95.6 ± 5.8
	S_{start} 8.8	0.1	44.3 ± 0.2	52.3 ± 1.1	91.4 ± 3.3
	S_{start} 13.1		45.0 ± 0.1	53.3 ± 0.3	88.9 ± 4.3
c) Supplied current	80% I_{lim}	0.5	48.1 ± 0.3	58.8 ± 1.5	–
	50% I_{lim}		56.4 ± 1.2	66.8 ± 1.8	–
	80% I_{lim}	0.1	43.0 ± 0.5	54.7 ± 0.8	–
	50% I_{lim}		43.8 ± 0.1	55.7 ± 3.9	–
d) Sample pH	pH 7	0.5	54.6 ± 0.4	73.7 ± 1.8	–
	pH 4		57.8 ± 0.6	76.2 ± 3.6	–
	pH 10		56.3 ± 0.4	61.4 ± 3.4	–
	pH 7	0.1	41.3 ± 0.3	56.8 ± 1.3	–
	pH 4		41.2 ± 0.5	51.7 ± 0.3	–
	pH 10		42.4 ± 0.1	48.3 ± 2.4	–

The influence of the supplied current was investigated by reducing the applied current from 80% to 50% of the limiting current (I_{lim}) below S = 2.7. Additionally, the voltage was limited to 5 V below S = 0.5. These adjustments led to an increase of DOC and DON recoveries by approx. 8% at S = 0.5 (Table 1c). Nonetheless, at the end of the ED run, at S = 0.1, recoveries were similar, regardless of the supplied current. Moreover, reducing the applied current led to an increased processing time of 30 min.

The recovery of bulk organic matter was also studied when the ED process was conducted at varying sample pH. If left unadjusted, sample pH changed slightly during ED experiments. It increased by 0.20 ± 0.04 pH units (n = 9) during desalination to S = 2.7 and, thereafter, it decreased by 0.55 ± 0.13 pH units due to exceeding of the limiting current at low sample salinity (Bell et al., 2017). The pH of acidified/alkalized water samples changes towards 7 during the ED process, especially at low salinity, because the added acid or base is removed in the ED cell. As a consequence, the pH needs to be readjusted regularly, if constant pH during the ED process is required.

In our experiments, we maintained a sample pH of 4, 7 or 10 through the addition of 5 M HCl or NaOH throughout the ED process. DOC recoveries were similar at pH 4, 7 and 10, meaning that sample pH did not affect DOC recovery (Table 1d). DON recovery was also similar at pH 4 and 7, but slightly lower DON recovery at pH 10 compared to pH 7 was observed.

3.4. Recovery of target analytes

The recovery of a total of 271 environmentally relevant target analytes, mainly pesticides, was analyzed during electrodialysis experiments. A Baltic Sea water sample was spiked with the various compounds at concentrations that assure detection with the respective analysis method (Table S4). The analytes had molecular weights between 96 and 732 Da. The spiked sample was processed with ED in triplicate and subsamples for the respective target analyses were taken. Only those analytes, which (1) showed < 10% RSD for the triplicates, and (2) did not show concentration increases of > 10% during ED, were considered for further evaluation (n = 184). Since the recovery of the target analytes was found to correlate with their *n*-octanol water partition coefficients $logK_{ow}$ (Fig. 3), the selection of compounds was further limited to those, for which an experimentally determined $logK_{ow}$ could be found in the literature (n = 103, Table S4).

Highest recoveries were found for compounds with a $logK_{ow}$ between −1 and 3. For these analytes, observed recoveries were usually above 80%. This indicates that, for our selection of target compounds, those in the described $logK_{ow}$ range are favorably retained in our ED system. For hydrophilic target analytes with $logK_{ow}$ below −1, recoveries decreased approximately linearly with decreasing $logK_{ow}$ (Fig. 3). Many compounds in this $logK_{ow}$ range are negatively charged at pH 7. The twice negatively charged compounds had a lower $logK_{ow}$ and, consequently, lower recoveries than the single negatively charged ones. The lowest determined recovery in this range was 26.6% for glyphosate ($logK_{ow}$ = −3.40). Similarly, for more hydrophobic compounds with $logK_{ow}$ above 3, recoveries also decreased approximately linearly with increasing $logK_{ow}$ (Fig. 3). The lowest determined recovery in this range was 21.2% for 2,4,6-tribromoanisole ($logK_{ow}$ = 4.48).

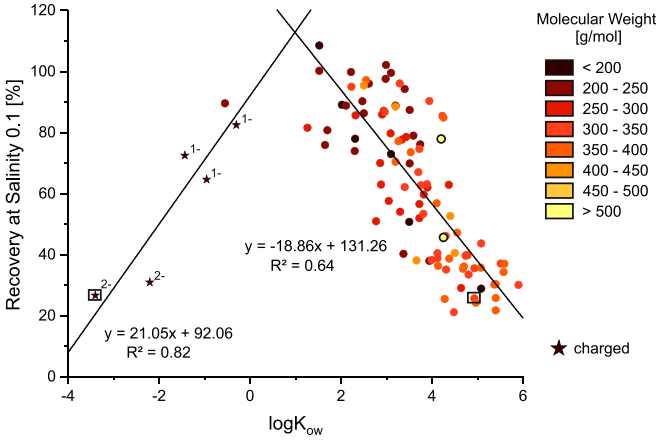

Fig. 3. Correlation between the recovery of target analytes at S = 0.1 and their *n*-octanol water partition coefficient $logK_{ow}$. The individual data points are color-coded according to the compounds' molecular weight. The stars mark charged compounds at pH 7; the adjacent numbers state the respective charge. The data points in boxes mark glyphosate (left) and buprofezin (right), for which the recovery curves are depicted in Fig. 4.

For the analyzed pool of target compounds, the molecular weight was apparently not a dominant influence factor on recovery in the ED system (Fig. 3).

The course of the target compound recovery during the electrodialysis process differed for analytes of high and low $logK_{ow}$ (Fig. 4), suggesting that different mechanisms drove analyte loss in both cases. For hydrophilic compounds in the low $logK_{ow}$ range, e.g. glyphosate (Fig. 4a), loss occurred predominately in the late stage of the ED process; for hydrophobic compounds in the high $logK_{ow}$ range, i.e. buprofezin (Fig. 4b), loss occurred throughout the entire ED process. In the case of glyphosate, the salinity-dependent recovery follows a logarithmic trend below S = 2.7, corresponding to increasing loss rates with decreasing salinity. In contrast, the salinity-dependent recovery of buprofezin follows a linear trend. It will be discussed below that a time-dependent depiction might be more suitable for hydrophobic compounds. The recovery of buprofezin decreases exponentially with time.

During the analysis of target analyte recovery in the ED system, another interesting advantage of sample desalination was discovered. Among the originally targeted compounds, there were 21 that could not be evaluated in the above context, because strong matrix-dependent ion suppression in the mass spectrometers was observed (Table S5). For these compounds, signal response was low in the early stage of the ED process, but with removal of the matrix, the signal response increased by 25 to 620% (Fig. 5, Table S5). This shows that through the removal of the salt matrix, the sensitivity and, thus, the LOD of LC-MS- or GC–MS-based analysis methods can be significantly improved.

4. Discussion

4.1. Analyte recovery during ED – loss mechanisms and influence factors

In general, different mechanisms through which the loss of organic and inorganic compounds from a sample in an electrodialysis system occurs can be described. On the one hand, compounds can transfer through the ion exchange membranes and into the concentrate solution; on the other hand, compounds can adsorb to membrane surfaces and system walls. In the first case, the respective molecules/ions (1) have to be transported into the boundary layer at the membrane surface and (2) need to be able to pass through the membrane pores. The former can occur either though diffusion or active migration driven by the electric field. Therefore, compounds that are prone to be lost via this mechanism would be charged and easily migrate through the ED membranes. Size certainly plays a decisive role in this process; however, other factors like the current density, solution pH and individual molecular properties are of influence, as well (Bell et al., 2017; Zhang et al., 2011). For our utilized membranes, permeability should be given for molecules below 200 Da, as specified by the manufacturer. Loss of compounds via adsorption to system surfaces is determined by the utilized materials, because surface adsorption is dependent on the affinity and steric fit between functional groups of the adsorbent and the material surface. The walls and tubing of the herein used ED system are made of different types of plastic and should, therefore, predominantly

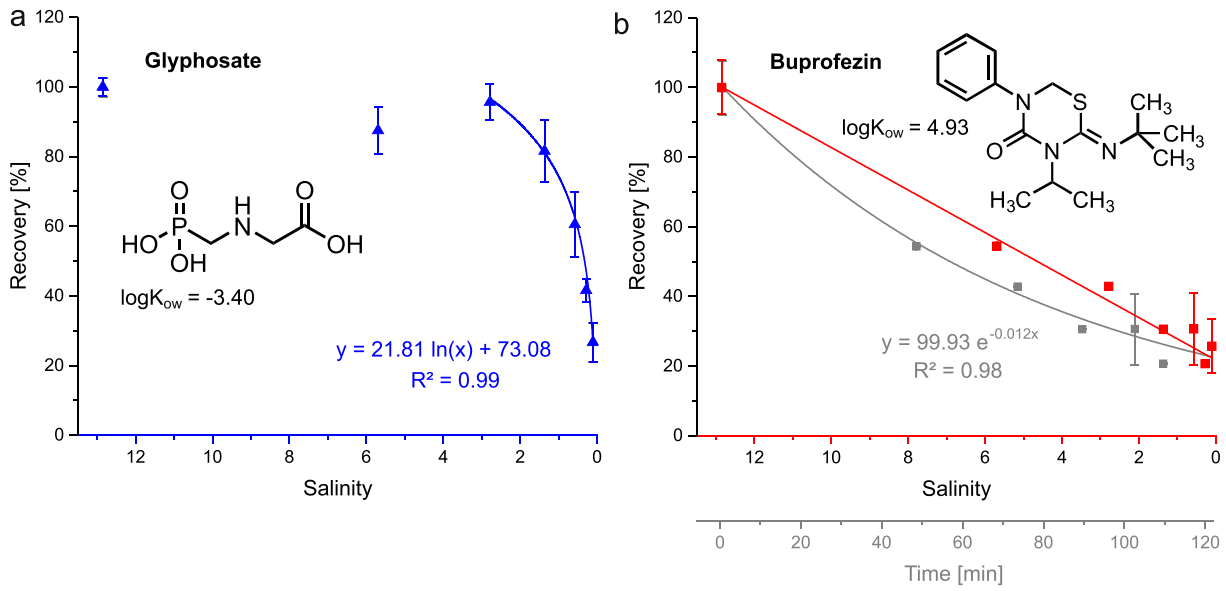

Fig. 4. Course of target compound recovery with decreasing sample salinity for two exemplary compounds with high and low logK$_{ow}$, (a) glyphosate (logK$_{ow}$ = −3.40; n = 3); (b) buprofezin (logK$_{ow}$ = 4.31; n = 1, except at S = 12.9, 0.5 and 0.1: n = 3). For buprofezin, the time-dependent recovery is also depicted.

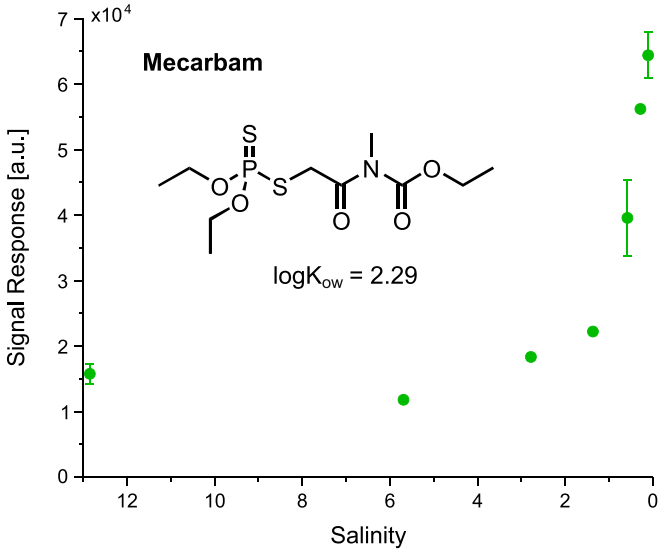

Fig. 5. Salinity-dependent LC-MS/MS signal response of the target analyte mecarbam (n = 1, except at S = 12.9, 0.5 and 0.1: n = 3). Due to strong matrix-dependent ion suppression, signal response was low in the early stage of the ED process, but increased strongly with removal of the salt matrix.

attract nonpolar compounds.

Most of the herein analyzed matrix components are small, charged ions and their loss should, consequently, occur almost exclusively through the ED membranes. From the obtained recovery curves (Fig. 1), it can be derived that a competitive process takes place. Fastest transport into the boundary layer and transfer trough the ED membranes occurred for ions with high charge and small size and, therefore, high mobility. Both lowered charge and increased size resulted in delayed removal from the sample. Phosphate and sulphate, which are the largest among the analyzed matrix components, were only removed late in the ED process, when the supply of other matrix ions was already lowered. Silicic acid showed minimal loss during ED, because it is not charged at circumneutral pH (pK$_{a1}$ 9.9). Green et al. (2014) also reported the retention of inorganic forms of silicon during ED/RO processing of seawater. Koprivnjak et al. (2006) showed that silicic acid can be removed with ED when increasing the pH above 9, which our data from the experiment at pH 10 confirm (data not shown).

Our conducted target analyte recovery experiment enables a detailed evaluation of the behavior of organic molecules in the utilized ED system. Our data indicates that for hydrophilic compounds, their recovery is strongly dependent on the desalination process itself (Fig. 4a), while the recovery of hydrophobic compounds is rather determined by the temporal progress of the ED procedure (Fig. 4b).

Hydrophilic molecules of low logK$_{ow}$ of < 0, especially the charged ones, are prone to loss through the ED membranes, as described above. Consequently, they compete with the matrix components in this process. Since the organic target analytes are larger and, therefore, less mobile than the matrix components, their loss occurs only in the late stage of the ED process, when the concentration of matrix components is already lowered (Bell et al., 2017; Gurtler et al., 2008; Vetter et al., 2007). As a result, the recovery of these compounds is highly salinity-dependent (Fig. 4a). The majority of the herein targeted hydrophilic compounds was of low molecular weight and charged at ED operating pH of 7–8. For these molecules, recoveries decreased with increasing charge (Fig. 3). This confirms that small and charged molecules are prone to loss through the ED membranes, as previously shown for the analyzed matrix components. From previous studies (Bell et al., 2017; Chambers et al., 2016), it is known that both increased size and decreased charge promote higher recoveries in ED systems, despite a low logK$_{ow}$ (e.g. glucose, logK$_{ow}$ −3.3, charge 0, recovery 90% (Chambers et al., 2016)). Decreased charge reduces the influence of the electric field and, therefore, the transport of a compound into the boundary layer. Increased size reduces the compounds' ability to migrate through the membrane pores.

The hydrophobic target compounds with high logK$_{ow}$ of > 2 potentially have high affinity towards the system walls and tubing. Adsorption generally depends on the available sites at the solid phase and the concentration of the adsorbent. Both of these factors decrease as adsorption continues over time and, consequently, the time-dependent recovery of hydrophobic compounds progresses exponentially (Fig. 4b). Recoveries of hydrophobic compounds decreased with increasing logK$_{ow}$ (Fig. 3), i.e. rising affinity towards the system walls. Within this group of molecules, size did not impact recoveries, which is understandable, since surface adsorption is not limited through this factor.

For compounds of moderate hydrophobicity/hydrophilicity, i.e. medium $logK_{ow}$ of 0–2, both loss mechanisms might apply in parallel. Nonetheless, neither seems to occur to a considerable extent, since compounds of medium $logK_{ow}$ always showed recoveries of above 80% (Fig. 3).

In conclusion, knowledge of a target molecules' $logK_{ow}$, molecular mass and charge at ED operating pH can help estimate its recovery in an ED system. Nonetheless, since recoveries will also be dependent on the used system and possibly the sample matrix, only experimentally determined recoveries will give definite confirmation.

4.2. Interpretation of bulk DOM recovery

In general, our achieved bulk organic matter recoveries are comparable to previously collected data. Our DOC recoveries at S = 0.1 were on average 44% (Fig. 2), which is among the lower recovery values achieved with ED and ED/RO systems. Similar values were reported for samples from the North Atlantic Ocean (50% (Chambers et al., 2016), 46 and 40% (Chen et al., 2014; Helms et al., 2015)) and the Amundsen Sea (44% (Young and Ingall, 2010)). The final salinity in these studies was 0.75 (Chambers et al., 2016), 0.25 (Chen et al., 2014; Helms et al., 2015) and 0.5 (Young and Ingall, 2010), respectively. DON recoveries have previously been reported to be similar to DOC recoveries (Chambers et al., 2016; Green et al., 2014), which our data confirm. Our obtained DOP recoveries that ranged from 76 to 100% with an average of 88.8 ± 8.7% were very similar to those reported by Bell et al. (2017) for ED/RO of North Atlantic coastal water. Their recoveries ranged from 72 to 100%, with an average of 83.8 ± 10.7% at a final salinity of 0.5.

Results from the target analyte recovery experiments can help interpret the achieved bulk DOM recoveries (Fig. 2). As shown above, the obtained recovery curves can hint at the occurring loss mechanism. Final DOP recoveries in our electrodialysis system were at 89% (Fig. 2), which indicates that the phosphorus-containing molecules in the analyzed samples had properties that favor retention in the ED system. They were possibly of medium to low $logK_{ow}$ and either uncharged or too large to fit through the membrane pores, despite their charge. Possible molecules that meet the derived criteria are, for example, polyphosphates, adenosine-triphosphate (ATP), nucleotides or ribonucleic acid (RNA) (Bell et al., 2017). Since DOP was only lost below S = 2 membrane passage of smaller DOP components was probably the dominant loss mechanism.

In contrast, both DOC and DON loss occurred throughout the entire ED process (Fig. 2), but increased towards the end. This indicates that DOC and DON loss was driven by a combination of both described mechanisms. Small and charged molecules from the DOC/DON-pool, for example amino acids, passed through the ED membranes, while the more hydrophobic fraction of DON/DON adsorbed to the system walls.

Overall, the wide range of recoveries achieved for single compounds (Fig. 3 (Bell et al., 2017; Chambers et al., 2016)) shows that a compositional variation in DOM can certainly influence the bulk organic matter recovery in ED and ED/RO systems. If, in addition, factors like system design, membrane type and processing protocol are taken into account, the wide range of achieved DOM recoveries within and in between different studies (Chambers et al., 2016) can be explained. Therefore, it is advisable to conduct comparative measurements of DOC, DON and DOP for a comprehensive understanding of DOM recovery after ED.

4.3. Measures to improve recoveries

Knowledge of the mechanisms and molecular properties that drive analyte recovery enables the design of the electrodialysis process to counteract analyte loss. To avoid membrane passage of analytes, one could (1) eliminate their charge, e.g. by adjusting the sample pH, or (2) refine the supplied current in order to reduce transport of analytes into the boundary layer.

Since bulk DOM is negatively charged at circumneutral pH (Gurtler et al., 2008), especially a lowered pH could potentially increase DOM recovery, because charges on acidic functional groups are eliminated (Bell et al., 2017). Similarly, increasing the pH might remove charges from nitrogen-containing basic functional groups. In this study, it was chosen to adjust sample pH to 4 and 10, respectively, because more extreme pH values might induce compositional changes in the sample material and are difficult to maintain during the ED process. Moreover, since the pK_a values of many organic acids are above 4, the majority of these compounds should be without charge at pH 4. Surprisingly, no improvement on DOC or DON recovery could be achieved through adjusting of the sample pH (Table 1d), even though the investigations with target compounds suggested that molecule charge does influence analyte recovery (Fig. 3). This discrepancy might be owed to counteracting loss mechanisms. Possibly, the eliminated charge reduced the membrane passage, but favored the adsorption of DOM to the membranes or the system walls. It was previously shown that adsorption of DOM to solid materials is pH-dependent (Dittmar et al., 2008; Kim et al., 2002). It might also be that the chosen pH values were not extreme enough for a measurable effect on recoveries.

Membrane passage of analytes can also be counteracted by refining the supplied current and thereby increasing the membrane selectivity (Zhang et al., 2011; Zhang et al., 2009). We hypothesized that decreasing the current from 80 to 50% of the limiting current might increase DOM recoveries at low salinity. Indeed, both DOC and DON recoveries could be improved by 8% at S = 0.5 (Table 1c). However, this effect was no longer apparent when desalination was continued to S = 0.1, probably due to the elongated runtime, which compensated for the increased selectivity.

Terminating the ED process at a higher salinity is another straightforward method to improve analyte recoveries. For example, with respect to glyphosate, ending the process at S = 0.5 instead of 0.1 would increase the recovery from 26 to 58% (Fig. 4a).

4.4. Suitability of electrodialysis for target analysis

In view of current analytical challenges, the use of electrodialysis might improve or even enable analysis of polar compounds in seawater which can, so far, not be analytically addressed due to matrix interferences. For a subsequent target analysis to be successful, analyte recovery in the ED system needs to be sufficient and the obtained isolate has to be compatible with the subsequent enrichment and analysis method.

The retention of polar analytes is possible in our ED system; however, desalination needs to be terminated before significant loss of the analytes occurs. When, for example, a subsequent SPE enrichment of the analytes is to be conducted, the chosen final salinity will be a compromise between obtained recovery and tolerable remaining salt content for the SPE columns. As a consequence, the final salinity needs to be specifically evaluated for the target compound and analysis method in question.

Our ED system is rather unsuitable for the retention of hydrophobic molecules, but those compounds are usually well extractable from water samples with organic solvents or ion exchange resins, thus making sample processing with ED unnecessary.

Nevertheless, matrix-dependent ion suppression was found to be reduced in ED isolates, giving rise to increased instrumental sensitivity of subsequent LC-MS/MS and GC–MS/MS methods, which can benefit the analysis of both hydrophilic and hydrophobic compounds.

5. Conclusion

Within this work, the drivers of compound loss during the electrodialysis of seawater were studied through a combination of bulk and target analysis of ED isolates. In addition, the desalination process itself

was investigated through the analysis of matrix components. It was found that small, charged compounds and highly hydrophobic compounds are both prone to loss from the samples via membrane passage and adsorption to system walls, respectively. Recoveries of bulk and target compounds can be improved by refining the supplied current and by terminating the ED process at elevated salinity.

Special focus was laid on the suitability of electrodialysis for coupling to target analysis with LC-MS/MS or GC–MS/MS. Sample processing with ED was deemed beneficial for the analysis of polar compounds, as they are only lost from samples in the late stage of the procedure. Generally, the sample processing protocol should be adjusted to maximize the recovery of the target analyte. The most influential parameter is, in this case, the chosen final salinity, which is always a compromise between obtained recovery and tolerable remaining salt content for subsequent sample processing.

The suitability of ED in combination with target analysis should be also discussed along with economic aspects. As a matter of fact, ED is an elaborate technique (Chambers et al., 2016; Green et al., 2014). Depending on the initial salinity, sample volume and applied settings, desalination with the herein used ED system took between 90 and 135 min. The overall ED processing time, including system preparation and cleaning was approx. 5 h. Therefore, the processing time of a single sample, including filtration, electrodialysis, enrichment (e.g. SPE) and measurement could take several days, which would not enable the high sample throughput often required in analytical laboratories. As a consequence, measures to increase the economic efficiency of such a procedure are commendable. This could include (1) downscaling of the ED system to reduce processing time, (2) further automatization to reduce the workload or (3) performing several analyses of different compounds from the same ED-processed sample. Nonetheless, electrodialysis was found to be a promising processing tool for seawater samples that can enable previously impossible analyses.

Acknowledgements

This work was supported by the funding line strategic networks of the Leibniz Association within the scope of the Leibniz ScienceCampus Phosphorus Research Rostock. The authors further appreciate funding for instrumentation from the German Federal Ministry of Education and Research through the project PROSO (MARE: N 0307779A).

The authors would like to thank the members of the IOW marine chemistry section, namely Jenny Jeschek, Birgit Sadkowiak, Christoph Kamper, Lisa Rönspieß and Malte Pallentin for their assistance during the analysis of bulk organic matter parameters and nutrients. Furthermore, we thank Dr. Olaf Dellwig and Anne Köhler from the IOW marine geology department for analyzing the ICP-OES samples. Finally, we thank Dr. Angela Vogts for her helpful comments on the manuscript.

Appendix A. Supplementary data

Supplementary data to this article can be found online at https://doi.org/10.1016/j.marchem.2019.103719.

References

Abdulla, H.A.N., Minor, E.C., Hatcher, P.G., 2010. Using two-dimensional correlations of 13C NMR and FTIR to investigate changes in the chemical composition of dissolved organic matter along an estuarine transect. Environ. Sci. Technol. 44, 8044–8049.

Bell, D.W., Pellechia, P., Chambers, L.R., Longo, A.F., McCabe, K.M., Ingall, E., Benitez-Nelson, C.R., 2017. Isolation and molecular characterization of dissolved organic phosphorus using electrodialysis-reverse osmosis and solution 31P-NMR. Limnol. Oceanogr. Meth. 15 (5), 436–452.

Bjorklund, E., Svahn, O., Bak, S., Bekoe, S.O., Hansen, M., 2016. Pharmaceutical residues affecting the UNESCO biosphere reserve Kristianstads Vattenrike wetlands: sources and sinks. Arch. Environ. Contam. Toxicol. 71 (3), 423–436.

Brzezinski, M.A., Nelson, D.M., 1986. A solvent extraction method for the colorimetric determination of nanomolar concentrations of silicic acid in seawater. Mar. Chem. 19, 139–151.

Chambers, L.R., Ingall, E.D., Saad, E.M., Longo, A.F., Takeuchi, M., Tang, Y., Benitez-Nelson, C., Haley, S.T., Dyhrman, S.T., Brandes, J., Stubbins, A., 2016. Enhanced dissolved organic matter recovery from saltwater samples with electrodialysis. Aquat. Geochem. 22 (5–6), 555–572.

Chen, H., Stubbins, A., Perdue, E.M., Green, N.W., Helms, J.R., Mopper, K., Hatcher, P.G., 2014. Ultrahigh resolution mass spectrometric differentiation of dissolved organic matter isolated by coupled reverse osmosis-electrodialysis from various major oceanic water masses. Mar. Chem. 164, 48–59.

Corbera, M., Hidalgo, M., Salvadó, V., Wieczorek, P.P., 2005. Determination of glyphosate and aminomethylphosphonic acid in natural water using the capillary electrophoresis combined with enrichment step. Anal. Chim. Acta 540 (1), 3–7.

Cowan, D.A., Brown, J.H., 1959. Effect of turbulece on limiting current in electrodialysis cells. Ind. Eng. Chem. 51 (12), 1445–1448.

Dittmar, T., Koch, B., Hertkorn, N., Kattner, G., 2008. A simple and efficient method for the solid-phase extraction of dissolved organic matter (SPE-DOM) from seawater. Limnol. Oceanogr. Meth. 6, 230–235.

Fisch, K., Waniek, J.J., Schulz-Bull, D.E., 2017. Occurrence of pharmaceuticals and UV-filters in riverine run-offs and waters of the German Baltic Sea. Mar. Pollut. Bull. 124 (1), 388–399.

Green, N.W., Perdue, E.M., Aiken, G.R., Butler, K.D., Chen, H., Dittmar, T., Niggemann, J., Stubbins, A., 2014. An intercomparison of three methods for the large-scale isolation of oceanic dissolved organic matter. Mar. Chem. 161, 14–19.

Gurtler, B.K., Vetter, T.A., Perdue, E.M., Ingall, E., Koprivnjak, J.F., Pfromm, P.H., 2008. Combining reverse osmosis and pulsed electrical current electrodialysis for improved recovery of dissolved organic matter from seawater. J. Membrane Sci. 323 (2), 328–336.

Habedank, F., Abraham, M., Tardel, H., Feldhusen, F., Schulz-Bull, D.E., 2017. Determination of organophosphate pesticides in sea and surface water with ultrasound-assisted dispersive liquid–liquid micro-extraction coupled to GC-MS/MS analysis. Int. J. Environ. Anal. Chem. 97 (9), 819–830.

Hanke, I., Singer, H., Hollender, J., 2008. Ultratrace-level determination of glyphosate, aminomethylphosphonic acid and glufosinate in natural waters by solid-phase extraction followed by liquid chromatography-tandem mass spectrometry: performance tuning of derivatization, enrichment and detection. Anal. Bioanal. Chem. 391 (6), 2265–2276.

Hansell, D.A., Carlson, C.A., Repeta, D.J., Schlitzer, R., 2009. Dissolved organic matter in the ocean: a controversy stimulates new insights. Oceanography 22 (4), 202–211.

Hansell, D.A., Carlson, C.A., Schlitzer, R., 2012. Net removal of major marine dissolved organic carbon fractions in the subsurface ocean. Global Biogeochem. Cycles 26(1). In: GB1016.

Helms, J.R., Stubbins, A., Ritchie, J.D., Minor, E.C., 2008. Absorption spectral slopes and slope ratios as indicators of molecular weight, source, and photobleaching of chromophoric dissolved organic matter. Limnol. Oceanogr. 53 (3), 955–969.

Helms, J.R., Mao, J., Chen, H., Perdue, E.M., Green, N.W., Hatcher, P.G., Mopper, K., Stubbins, A., 2015. Spectroscopic characterization of oceanic dissolved organic matter isolated by reverse osmosis coupled with electrodialysis. Mar. Chem. 177, 278–287.

Hertkorn, N., Stubbins, A., Ritchie, J.D., Minor, E.C., 2008. Natural organic matter and the event horizon of mass spectrometry. Anal. Chem. 80 (23), 8908–8919.

Kaiser, K., Benner, R., 2012. Organic matter transformations in the upper mesopelagic zone of the North Pacific: chemical composition and linkages to microbial community structure. J. Geophys. Res.: Oceans 117, C01023.

Káňavová, N., Machuča, L., 2014. A novel method for limiting current calculation in electrodialysis modules. Period. Polytech. Chem. Eng. 58 (2), 125–130.

Karl, D.M., Björkman, K.M., 2015. Dynamics of dissolved organic phosphorus. In: Hansell, D.A., Carlson, C.A. (Eds.), Biogeochemistry of Marine Dissolved Organic Matter. Elsevier, pp. 233–334.

Kim, D.H., Moon, S.-H., Cho, J., 2002. Investigation of the adsorption and transport of natural organic matter (NOM) in ion-exchange membranes. Desalination 15, 11–20.

Koponen, J., Airaksinen, R., Hallikainen, A., Vuorinen, P.J., Mannio, J., Kiviranta, H., 2015. Perfluoroalkyl acids in various edible Baltic, freshwater, and farmed fish in Finland. Chemosphere 129, 186–191.

Koprivnjak, J.F., Perdue, E.M., Pfromm, P.H., 2006. Coupling reverse osmosis with electrodialysis to isolate natural organic matter from fresh waters. Water Res. 40 (18), 3385–3392.

Koprivnjak, J.F., Pfromm, P.H., Ingall, E., Vetter, T.A., Schmitt-Kopplin, P., Hertkorn, N., Frommberger, M., Knicker, H., Perdue, E.M., 2009. Chemical and spectroscopic characterization of marine dissolved organic matter isolated using coupled reverse osmosis–electrodialysis. Geochim. Cosmochim. Acta 73 (14), 4215–4231.

Lee, H.-J., Strathmann, H., Moon, S.-H., 2006. Determination of the limiting current density in electrodialysis desalination as an empirical function of linear velocity. Desalination 190 (1–3), 43–50.

Letscher, R.T., Hansell, D.A., Carlson, C.A., Lumpkin, R., Knapp, A.N., 2013. Dissolved organic nitrogen in the global surface ocean: distribution and fate. Glob. Biogeochem. Cycles 27 (1), 141–153.

Li, Y., Harir, M., Uhl, J., Kanawati, B., Lucio, M., Smirnov, K.S., Koch, B.P., Schmitt-Kopplin, P., Hertkorn, N., 2017. How representative are dissolved organic matter (DOM) extracts? A comprehensive study of sorbent selectivity for DOM isolation. Water Res. 116, 316–323.

Lohrer, C., Cwierz, P.P., Wirth, M.A., Schulz-Bull, D.E., Kanwischer, M., 2019. Methodological aspects of methylphosphonic acid analysis: determination in river and coastal water samples. Talanta, submitted.

Macdonald, M.J., Minor, E.C., 2013. Photochemical degradation of dissolved organic matter from streams in the western Lake Superior watershed. Aquat. Sci. 75 (4), 509–522.

Mao, J., Kong, X., Schmidt-Rohr, K., Pignatello, J.J., Perdue, E.M., 2012. Advanced solid-state NMR characterization of marine dissolved organic matter isolated using the

coupled reverse osmosis/electrodialysis method. Environ. Sci. Technol. 46 (11), 5806–5814.
McGill, D.A., 1964. The distribution of phosphorus and oxygen in the Atlantic Ocean as observed during the I.G.Y., 1957–1958. Prog. Oceanogr. 2, 127–211.
Meyers-Schulte, K.J., Hedges, J.I., 1986. Molecular evidence for a terrestrial component of organic matter dissolved in ocean water. Nature 321, 61–63.
Minor, E.C., Swenson, M.M., Mattson, B.M., Oyler, A.R., 2014. Structural characterization of dissolved organic matter: a review of current techniques for isolation and analysis. Environ. Sci.: Proc. Imp. 16 (9), 2064–2079.
Mopper, K., Stubbins, A., Ritchie, J.D., Bialk, H.M., Hatcher, P.G., 2007. Advanced instrumental approaches for characterization of marine dissolved organic matter: extraction techniques, mass spectrometry, and nuclear magnetic resonance spectroscopy. Chem. Rev. 107, 419–442.
Moran, M.A., Kujawinski, E.B., Stubbins, A., Fatland, R., Aluwihare, L.I., Buchan, A., Crump, B.C., Dorrestein, P.C., Dyhrman, S.T., Hess, N.J., Howe, B., Longnecker, K., Medeiros, P.M., Niggemann, J., Obernosterer, I., Repeta, D.J., Waldbauer, J.R., 2016. Deciphering ocean carbon in a changing world. Proc. Natl. Acad. Sci. U. S. A. 113 (12), 3143–3151.
Naumann, M., Umlauf, L., Mohrholz, V., Kuss, J., Siegel, H., Waniek, J.J., Schulz-Bull, D.E., 2018. Hydrographic-Hydrochemical Assessment of the Baltic Sea 2017. Leibniz Institute for Baltic Sea Research Warnemuende, Warnemuende.
Nebbioso, A., Piccolo, A., 2013. Molecular characterization of dissolved organic matter (DOM): a critical review. Anal. Bioanal. Chem. 405 (1), 109–124.
Nightingale, E.R., 1959. Phenomenological theory of ion solvation. Effective radii of hydrated ions. J. Phys. Chem. 63, 1381–1387.
Panagiotopoulos, C., Repeta, D.J., Mathieu, L., Rontani, J.-F., Sempéré, R., 2013. Molecular level characterization of methyl sugars in marine high molecular weight dissolved organic matter. Mar. Chem. 154, 34–45.
Porcal, P., Koprivnjak, J.F., Molot, L.A., Dillon, P.J., 2009. Humic substances-part 7: the biogeochemistry of dissolved organic carbon and its interactions with climate change. Environ. Sci. Pollut. Res. Int. 16 (6), 714–726.
Remucal, C.K., 2014. The role of indirect photochemical degradation in the environmental fate of pesticides: a review. Environ. Sci. Proc. Imp. 16 (4), 628–653.
Repeta, D.J., 2015. Chemical characterization and cycling of dissolved organic matter. In: Hansell, D.A., Carlson, C.A. (Eds.), Biogeochemistry of Marine Dissolved Organic Matter. Elsevier, pp. 21–63.
Ridgwell, A., Arndt, S., 2015. Why dissolved organics matter. In: Hansell, D.A., Carlson, C.A. (Eds.), Biogeochemistry of Marine Dissolved Organic Matter. Elsevier, pp. 1–20.
Sanderman, J., Lohse, K.A., Baldock, J.A., Amundson, R., 2009. Linking soils and streams: sources and chemistry of dissolved organic matter in a small coastal watershed. Water Resour. Res. 45 (3).
Seidel, M., Manecki, M., Herlemann, D.P.R., Deutsch, B., Schulz-Bull, D.E., Jürgens, K., Dittmar, T., 2017. Composition and transformation of dissolved organic matter in the Baltic Sea. Front. Earth Sci. 5.
Sillanpää, M., Shestakova, M., 2017. Electrochemical Water Treatment Methods. Elsevier.
Sipler, R.E., Bronk, D.A., 2015. Dynamics of dissolved organic nitrogen. In: Hansell, D.A., Carlson, C.A. (Eds.), Biogeochemistry of Marine Dissolved Organic Matter. Elsevier, pp. 127–232.
Skeff, W., Neumann, C., Schulz-Bull, D.E., 2015. Glyphosate and AMPA in the estuaries of the Baltic Sea method optimization and field study. Mar. Pollut. Bull. 100 (1), 577–585.
Sleighter, R.L., McKee, G.A., Liu, Z., Hatcher, P.G., 2008. Naturally present fatty acids as internal calibrants for Fourier transform mass spectra of dissolved organic matter. Limnol. Oceanogr. Meth. 6, 246–253.
Svahn, O., Björklund, E., 2019. Simple, fast and inexpensive large “whole water” volume sample SPE-loading using compressed air and finely ground sand. Anal. Meth. 11 (7), 894–896.
Vetter, T., Perdue, E., Ingall, E., Koprivnjak, J., Pfromm, P., 2007. Combining reverse osmosis and electrodialysis for more complete recovery of dissolved organic matter from seawater. Separ. Purif. Technol. 56 (3), 383–387.
Wakeham, S.G., Pease, T.K., Benner, R., 2003. Hydroxy fatty acids in marine dissolved organic matter as indicators of bacterial membrane material. Org. Geochem. 34 (6), 857–868.
Walker, B.D., Beaupré, S.R., Guilderson, T.P., Druffel, E.R.M., McCarthy, M.D., 2011. Large-volume ultrafiltration for the study of radiocarbon signatures and size vs. age relationships in marine dissolved organic matter. Geochim. Cosmochim. Acta 75 (18), 5187–5202.
Wenk, J., von Gunten, U., Canonica, S., 2011. Effect of dissolved organic matter on the transformation of contaminants induced by excited triplet states and the hydroxyl radical. Environ. Sci. Technol. 45 (4), 1334–1340.
Wünsch, U.J., Geuer, J.K., Lechtenfeld, O.J., Koch, B.P., Murphy, K.R., Stedmon, C.A., 2018. Quantifying the impact of solid-phase extraction on chromophoric dissolved organic matter composition. Mar. Chem. 207, 33–41.
Yamashita, Y., Tanoue, E., 2003. Distribution and alteration of amino acids in bulk DOM along a transect from bay to oceanic waters. Mar. Chem. 82 (3–4), 145–160.
Young, C.L., Ingall, E.D., 2010. Marine dissolved organic phosphorus composition: insights from samples recovered using combined electrodialysis/reverse osmosis. Aquat. Geochem. 16 (4), 563–574.
Zhang, Y., Van der Bruggen, B., Pinoy, L., Meesschaert, B., 2009. Separation of nutrient ions and organic compounds from salts in RO concentrates by standard and monovalent selective ion-exchange membranes used in electrodialysis. J. Membrane Sci. 332 (1–2), 104–112.
Zhang, Y., Pinoy, L., Meesschaert, B., Van der Bruggen, B., 2011. Separation of small organic ions from salts by ion-exchange membrane in electrodialysis. AICHE J. 57 (8), 2070–2078.
Zhuang, W.E., Yang, L., 2018. Impacts of global changes on the biogeochemistry and environmental effects of dissolved organic matter at the land-ocean interface: a review. Environ. Sci. Pollut. Res. Int. 25 (5), 4165–4173.

Publication 2

The challenge of detecting the herbicide glyphosate and its metabolite AMPA in seawater – Method development and application in the Baltic Sea

by

Marisa A. Wirth, Detlef E. Schulz-Bull, Marion Kanwischer

Chemosphere

Year 2021, Volume 262, Page 128327 ff.

DOI: 10.1016/j.chemosphere.2020.128327

Chemosphere 262 (2021) 128327

Contents lists available at ScienceDirect

Chemosphere

journal homepage: www.elsevier.com/locate/chemosphere

The challenge of detecting the herbicide glyphosate and its metabolite AMPA in seawater – Method development and application in the Baltic Sea

Marisa A. Wirth*, Detlef E. Schulz-Bull, Marion Kanwischer

Leibniz Institute for Baltic Sea Research Warnemünde, Department of Marine Chemistry, Seestraße 15, 18119, Rostock, Germany

HIGHLIGHTS

- A new methodology was developed to determine glyphosate and AMPA in seawater.
- Salt-matrix sensitivity of different solid phase extraction materials was evaluated.
- Low detection limits of 0.12 and 0.22 ng/L for glyphosate and AMPA were achieved.
- Measured glyphosate levels in the Baltic Sea were between 0.42 and 1.22 ng/L.
- This is the first report on the occurrence of glyphosate and AMPA in seawater.

GRAPHICAL ABSTRACT

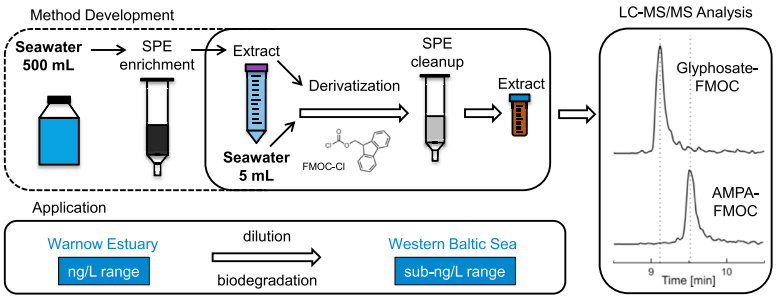

ARTICLE INFO

Article history:
Received 17 July 2020
Received in revised form
7 September 2020
Accepted 10 September 2020
Available online 16 September 2020

Handling Editor: Keith Maruya

Keywords:
Glyphosate
Seawater
Salt matrix
Solid phase extraction
LC-MS/MS
Baltic Sea

ABSTRACT

The globally used herbicide glyphosate and its metabolite aminomethylphosphonic acid (AMPA) have not yet been reported to occur in the marine environment, presumably due to a lack of suitable analytical methods. In this study, we developed two new methods for the analysis of glyphosate and AMPA in seawater: a small-scale method, which includes an SPE cleanup step that minimizes salt-matrix effects during LC-MS/MS analysis, and a large-scale method that employs an additional SPE preconcentration step. Different SPE materials were evaluated for their suitability to enrich glyphosate and AMPA from saltwater and a molecularly imprinted polymer was selected. Both methods were validated in ultrapure water and environmental seawater. Achieved limits of detection with the small-scale method were 6 and 8 ng/L for glyphosate and AMPA, while the large-scale method achieved 0.12 and 0.22 ng/L, respectively. The small-scale method was used to analyze environmental samples from the Warnow Estuary in Germany. Glyphosate and AMPA could be successfully detected in the samples, but could not be measured beyond the saline estuary due to dilution and degradation effects. A set of samples from the western Baltic Sea was analyzed with the large-scale method. Glyphosate and AMPA could be detected in all Baltic Sea samples, especially at stations close to estuaries. To the best of our knowledge, this is the first report on the occurrence of glyphosate and AMPA in seawater.

* Corresponding author.
E-mail address: marisa.wirth@io-warnemuende.de (M.A. Wirth).

https://doi.org/10.1016/j.chemosphere.2020.128327
0045-6535/

1. Introduction

Glyphosate [*N*-(phosphonomethyl)glycine] is a broad-spectrum herbicide that is among the most frequently applied ones worldwide (Duke and Powles, 2008; Richmond, 2018). Despite a relatively high sorption potential to soil (Glass, 1987; Gros et al., 2017), it is known to be transported into surface waters through spray drift, surface runoff and wind erosion (Silva et al., 2018; Skeff et al., 2015). Glyphosate has been frequently detected in freshwater ecosystems, e.g., rivers and lakes across the globe, usually together with its metabolite aminomethylphosphonic acid (AMPA) (Battaglin et al., 2005; Coupe et al., 2012; Daouk et al., 2013; Huntscha et al., 2018).

To the best of our knowledge, there have not yet been any reports on the occurrence of glyphosate and AMPA in the marine environment. The interest in the analysis of both compounds in seawater has been evident in the literature for several years. There have been laboratory studies characterizing the influence of glyphosate and AMPA on marine organisms (Milan et al., 2018; Stachowski-Haberkorn et al., 2008; Tsui and Chu, 2003) and the degradation of glyphosate in seawater (Janβen et al., 2019; Mercurio et al., 2014). Previously, Skeff et al. (2015) detected glyphosate and AMPA in German estuaries discharging into the Baltic Sea, which confirmed that both compounds are transported into the marine environment. However, their method was not sensitive enough to detect the low-concentrated analytes beyond the estuaries (Skeff et al., 2016).

The analysis of glyphosate and AMPA in seawater seems to be mainly hampered through methodological difficulties. As stated above, target analytes can be strongly diluted in seawater. Hence, a preconcentration step is required before instrumental analysis, which can, for example, be achieved with solid phase extraction (SPE) (Claude et al., 2017; Corbera et al., 2005; Hanke et al., 2008; Hidalgo et al., 2004; Ibanez et al., 2005; Küsters and Gerhartz, 2010; Montiel-León et al., 2019; Sanchís et al., 2012). However, it is challenging to use this technique for glyphosate and AMPA enrichment from seawater. Both analytes are very polar and SPE materials that are able to bind them, typically ion exchange resins (IERs) (Corbera et al., 2005, 2006; Delmonico et al., 2014; Jiang and Lucy, 2007; Patsias et al., 2001), are also able to bind salt ions. Consequently, competiton of salt ions and analytes for binding sites on the solid phase hampers the enrichment (Corbera et al., 2005; Jiang and Lucy, 2007; Patsias et al., 2001). For successful preconcentration, it is required to either separate the analytes from the salt matrix prior to SPE, or to employ a salt matrix insensitive material. Promising candidates for such materials are molecularly imprinted polymers (MIPs), which allow highly selective binding of target analytes from complex matrices and have gained increasing attention in analytical chemistry in the past years (Ansari and Karimi, 2017; Claude et al., 2017). Separation of analytes and salt matrix before SPE can, for example, be achieved with electrodialysis. During this desalination technique, salt ions are removed from a seawater sample through ion exchange resins under the influence of an electric field (Wirth et al., 2019).

Further methodological challenges can arise during the instrumental analysis of glyphosate and AMPA in seawater. A common way to analyze both compounds in water samples is the derivatization with fluorenylmethoxycarbonyl chloride (FMOC-Cl) followed by reversed-phase liquid chromatography (LC) coupled to flourescence detection (FLD) or mass spectrometry (MS) (Hidalgo et al., 2004; Ibanez et al., 2005; Le Fur et al., 2000; Pinto et al., 2018; Skeff et al., 2015). Laboratory experiments have demonstrated that this derivatization procedure can be successfully conducted in seawater (Skeff et al., 2016; Wang et al., 2016). However, it was also shown that salt matrices can highly influence the LC-MS/MS analysis of glyphosate-FMOC and AMPA-FMOC by causing retention time shifts and strong matrix effects.

Hence, a method that is capable to detect glyphosate and AMPA in seawater has to include (1) a preconcentration step as well as (2) an analysis procedure that are both salt-matrix-insensitive. The aim of this study was to develop and apply a methodology that meets the above criteria. For this purpose, we evaluated different potential SPE materials for the enrichment of glyphosate and AMPA from seawater and determined their salt sensitivity by combining SPE with electrodialysis. Furthermore, we introduced an SPE cleanup step after analyte derivatization with FMOC-Cl and investigated its effect on the chromatographic behavior and MS-detection of the analytes. Based on this, we set up two new methods for the analysis of glyphosate and AMPA in seawater: a small-scale method without elaborate preconcentration, which is suitable for coastal areas, and a more sensitive large-scale method which uses a molecularly imprinted polymer for SPE enrichment of the analytes. Both methods were validated and tested on environmental samples collected in the Warnow Estuary in the city of Rostock (Germany) and in the western Baltic Sea. To the best of our knowledge, this constitutes the first report on the occurrence of glyphosate and AMPA in seawater.

2. Material and methods

A list of all utilized chemicals and materials and their suppliers is provided in the supplement (Table S1).

2.1. Material evaluation for SPE preconcentration

Three different materials were evaluated for the SPE enrichment of glyphosate and AMPA from seawater. Two ion exchange resins, Chromabond PS-OH^- and Amberlite IRA 900 Cl (Corbera et al., 2006), as well as the molecularly imprinted polymer Affinimip Glyphosate (Claude et al., 2017) were tested.

All materials were first evaluated in ultrapure water in triplicate. For this, 100 mL of water were spiked with glyphosate, AMPA and the internal standards (IS) 1,2-^{13}C—^{15}N-glyphosate and ^{13}C—^{15}N-AMPA at 5 ng/L and extracted with the SPE columns according to the procedures described in Table 1. Recoveries were determined by comparison with reference samples, for which the same amounts of glyphosate, AMPA and the IS were added directly into the elution solutions. Aliquots of the obtained eluates and reference samples were derivatized as described in section 2.2. No additional KCl was added to the KCl eluates. The HCl eluates were neutralized with 167 μL of 5 M NaOH prior to derivatization.

2.2. Sample derivatization and SPE cleanup

The different SPE procedures described in Table 1 required the derivatization of different sample volumes. In the following, the basic procedure using 1 mL of derivatization solution will be described. The amounts of added reagents were adapted proportionally when higher sample volumes were used. For the derivatization: 760 μL of 0.45 μm filtered sample were transferred into a polypropylene tube with 0.052 g solid KCl (c_{final} = 0.7 M). The purpose of KCl is to increase the polarity of the derivatization solution to enable the binding of the FMOC-derivatives on the subsequently used SPE material. After dissolution of KCl, 20 μL of the internal standard (IS) containing 1,2-^{13}C—^{15}N-glyphosate and ^{13}C—^{15}N-AMPA (c_{stock} = 10 μg/L, v = 20 μL) and 20 μL EDTA solution (c_{stock} = 100 mM) were added. Samples were incubated for 30 min at room temperature to allow breaking of glyphosate-metal-complexes with EDTA and equilibration with the IS. Afterwards, 100 μL of $Na_2B_4O_7$ buffer (c_{stock} = 52 mM, pH 9) and 100 μL of

Table 1
Utilized SPE materials and employed procedures for the enrichment of glyphosate and AMPA.

Material	Conditioning	Sample Loading Rate	Washing and Drying	Elution
Chromabond PS-OH^- 200 mg/3 mL	4 mL ultrapure water 4 mL 1 M $NaHCO_3$ 4 mL ultrapure water	3 mL/min	10 min drying with clean air	2 mL 1 M KCl
Amberlite IRA 900 Cl (1 g sorbent)	5 mL ultrapure water	5 mL/min	–	15 mL 1 M KCl
Affinimip Glyphosate 6 mL	6 mL ultrapure water	2 mL/min	washing with 6 mL ultrapure water	8 mL 0.1 M HCl

FMOC-Cl in acetonitrile (c_{stock} = 1 mM) were added. After mixing, the derivatization solutions were incubated for 3 h at room temperature. They were then extracted with 100 mg Chromabond C_{18} hydra columns at approx. 5 mL/min. The FMOC-derivatives and the excess derivatization agent favor bonding to the SPE material compared to the saline derivatization solution. Columns were previously conditioned with 600 μL of methanol and 600 μL of ultrapure water. After drying, the FMOC-derivatives were eluted with 500 μL of ultrapure water with 1 vol-% acetonitrile. Compared to the solid phase, this elution solution is favored by the FMOC-derivatives, but not by the excess derivatization agent, resulting in their separation. Instrumental analysis of the FMOC-derivatives was carried out with a LC-2040C Nexera-I and a triple quadrupole mass spectrometer LCMS-8060 (Shimadzu, Duisburg, Germany), as described in Wirth et al. (2019), but with an injection volume of 50 μL.

2.3. Salt sensitivity of SPE procedures

To evaluate the salt matrix sensitivity of the SPE preconcentration materials introduced in section 2.1, the enrichment of glyphosate and AMPA was carried out in seawater samples with different salinity (S). The required sample material was generated with an electrodialysis system. For this, a Baltic Sea water sample was collected at the Heiligendamm pier in Mecklenburg-Western Pomerania, Germany (54°08′46.7″ N, 11°50′36.1″ E) in June 2019. The sample was filtered (0.7 μm) and processed with electrodialysis, as described in Wirth et al. (2019). At specific residual salinities, 1 L subsamples were taken from the system.

The analytes and IS (both c = 5 ng/L) were subsequently spiked into 100 mL of the original seawater sample (S = 10 (PSU scale)) and the subsamples taken at S = 1.3, 0.5, 0.2 and 0.1. SPE enrichment was carried out with all three materials according to the above described protocols. Recoveries were also determined as described above.

The salt matrix sensitivity of the SPE cleanup procedure introduced in section 2.2 was evaluated similarly. The analytes and IS (both c = 1 μg/L) were spiked into 1 mL subsamples of different salinity and derivatization and cleanup was carried out. The salt matrix influence was investigated by calculating absolute and effective matrix effects, as shown in the supplement (Equation S1, S2).

2.4. Optimized sample treatment methods

2.4.1. Small-scale (5 mL) method

For the small-scale method, 3.88 mL of 0.45 μm filtered sample were directly derivatized without SPE preconcentration, as described in section 2.2. The added reagents were 0.26 g KCl, 100 μL EDTA, 500 μL $Na_2B_4O_7$ buffer and 500 μL FMOC-Cl, resulting in a derivatization solution volume of 5 mL. The elution volume after SPE cleanup was maintained at 500 μL, resulting in an enrichment factor of ~8 for the cleanup step.

2.4.2. Large-scale (500 mL) method

For the large-scale method, 500 mL of 0.7 μm filtered sample were preconcentrated with the selected MIP, as described in section 2.1. The obtained eluates (9 mL after neutralization) were mixed with 0.60 g KCl, 230 μL EDTA, 1150 μL $Na_2B_4O_7$ buffer and 1150 μL FMOC-Cl. Since the capacity of the utilized cleanup columns was insufficient for the obtained 11.5 mL derivatization solution, the cleanup column was switched to 500 mg Chromabond C_{18} hydra, which was conditioned with 3 mL of methanol and 3 mL of ultrapure water, sequentially. The elution volume for the larger columns was 3 mL. Finally, the obtained eluates were evaporated to a volume of approx. 500 μL at 40 °C under a stream of clean air and filtrated over 0.45 μm syringe filters, resulting in a combined enrichment factor of ~1000 for both SPE steps.

2.5. Quantitation, validation and quality assurance

Compounds were analyzed with LC-MS/MS through multiple reaction monitoring (MRM) events (Table S2). Exemplary chromatograms for both methods are shown in the supplement (Figs. S1 and S2). Analyte-to-IS ratios were considered for quantitation. The identity of the detected compounds was considered as confirmed when (1) the LC-retention time R_T of the analytes and internal standards was identical with a tolerance of R_T = 0.03 min, (2) all monitored mass transitions were present and (3) the ratio between the different transitions was identical compared to standard measurements, with a tolerance of ±30% (Bratinova et al., 2009).

Both developed methods were validated by assessing the linearity of five-point calibration curves after triplicate injection with the Mandel-Test for linearity (5 mL method: 0, 10, 40, 80 and 200 ng/L, IS = 40 ng/L; 500 mL method: 0.0, 0.2, 0.5, 1.0 and 1.5 ng/L, IS = 1.0 ng/L), as shown in the supplement (Equation S3, S4) (Bratinova et al., 2009). Furthermore, a standard sample and an environmental seawater sample were processed in triplicate with each method, to calculate precision and accuracy in terms of relative standard deviation (RSD%) and relative error (RE%), as shown in the supplement (Equation S5, S6). Lastly, the utilized environmental samples were spiked with three different analyte concentrations to assess method accuracy (i.e. spiking recovery) in the presence of matrix components. The environmental seawater sample for the small-scale method was collected from station 2 in the Warnow Estuary, the one for the large-scale method was taken from the Baltic Sea at Heiligendamm pier, since these samples were expected to contain representative matrix components for the targeted environmental compartments. Limits of detection and quantification (LOD and LOQ) for both methods were calculated according to Miller (1991) as shown in the supplement (Equation S7, S8).

For further quality assurance, blank samples were always included during both SPE and derivatization procedures to ensure that all utilized solutions were free of contamination. Blanks were accepted when the analyte concentration was < LOD. When environmental samples were analyzed, five-point calibration curves were always included for quantitation and to assure the robustness of the method.

2.6. Environmental sampling

The small-scale method was tested on a set of 13 surface water samples collected aboard the R/V Klaashahn in the Warnow Estuary on September 26, 2019. The 155 km long river Warnow, which discharges into the estuary, flows through agricultural land in Mecklenburg-Western Pomerania, Germany. The estuary itself is an urban site, surrounded by the city of Rostock and the Rostock Port. The sampled stations represent a transect along the estuary with the final station 12 located in the Baltic Sea. Moreover, a sample was collected close to the city's wastewater treatment plant (WWTP) outlet, which discharges into the estuary. Samples were collected at the immediate surface with a pre-rinsed bucket. The salinity of the collected samples ranged from 1.7 at station 2, to 12.8 at station 8 and 16.3 at station 12.

The large-scale method was used to analyze seven surface water samples collected in the western Baltic Sea aboard the R/V Elisabeth Mann Borgese between 29th and July 31, 2019. Some sampling stations are located close to the coast and near the mouths of the rivers Trave (TF022), Warnow (TFO5) and Oder (OBBoje). The remaining stations are located further offshore in the Bight of Kiel (TF360), the Bight of Mecklenburg (TF012, TF045) and the Arkona basin (TF145). Samples were collected with a CTD rosette system (SBE911) at 1–2 m depth. The salinities of the samples ranged from 7.7 at OBBoje to 13.1 at TF360. All collected samples were stored in 1 L polypropylene containers and kept frozen at −20 °C until analysis. A complete list of all sampling stations describing location, water temperature, surface salinity and determined analyte concentrations is given in the supplement (Tables S3 and S4).

3. Results and discussion

3.1. Suitability of SPE procedures for seawater

3.1.1. SPE preconcentration step

The SPE materials that were considered for the preconcentration of glyphosate and AMPA from seawater were first evaluated in ultrapure water and, afterwards, in Baltic Sea water of different salinity. Using an environmental sample that was desalted with electrodialysis rather than artificial seawater samples means that both salt matrix and organic matter effects were accounted for.

All three materials were suitable to enrich the analytes in ultrapure water (Fig. 1). Both the IER Amberlite IRA 900 Cl and the MIP Affinimip Glyphosate gave high average recoveries for glyphosate and AMPA, with 89 and 77% (IER) (Kanwischer et al., 2019) and 86 and 68% (MIP), respectively. The second IER, Chromabond PS-OH$^-$, showed lower average recoveries of 62 and 35%.

The experiments with Baltic Sea water of different salinity showed that both IERs are highly matrix-sensitive (Fig. 1 a,b). In the original seawater sample (S = 10), no glyphosate or AMPA could be recovered with both IERs. With Chromabond PS-OH$^-$, recoveries increased below S = 0.5. Only at the lowest evaluated salinity of S = 0.1 were the results comparable to the data obtained in pure water. When using Amberlite IRA 900 Cl, high recoveries for glyphosate could be obtained at S = 0.5 and lower. However, AMPA recoveries never became similar to those obtained in pure water, even at S = 0.1. Our results are well comparable to those obtained by Corbera et al. (2005), who evaluated the SPE recovery of glyphosate and AMPA with Amberlite 900 IRA Cl in tap and river water samples of varying conductivity. In their experiments, they also found decreasing SPE recoveries with increasing sample conductivity. Like in our experiments, AMPA recoveries were more sensitive to matrix ions than glyphosate. Consequently, both IERs were deemed unsuitable for the direct SPE enrichment of glyphosate and AMPA from seawater.

As stated above, an electrodialysis (ED) step could be implemented to reduce the salt content of seawater samples prior to SPE with IERs. Seawater samples would have to be desalted down to a salinity of at least 0.2 for acceptable SPE recoveries with the herein evaluated materials. However, the recoveries of glyphosate and AMPA during the ED process also need to be considered during this assessment. Analytes can be lost from the sample during ED via wall adsorption or membrane passage. In our previous work (Wirth et al., 2019), we examined the ED recoveries of glyphosate and AMPA, and found that at S = 0.2, the ED recoveries for glyphosate and AMPA were 42 and 80%. When using Amberlite IRA 900 Cl at a residual salinity of S = 0.2, the calculated combined ED and SPE recovery would, thus, be 34% for glyphosate and 16% for AMPA. Hence, this approach would result in high overall analyte losses and low method sensitivity. Moreover, sample processing with ED is elaborate and at maximum two samples per day can be processed with our system.

The third evaluated material, Affinimip Glyphosate, only showed moderate matrix sensitivity (Fig. 1c). Glyphosate recoveries were only slightly lower in the original Baltic Sea water sample (75%) than in ultrapure water (86%). AMPA recoveries were almost identical in both media (69 and 68%) and even slightly decreased in the desalted samples (e.g. 50% at S = 0.1). These findings are in agreement with Claude et al. (2017), who introduced the herein used MIP and stated that it can be used to enrich glyphosate and AMPA from seawater. They tested the material with seawater spiked with glyphosate and AMPA at 100 ng/L and found recoveries of 96 and 121%, respectively. In light of these findings, the MIP was chosen as the material for SPE preconcentration.

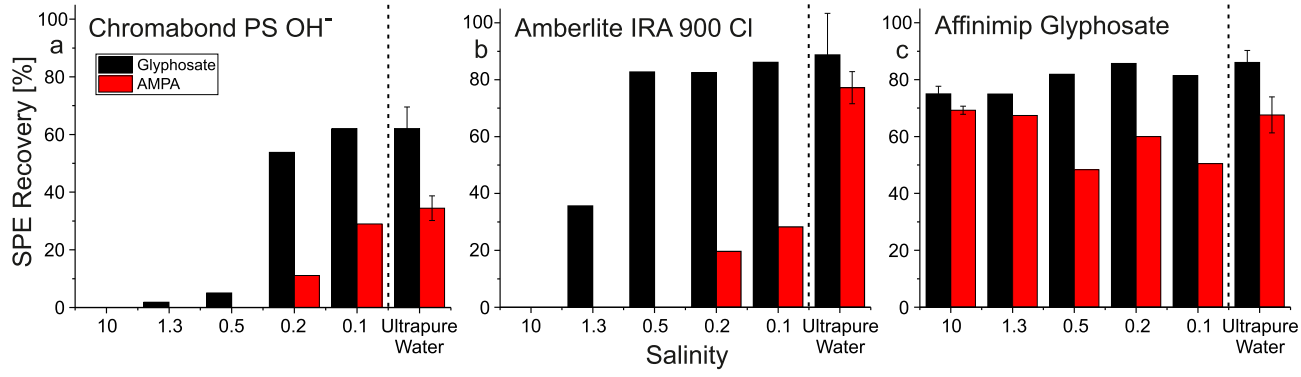

Fig. 1. SPE recoveries of glyphosate and AMPA utilizing two ion exchange resins (a,b) and one molecularly imprinted polymer (c) at different salinities compared to ultrapure water. Error bars represent the standard deviation from triplicate experiments (conducted in ultrapure water for a, b and c and at S = 10 for c).

3.1.2. SPE cleanup step

The applicability of the developed SPE cleanup step and subsequent LC-MS/MS analysis in the presence of inorganic as well as organic matrix components was tested by applying it to Baltic Sea water of different salinity, which was obtained through electrodialysis. This evaluation is crucial, since LC-MS/MS analysis, especially with electrospray ionization (ESI), is particularly susceptible to matrix effects (Gosetti et al., 2010; Trufelli et al., 2011). From the obtained signals, absolute and effective matrix effects were calculated and were classified as low when < ± 20%, as moderate between ±20% and ±50% and as high when > ± 50% (Economou et al., 2009). Low absolute matrix effects were observed for both analytes at all tested salinities, except for AMPA at S = 10, where the effect was moderate with −22.3% (Fig. 2a). Generally, signal suppression rather than enhancement was the dominant observed phenomenon. These low to moderate suppression effects are likely owed either to reduced analyte recovery during SPE cleanup or to matrix-induced ion suppression during the LC-MS/MS measurement. Nonetheless, effective matrix effects were below 5% for both analytes in all samples (Fig. 2b), indicating that internal standard correction efficiently compensates matrix interferences. This confirms that glyphosate and AMPA can be analyzed in seawater without considerable matrix limitations when using the employed SPE cleanup step.

Skeff et al. (2016) previously investigated the influence of salt matrices on the LC-MS/MS analysis of glyphosate and AMPA after FMOC-derivatization. They performed direct injection of the derivatization solutions without any sample cleanup steps. Glyphosate was reported to form metal complexes with divalent matrix cations, which caused retention time shifts of several minutes or prevented glyphosate detection entirely. Moreover, high matrix effects of up to +181% were observed for the glyphosate-FMOC signal. Wang et al. (2016) also reported retention time shifts and enhancing matrix effects during the LC-FLD analysis of glyphosate.

In our experiments, the LC-retention times for both analytes remained constant regardless of the sample salinity (Table S5). Furthermore, only low to moderate matrix effects were observed. This indicates that our employed sample cleanup protocol prevented the above described effects and facilitated the LC-MS/MS analysis compared to direct injection techniques.

3.2. Method optimization, validation and performance assessment

Based on the results from the salt sensitivity experiments, we chose to develop two different sample processing methods. Since the SPE cleanup step alone enabled the LC-MS/MS measurement of glyphosate and AMPA without salt matrix limitations, a more straightforward, small-scale method without SPE preconcentration, as well as a large-scale method including SPE preconcentration were set up. Intended application areas for the small-scale method are coastal or highly polluted areas, whereas the large-scale method can be applied to open seawater with lower analyte concentrations.

The optimization of the sample volumes used for both methods is described in the supplemental material (Figs. S3 and S4). Briefly, highest sensitivity in terms of lowest detection limits for the small-scale method was obtained when using 5 mL of derivatization volume. The optimized sample volume for the large-scale method was determined to be 500 mL.

The two optimized methods were validated by statistically evaluating the obtained calibration curves in standard samples and environmental seawater samples. Furthermore, precision and accuracy in terms of RSD% and RE% were calculated for both media. The methods showed high linearity in ultrapure water and environmental water for glyphosate and AMPA. The Mandel-Test for linearity was significant at P = 99% for all calibration curves (Figs. S5 and S6). The slopes of the calibration curves were similar in ultrapure water and environmental seawater, which is another indication for low effective matrix effects. For AMPA, there was a difference in the calibration curve slopes between ultrapure water and seawater when using the large scale method, which indicates that matrix-matched calibration might be better suited in that case. Nonetheless, since the validation data showed high accuracy and precision (RSD% and RE% < 12%) in ultrapure water and in seawater for both compounds and both methods, calibration in ultrapure water was deemed applicable. (Table 2 a,b).

The calculated LODs for the small-scale method were 6 and 8 ng/L for glyphosate and AMPA, while the LOQs were 10 and 15 ng/L. These are similar results compared to other methods employing a small-scale SPE-step after FMOC-derivatization followed by LC-MS/MS analysis. Ibanez et al. (2005) used 4.3 mL water samples and enriched the derivatization products on Oasis HLB columns, which resulted in an LOD of 5 ng/L for both glyphosate and AMPA. Poiger

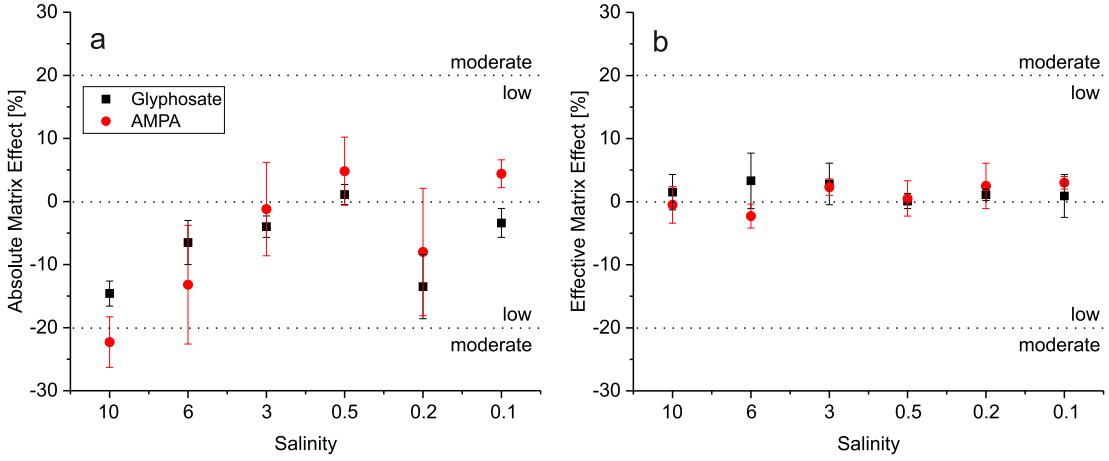

Fig. 2. Absolute (a, analyte signal) and effective (b, analyte signal weighted with IS) matrix effects for glyphosate and AMPA at different salinities after SPE cleanup. Error bars represent the standard deviation from triplicate experiments. Values > 0 represent signal enhancement, values < 0 represent signal suppression.

Table 2
Validation results in terms of determined accuracy (relative error, RE%) and precision (relative standard deviation, RSD%) for both developed methods. During calculation of accuracy in the spiked environmental sample, the natural background value was subtracted before calculation. These values were 16.4 and 123.7 ng/L for glyphosate and AMPA for the small-scale method and 1.17 and 2.91 ng/L for glyphosate and AMPA for the large-scale method.

Small-Scale (5 mL) Method					
(a)		**Glyphosate**		**AMPA**	
	Spike Level		**Precision (RSD%)**		**Precision (RSD%)**
Standard Sample	40 ng/L		6.0%		7.3%
Env. Sample	–		4.2%		0.3%
		Determined Conc. [ng/L]	**Accuracy (RE%)**	**Determined Conc. [ng/L]**	**Accuracy (RE%)**
Standard Sample	40 ng/L	37.2	−7.0%	39.1	−2.2%
Env. Sample	10 ng/L	9.2	−7.5%	11.1	10.9%
Env. Sample	40 ng/L	39.9	−0.1%	39.7	−0.7%
Env. Sample	80 ng/L	80.2	0.3%	80.0	0.0%
Large-Scale (500 mL) Method					
(b)		**Glyphosate**		**AMPA**	
	Spike Level		**Precision (RSD%)**		**Precision (RSD%)**
Standard Sample	1.0 ng/L		0.9%		0.7%
Env. Sample	–		4.1%		5.6%
		Determined Conc. [ng/L]	**Accuracy (RE%)**	**Determined Conc. [ng/L]**	**Accuracy (RE%)**
Standard Sample	1.0 ng/L	1.05	4.8%	0.97	−2.6%
Env. Sample	0.2 ng/L	0.20	−0.2%	0.22	11.8%
Env. Sample	0.5 ng/L	0.53	5.8%	0.49	−2.4%
Env. Sample	1.0 ng/L	1.00	−0.4%	1.00	0.1%

et al. (2017) and Sanchís et al. (2012) both used online-SPE after FMOC-derivatization of 5 and 2 mL water samples, respectively, and achieved LODs of 5 and 3.2 ng/L for glyphosate. The only previous analysis method that was specifically designed for and tested in seawater had LODs of 600 and 300 ng/L for glyphosate and AMPA (Wang et al., 2016). Comparatively, the herein presented method represents a significant improvement in sensitivity. Furthermore, as discussed above, previously reported salt matrix limitations during LC-MS/MS analysis (Skeff et al., 2016; Wang et al., 2016) could be prevented through the herein introduced SPE cleanup step.

The additional preconcentration SPE step employed during the large-scale method resulted in lower LODs of 0.12 and 0.22 ng/L for glyphosate and AMPA. The respective LOQs were 0.17 and 0.31 ng/L. The only previous method for the analysis of glyphosate and AMPA with LODs in the sub-ng/L-range was published by Hanke et al. (2008). They enriched glyphosate-FMOC and AMPA-FMOC on 200 mg Strata-X columns after the derivatization and reported an LOD of 0.2 ng/L for both compounds. However, this procedure has the important disadvantage of producing large amounts of special waste, i.e. 200 mL of derivatization solution for each sample. Moreover, this method was not tested on seawater and, thus, its suitability for this field of application is unknown.

Of course, the increase in method sensitivity that was achieved by introducing an SPE preconcentration step made the sample processing a lot more elaborate. The overall time to process 20 samples with the large-scale method, including preparation, SPE, derivatization and analysis, increased to 4 days, compared to one day with the small-scale method.

We developed the large-scale method with seawater from the brackish Baltic Sea, which has lower salinity ($S \approx 5–20$) than the world oceans ($S \approx 35$). To verify that this salinity difference does not limit the applicability of the method, it was also tested on artificial seawater of salinity 35. Results are shown in the supplemental material (Fig. S7). The achieved peak areas as well as the ratios of analyte to IS were similar in ultrapure water and artificial seawater, which confirms that the MIP-SPE columns are presumably also suitable for the enrichment of glyphosate and AMPA from seawater with $S = 35$.

3.3. Occurrence of glyphosate and AMPA in marine surface water

3.3.1. Warnow Estuary

To assess the performance of the developed small-scale method, 13 environmental samples collected in the Warnow Estuary in the city of Rostock were analyzed. Both glyphosate and AMPA could be detected in the samples (Fig. 3). Highest glyphosate concentrations of 26–28 ng/L were measured at stations close to the Warnow River (no. 1–3). Concentrations generally decreased towards the Baltic Sea and beyond station 9, glyphosate levels fell below LOQ. At the Baltic Sea station (no. 12), the glyphosate concentration was below LOD.

AMPA concentrations at stations near the Warnow river were up to 181 ng/L (no. 3) and, similar to glyphosate, generally decreased towards the Baltic Sea. AMPA was also not detectable beyond the estuary (< LOD, station 12). The sample collected close to the WWTP outlet contained glyphosate and AMPA at concentrations of 106 and 2633 ng/L, respectively. The input from this point source presumably caused the relative increase of AMPA concentrations at stations 8 and 9, downstream from the WWTP outlet. It is important to note that the AMPA that was detected close to the WWTP outlet may not necessarily have originated from glyphosate degradation. AMPA is also the metabolite of several industrial organophosphonates, which are, for example, used as detergents in the textile industry (Jaworska et al., 2002; Nowack, 2003). Therefore, especially given the much higher amounts of AMPA near the WWTP compared to glyphosate, it is likely that at least part of the detected AMPA originated from industrial sources rather than from glyphosate degradation.

Samples from the Warnow River upstream from the estuary have been previously analyzed for glyphosate and AMPA by Skeff et al. (2015) in the summer months of 2012. They reported glyphosate concentrations from < LOD (27 ng/L) to 29 ng/L and AMPA concentrations of 99–150 ng/L. These values compare well to the

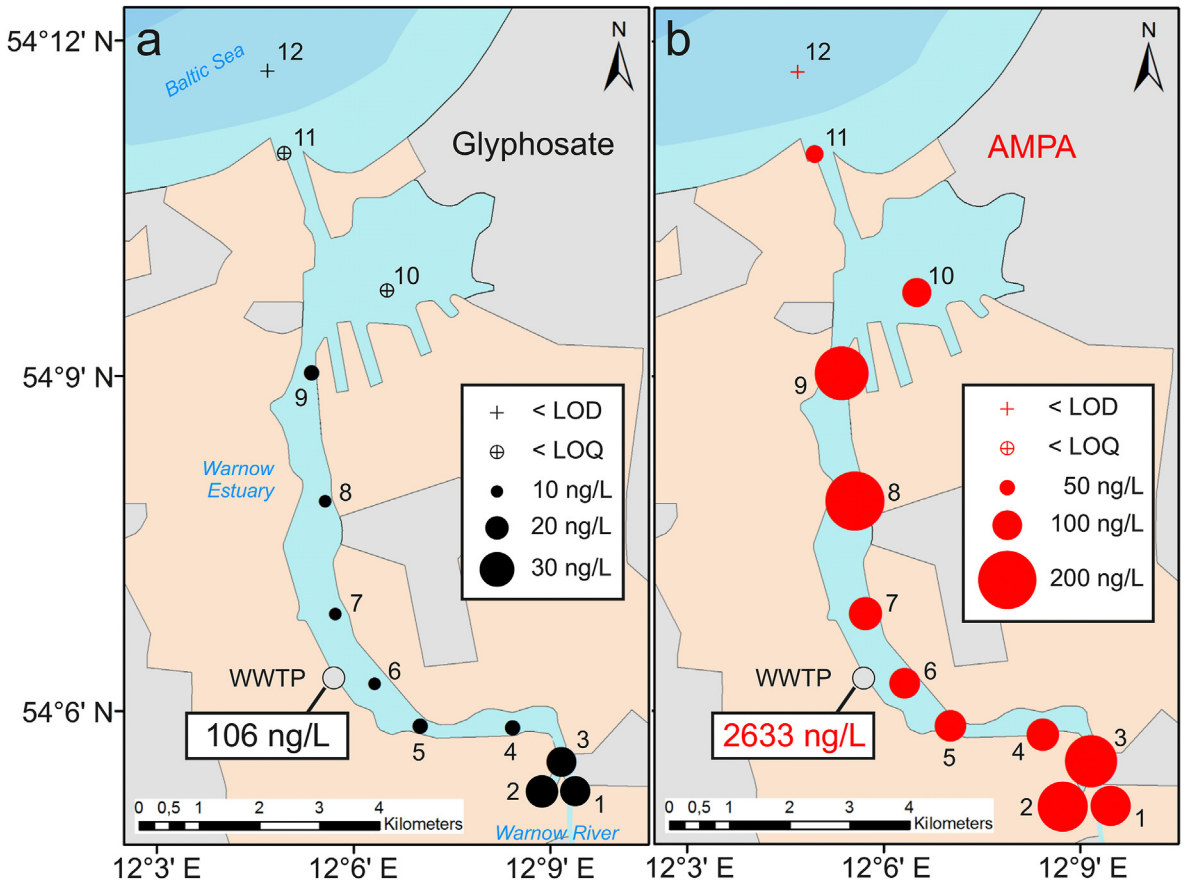

Fig. 3. Determined concentrations of glyphosate (a) and AMPA (b) in the Warnow Estuary in September 2019, measured with the small-scale (5 mL) method.

herein determined concentrations at stations close to the Warnow River (no. 1–3), indicating that glyphosate input into the river has not substantially changed between these years.

The observed decrease in glyphosate and AMPA concentrations towards the Baltic Sea could be owed to degradation and/or dilution of the analytes. The concentration ratio of a parent compound to its transformation product (Equation S9, supplement) can be indicative of environmental fate and transport processes (Battaglin et al., 2005). Smaller ratios suggest spatial or temporal proximity to the application point, while higher ratios hint at increased spatial or temporal distance. The AMPA to glyphosate ratios in the Warnow Estuary (Table S3) were between 5.3 and 18.3. These high ratios generally indicate considerable distance to the herbicide source. From station 1 to 7, ratios consistently increased from 5.3 to 10.2, indicating glyphosate degradation along the flow path. The influence of the WWTP as a considerable AMPA point source is also evident from the ratios (24.9 near WWTP outlet). From stations 8 to 11, ratios consistently decreased from 18.3 down to 7.8. However, since glyphosate levels were < LOQ at stations 10 and 11, the respective calculated ratios have higher uncertainty (Equation S9). The observed ratio decrease in this section of the estuary was apparently brought on by faster decrease of AMPA concentrations towards the Baltic Sea compared to glyphosate (Table S3). This could indicate faster removal of AMPA from surface water under increasingly marine conditions, a trend that was also apparent in the Baltic Sea (see section 3.3.2).

Nonetheless, the measured concentrations of glyphosate and AMPA in the Warnow Estuary also show a linear correlation with the salinity (Fig. 4). This indicates that the observed general concentration decrease is also owed to mixing of water from the Warnow River with saline water from the Baltic Sea, which results in a dilution of glyphosate and AMPA. The influence of the WWTP as a point source is clearly visible for AMPA (Fig. 4b), since the stations downstream from the plant showed higher concentrations despite the increasing dilution with Baltic Sea water. For glyphosate, the WWTP did not cause a significant increase of concentrations at the respective stations (Fig. 4a). In summary, the data provide evidence for the occurrence of both biodegradation and dilution processes that cause a decrease of glyphosate and AMPA in the Warnow Estuary and towards the Baltic Sea.

The data from the Warnow Estuary underline the suitability of the small-scale method for seawater, because the IS signals in the analyzed samples showed little variation between the different stations, even though salinity increased from 1.7 to 16.3 along the transect (Fig. S8). This finding confirms the low matrix sensitivity of the SPE cleanup step and the LC-MS/MS analysis. Nonetheless, the data also highlights the necessity for further analyte enrichment to determine the concentrations of glyphosate and AMPA beyond coastal regions, since both analytes were undetectable beyond the estuary.

3.3.2. Western Baltic Sea

The large-scale method was tested on seven surface water samples collected in the western Baltic Sea in July 2019. Both glyphosate and AMPA could be detected in the samples (Fig. 5). Glyphosate levels were relatively constant between the different stations, with concentrations between 0.42 ng/L (TF012) and 0.49 ng/L (TF046), for all sampling stations except one. The exception was TF022 in the Bight of Lübeck, where a higher glyphosate concentration of 1.22 ng/L was measured. AMPA

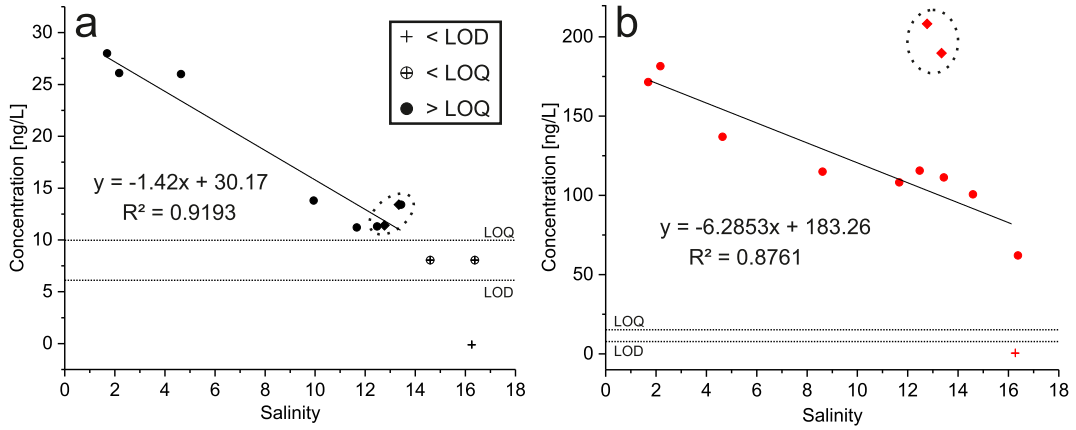

Fig. 4. Correlation between salinity and measured concentration of glyphosate (a) and AMPA (b) in the Warnow Estuary. The circled data points displayed as diamonds (◆) are stations 8 and 9, downstream from the WWTP. They were not included in the regression calculation.

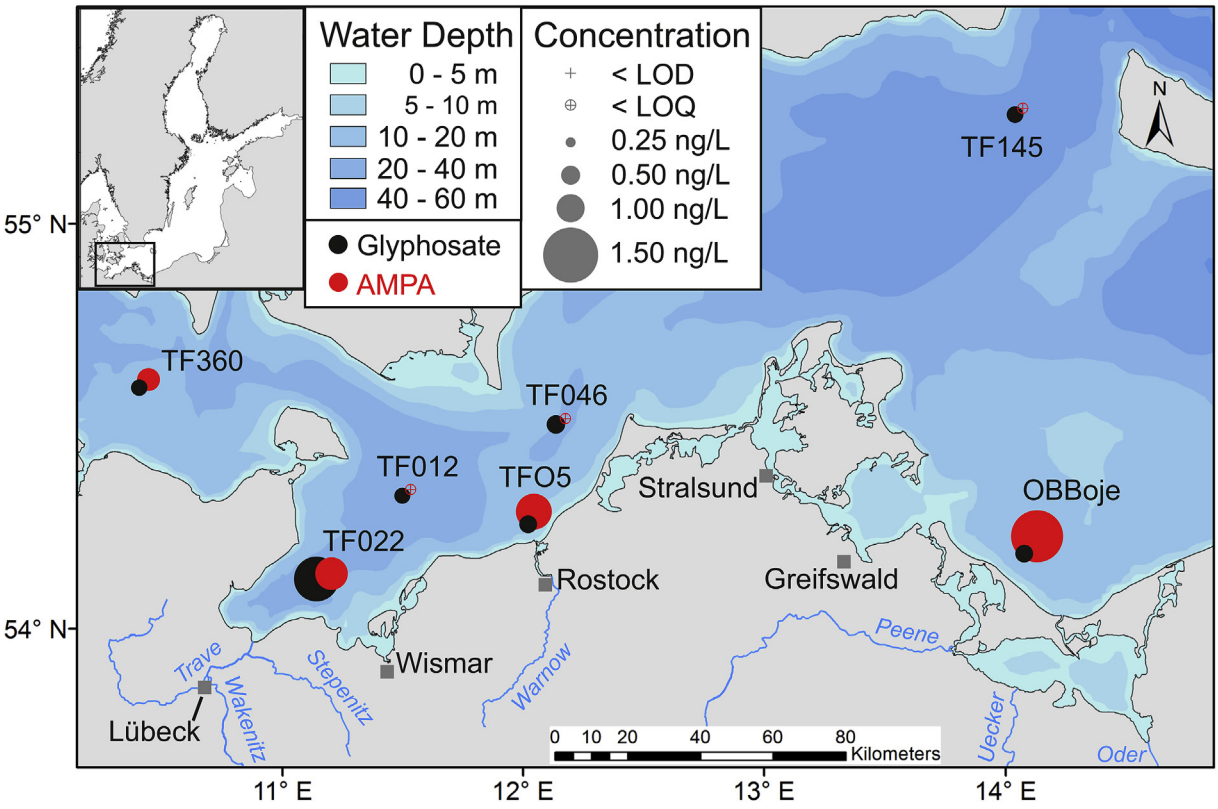

Fig. 5. Concentrations of glyphosate (black) and AMPA (red) in the western Baltic Sea in July 2019 measured with the large-scale (500 mL) method.

concentrations were generally higher at stations close to the coast, e.g., in the Pomeranian Bight close to the mouth of the river Oder (OBBoje, 1.42 ng/L) or close to the Warnow Estuary (TFO5, 0.97 ng/L). At stations further away from the coast, AMPA concentrations fell below LOQ, (stations TF012, TF046 and TF145).

In the summer months of 2012, Skeff et al. (2015) measured glyphosate and AMPA in ten estuaries discharging into the Baltic Sea along the German coast. They could show that most of the sampled rivers transported both compounds into the marine environment and reported highly variable mean concentrations of 29–665 ng/L for glyphosate and 66–1445 ng/L for AMPA. We determined highest concentrations of both glyphosate and AMPA at stations close to estuaries, which indicates that riverine discharge significantly contributes to the measured marine concentrations. Nonetheless, the marine concentrations were much lower compared to riverine values.

Interestingly, our data generally show a much stronger concentration gradient between coastal and offshore stations for AMPA compared to glyphosate (Fig. 5). Moreover, the AMPA to glyphosate ratios were higher at coastal (0.7–3.0) compared to offshore (0.6) stations and were thus, increasingly indicative of close spatial or temporal proximity to the herbicide source. Assuming that both compounds originate from landbased sources, these results are contradictory. A possible explanation is that, contrary to degradation patterns observed in soil (Borggaard and Gimsing, 2008), AMPA is degraded faster in marine surface water than glyphosate.

This deduction is supported by two laboratory studies that investigated the microbial degradation of glyphosate in seawater from the Baltic Sea (Janβen et al., 2019) and the Pacific Ocean (Mercurio et al., 2014). In both experiments, AMPA concentrations remained low compared to glyphosate. This suggested that AMPA was subject to faster biodegradation than glyphosate, which is supported by the herein determined pattern of environmental concentrations. Moreover, both studies concluded that glyphosate might potentially persist in seawater. The herein determined relatively constant glyphosate levels at different Baltic Sea stations provide additional evidence that supports this hypothesis. It should be emphasized that the above considerations were made based on only a small set of samples and can, thus, only be regarded as first hints towards the behavior and transport of glyphosate and AMPA in marine surface water.

4. Conclusion

In the present work, sensitive tools to analyze the herbicide glyphosate and its metabolite AMPA in marine surface water were developed. The SPE enrichment of both compounds from seawater is challenging and can currently only be achieved with a tailored molecularly imprinted polymer. Furthermore, successful application of the developed methods could be demonstrated. To the best of our knowledge, the above presented measurements from the Baltic Sea represent the first report on the occurrence of glyphosate and AMPA in seawater worldwide. We found indications that riverine discharge is likely an important contributor to the measured marine concentrations. Moreover, consistent with previous studies, our data suggest faster degradation of AMPA in marine surface water compared to glyphosate. The newly developed methodology enables monitoring programs and future studies, which can address current research questions, e.g., regarding the transport, persistence and biodegradation of glyphosate and AMPA in the marine environment.

Author statement

Marisa A. Wirth: Conceptualization, Methodology, Validation, Formal analysis, Investigation, Writing - original draft, Writing - review & editing, Visualization. Detlef E. Schulz-Bull: Conceptualization, Writing - review & editing, Supervision, Project administration, Funding acquisition. Marion Kanwischer: Conceptualization, Writing - review & editing, Supervision, Project administration, Funding acquisition.

Funding sources

This work was supported by the funding line strategic networks of the Leibniz Association within the scope of the Leibniz ScienceCampus Phosphorus Research Rostock (W19/2018).

Declaration of competing interest

The authors declare that they have no known competing financial interests or personal relationships that could have appeared to influence the work reported in this paper.

Acknowledgement

We would like to thank the crews or R/V Klaashahn and R/V Elisabeth Mann Borgese for their assistance during sample collection, specifically Ines Hand and Paul Philipp Cwierz. We thank Eva Fritzsche for her preliminary work on the SPE of glyphosate, on which we could build for this study. Furthermore, we thank Niels Nitzsche for his lab assistance during the SPE procedure development. Lastly, we thank the two anonymous reviewers for their helpful comments on the manuscript.

Appendix A. Supplementary data

Supplementary data to this article can be found online at https://doi.org/10.1016/j.chemosphere.2020.128327.

References

Ansari, S., Karimi, M., 2017. Novel developments and trends of analytical methods for drug analysis in biological and environmental samples by molecularly imprinted polymers. Trends Anal. Chem. 89, 146–162. https://doi.org/10.1016/j.trac.2017.02.002.

Battaglin, W.A., Kolpin, D.W., Scribner, E.A., Kuivila, K.M., Sandstrom, M.W., 2005. Glyphosate, other herbicides, and transformation products in Midwestern streams, 2002. J. Am. Water Resour. Assoc. 323–332. https://doi.org/10.1111/j.1752-1688.2005.tb03738.x.

Borggaard, O.K., Gimsing, A.L., 2008. Fate of glyphosate in soil and the possibility of leaching to ground and surface waters: a review. Pest Manag. Sci. 64 (4), 441–456. https://doi.org/10.1002/ps.1512.

Bratinova, S., Raffael, B., Simoneau, C., 2009. Guidelines for Performance Criteria and Validation Procedures of Analytical Methods Used in Controls of Food Contact Materials. European Commision. https://doi.org/10.2788/49046.

Claude, B., Berho, C., Bayoudh, S., Amalric, L., Coisy, E., Nehme, R., Morin, P., 2017. Preliminary recovery study of a commercial molecularly imprinted polymer for the extraction of glyphosate and AMPA in different environmental waters using MS. Environ. Sci. Pollut. Res. Int. 24 (13), 12293–12300. https://doi.org/10.1007/s11356-017-8844-5.

Corbera, M., Hidalgo, M., Salvadó, V., 2006. Extraction and preconcentration of the herbicide glyphosate and its metabolite AMPA using anion-exchange solid phases. Microchim. Acta 153 (3–4), 203–209. https://doi.org/10.1007/s00604-005-0462-0.

Corbera, M., Hidalgo, M., Salvadó, V., Wieczorek, P.P., 2005. Determination of glyphosate and aminomethylphosphonic acid in natural water using the capillary electrophoresis combined with enrichment step. Anal. Chim. Acta 540 (1), 3–7. https://doi.org/10.1016/j.aca.2004.12.028.

Coupe, R.H., Kalkhoff, S.J., Capel, P.D., Gregoire, C., 2012. Fate and transport of glyphosate and aminomethylphosphonic acid in surface waters of agricultural basins. Pest Manag. Sci. 68 (1), 16–30. https://doi.org/10.1002/ps.2212.

Daouk, S., Copin, P.J., Rossi, L., Chevre, N., Pfeifer, H.R., 2013. Dynamics and environmental risk assessment of the herbicide glyphosate and its metabolite AMPA in a small vineyard river of the Lake Geneva catchment. Environ. Toxicol. Chem. 32 (9), 2035–2044. https://doi.org/10.1002/etc.2276.

Delmonico, E.L., Bertozzi, J., de Souza, N.E., Oliveira, C.C., 2014. Determination of glyphosate and aminomethylphosphonic acid for assessing the quality tap water using SPE and HPLC. Acta Sci. Technol. 3, 513–519. https://doi.org/10.4025/actascitechnol.v36i3.22406.

Duke, S.O., Powles, S.B., 2008. Glyphosate: a once-in-a-century herbicide. Pest Manag. Sci. 64 (4), 319–325. https://doi.org/10.1002/ps.1518.

Economou, A., Botitsi, H., Antoniou, S., Tsipi, D., 2009. Determination of multi-class pesticides in wines by solid-phase extraction and liquid chromatography-tandem mass spectrometry. J. Chromatogr., A 1216 (31), 5856–5867. https://doi.org/10.1016/j.chroma.2009.06.031.

Glass, R.L., 1987. Adsorption of glyphosate by soils and clay minerals. J. Agric. Food Chem. 35, 497–500. https://doi.org/10.1021/jf00076a013.

Gosetti, F., Mazzucco, E., Zampieri, D., Gennaro, M.C., 2010. Signal suppression/enhancement in high-performance liquid chromatography tandem mass spectrometry. J. Chromatogr. A 1217 (25), 3929–3937. https://doi.org/10.1016/j.chroma.2009.11.060.

Gros, P., Ahmed, A., Kuhn, O., Leinweber, P., 2017. Glyphosate binding in soil as revealed by sorption experiments and quantum-chemical modeling. Sci. Total Environ. 586, 527–535. https://doi.org/10.1016/j.scitotenv.2017.02.007.

Hanke, I., Singer, H., Hollender, J., 2008. Ultratrace-level determination of glyphosate, aminomethylphosphonic acid and glufosinate in natural waters by solid-phase extraction followed by liquid chromatography-tandem mass spectrometry: performance tuning of derivatization, enrichment and detection. Anal. Bioanal. Chem. 391 (6), 2265–2276. https://doi.org/10.1007/s00216-008-2134-5.

Hidalgo, C., Rios, C., Hidalgo, M., Salvado, V., Sancho, J.V., Hernandez, F., 2004. Improved coupled-column liquid chromatographic method for the determination of glyphosate and aminomethylphosphonic acid residues in environmental waters. J. Chromatogr., A 1035 (1), 153–157. https://doi.org/10.1016/j.chroma.2004.02.044.

Huntscha, S., Stravs, M.A., Buhlmann, A., Ahrens, C.H., Frey, J.E., Pomati, F., Hollender, J., Buerge, I.J., Balmer, M.E., Poiger, T., 2018. Seasonal dynamics of glyphosate and AMPA in lake greifensee: rapid microbial degradation in the epilimnion during summer. Environ. Sci. Technol. 52 (8), 4641–4649. https://doi.org/10.1021/acs.est.8b00314.

Ibanez, M., Pozo, O.J., Sancho, J.V., Lopez, F.J., Hernandez, F., 2005. Residue

determination of glyphosate, glufosinate and aminomethylphosphonic acid in water and soil samples by liquid chromatography coupled to electrospray tandem mass spectrometry. J. Chromatogr., A 1081 (2), 145–155. https://doi.org/10.1016/j.chroma.2005.05.041.

Janßen, R., Skeff, W., Werner, J., Wirth, M.A., Kreikemeyer, B., Schulz-Bull, D., Labrenz, M., 2019. A glyphosate pulse to brackish long-term microcosms has a greater impact on the microbial diversity and abundance of planktonic than of biofilm assemblages. Front. Mar. Sci. 6 https://doi.org/10.3389/fmars.2019.00758.

Jaworska, J., Van Genderen-Takken, H., Hanstveit, A., van de Plassche, E., Feijtel, T., 2002. Environmental risk assessment of phosphonates, used in domestic laundry and cleaning agents in The Netherlands. Chemosphere 47, 655–665. https://doi.org/10.1016/S0045-6535(01)00328-9.

Jiang, J., Lucy, C.A., 2007. Determination of glyphosate using off-line ion exchange preconcentration and capillary electrophoresis-laser induced fluorescence detection. Talanta 72 (1), 113–118. https://doi.org/10.1016/j.talanta.2006.10.001.

Kanwischer, M., Wirth, M.A., Schulz-Bull, D.E., 2019. Analyse von organischen Spurenstoffen in der Ostsee. WasserFORUM 11, 54–56.

Küsters, M., Gerhartz, M., 2010. Enrichment and low-level determination of glyphosate, aminomethylphosphonic acid and glufosinate in drinking water after cleanup by cation exchange resin. J. Separ. Sci. 33, 1139–1146. https://doi.org/10.1002/jssc.200900556.

Le Fur, E., Colin, R., Charrêteur, C., Dufau, C., Péron, J.J., 2000. Determination of glyphosate herbicide and aminomethylphosphonic acid in natural waters by liquid chromatography using pre-column fluorogenic labeling. Part I: direct determination at the 0.1 μg/L level using FMOC. Analusis 28 (9), 813–818. https://doi.org/10.1051/analusis:2000148.

Mercurio, P., Flores, F., Mueller, J.F., Carter, S., Negri, A.P., 2014. Glyphosate persistence in seawater. Mar. Pollut. Bull. 85 (2), 385–390. https://doi.org/10.1016/j.marpolbul.2014.01.021.

Milan, M., Dalla Rovere, G., Smits, M., Ferraresso, S., Pastore, P., Marin, M.G., Bogialli, S., Patarnello, T., Bargelloni, L., Matozzo, V., 2018. Ecotoxicological effects of the herbicide glyphosate in non-target aquatic species: transcriptional responses in the mussel Mytilus galloprovincialis. Environ. Pollut. 237, 442–451. https://doi.org/10.1016/j.envpol.2018.02.049.

Miller, J.N., 1991. Basic statistical methods for analytical chemistry Part 2. Calibration and regression methods. A review. Analyst 116, 3–14. https://doi.org/10.1039/AN9911600003.

Montiel-León, J.M., Munoz, G., Duy, S.V., Do, D.T., Vaudreuil, M.-A., Goeury, K., Guillemette, F., Amyot, M., Sauvé, S., 2019. Widespread occurrence and spatial distribution of glyphosate, atrazine, 2 and neonicotinoids pesticides in the St. Lawrence and tributary rivers. Environ. Pollut. 250, 29–39. https://doi.org/10.1016/j.envpol.2019.03.125.

Nowack, B., 2003. Environmental chemistry of phosphonates. Wat. Res. 37 (11), 2533–2546. https://doi.org/10.1016/s0043-1354(03)00079-4.

Patsias, J., Papadopoulou, A., Papadopoulou-Mourkidou, E., 2001. Automated trace level determination of glyphosate and aminomethyl phosphonic acid in water by on-line anion-exchange solid-phase extraction followed by cation-exchange liquid chromatography and post-column derivatization. J. Chromatogr. A 932, 83–90. https://doi.org/10.1016/s0021-9673(01)01253-5.

Pinto, E., Soares, A.G., Ferreira, I.M., P L V O, 2018. Quantitative analysis of glyphosate, glufosinate and AMPA in irrigation water by in situ derivatization–dispersive liquid–liquid microextraction combined with UPLC-MS/MS. Anal. Meth. 10 (5), 554–561. https://doi.org/10.1039/c7ay02722b.

Poiger, T., Buerge, I.J., Balmer, M.E., Bächli, A., Müller, M.D., 2017. Occurrence of the herbicide glyphosate and its metabolite AMPA in surface waters in Switzerland determined with on-line solid phase extraction LC-MS/MS. Environ. Sci. Pollut. Res. 24, 1588–1596. https://doi.org/10.1007/s11356-016-7835-2.

Richmond, M.E., 2018. Glyphosate: a review of its global use, environmental impact, and potential health effects on humans and other species. J. Environ. Stud. Sci. 8, 416–434. https://doi.org/10.1007/s13412-018-0517-2.

Sanchís, J., Kantiani, L., Llorca, M., Rubio, F., Ginebreda, A., Fraile, J., Garrido, T., Farré, M., 2012. Determination of glyphosate in groundwater samples using an ultrasensitive immunoassay and confirmation by on-line solid-phase extraction followed by liquid chromatography coupled to tandem mass spectrometry. Anal. Bioanal. Chem. 402, 2335–2345. https://doi.org/10.1007/s00216-011-5541-y.

Silva, V., Montanarella, L., Jones, A., Fernandez-Ugalde, O., Mol, H.G.J., Ritsema, C.J., Geissen, V., 2018. Distribution of glyphosate and aminomethylphosphonic acid (AMPA) in agricultural topsoils of the European Union. Sci. Total Environ. 621, 1352–1359. https://doi.org/10.1016/j.scitotenv.2017.10.093.

Skeff, W., Neumann, C., Schulz-Bull, D.E., 2015. Glyphosate and AMPA in the estuaries of the Baltic Sea method optimization and field study. Mar. Pollut. Bull. 100 (1), 577–585. https://doi.org/10.1016/j.marpolbul.2015.08.015.

Skeff, W., Recknagel, C., Schulz-Bull, D.E., 2016. The influence of salt matrices on the reversed-phase liquid chromatography behavior and electrospray ionization tandem mass spectrometry detection of glyphosate, glufosinate, aminomethylphosphonic acid and 2-aminoethylphosphonic acid in water. J. Chromatogr. A 1475, 64–73. https://doi.org/10.1016/j.chroma.2016.11.007.

Stachowski-Haberkorn, S., Becker, B., Marie, D., Haberkorn, H., Coroller, L., de la Broise, D., 2008. Impact of Roundup on the marine microbial community, as shown by an in situ microcosm experiment. Aquat. Toxicol. 89 (4), 232–241. https://doi.org/10.1016/j.aquatox.2008.07.004.

Trufelli, H., Palma, P., Famiglini, G., Cappiello, A., 2011. An overview of matrix effects in liquid chromatography mass spectrometry. Mass Spectrom. Rev. 30, 491–509. https://doi.org/10.1002/mas.20298.

Tsui, M.T.K., Chu, L.M., 2003. Aquatic toxicity of glyphosate-based formulations: comparison between different organisms and the effects of environmental factors. Chemosphere 52 (7), 1189–1197. https://doi.org/10.1016/s0045-6535(03)00306-0.

Wang, S., Liu, B., Yuan, D., Ma, J., 2016. A simple method for the determination of glyphosate and aminomethylphosphonic acid in seawater matrix with high performance liquid chromatography and fluorescence detection. Talanta 161, 700–706. https://doi.org/10.1016/j.talanta.2016.09.023.

Wirth, M.A., Sievers, M., Habedank, F., Kragl, U., Schulz-Bull, D.E., Kanwischer, M., 2019. Electrodialysis as a sample processing tool for bulk organic matter and target pollutant analysis of seawater. Mar. Chem. 217, 103719. https://doi.org/10.1016/j.marchem.2019.103719.

Publication 3

Methodological aspects of methylphosphonic acid analysis: Determination in river and coastal water samples

by

Constantin Lohrer, Paul P. Cwierz, **Marisa A. Wirth**, Detlef E. Schulz-Bull, Marion Kanwischer

Talanta

Year 2020, Volume 211, Page 120724 ff.

DOI: 10.1016/j.talanta.2020.120724

Talanta 211 (2020) 120724

Contents lists available at ScienceDirect

Talanta

journal homepage: www.elsevier.com/locate/talanta

Methodological aspects of methylphosphonic acid analysis: Determination in river and coastal water samples

Constantin Lohrer*, Paul P. Cwierz, Marisa A. Wirth, Detlef E. Schulz-Bull, Marion Kanwischer

Leibniz Institute for Baltic Sea Research Warnemuende, Department of Marine Chemistry, Seestrasse 15, 18119, Rostock, Germany

ARTICLE INFO

Keywords:
Methylphosphonic acid
Solid-phase extraction
Brackish water
GC/MS
Electrodialysis

ABSTRACT

Methylphosphonic acid (MPn) is suspected to play an important role in aquatic systems like rivers or the open ocean. To gain more insights into the importance of MPn, e.g., for the aquatic phosphorus cycle, an analytical method for its quantitative determination was developed. The method is based on the use of an isotopically-labelled internal standard and sample preparation including solid-phase extraction (SPE). Instrumental detection was done using GC-MS after derivatisation of MPn with *N-tert*-Butyldimethylsilyl-*N*-methyltrifluoroacetamide (MTBSTFA). The study compares different isotopically-labelled compounds as well as different SPE-materials. As water samples with high salt content decrease the recovery of the chosen SPE-material, a desalting procedure using electrodialysis was implemented. Finally, water samples from different aquatic systems located at the German Baltic Sea coastal area were analysed to gain first insights into the relevance of MPn in these systems. MPn-concentrations in the low µg/L-range were detected.

1. Introduction

Naturally occurring organophosphonates comprise a class of P organic compounds, whose origin and function still is a puzzling subject of environmental research. Since organophosphonates contain a C–P bond, organisms require a different enzyme apparatus and more energy for their biochemical utilization compared to the oxygen-containing C–O–P phosphate ester group, which is the fundamental biochemical backbone for current life [1].

Organophosphonates are considered as the preceding form of phosphate in early life forms. However, they remained at particular sites at which their presence presumably is advantageous to life. In this regard, it was shown through ^{31}P nuclear magnetic resonance (^{31}P NMR) analysis that phosphonates make up 25% of the marine high molecular weight dissolved organic phosphorus pool [2]. Therefore, organophosphonate compounds presumably relevantly contribute to the marine biogeochemical P-cycle. Metabolic pathways for C–P cleavage have been conserved among a number of organisms in particular for those of the marine environment. It was shown that under P starvation conditions, in particular, methylphosphonic acid (MPn) was utilized by marine bacteria; *vice versa* for some marine microorganisms, the presence of an MPn synthesis was shown, too [3,4]. In this regard, MPn receives great interest, as it is discussed in view of the methane paradox in the aquatic environment [4–7].

However, there is limited information on concentrations of this small organophosphonate compound in the environment, which is probably due to the ionic behaviour conferred through the phosphonate group and, therefore, the high solubility in water.

There are several analytical methods for the determination of MPn in different sample matrices. These methods are mostly described in the context of chemical warfare analysis, as MPn is also a degradation product of organophosphorus nerve agents [8], and most of them base on gas chromatography (GC) [8–11] or liquid chromatography (LC) [12–14] coupled to mass spectrometry (MS). For MPn analysis through GC, a derivatisation step, e.g. methylation or silylation [15], is required to confer sufficient volatility for GC separation. Methods based on LC can also involve a derivatisation step, either to change the chromatographic behaviour [12] or to increase the sensitivity of the detection method [16].

When using silylation reactions for derivatisation, the separation of MPn from the water matrix is necessary, as silyl reagents are sensitive to water. However, a direct extraction with an organic solvent is not possible due to the ionic behaviour of MPn. To accomplish this, selected methods dry the sample with a stream of nitrogen gas or employ a rotary evaporator [8,12,17]. This is only useful when small amounts of water sample are used, and also if other matrix components are not disturbing the derivatisation of MPn. Another useful technique for sample preparation is solid-phase extraction (SPE). There are several

* Corresponding author.
E-mail address: constantin.lohrer@io-warnemuende.de (C. Lohrer).

https://doi.org/10.1016/j.talanta.2020.120724
Received 29 July 2019; Received in revised form 3 January 2020; Accepted 7 January 2020
Available online 07 January 2020
0039-9140/

methods which exploit strong anion-exchange materials [11,18–22]. However, only Kataoka et al. investigated the influence of saltwater on the recovery of MPn with anion exchange-materials and found a recovery of ~60% [19]. Owens and Koester used a reversed-phase SPE method and reported a recovery of 16–60% for MPn in different beverages [13]. The use of liquid-liquid extraction with nonpolar organic solvents is not possible due to the ionic behaviour of MPn in water and its low solubility in nonpolar organic solvents [23].

Many of these methods have in common that the high amount of salt in the studied water samples may cause negative effects during SPE enrichment and sample analysis (e.g. chromatographic behaviour, derivatisation yield). Therefore, desalination of the matrix before further analysis should improve the performance of the analytical methods. Such a reduction of the salt matrix can be achieved by subjecting the samples to electrodialysis [24–26].

Herein, we report on further method development for the analysis of MPn in river and coastal water based on sample purification and enrichment through SPE with subsequent silylation and GC-MS analysis. We present data on the usage of two types of internal standard for MPn quantification and show our investigations on two different SPE-materials and their performance using salt-containing samples. The resulting method was validated in terms of accuracy and precision. Its analytical performance was described with figures of merit and accuracy studies were conducted using the elliptic joint confidence region (EJCR) test. In addition, we tested electrodialysis for sample processing in order to reduce the saline matrix load for coastal marine water. Finally, the developed method was tested for the analysis of MPn in riverine and coastal water samples in Mecklenburg-Western Pomerania, Germany.

2. Experimental

2.1. Chemicals and reagents

Methylphosphonic acid (98% purity) was purchased from VWR International GmbH (Hannover, Germany) and stock and working solutions were prepared using MilliQ-water (18.2 MΩ, Merck Millipore, Schwalbach, Germany). Deuterated methylphosphonic acid (D_3-MPn, 98% purity, 100 µg/mL in methanol, Sigma-Aldrich, Taufkirchen, Germany) was used as internal standard (IS) and working solutions were prepared with MilliQ-water as well. ^{13}C-methylphosphonic acid (99 atom-% ^{13}C, 98% purity, Sigma-Aldrich, Taufkirchen, Germany) was prepared by dissolving 10 mg in 10 mL LC-MS grade water (VWR International GmbH, Hannover, Germany) resulting in a 1 g/L-stock solution and tested as internal standard during method development.

Acetonitrile (ACN) and methanol (MeOH) were purchased from Walter-CMP (Kiel, Germany) and were of LC-MS grade. Barrelled n-hexane was obtained from Mallinkrodt Baker B. V and was purified through distillation. Ammonia solution 32% (v/v) in water was purchased from VWR International GmbH. *N-tert*-Butyldimethylsilyl-*N*-methyltrifluoroacetamide (MTBSTFA) with 1% *tert*-Butyldimethylchlorosilane (TBDMSCl) (assay ≥95%) was obtained from VWR. Sodium sulphate (Merck KGaA) and GC vials were combusted at 450 °C for 15 h. Artificial seawater for method development and electrodialysis was prepared using Tropic Marin® Sea Salt Classic (Tropic Marin AG, Hünenberg, Switzerland).

2.2. Sampling

Sampling was conducted in summer 2017 and 2018 as well as in winter 2018/2019 from freshwater, brackish and coastal waters. Surface water samples were collected from the Mühlenfließ (MF), a small tributary to the Baltic Sea, and the river Warnow in the German federal state Mecklenburg-Western Pomerania (Table 1). The Warnow is characterised by a large lowland catchment area discharging into the Baltic Sea (for a detailed description see Bitschofsky and Nausch, [27]). Samples were obtained from the upper freshwater course (W-1 to W-9) and from the brackish water part influenced through Baltic Sea coastal water (W-10). Baltic Sea coastal water samples were obtained from the pier at the site Heiligendamm (HD). The water samples were collected from a river bank or from bridges and filled into pre-rinsed polypropylene bottles. They were stored at −20 °C until further analysis.

2.3. Sample preparation

The final sample preparation included an enrichment and purification step on Strata-X-AW (500 mg/3 mL, Phenomenex, Aschaffenburg, Germany) cartridges with subsequent derivatisation of MPn to its silylated derivative. For this, the cartridges were conditioned with 5 mL methanol and water each. A volume of 5 mL water sample was spiked with the internal standard and directed through the column with a flow rate of approx. 1–2 mL/min. The column was washed with 2 mL MilliQ-water and methanol each and dried thereafter with a stream of nitrogen. Elution was conducted with 10 mL of 5% (v/v) NH_3 in methanol. The eluates were evaporated to dryness at 40 °C under a stream of clean-air (TurboVap, LV, Zymark, USA).

Derivatisation was done according to previously published protocols [8,9,28] with slight modifications. Thus, 100 µL ACN and 50 µL MTBSTFA were added to the dried sample and the reaction mixture was incubated for 2 h at 60 °C in a water bath. To extract the derivatisation products, 100 µL MilliQ-water and 250 µL *n*-hexane were added, the suspension was vortexed and centrifuged for phase separation (10 min, 1000 rpm). The above hexane layer was shortly dried on sodium sulphate and transferred into a GC-vial for GC-MS analysis.

During method development, sample preparations varied. For those data, methodological differences are stated in the further descriptions.

2.4. Instrumentation and GC-MS analysis of MPn-Derivatives

Analysis of derivatised methylphosphonic acid was conducted on a Trace-DSQ-GC-MS system (Thermo Fisher Scientific, Waltham, USA) equipped with a TriPlus autosampler. A DB-5MS capillary column (60 m × 0.25 mm I.D., 0.25 µm film thickness, Agilent, Waldbronn, Germany) was used for gas chromatographic separation. A sample volume of 1 µL was injected into the heated injector (50 °C) operating in splitless mode with a purge time of 1 min and a purge flow of 50 mL/min. Helium was used as carrier gas with an initial flow of 1.5 L/min. The oven temperature program started at a temperature of 50 °C for 1 min following a temperature ramp of 10 °C/min to a temperature of 220 °C and with a second ramp of 20 °C/min to 280 °C with a final hold for 20 min. The transfer line was set to 250 °C and the MS source to 240 °C. Electron impact (70 eV) was used for ionization.

Full scan mode (m/z = 50–550) was used to identify the retention times of the analytes and to determine the characteristic mass fragments, which were m/z = 267 and 309 for MPn and m/z = 270 and 312 for D_3-MPn. However, as the mass fragments m/z = 309, 312 had an abundance of only 4.5% of the more intensive fragments, we excluded them from the observation. Quantitative analysis was performed in the SIM mode with a dwell time of 100 ms for the monitored fragments.

Operation of the GC-MS system and evaluation of the data was done with XCalibur 3.0 (Thermo, USA). Only data with a signal-to-noise ratio (S/N) above 3 were used for further evaluation.

2.5. Calibration and quantification

D_3-MPn was used as internal standard (IS). Within this study, different concentration ranges of MPn were studied. For precise quantification including the low concentration range, calibrations for three concentration ranges were obtained. For each calibration range, a different amount of IS was used (Table Suppl. 2).

For validation, precision (RSD%) and accuracy (RE) were determined as described in Equations Suppl. 1 and 2.

Table 1
List of stations for the sampling of surface water including the corresponding sampling dates, the salinity and the detected MPn-concentration (n.d.: not detected, *: result achieved by exponential extrapolation).

Station	Coordinates	Sampling date	Salinity S [PSU scale]	MPn [µg/L]
Mühlenfließ (MF)	N54° 07.02 E11° 54.87	November 22, 2018	0.3	n.d.
Heiligendamm (HD)	N54° 08.78 E11° 50.60	September 25, 2018 /February 26, 2019	12.8 /10.4	1.8*
Warnow-1 (W1)	N53° 43.07 E11° 44.87	August 02, 2017	0.25	n.d.
Warnow-2 (W2)	N53° 44.70 E11° 49.95	August 02, 2017	0.26	n.d.
Warnow-3 (W3)	N53° 47.06 E11° 50.29	August 02, 2017	0.25	n.d.
Warnow-4 (W4)	N53° 50.27 E11° 58.55	August 01, 2017	0.26	n.d.
Warnow-5 (W5)	N53° 53.79 E12° 05.79	August 01, 2017	0.28	n.d.
Warnow-6 (W6)	N53° 56.85 E12° 07.25	August 01, 2017	0.29	n.d.
Warnow-7 (W7)	N54° 03.85 E12° 10.27	July 31, 2017 /December 07, 2018	0.29 /0.1	n.d. /0.41
Warnow-8 (W8)	N54° 04.69 E12° 09.26	December 07, 2018	0.1	0.47
Warnow-9 (W9)	N54° 05.03 E12° 09.08	July 31, 2017 /December 07, 2018	0.29 /0.1	n.d. /0.57
Warnow-10 (W10)	N54° 05.22 E12° 09.13	December 07, 2018	1.1	n.d.

2.6. Electrodialysis

The water sample collected at station Heiligendamm (HD) was subjected to electrodialysis (ED), in order to reduce their salt content and possibly improve the recovery of the subsequent SPE step. The procedure was conducted with an ED system from Deukum GmbH (Frickenhausen, Germany) as described by Wirth et al. [26]. In an electrodialysis cell, anion- and cation exchange membranes are alternatingly positioned between a set of electrodes. The sample (diluate) and a receiving solution (concentrate) are circulated through the alternating interspaces between the membranes. An electric field is applied perpendicular to the membrane surfaces, which causes salt ions in the diluate to be transported through the membranes and into the concentrate. A third solution (electrode rinse) is circulated along the electrodes to carry off oxygen and hydrogen gas formed due to water splitting at the electrodes.

The ED system was carefully cleaned with aqueous HCl (pH 2, 3%) and MilliQ water before sample processing. Afterwards, the filtered sample (GF/F filters Ø 47 mm, 0.7 µm; Whatman GmbH, Dassel, Germany) was filled into the diluate channel. The concentrate was a 0.2 g/L salt solution prepared with artificial sea salt in MilliQ water. The electrode rinse was a 5 g/L Na_2SO_4 solution prepared in MilliQ water. During the ED run, the diluate and concentrate were circulated in the system at a flow rate of 50 L/h, while the electrode rinse was circulated at 125 L/h. Desalination of the sample is achieved through the electric field provided by the laboratory power supply. The supplied current was adjusted so that it never exceeded 80% of the limiting current. In order to maintain the concentration gradient along with the membrane stack, ~80% of the concentrate was replaced with MilliQ water whenever concentrate conductivity was 2 mS/cm above diluate conductivity.

Subsamples from the diluate tank were taken at the beginning, as well as at conductivities of 15, 10, 5, 2.5, 1, 0.5 and 0.2 mS/cm. At 25 °C, this corresponds to salinities of 8.7, 5.6, 2.7, 1.3, 0.5, 0.2 and 0.1. After the final subsamples were taken, the current was switched off, the solutions were drained from the system and their residual volume was measured. Subsamples taken during the ED run were stored frozen at −20 °C until analysis.

The determined MPn concentrations were corrected for sample volume loss that occurred during the ED process. Small amounts of water (~0.2–0.4 L) are transported through the membranes alongside the salt. Therefore, the theoretical sample volume was corrected as described in Wirth et al. [26]. MPn recoveries were calculated using the determined concentrations and the sample volume, which was corrected for water loss and subsample removal.

Initially, to test the retention of MPn during the ED process, a coastal Heiligendamm water sample (Table 1) was spiked with MPn and processed in triplicate (MPn concentration in the ED start sample about 1 mg/L, see Wirth et al. [26]). During the ED, subsamples were taken at distinct sample conductivities and analysed for MPn.

3. Results and discussion

3.1. Instrumental calibration and validation

It was the aim to quantify MPn through the use of an isotopically-labelled internal standard. The ^{13}C-MPn and the D_3-MPn are currently commercially available. The ^{13}C-MPn has a mass difference of only 1 Da to the natural MPn. However, within our studies, we evaluated using ^{13}C-MPn as an internal standard as well. For this, a calibration in the range of 0.27–2.77 µg/mL was prepared (MPn-concentration in the measured solution, Fig. 1) and a non-linear course of the calibration curve, even at small MPn amounts, was observed. A statistical assessment revealed that a non-linear regression model fits best (Mandel: TV = 18.48, F(f1 = 1, f2 = N-3, P = 99%) = 12.25). It was discussed before by Rule et al. [29] that when using an isotopically-labelled compound as internal standard, interferences between the analyte and the internal standard may occur, leading to this non-linear behaviour. In the present case, the mass difference between the analyte and the internal standard was only 1 Da and, therefore, such interferences might play a crucial role.

Examination of the obtained mass spectra (Fig. 1) revealed an isotopic peak for natural MPn (m/z = 268), which overlays with the mass fragment of the ^{13}C-MPn used for quantification. Moreover, the signal of the mass fragment m/z = 266.9 of ^{13}C-MPn contributes to one of the characteristic mass fragments of ^{12}C-MPn. This is what Rule et al. described as the basic underlying cause for the interference [29]. Therefore, the non-linear fitting curve of the calibration data was calculated according to their study with Equation Suppl. 3 and compared to a linear fit. Obtained R^2-values for both regression models indicate a higher correlation to the fitted non-linear regression (R^2 = 0.997) than for the linear (R^2 = 0.967). As it can be seen in Fig. 1, using a linear regression model might cause overestimation of the concentration levels in the low and high concentration ranges and underestimation in the middle concentration range, which is in agreement with the results obtained by Rule et al. [29].

Since the deuterated MPn (D_3-MPn) internal standard has a mass difference of 3 Da to the natural MPn, linearity over a wide MPn mass range can be assumed. We obtained calibrations with the D_3-MPn as internal standard up to 2 µg/mL of MPn (Fig. 2, Table Suppl. 2) and the linearity test (F-test) revealed that a linear regression model fits best for all measured concentration ranges (see Table Suppl. 2 for further figures of merit of the calibration).

To further characterize the method, the instrumental limit of detection (LOD, resp. detection capability L_D [30]) was assessed from the calibrations as described by Miller and Miller (Equation Suppl. 4) [31] and was 0.008 µg/mL respectively 8 µg/L (MPn-concentration in the final measured solution). This is in the same range as another method published before by Baygildiev et al., which was based on LC-MS/MS and was characterised by a LOD of 10 µg/L [14]. Compared to other

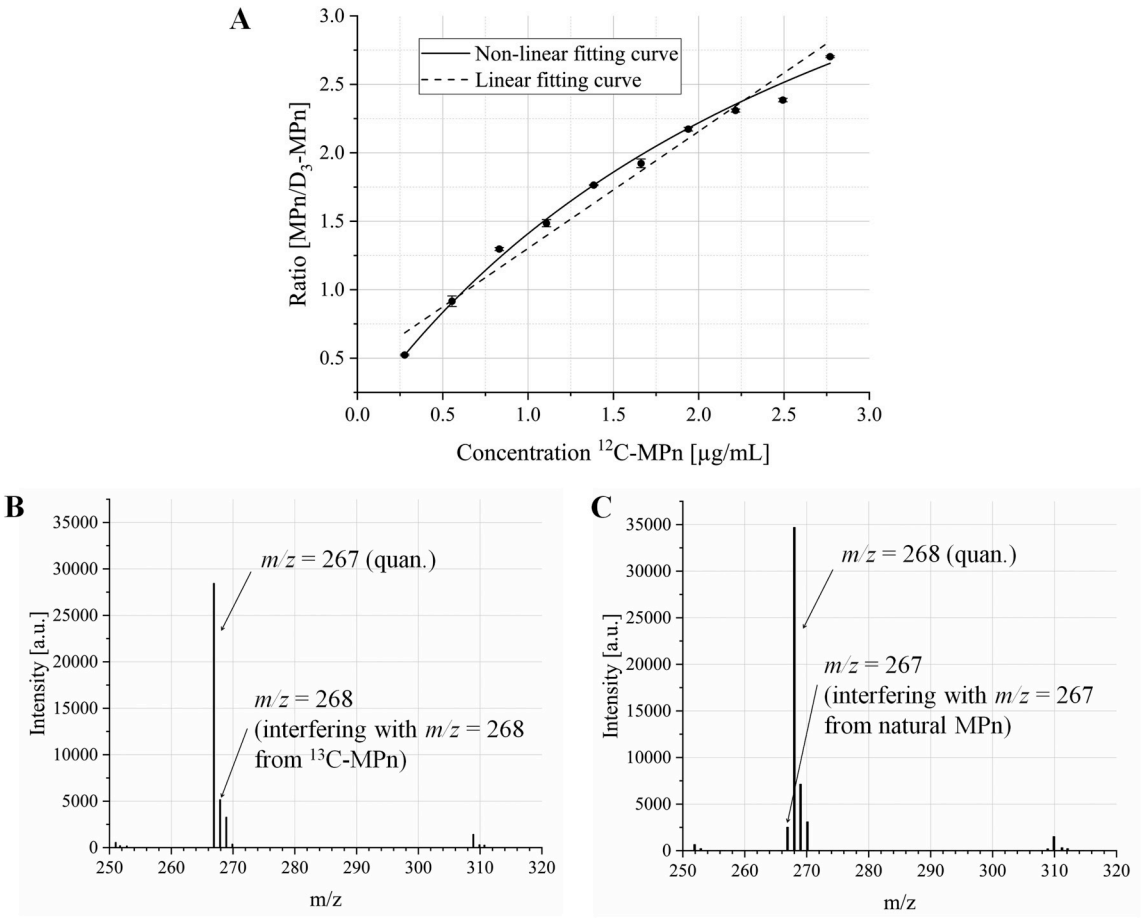

Fig. 1. A: Calibration of MPn using ^{13}C-MPn as internal standard (c = 0.333 µg/mL in measured solution). A linear fit as well as a non-linear fit are shown. Here, the samples were derivatised at 80 °C for 2 h in ACN/MTBSTFA (100 µL/50 µL). Afterwards the solution was diluted 1:10 with ACN and directly conducted to GC-MS-analysis. Each data point was achieved by triplicate injection; B: Mass spectra of the derivatised natural ^{12}C-MPn standard in the range of *m/z* = 250–320 (c = 0.243 µg/mL in measured solution); C: Mass spectra of the derivatised ^{13}C-MPn standard in the range of *m/z* = 250–320 (c = 0.666 µg/mL in measured solution).

GC-MS-based methods by Richardson and Caruso (LOD = 5 µg/L, [8]) or by Singh et al. (LOD = 0.1 µg/L, [11]), our method showed a slightly higher LOD [8,11]. For this current study, we decided to continue with the D_3-MPn as internal standard compound.

For quality assurance, MPn control samples were regularly included into sample sequences to verify the instrumental calibration (e.g., Table Suppl. 3A). The obtained data show that the described method leads to satisfying results for MPn-analysis for the tested combinations. Accuracy was mostly below 20%; however, in the lower concentration range, higher uncertainties must be considered. With RSD of less than 15%, the method can be considered as precise.

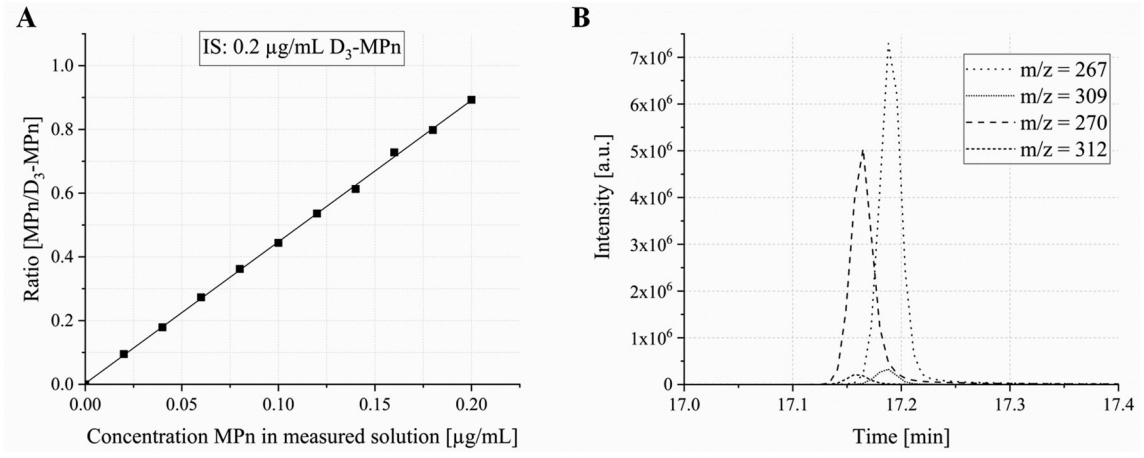

Fig. 2. A: Calibration curve for MPn using D_3-MPn as internal standard. Each data point represents a single measurement; B: Chromatograms of MPn (1 µg/mL) and D_3-MPn (0.8 µg/mL). For each substance, both recorded mass fragments are shown.

3.2. Development of sample enrichment through SPE

Solid-phase extraction of MPn is necessary in order to change the sample matrix, as the silylation reaction cannot be conducted in water. Evaporation of the water matrix with a stream of nitrogen or through rotary evaporation, as it was done by Richardson and Caruso [8], was not successful, probably due to the salt residue which was obtained even in samples with low salinity (S ~0.1, data not shown), inhibiting subsequent derivatisation.

Two different SPE materials were tested for their ability to extract MPn from brackish water samples. Strata-X is a polymeric reversed-phase material, which presumably interacts with the methyl group of MPn. This material was used by Owens and Koester for analysis of MPn in beverages with a recovery of about 30% for most matrices [13]. The second SPE material investigated was the Strata-X-AW material, which is a weak anion-exchange material. Both materials were previously used for MPn analysis [21,32]. However, the influence of salt-containing matrices on the recovery is poorly studied [19].

Our results (Fig. 3) show that MPn is retained to different degrees by the tested SPE materials when MPn was applied in MilliQ-water, with superior recovery with the ion-exchange material (Fig. 3C). Upon using salt-containing matrices, MPn was hardly detectable with the reversed-phase material (Fig. 3A and B), which might result from salt precipitations interfering with the derivatisation procedure. To mitigate this, a washing step with 2 mL of MilliQ-water (pH 1) was added after the sample was loaded onto the SPE cartridge. With the washing step, the salt residue in the eluent was reduced. However, the recovery also for MilliQ-water samples clearly decreased (Fig. 3A and B). This implies that the interaction between MPn and the reversed-phase material is too weak and, therefore, we precluded this material for further use.

Upon using the weak anion-exchange material, high recovery (about 100%) of MPn was obtained for MilliQ-water as the matrix (Fig. 3C), which is in good agreement with earlier studies [20]. However, for salt-containing water samples, a clear decrease in the recovery from about 100% to 4% was observed (Fig. 3C). We think that this is due to the matrix anions which probably compete with the target analyte for the active sites of the sorbent. Furthermore, the matrix cations might increase the eluting strength of the matrix. Therefore, we conclude that this SPE material should be used only for low salinity, i.e. fresh and brackish water samples.

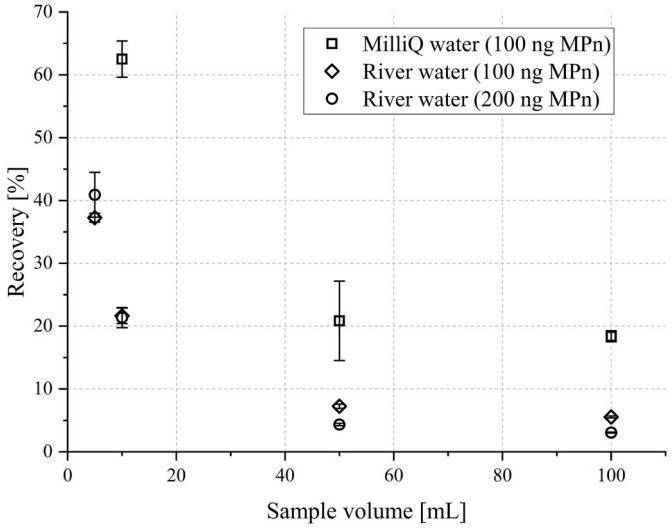

Fig. 4. Recovery of MPn after SPE from different matrices depending on the sample volume. The given amount of MPn is the total amount added to the different sample volumes prior the SPE processing.

To investigate the operational capability of the entire method, the SPE step was further characterised, i.e. with respect to the influence of the low salinity matrix, sample volume and MPn concentration. For this, we utilized MilliQ as matrix-free sample and a river sample of low salinity (river Mühlenfließ, Table 1) spiked with MPn. Before the analysis, the samples were analysed for MPn, which was below LOD for both.

Fig. 4 shows the obtained recovery for MPn in the spiked MilliQ- and river samples. A clear difference between the recovery of MPn in 10 mL of MilliQ- (~60%) and river water (~20%) was obtained. The fact that the salinity of the river sample was only 0.3 indicates that not

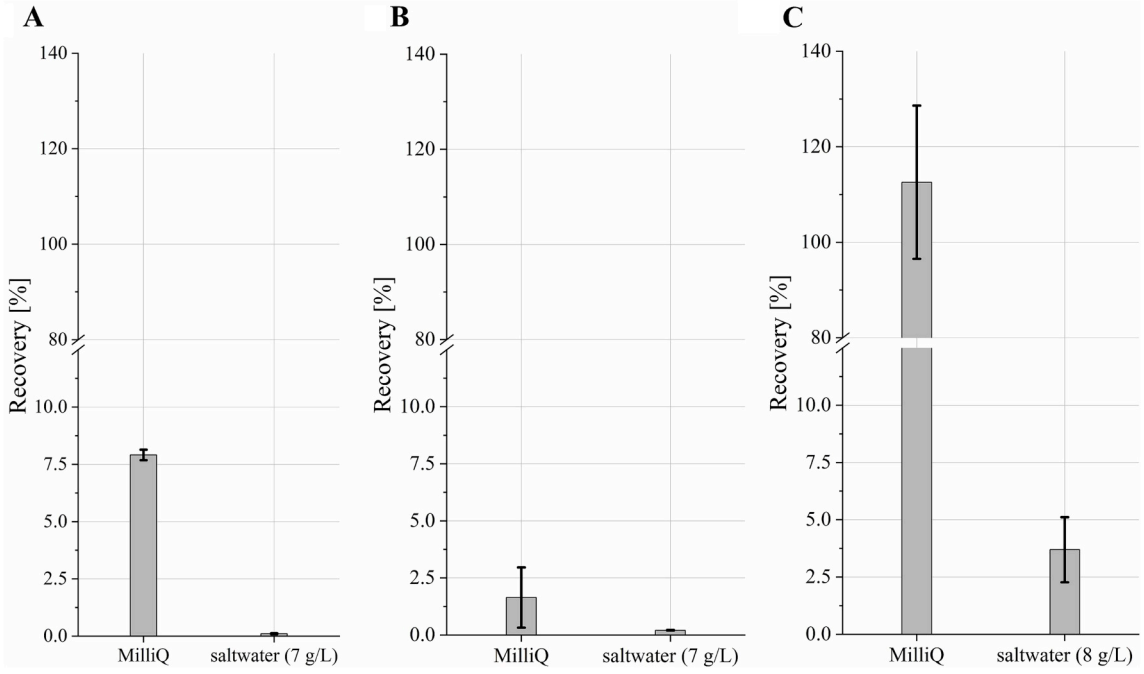

Fig. 3. Comparison of two different SPE materials and recovery of MPn from different water matrices (2 mL each). A: Strata-X (500 mg/3 mL, Phenomenex, Aschaffenburg, Germany) without washing step (Conditioning: 10 mL MeOH, 10 mL pH 1 water /loaded sample acidified to pH 1/elution: 10 mL ACN) B: Strata-X incl. a washing step C: Strata-X-AW incl. a. washing step. Error bars present triplicate injections.

only the salt matrix interferes with the SPE, but also other matrix components. With increasing sample volume, MPn recovery decreased further for MilliQ as well as for river water. Therefore, only small sample volumes of river water should be used for quantitative analysis, because even if the internal standard corrects for losses during SPE fortification, a low recovery has a large impact on the sensitivity of the method. Thus, for the river sample, a sample volume of 5 mL was additionally tested. The results show that the recovery for 5 mL is twice as high as for 10 mL. Based on these results and to keep matrix effects to a minimum, we suggest using sample volumes of not more than 5–10 mL, depending on the sample type and, in particular, the sample matrix.. Furthermore, Fig. 4 indicates that the total amount of MPn in the river sample is not affecting the recovery of MPn, when a total amount of up to 200 ng is added to the SPE-cartridge. On the basis of these results, we conclude that the recovery of MPn from the SPE depends on sample matrix and also largely on the sample volume. Hence, MPn fortification through SPE is strongly limited.

Moreover, the method was validated for MilliQ and river water samples which were processed through SPE in terms of accuracy (RE) and reproducibility (RSD%) by triplicate analysis at two different MPn-levels (Table Suppl. 3B). With obtained data for RSD% and RE% below 15%, the results indicate that the method is valid even with decreased recovery at a larger sample volume of 100 mL.

Finally, considering the determined instrumental LOD of 8 µg/L MPn and a sample volume of 5 mL, the entire method is characterised by a method LOD of 0.4 µg/L in the initial water sample. This is comparable to other methods published previously [12,14,33].

To test whether the instrumental calibration is also valid for the samples after their processing through SPE as well as in view of possible matrix effects, we conducted matrix-matched calibration in 10 mL of MilliQ and river water, obtained from Mühlenfließ, which were spiked with MPn up to 500 ng and D_3-MPn (200 ng) as internal standard. MPn concentrations were determined using the instrumental calibration and compared to the spiked concentration (Figure Suppl. 1). For statistical analysis of the method accuracy, the elliptic joint confidence region (EJCR) for the true slope and intercept of the linear regression were calculated (Figure Suppl. 1) [34]. The ideal point (0; 1 (intercept; slope)) is within the ellipse for river water, but not for MilliQ-water. This results from the larger area of the ellipse for river water, which is due to the lower precision of the river water data compared to the MilliQ-water data. However, this analysis shows that for matrix affected environmental samples the analytical method results in accurate quantitative data.

3.3. Matrix reduction through electrodialysis

As the sample matrix was identified to be an obstacle for MPn sample preparation, electrodialysis was tested to reduce the seawater matrix load and to analyse the effect of reducing salinity on the efficiency of the solid-phase extraction. In a recent study by Wirth et al. it was shown that at a final salinity of 0.1 not more than 30% of initially added MPn could be recovered [26]. However, aiming at optimising the method for MPn analysis, we analysed MPn recovery during the electrodialysis course in more detail (Fig. 5A). Basically, the recovery of MPn during the ED follows an exponential course with a sample salinity of about 1.4 as the critical point at which MPn is lost through the electrodialysis membrane, which is probably due to the ionic behaviour of MPn. With a $\log K_{OW}$ of −2.28, MPn is a very hydrophilic compound [35]. In addition, during electrodialysis, pH usually slightly increased up to a pH of about 7.8, so that MPn partially was twice negatively charged [26,36]. This presumably led to an increasing loss during electrodialysis with decreasing salinity, as it was described for other hydrophilic compounds such as glyphosate [26]. However, our data show that MPn recovery stays above 90% until a salinity of 1.4, which implies that until this point, the sample matrix can be reduced without major MPn loss. However, the influence of sample matrices on sample preparation may vary significantly from one sample to another. Therefore, for MPn analysis, the electrodialysis terminating point is a compromise of MPn recovery and salt tolerance of subsequent

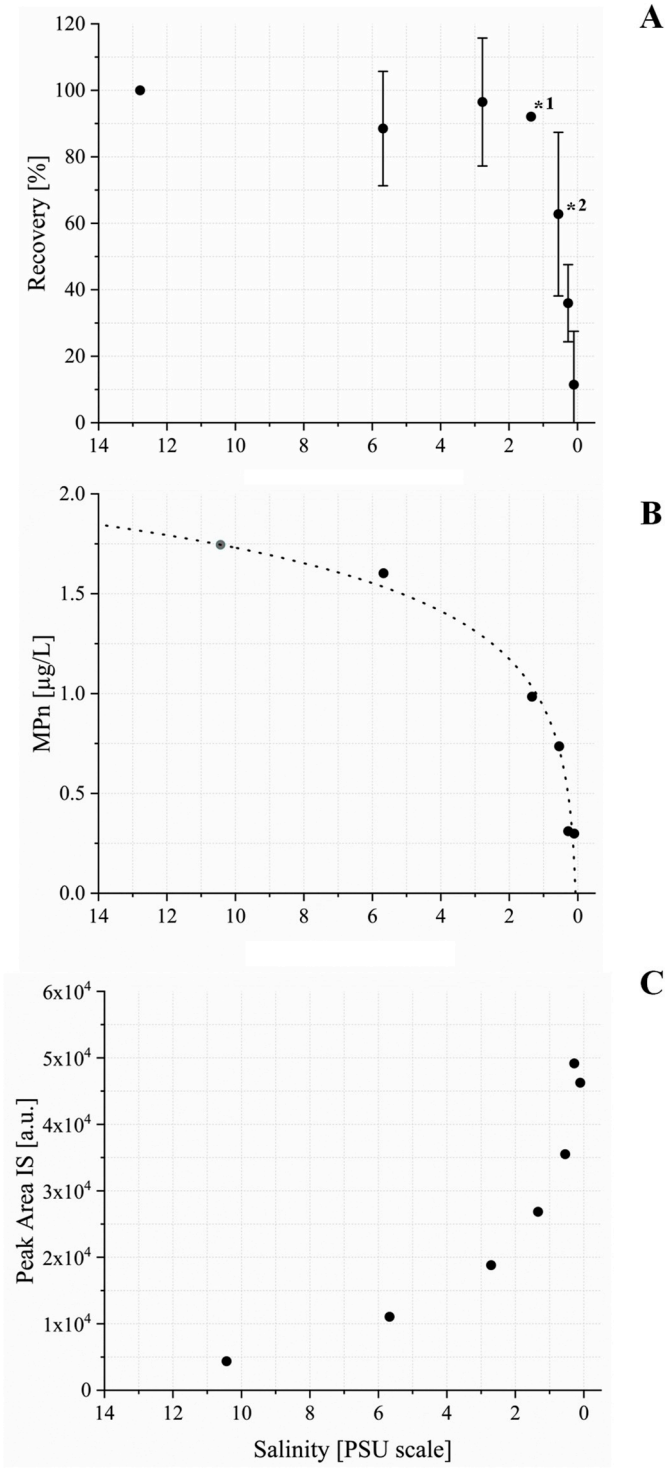

Fig. 5. A: Three batches of the same coastal water sample which were spiked with MPn were electrodialysed and subsamples at distinct sample conductivities were analysed for MPn. All measured values were corrected by the MPn-blank of the individual run (*1 single analysis, *2 duplicate analysis, see also [26]) B: A coastal water sample from the same site (without MPn addition) was electrodialysed and subsamples were analysed for MPn (bright circle: calculated MPn concentration of 1.8 µg/L upon an exponential correlation of the obtained MPn data). All measured values were blank-corrected. C: The IS peak area of the MPn measurements in B increased exponentially.

processing steps as it was discussed before [26]. In this regard, the application of an internal standard before electrodialysis processing seems essential.

However, this analysis also showed that MPn is detectable at the initial marine water salinity if concentrations are high enough. Thus, the matrix *per se* does not inhibit MPn recovery from SPE, but it is determined, on the one hand, by the sample's MPn concentration and, on the other hand, by the sample matrix.

3.4. Environmental samples

The described method was then tested by analysing several samples from the river Warnow, located in Mecklenburg-Western Pomerania, Germany (Section 2.6, Table 1). Analysis of the samples W1 – W7 and W9 from the freshwater part of the Warnow collected in summer 2017 and from the river Mühlenfließ in December 2018 revealed MPn concentrations below LOD. However, we observed MPn concentrations between 0.4 and 0.6 µg/L for the freshwater samples W7 – W9 collected in winter 2018. MPn was not detectable at the adjacent site W10 which might be derived from matrix dependent lower SPE recovery due to the higher salinity of 1.1 at this site compared to W7 – W9. The samples W7 and W9 were analysed twice (Table Suppl. 3C) and the results indicate satisfactory values for the precision of the method.

Several publications indicate the possible role of MPn in the marine methane system [5,37,38]. However, there are hardly any data for MPn in marine water samples available, which we attribute to missing analytical methods for this challenging matrix. It was already shown above, that the SPE-method is sensitive to the salt matrix resulting in decreased recovery. To test if a reduction of the seawater matrix might enable MPn analysis in these sample types, a Baltic Sea coastal water sample (Heiligendamm, salinity 10.4, Table 1) was electrodialysed and subsamples at distinct sample conductivities were analysed for MPn (Fig. 5B). Interestingly, at sea salt reduction to a salinity of 5.6, MPn was already detectable. At lower salinities, MPn concentrations decreased exponentially, as described above for the spiked water sample (Fig. 5A and B). Based on the determined MPn concentration at the salinity of 5.6 and the exponential course of MPn loss during the ED, an exponential extrapolation was used to determine an approximate value for the MPn-concentration in the initial sample. Based on this, we propose an MPn concentration of about 1.8 µg/L in the initial water sample (exponential correlation: $R^2 = 0.9486$). At this point, it is certainly preferable to determine the MPn-concentration by direct quantification, i.e., through addition of the internal standard before the electrodialysis. However, for the herein utilized electrodialysis system a sample volume of at least 3 L has to be processed which would be very costly. However, our results indicate that the approach through extrapolation results in reliable semi-quantitative data which might provide a first indication on the concentration range of MPn in marine water samples. Here, more work is necessary for reliable MPn quantification. In this regard, a reduction of the sample volume after the electrodialysis, e.g. through reverse osmosis, might further improve the sensitivity of the method [39].

The improvement of the sensitivity of the sample preparation method through reduction of the sample matrix can also be viewed through the determined peak area of the IS, which was added in same concentrations to the subsamples after electrodialysis (Fig. 5C). It increased exponentially with decreasing sample salinity, which is due to the higher recovery of the SPE-method at lower values for salinity.

Based on our obtained data, we postulate different ranges of MPn concentrations for the analysed river- and coastal-water samples. Our data indicate that MPn is with a concentration above 1 µg/L by far higher concentrated in coastal water than in river water, which was mostly below LOD. This implies a particular relevance of MPn for the marine environment, which was discussed previously [5,37,38].

4. Conclusion

This study presents an analytical method for the quantitative determination of methylphosphonic acid in environmental water samples. The critical extraction of MPn from different water samples with sufficient recovery was done by using a weak-anion exchange SPE-material with sufficient recovery. We show that recovery of MPn using SPE decreases with increasing salt concentration and, consequently, the analysis of brackish as well as marine samples results in lower sensitivity. To overcome this problem, the use of electrodialysis for desalting of water samples was successfully tested for a brackish water sample. Finally, MPn was detected at a low µg/L-level in water samples from the German river Warnow and the German Baltic Sea coastal area.

The presented method enables the possibility to quantify MPn in different aquatic systems. Therefore, the results of this work may help to study the role of MPn in these systems. As described before, an important role of MPn in aquatic systems was often assumed [4,5]. Our results indicate that MPn is present in river as well as coastal waters. However, more work is necessary to fully understand sinks and sources of MPn, as well as regional and seasonal changes of its concentration.

Declaration of competing interest

No potential conflict of interest was reported by the authors.

Acknowledgements

This work was supported by the funding line strategic networks of the Leibniz Association within the scope of the Leibniz ScienceCampus Phosphorus Research Rostock (SAS-2015-IOW-LWC).

The authors are grateful to Nadine Hollmann and Dr. Wael Skeff for helpful contributions during the development of the GC-MS- and the SPE-method, to Christoph Kamper, Dr. Franziska Bitschofsky and Lisa Rönspieß for providing samples and to Dr. Kathrin Fisch for helping with the map.

Appendix A. Supplementary data

Supplementary data to this article can be found online at https://doi.org/10.1016/j.talanta.2020.120724.

References

[1] J.W. McGrath, J.P. Chin, J.P. Quinn, Organophosphonates revealed: new insights into the microbial metabolism of ancient molecules, Nat. Rev. Microbiol. 11 (2013) 412–419.
[2] L.L. Clark, E.D. Ingall, R. Benner, Marine organic phosphorus cycling: novel insights from nuclear magnetic resonance, Am. J. Sci. 299 (1999) 724–737.
[3] L.W.J. Anderson, Potential for sediment-applied acetic acid for control of invasive Spartina alterniflora, J. Aquat. Plant Manage. 45 (2007) 100–105.
[4] W.W. Metcalf, B.M. Griffin, R.M. Cicchillo, J. Gao, S.C. Janga, H.A. Cooke, B.T. Circello, B.S. Evans, W. Martens-Habbena, D.A. Stahl, W.A. van der Donk, Synthesis of methylphosphonic acid by marine microbes: a source for methane in the aerobic ocean, Science 337 (2012) 1104–1107.
[5] D.M. Karl, L. Beversdorf, K.M. Bjorkman, M.J. Church, A. Martinez, E.F. DeLong, Aerobic production of methane in the sea, Nat. Geosci. 1 (2008) 473–478.
[6] J.E. Teikari, D.P. Fewer, R. Shrestha, S.W. Hou, N. Leikoski, M. Makela, A. Simojoki, W.R. Hess, K. Sivonen, Strains of the toxic and bloom-forming Nodularia spumigena (cyanobacteria) can degrade methylphosphonate and release methane, ISME J. 12 (2018) 1619–1630.
[7] M. Yao, C. Henny, J.A. Maresca, Freshwater bacteria release methane as a by-product of phosphorus acquisition, appl, Environ. Microbiol. 82 (2016) 6994–7003.
[8] D.D. Richardson, J.A. Caruso, Derivatization of organophosphorus nerve agent degradation products for gas chromatography with ICPMS and TOF-MS detection, Anal. Bioanal. Chem. 388 (2007) 809–823.
[9] J.G. Purdon, J.G. Pagotto, R.K. Miller, Preparation, stability and quantitative analysis by gas chromatography and gas chromatography—electron impact mass spectrometry of tert.-butyldimethylsilyl derivatives of some alkylphosphonic and alkyl methylphoshonic acids, J. Chromatogr. A 475 (1989) 261–272.
[10] Y. Seto, M. Tachikawa, M. Kanamori-Kataoka, K. Sasamoto, N. Ochiai, Target analysis of tert-butyldimethylsilyl derivatives of nerve agent hydrolysis products by selectable one-dimensional or two-dimensional gas chromatography-mass

spectrometry, J. Chromatogr. A 1501 (2017) 99–106.
[11] V. Singh, S. Chinthakindi, A.K. Purohit, D. Pardasani, V. Tak, D.K. Dubey, Single vial sample preparation of markers of nerve agents by dispersive solid-phase extraction using magnetic strong anion exchange resins, J. Chromatogr. A 1395 (2015) 48–56.
[12] I. Rodin, T. Baygildiev, A. Stavrianidi, A. Braun, I. Rybalchenko, O. Shpigun, Hydrophilic interaction liquid chromatography tandem mass spectrometry methylphosphonic acid determination in water samples after derivatization with p-bromophenacyl bromide, Chromatographia 78 (2015) 585–591.
[13] J. Owens, C. Koester, Quantitative analysis of chemical warfare agent degradation products in beverages by liquid chromatography tandem mass spectrometry, J. Agric. Food Chem. 57 (2009) 8227–8235.
[14] T.M. Baygildiev, I.A. Rodin, A.N. Stavrianidi, A.V. Braun, D.I. Akhmerova, O.A. Shpigun, I.V. Rybal'chenko, Time-efficient LC/MS/MS determination of low concentrations of methylphosphonic acid, Inorg. Mater. 53 (2017) 1382–1385.
[15] R.M. Black, B. Muir, Derivatisation reactions in the chromatographic analysis of chemical warfare agents and their degradation products, J. Chromatogr. A 1000 (2003) 253–281.
[16] W.R. Creasy, Postcolumn derivatization liquid chromatography mass spectrometry for detection of chemical-weapons-related compounds, J. Am. Soc. Mass Spectrom. 10 (1999) 440–447.
[17] D.D. Richardson, J.A. Caruso, Screening organophosphorus nerve agent degradation products in pesticide mixtures by GC-ICPMS, Anal. Bioanal. Chem. 389 (2007) 679–682.
[18] M. Noami, M. Kataoka, Y. Seto, Improved tert-butyldimethylsilylation gas chromatographic/mass spectrometric detection of nerve gas hydrolysis products from soils by pretreatment of aqueous alkaline extraction and strong anion-exchange solid-phase extraction, Anal. Chem. 74 (2002) 4709–4715.
[19] M. Kataoka, K. Tsuge, Y. Seto, Efficiency of pretreatment of aqueous samples using a macroporous strong anion-exchange resin on the determination of nerve gas hydrolysis products by gas chromatography–mass spectrometry after tert.-butyldimethylsilylation, J. Chromatogr. A 891 (2000) 295–304.
[20] Q. Wang, J. Xie, M. Gu, J. Feng, J. Ruan, Gas chromatographic–mass spectrometric method for quantitation of trimethylsilyl derivatives of nerve agent degradation products in human plasma, using strong anion–exchange solid-phase extraction, Chromatographia 62 (2005) 167–173.
[21] R. Wagner, S.J. Wetzel, J. Kern, H.M.S. Kingston, Improved sample preparation of glyphosate and methylphosphonic acid by EPA method 6800A and time-of-flight mass spectrometry using novel solid-phase extraction, J. Mass Spectrom. 47 (2012) 147–154.
[22] M. Kanamori-Kataoka, Y. Seto, Laboratory identification of the nerve gas hydrolysis products alkyl methylphosphonic acids and methylphosphonic acid, by gas chromatography-mass spectrometry after tert-butyidimethylsilylation, J. Health Sci. 54 (2008) 513–523.
[23] X.Z. Shao, H.G. Ge, Z.Z. Li, C.Q. Ren, J.H. Wang, Solubility of methylphosphonic acid in selected organic solvents, Fluid Phase Equilib. 390 (2015) 7–13.
[24] L.R. Chambers, E.D. Ingall, E.M. Saad, A.F. Longo, M. Takeuchi, Y. Tang, C. Benitez-Nelson, S.T. Haley, S.T. Dyhrman, J. Brandes, A. Stubbins, Enhanced dissolved organic matter recovery from saltwater samples with electrodialysis, Aquat. Geochem. 22 (2016) 555–572.
[25] D.W. Bell, P. Pellechia, L.R. Chambers, A.F. Longo, K.M. McCabe, E.D. Ingall, C.R. Benitez-Nelson, Isolation and molecular characterization of dissolved organic phosphorus using electrodialysis-reverse osmosis and solution 31P-NMR, Limnol Oceanogr. Methods 15 (2017) 436–452.
[26] M.A. Wirth, M. Sievers, F. Habedank, U. Kragl, D.E. Schulz-Bull, M. Kanwischer, Electrodialysis as a sample processing tool for bulk organic matter and target pollutant analysis of seawater, Mar. Chem. 217 (2019) 103719.
[27] F. Bitschofsky, M. Nausch, Spatial and seasonal variations in phosphorus speciation along a river in a lowland catchment (Warnow, Germany), Sci. Total Environ. 657 (2019) 671–685.
[28] G.W. Cooper, W.M. Onwo, J.R. Cronin, Alkyl phosphonic acids and sulfonic acids in the Murchison meteorite, Geochem. Cosmochim. Acta 56 (1992) 4109–4115.
[29] G.S. Rule, Z.D. Clark, B. Yue, A.L. Rockwood, Correction for isotopic interferences between analyte and internal standard in quantitative mass spectrometry by a nonlinear calibration function, Anal. Chem. 85 (2013) 3879–3885.
[30] L.A. Currie, Detection and quantification limits: origins and historical overview, Anal. Chim. Acta 391 (1999) 127–134.
[31] J.C. Miller, J.N. Miller, Statistics for Analytical Chemistry, 2 ed., Ellis Horwood, Halsted Press, Chichester, England, 1988.
[32] B. Maddah, A. Motahari, A. Moghimi, High capacity anion-exchange resin as a solid-phase extraction for determination of methylphosphonic acid, Separ. Sci. Technol. 45 (2010) 2363–2367.
[33] P.J. Li, B. Hu, X.Y. Li, Zirconia coated stir bar sorptive extraction combined with large volume sample stacking capillary electrophoresis-indirect ultraviolet detection for the determination of chemical warfare agent degradation products in water samples, J. Chromatogr. A 1247 (2012) 49–56.
[34] A.G. González, M.A. Herrador, A.G. Asuero, Intra-laboratory testing of method accuracy from recovery assays, Talanta 48 (1999) 729–736.
[35] M.J. Small, Compounds Formed from the Chemical Decontamination of HD, GB, and VX and Their Environmental Fate. AD-A149 515. Ft, Army Medical Bioengineering Research and Development Laboratory, Detrick, MD, 1984.
[36] E.P. Serjeant, B. Dempsey, Ionisation Constants of Organic Acids in Aqueous Solution, IUPAC Chemical Data Series No. 23, International Union of Pure and Applied Chemistry (IUPAC), Pergamon Press, Inc., New York, 1979, p. 12.
[37] D.A. del Valle, D.M. Karl, Aerobic production of methane from dissolved water-column methylphosphonate and sinking particles in the North Pacific Subtropical Gyre, Aquat. Microb. Ecol. 73 (2014) 93–105.
[38] A.Y. Kallistova, A.Y. Merkel, I.Y. Tarnovetskii, N.V. Pimenov, Methane formation and oxidation by prokaryotes, Microbiology 86 (2017) 671–691.
[39] T. Vetter, E. Perdue, E. Ingall, J. Koprivnjak, P. Pfromm, Combining reverse osmosis and electrodialysis for more complete recovery of dissolved organic matter from seawater, Separ. Purif. Technol. 56 (2007) 383-387.5.

Publication 4

Leaching and degradation of (13)C2-(15)N-glyphosate in field lysimeters

by

Peter Gros, Ralf Meissner, **Marisa A. Wirth**, Marion Kanwischer, Holger Rupp, Detlef E. Schulz-Bull, Peter Leinweber

Environmental Monitoring and Assessment

Year 2020, Volume 192, Issue 2, Page 127 ff.

DOI: 10.1007/s10661-019-8045-4

Environ Monit Assess (2020) 192:127
https://doi.org/10.1007/s10661-019-8045-4

Leaching and degradation of $^{13}C_2$-^{15}N-glyphosate in field lysimeters

Peter Gros · Ralph Meissner · Marisa A. Wirth · Marion Kanwischer · Holger Rupp · Detlef E. Schulz-Bull · Peter Leinweber

Received: 3 July 2019 / Accepted: 17 December 2019

Abstract Glyphosate (GLYP), the globally most important herbicide, may have effects in various compartments of the environment such as soil and water. Although laboratory studies showed fast microbial degradation and a low leaching potential, it is often detected in various environmental compartments, but pathways are unknown. Therefore, the objective was to study GLYP leaching and transformations in a lysimeter field experiment over a study period of one hydrological year using non-radioactive $^{13}C_2$-^{15}N-GLYP labelling and maize cultivation. ^{15}N and ^{13}C were selectively measured using isotopic ratio mass spectrometry (IR-MS) in leachates, soil, and plant material. Additionally, HPLC coupled to tandem mass spectrometry (HPLC-MS/MS) was used for quantitation of GLYP and its main degradation product aminomethylphosphonic acid (AMPA) in different environmental compartments (leachates and soil). Results show low recoveries for GLYP (< 3%) and AMPA (< level of detection) in soil after the study period, whereas recoveries of ^{15}N (11–19%) and ^{13}C (23–54%) were higher. Time independent enrichment of ^{15}N and ^{13}C and the absence of GLYP and AMPA in leachates indicated further degradation. ^{15}N was enriched in all compartments of maize plants (roots, shoots, and cobs). ^{13}C was only enriched in roots. Results confirmed rapid degradation to further degradation products, e.g., $^{15}NH_4^+$, which plausibly was taken up as nutrient by plants. Due to the discrepancy of low GLYP and AMPA concentrations in soil, but higher values for ^{15}N and ^{13}C after the study period, it cannot be excluded that non-extractable residues of GLYP remained and accumulated in soil.

Keywords Pesticide · Fate · IR-MS · HPLC-MS/MS · Stable isotopes · Environmental detection

Introduction

Glyphosate (GLYP) is an important herbicide in the world, annually > 1 million tonnes are applied (Richmond 2018). GLYP reaches the soil either by direct spraying or indirectly by release through plant roots (Neumann et al. 2006; Laitinen et al. 2007). Rapid microbial degradation has been reported in soil, leading to the most predominant degradation product aminomethylphosphonic acid (AMPA). This pathway has been documented extensively and was reviewed by Borggaard and Gimsing (2008). Degradation

Electronic supplementary material The online version of this article (https://doi.org/10.1007/s10661-019-8045-4) contains supplementary material, which is available to authorized users.

P. Gros (✉) · P. Leinweber
Agricultural and Environmental Science, Soil Science, University of Rostock, Justus-von-Liebig-Weg 6, 18051 Rostock, Germany
e-mail: peter.gros@uni-rostock.de

R. Meissner · H. Rupp
Department of Soil System Science, Helmholtz Centre for Environmental Research, Lysimeter Station, Falkenberg 55, 39615 Altmärkische Wische, Germany

M. A. Wirth · M. Kanwischer · D. E. Schulz-Bull
Department of Marine Chemistry, Leibniz Institute for Baltic Sea Research Warnemünde, Seestrasse 15, 18119 Rostock, Germany

Published online: 21 January 2020

products can further react to CO_2 and NH_4^+. Degradation rates for GLYP vary significantly and half-life values from 2 to 180 days have been reported (Borggaard and Gimsing 2008; Tang et al. 2019). GLYP can interact strongly with organic and inorganic molecules at a variety of binding sites such as (i) the soil organic matter, e.g., peptides, carbohydrates, or phenolic structures (Gros et al. 2017; Ahmed et al. 2018) or (ii) mineral surfaces, e.g., goethite or montmorillonite, as has been demonstrated in laboratory experiments and quantum chemical modeling (Morillo et al. 1997; Ahmed et al. 2017). These interactions lead to strong and high sorption, as has been shown in laboratory batch sorption experiments (Dion et al. 2001; Okada et al. 2016; Gros et al. 2017). Although strong sorption and degradation are antagonistic effects, both are supported under normal or low tillage soil management and should prevent GLYP from distributing through soil (Kjær et al. 2005; Bergström et al. 2011). Contrary to this assumption, GLYP frequently has been detected in ground and surface water (Coupe et al. 2012) even above the regulatory limit of 0.1 μg L^{-1} in the EU (Van Stempvoort et al. 2014; Skeff et al. 2015). The mechanisms of GLYP translocation from place of application through the drainage system into waterways and estuaries are still unclear but need to be understood for preventing these undesired translocations.

Lysimeters are suitable research facilities that enable monitoring and assessing of nutrient or pollutant balances in disturbed or undisturbed soil columns (Führ et al. 1998). Only a few field lysimeter experiments have been conducted with non-labeled GLYP (Malone et al. 2004), where leachate waters were analyzed through fluorescence detection after derivatization of the analyte. In the laboratory, lysimeter experiments with GLYP often have been conducted using non-stable, radioactive ^{14}C isotopic labelling, which provides advantages of sensitive quantitation and recovery by scintillation (e.g., Al-Rajab et al. 2008). Safety restrictions for the use of radioactively labeled substances make it necessary to evaluate experimental data from laboratory experiments under more practically relevant field conditions. Utilization of $^{13}C_2$-^{15}N-GLYP (GLYP*i*), which contains stable isotopes, combines the advantages of non-radioactive GLYP for field studies with the sensitivity of labelling (in analogy to ^{14}C-GLYP) for environmental monitoring in laboratory experiments (Muskus et al. 2019). Using that non-radioactively labeled GLYP*i* enables the detection using isotopic ratio mass spectrometry (IR-MS) complementary to high performance liquid chromatography coupled to electrospray ionization mass spectrometry (HPLC-ESI-MS/MS) for environmental measurements of extractable residues of GLYP*i* and AMPA*i*. This experimental approach has not been applied in field lysimeter studies so far. Therefore, we hypothesize that the methodological approach with GLYP*i*, IR-MS, and HPLC-ESI-MS/MS enables to study the fate and possible translocation of GLYP under field conditions.

Material and methods

The leaching experiment was set up in two field lysimeters (non-weighing zero tension), which were installed in the Lysimeter Station at the Helmholtz Centre for Environmental Research-UFZ (Falkenberg, Germany; 52°51′ N, 11°48′ E). These lysimeters were constructed in 1981 in sheet steel vessels with cuboid shape of 1 × 1 m surface area and 1.25 m depth. The lysimeters were filled with sandy loam (0–30 cm topsoil: 74% sand, 14% silt, 12% clay, pH 4.8, organic C = 1.1%; 30–100 cm subsoil: 75% sand, 17% silt, 8% clay, pH 5.6, organic C = 0.2%) and an additional 25 cm-drainage layer composed of three sublayers (sand, gravel, and coarse gravel) at the bottom. The soil texture is representative for the river Elbe valley in the Federal State Saxony-Anhalt. Conventional agricultural management was oriented according to best management practice. In 2017, maize was planted which was embedded in a regionally typical crop rotation of sugar beets-winter wheat-potatoes-winter barley-maize. Details on the lysimeter site and management history have been published previously (Meissner et al. 2010; Rupp et al. 2018). The present study investigated a period of one hydrological year starting in the hydrological summer semester in May 2017. Any weeds were removed mechanically, followed by GLYP*i* application (2017/24/04) via spraying as a worst-case scenario. Application rate was equivalent to maximum allowed annual for Germany (3.6 kg ha^{-1} a^{-1}) with practical concentration of GLYP formulations (480 g kg^{-1}) (360 mL GLYP*i*, dissolved in 750 mL H_2O). Drift by air flow was prevented by temporally fencing the application area with a ring of steel (1 m in height). Three days after GLYP*i* application, 5 L of the conservative KBr tracer solution was applied at a rate corresponding to 40 kg KBr ha^{-1} to each of the lysimeters to provide

information on the movement of water through the soil column. Lysimeters were cultivated with maize (9 plants per lysimeter, equally spaced). No fertilizers or treatments for weeding were executed during the study period.

Sampling of leachates, soil, and plant material

Lysimeter soils were sampled from 0 to 5 cm depth (5 spots equally spaced in each lysimeter) at 4 dates over the study period (before and directly after application, 165 and 360 days after application). Soil sampling before application characterizes the basic level of GLYP*i* concentration, whereas the sample directly after application represents 100% of initial GLYP*i*. To keep the soil column intact, samples from the whole topsoil (0–30 cm) and the subsoil (30–60 cm) were taken only at the end (day 360 after application) of the study period. Soil samples were air dried and sieved (2 mm). Subsamples of the sieved soils were finely ground for further measurement with IR-MS. Residues of GLYP*i* and AMPA*i* were extracted from 5 g of the sieved soil in 40 mL of a 1 M KOH solution (shaking overnight and centrifugation for 10 min at 1558 g) and stored at − 20 °C until quantitation via HPLC-ESI-MS/MS.

Leachates were collected weekly in polyethylene canisters and volumes were recorded. Subsamples of 150 mL were taken and stored in a freezer at − 20 °C in 3 × 50 mL centrifuge tubes for further measurements with ion chromatography (IC) and HPLC-ESI-MS/MS. A total of 50 mL of each sample were lyophilized to dryness (− 50 °C, 0.025 mbar; Christ Alpha 1-4, Martin Christ Gefriertrocknungsanlagen GmbH, D-37250 Osterode, Germany) and solid residue amounts were weighed back and stored for measurements with isotopic ratio mass spectrometry (IR-MS).

Mature maize plants (roots, shoots, and cobs) were harvested in September 2017 from the two treated lysimeters and one untreated neighboring plot as reference. Subsamples of 3 plants per lysimeter were harvested for further measurements of plant biomass. Moist weight was determined followed by drying at 60 °C and measuring of dry matter weight. Plant compartment samples (root, shoot, and cobs) were shredded and subsequently finely ground separately and stored until further measurements with IR-MS.

Sample analyses

Conservative tracer and isotope ratio analyses

Br^- tracer analysis in the leachate was performed using ion chromatography (column: Metrosep A SUPP 5150 × 4.0 mm, pre-column: Metrosep A SUPP 4/5 Guard, eluent: 0.3 mM Na_2CO_3 and 1.0 mM $NaHCO_3$, flow: 0.7 mL min_{-1}, separation mode: isocratic; Metrohm, D-70794 Filderstadt, Germany).

Isotopic ratios for $^{15}N/^{14}N$ and $^{13}C/^{12}C$ in soil, plant compartments, and lyophilized leachate samples were measured through the elemental analyzer (Eurovector EA, Via F.lli Cuzio 42, 27100 PAVIA, Italy; IR-MS GV-Isoprome, Elementar Analysensysteme GmbH, Elementar-Straße 1, 63505 Langenselbold, Germany) in the Institute for Nutritional Sciences, University of Gießen, Germany. For this purpose, finely ground soil and plant samples from the two treated sites and one untreated site (reference) were measured in triplicates. Lyophilized leachate samples from lysimeter leachates were measured in duplicates. Equations 1 and 2 show the calculation of $\delta^{15}N$ and $\delta^{13}C$ derived from isotopic ratios of the sample in relation to defined standard isotopic ratios from air for N and Pee Dee Belemnite (PDB) for C; values are generally given in ‰.

$$\delta^{13}C = \left(\frac{\left({}^{13}C/{}^{12}C \right)_{\text{sample}}}{\left({}^{13}C/{}^{12}C \right)_{\text{PDB}}} - 1 \right) \quad (1)$$

$$\delta^{15}N = \left(\frac{\left({}^{15}N/{}^{14}N \right)_{\text{sample}}}{\left({}^{15}N/{}^{14}N \right)_{\text{air}}} - 1 \right). \quad (2)$$

GLYPi and AMPAi analyses

Soil extracts and leachate samples were analyzed for GLYP*i* and AMPA*i* with HPLC-ESI-MS/MS after derivatization with fluorenylmethyloxycarbonyl chloride (FMOC-Cl), as described in Wirth et al. (2019). The utilized system was composed of an LC-2040C Nexera-i and a triple quadrupole mass spectrometer LCMS-8060 (Shimadzu, Duisburg, Germany) equipped with a heated ESI-source. The FMOC derivatives were

separated on a Gemini 3 μm NX-C_{18} column (Column 1: 150 × 2 mm, Aschaffenburg, Phenomenex, Germany).

Non-isotope-labeled GLYP (LGC Standards, Wesel, Germany) was used as internal standard for GLYP*i* (Sigma Aldrich, Taufkirchen, Germany) quantitation. Since AMPA*i* is not commercially available as a standard substance, no HPLC-ESI-MS/MS-optimization and, thus, no calibration could be carried out for this compound. Therefore, AMPA*i* was determined only qualitatively. Analytes were detected in the multiple reaction monitoring (MRM) mode. The MRM transitions were determined and optimized utilizing standard compounds (Table 1). However, as AMPA*i* is not commercially available, instrumental MRM optimization for AMPA*i*-FMOC could not be performed. Therefore, the settings for the MRM transitions for this compound were chosen as follows: optimization was carried out for ^{13}C-^{15}N-AMPA-FMOC and AMPA-FMOC (LGC Standards, Wesel, Germany) and their fragmentation patterns were utilized to derive the expected masses of the precursor and product ions for ^{15}N-AMPA-FMOC (AMPA*i*-FMOC). Further parameters of the MRM transitions were set by averaging values for ^{13}C-^{15}N-AMPA-FMOC and AMPA-FMOC (Table 1).

To further verify that the targeted and detected compound was the ^{15}N-AMPA-FMOC, a selection of samples was additionally separated on a different LC-column (Column 2: Kinetex 2.6 μm EVO C18 100 Å, 150 × 2.1 mm, Phenomenex, Aschaffenburg, Germany). The proposed AMPA*i*-FMOC was eluted from both columns at similar retention times as AMPA-FMOC (Table 1) which confirms its presence. Due to the lack of an AMPA*i*-FMOC calibration, these data could be evaluated only semi-quantitatively. Quantitation of GLYP*i* was carried out through weighting with the glyphosate internal standard signal.

Results and discussion

Precipitation and leachate analysis

The study period from May 2017 to April 2018 was characterized by overall high amounts of precipitation that exceeded the monthly 30-year mean values (1981–2010) for this region, except for the months May, September, and February. Especially, June and July were characterized by heavy rainfall events that summed up to 123 and 125 mm per month precipitation, greatly exceeding the mean values of 57 ± 22 mm (June) and 61 ± 32 mm (July). These events resulted in large amounts of leachate in July 2017 (60.4 and 66.3 L). Weekly leachate amounts, collected from May 2017 until July 2017 to December 2017 until April 2018, had a mean volume of 5.1 L per week. For the period from August 2017 to November 2017, no leachates were received although precipitation occurred, most likely because of transpiration and water uptake by plants. Total volumes of leachates for the two lysimeters were 203 and 215 L over the study period. The Br^--breakthrough started in week 10 after application, where 35 and 37 L of leachate were received in the two tested lysimeters. Residues from the conservative tracer KBr were detected later on in all leachates. Due to the occurrence of Br^- in the leachates after 10 weeks and its slowly increasing concentrations over the following weeks along with continually received leachates, the main transport mechanism through the soil column can be assumed as matrix flow for the studied period.

For the natural ^{15}N background representing the ratio of $^{15}N/^{14}N$ of the air nitrogen, the $\delta^{15}N$ has been set to 0 (Fig. 1a). Discrepancies towards higher values indicate an enrichment of ^{15}N. In the first 2 weeks after application, a strong decrease of leachate $\delta^{15}N$ to negative values was detected, indicating an enrichment of ^{14}N. In the following weeks 3 to 10, the $\delta^{15}N$ in the leachate was constant between 0 and 1.7‰, and it increased over time from week 11 after GLYP*i* application. After the period with no leachates, the trend of $\delta^{15}N$ had a sigmoidal shape with an assumed maximum limit of about 50‰ for the last 10 weeks of the experimental period. This maximum level corresponds to a mass rate of about 10 μg $^{15}N\ week^{-1}$ of leached GLYP*i* active ingredient equivalent or its N-containing degradation products.

Values for $\delta^{13}C$ started at about − 8‰ and fluctuated between − 12 and − 6‰ for the first 10 weeks before they strongly increased and reached values of − 2.6 and − 0.5‰ in the two lysimeters (Fig. 1b). After the period with no leachates, the $\delta^{13}C$ started at lower levels of − 8.9 and − 2.1 in lysimeters 1 and 2, respectively. The trend of increasing $\delta^{13}C$ values starting at − 5.5‰ went on and ended at −2.3‰ for the remaining 20 weeks of the study, although with a less steep slope than in the first experimental phase.

Trends of ^{13}C and ^{15}N originating from GLYP*i* in the leachate (Fig. 1) did not correlate, which may be an indication for an independent movement of these

Table 1 Measurement modes for identification and quantitation of $^{13}C_2$-^{15}N-glyphosate and ^{15}N-aminomethylphosphonic acid using high performance liquid chromatography tandem mass spectrometry (HPLC-ESI-MS/MS)

Component	Measurement mode	Precursor m/z	Product m/z	Collision energy	Retention time column 1(min)	Retention time column 2 (min)
$^{13}C_2$-^{15}N-Glyphosate-FMOC (GLP*i*)	-	392.10	170.15	14	9.10	8.77
			152.20	24		
			63.10	48		
Glyphosate-FMOC	-	390.00	168.15	14	9.10	8.76
			150.20	23		
			63.05	49		
^{15}N-AMPA-FMOC* (AMPA*i*)	+	335.20	179.05	−23	9.47	9.18
			178.15	−48		
			157.05	−10		
			113.05	−15		
AMPA-FMOC	+	334.20	179.05	−23	9.47	9.19
			178.15	−46		
			156.00	−10		
			112.05	−15		
^{13}C-^{15}N-AMPA-FMOC	+	336.20	179.05	−22	9.46	n.a.
			178.10	−50		
			158.15	−10		
			114.10	−15		

*derived from the optimized MRM transitions of ^{13}C-^{15}N-AMPA-FMOC and AMPA-FMOC

isotopes through the soil column. Also, IR-MS cannot distinguish between GLYP*i* and its degradation products, but simultaneous occurrence and parallel trend would be an indication for a displacement of intact GLYP*i*, which appears unlikely from these data. The analyses for GLYP*i* and AMPA*i* using HPLC-ESI-MS/MS in the leachates showed no occurrence of residues of these compounds above detection limits (0.1 μg L^{-1}). Therefore, the leached ^{15}N and ^{13}C residues are most likely no constituents of intact GLYP*i* or AMPA*i* but originated from further degradation products.

Soil analyses

The concentrations of GLYP*i*, ^{15}N and ^{13}C in the lysimeter soils derived from HPLC-ESI-MS/MS and IR-MS, respectively, were normalized and set to 100% since GLYP*i* was not detectable in soil extracts sampled before GLYP*i* application (data not shown) (Fig. 2a). The $\delta^{15}N$ decreased within 165 days after application to 24 and 29% of the initial value and decreased further to 11 and 19% until the end of the study period. This indicates that amounts of the added artificial ^{15}N isotopes in soil decreased over time. The same was true for $\delta^{13}C$ which decreased down to 30 and 66% compared with the initial value and ended at 23 and 54% in the two lysimeters (Fig. 2b).

Measurement of the GLYP*i* residues through HPLC-ESI-MS/MS showed that about 4 and 6% of the initial GLYP*i* concentration remained in the soil after 165 days and the recovery decreased further down to 1 and 3% in the two lysimeters until the end of the study (Fig. 2c). AMPA*i* was detected in the topsoil extracts of all samples after application (Suppl. Fig. S1), and GLYP*i* and AMPA*i* were not detected in the subsoil (results not shown). This indicates that AMPA*i* had not been formed, and GLYP*i* was already decomposed by microorganisms or scarcely displaced from surface into subsoil. Therefore, leaching of GLYP*i* or AMPA*i* can be considered as insignificant in this experiment and rapid degradation to further products most likely happened. This confirms Borggaard and Gimsing (2008) who reported a fast GLYP degradation and limited leaching through soil. Nevertheless, it is still possible that strongly bound non-extractable, and therefore non-detected residues of GLYP*i* or AMPA*i* could have remained in soil too, partly explaining the higher

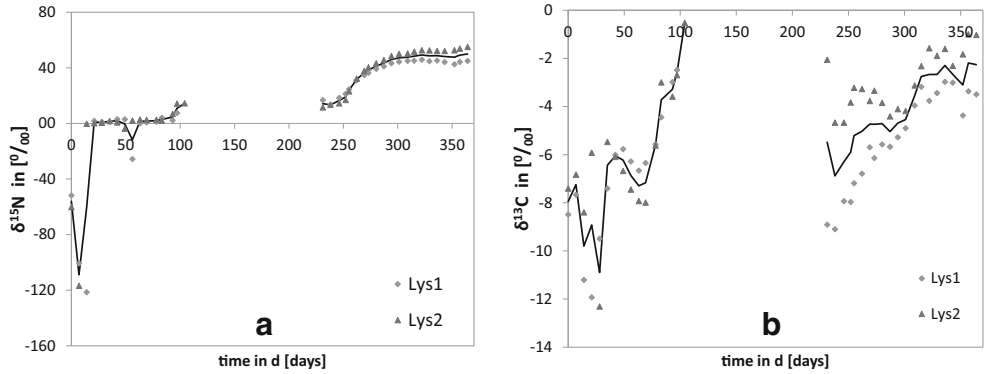

Fig. 1 $\delta^{15}N$ (**a**) and $\delta^{13}C$ (**b**) values for lyophilized leachates over the one-year study period in lysimeter 1 (Lys1) and lysimeter 2 (Lys2) and mean values (continuous line)

amounts of ^{13}C and ^{15}N after 165 and 360 days (Fig. 2a and b).

Plant material analyses

^{15}N was enriched highly significantly ($p < 0.01$) in all sampled plant compartments (root, 39 ± 10‰ and 54 ± 16; shoot, 28 ± 13‰ and 51 ± 16‰; cob, 34 ± 12‰ and 51 ± 14‰) compared with reference plant parts from a lysimeter that was not treated with GLYP*i* (root, 2.5 ± 1.6‰; shoot, 2.0 ± 0.9‰; cob, 4.0 ± 1.9‰) (Fig. 3). By comparison, ^{13}C was highly significantly enriched only in the plant roots from the two lysimeters treated with GLYP*i* (− 12.75 ± 0.07‰ and − 12.84 ± 0.06‰) compared with maize roots from the lysimeter with no herbicide treatment (− 13.03 ± 0.08‰). In contrast, ^{13}C was significantly depleted ($p < 0.01$) in the cob material of plants from lysimeters with GLYP*i* treatment (− 23.24 ± 0.18‰ and − 24.06 ± 0.96‰) compared with those with no treatment (− 22.84 ± 0.25‰). There was not a significant difference in the shoots between the treated (− 13.69 ± 0.06‰ and − 13.58 ± 0.05‰) and non-treated lysimeters (− 13.56 ± 0.45‰).

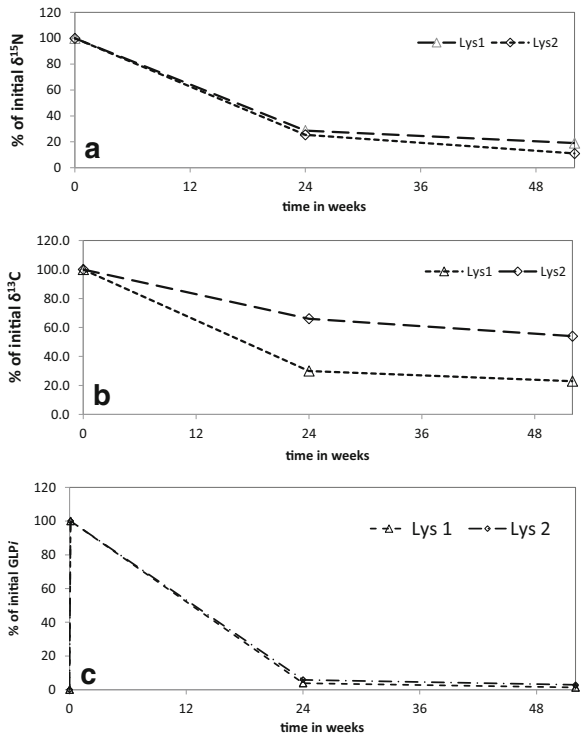

Fig. 2 Development of $\delta^{15}N$ (**a**), $\delta^{13}C$ (**b**), and $^{13}C_2$-^{15}N-glyphosate (**c**) in topsoil samples compared with initial values (set to 100%) over the studied period in lysimeter 1 (Lys1) and lysimeter 2 (Lys2)

The enrichment of ^{15}N in roots, shoots, and cobs can result only from uptake from the soil and distribution through the plant. Since ^{15}N is bound in GLYP*i* or its ^{15}N containing degradation products (Fig. 4), those degradation products must have acted as plant nutrients. Furthermore, as plants do not take up organic substances like GLYP*i* or AMPA*i* over the root system, the occurrence of ^{15}N can be plausibly explained only by an uptake of mineral ^{15}N ($^{15}NH_4^+$ and/or $^{15}NO_3^-$) as mineralized degradation products from GLYP*i,* which are formed by microbial degradation in the rhizosphere (Duke et al. 2012).

The enrichment of ^{13}C in the roots compared with plants from the non-treated lysimeter may either be a result of uptake or attachment to this plant compartment. The possibility of ^{13}C uptake should be excluded, since neither organic substances like GLYP*i* or AMPA*i* can be taken up by plant roots, nor were these substances further distributed into other plant compartments. Also, mineralized species of ^{13}C like $^{13}CO_2$ originating from

GLYP*i* degradation cannot be taken up by the roots. Therefore, enrichment of ^{13}C species is explained by attachment, possibly due to mycorrhizal fungi associated with the maize roots (Bott et al. 2011) that utilize organic substances as nutrients for growth.

In summary, since (i) ^{15}N has been taken up by the maize roots and distributed into all plant compartments and (ii) ^{13}C is only associated with the plant roots, the interaction of these labeled atoms with the plants most plausibly resulted from the independent interaction of the inorganic degradation products of GLYP*i*. $^{13}CO_2$ and $^{15}NH_3$ as the inorganic end-products of the degradation process can be emitted via the air path. This was shown for ^{14}C labeled GLYP (Grundmann et al. 2008). But since (i) $^{15}NH_3$ is water-soluble and forms $^{15}NH_4^+$ in soil solution and (ii) ^{15}N was taken up by plants, it is rather unlikely for inorganic N to be emitted into the air.

Summarizing discussion

Comparing the present approach with an overview of most important published GLYP-lysimeter studies, the compilation in Table 2 shows that most experiments have been conducted with radioactive labelling of GLYP ($n = 6$) in the laboratory or with non-labeled GLYP ($n = 3$). Among the latter studies, only two reflected field conditions. Filtered leachates for GLYP residues have been analyzed in all studies, but only four (Al-Rajab et al. 2008; Grundmann et al. 2008; Klier et al. 2008; Bergström et al. 2011) additionally analyzed extracted GLYP residues or its degradation products in soil. Thus, the present study was designed in detail so that field conditions are reflected and also all relevant compartments are considered.

In the present study, concentrations of extracted GLYP*i*-residues were low in soil at the end of the study period compared with the initial concentrations at the beginning. But fractions of ^{15}N and ^{13}C above extracted GLYP*i*-residues indicate that either non-extractable GLYP*i* is still left and/or further degradation products accumulated in soil. The latter explanation agrees with Al-Rajab et al. (2008), Grundmann et al. (2008), and Klier et al. (2008), who found low amounts of GLYP that remained in soil due to degradation of GLYP. Residues of GLYP and AMPA remained in topsoil (Bergström et al. 2011) and were either accumulated by organisms in the rhizosphere with low risk of leaching (Grundmann et al. 2008; Klier et al. 2008) or have been sorbed to soil particles with a risk of leaching (Al-Rajab et al. 2008).

The ^{13}C and ^{15}N are signals of leachates (Fig. 1), but absence or low concentrated (< LOD) residues of GLYP*i* and AMPA*i* indicate that further degradation products have been leached through the soil column, which partly confirms De Jonge et al. (2000), Fomsgaard et al. (2003), and Dousset et al. (2004). In contrast, leaching of GLYP and AMPA in lysimeters was reported for tilled soils and explained by particle transport (Fomsgaard et al. 2003; Malone et al. 2004; Kjær et al. 2005). This contradiction may result from different experimental designs, soil properties, and management measures that support or suppress particle-bound GLYP transport (Fomsgaard et al. 2003). Furthermore, the methods applied differ in their sensitivity to detect particle-bound GLYP or AMPA in leachates or soil extracts (Table 2). For instance, HPLC only provides information on the concentration of free or extractable amounts of GLYP or AMPA (Malone et al. 2004), since filtration is mandatory before HPLC-MS/MS measurements of liquid samples. However, HPLC cannot distinguish between bound (non-extractable) GLYP and further degradation products, since only free and recoverable GLYP can be detected. Most of the lysimeter studies complied in Table 2 used single ^{14}C labelling (radioactive), which can be assigned to GLYP or AMPA in leachates or extracts by its retention time and molecular mass and/or radioactive signal when measured by HLPC in combination with mass spectrometry and/or scintillation detection. However, molecule identification only by scintillation of solid samples is not possible, since the signal of a labeled C-atom originate come from intact GLYP or degradation products, even if the position of the labelling in the initial GLYP molecule is known. Therefore, the multi-labelling of GLYP with ^{15}N and ^{13}C in the present field lysimeter study, by avoiding disadvantages of previous studies, has shown (time-) independent occurrence of GLYP*i* decomposition products. The noncorrelated appearance of ^{13}C and ^{15}N signals in leachates (Fig. 1) makes the degradation pathway B in Fig. 4 rather unlikely, in agreement with Borggaard and Gimsing (2008). Instead, pathway A in Fig. 4 is supported by the noncorrelated appearance of ^{13}C and ^{15}N signals in leachates, among which ^{13}C can originate from glyoxylic acid and ^{15}N from detected AMPA*i* or further degradation products, such as methylamine and ammonium ions (Fig. 4). Along

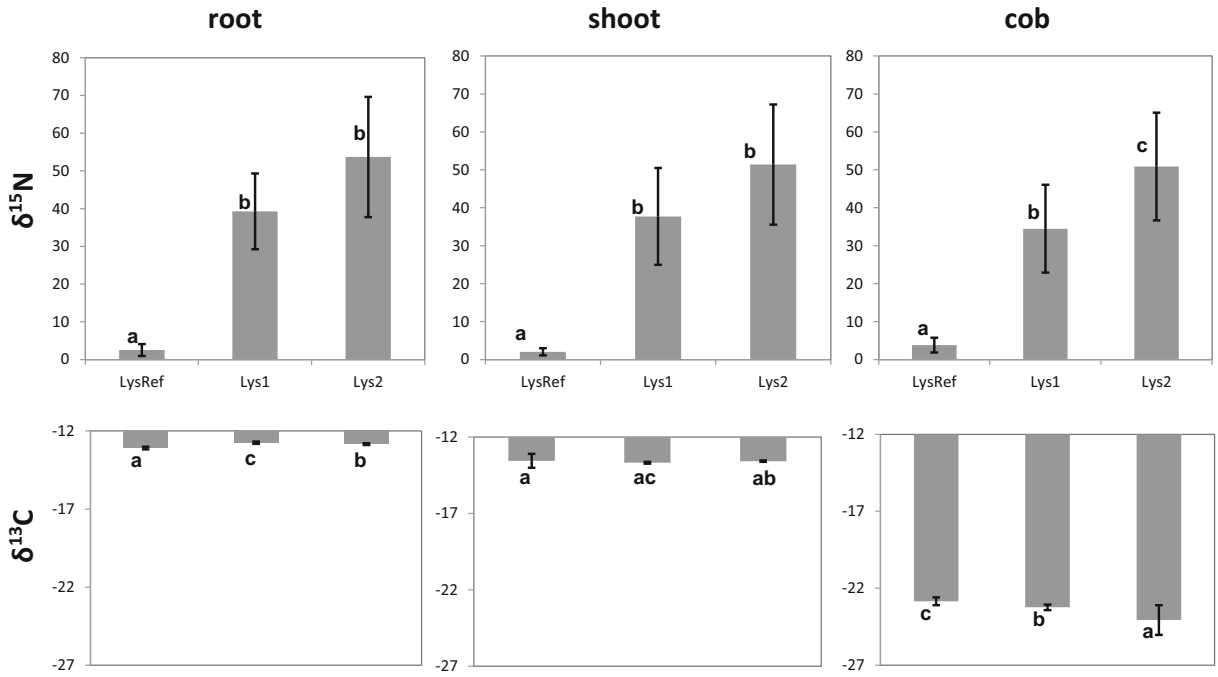

Fig. 3 $\delta^{15}N$ and $\delta^{13}C$ mean values in plant material of roots, shoots, and cobs of maize plants of the tested lysimeter 1(Lys1), lysimeter 2 (Lys2), and a reference lysimeter (LysRef)

with small concentrations of extracted GLYP*i* (Fig. 2c) under practically optimal leaching conditions in the very wet hydrological year 2017/2018, the present findings indicate that rapid degradation most likely is the best explanation for the absence of concentrations below LOD of GLYP*i* and AMPA*i* in leachates, which confirms previous findings as referenced in Table 2.

Conclusions

Isotopic ratios of $^{13}C/^{12}C$ and $^{15}N/^{14}N$ and resulting changes of $\delta^{13}C$ and $\delta^{15}N$ from isotopically labeled glyphosate (GLYP*i*) and its degradation products were successfully quantified using isotopic ratio mass spectrometry (IR-MS) in different compartments (leachates, soil, and plant material) of a field lysimeter. Therefore,

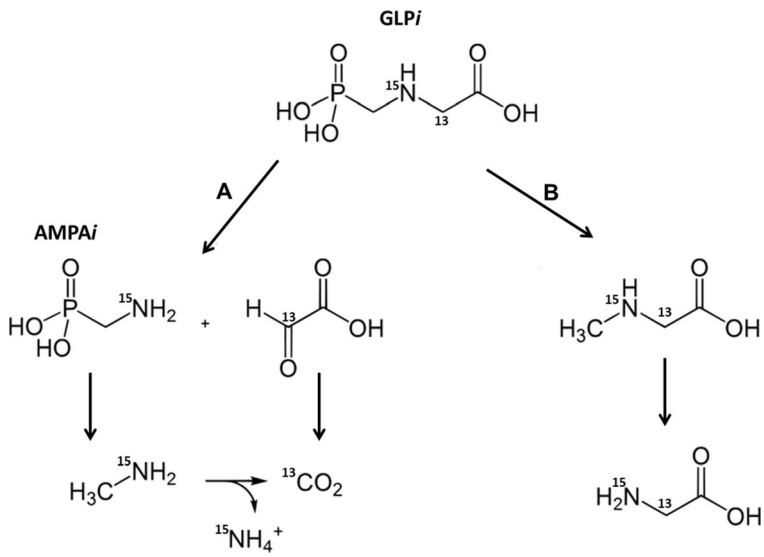

Fig. 4 Degradation pathways of isotopic labeled $^{13}C_2$-^{15}N-glyphosate (GLP*i*) and its main degradation product ^{15}N-aminomethylphosphonic acid (AMPA*i*) with indicated positions of labelling (modified from Giesy et al. 2000)

Table 2 Literature data of methods for lysimeter studies using glyphosate of different labelling

Reference	Country	Lysimeter soil column, site (10^3 cm^3)	Labelling	Application (kg ha^{-1})	Analytical detection	Studied compartment		
						Leachate	Soil	Plant
De Jonge et al. 2000	Denmark	8, laboratory	^{14}C	2.4	Scintillation	x	x	
Fomsgaard et al. 2003	Denmark	550, laboratory	^{14}C	0.8	GC-MS	x		
Dousset et al. 2004	France	3, laboratory	None	1.5	LC-ESI-MS/MS	x x		
Malone et al. 2004	USA	19,440, field	None	0.5	FLD	x		
Kjær et al. 2005	Denmark	*(drained field)*	None	1.44	HPLC-EI-MS	x		
Al-Rajab et al. 2008	France	2, laboratory	^{14}C	2.2	HPLC-FLD/RFD	x	x	
Grundmann et al. 2008	Germany	20, laboratory	^{14}C	3 × 1	Scintillation, HPLC-RFD	x	x	x
Klier et al. 2008	Germany	20, laboratory	^{14}C	10.8	Scintillation, HPLC-RFD	x	x	x
Bergström et al. 2011	Sweden	34, laboratory	^{14}C	1.5	GC–MS	x	x	
present study	Germany	1000, field	^{15}N-$^{13}C_2$	3.6	IR-MS, HPLC-ESI-MS/MS	x	x	x

GC, gas chromatography; *HPLC*, high performance liquid chromatography

ESI-MS/MS, electro spray ionization tandem mass spectrometry; *EI-MS*, electron impact mass spectrometry

FLD, fluorescence detection; *RFD*, radio flow detection

IR-MS, isotopic ratio mass spectrometry

this experimental approach was well suited to trace GLYP*i* under practice-near experimental conditions.

Since (i) the great decline of GLYP*i* content down to < 3% of initial amounts in soil during the one-year study period and (ii) a lower decline of ^{13}C (< 60%) and ^{15}N (< 20%), we conclude that either further degradation products had been formed and/or non-extractable and, therefore, strongly bound GLYP*i* remained in soil and accumulated. The disparate increase of $\delta^{13}C$ and $\delta^{15}N$ values in leachates and plant material is explained plausibly by (i) rapid degradation of GLYP*i* within one vegetation period and, also (ii) the selective uptake of mineralized ^{15}N species from degraded GLYP*i* as plant nutrient, most likely NH_4^+ or NO_3^-. These findings from a wet hydrological year support the assumption that the risk of leaching of applied GLYP to other waterbodies can be considered to be low under central European climatic conditions. Accumulation in soil may enhance the risk of further distribution in the environment by soil erosion.

Acknowledgements The authors thank Evelyn Bolzmann from the Department Soil Physics at the University of Rostock for her support in IC measurements of Br-, Melitta Stratschka from the lysimeter station Falkenberg for the support in the management and cultivation of the test sites and also Prof. Silvia Rudloff and Dr. Christian Borsch from the University of Gießen (Department of Nutritional Sciences) for their supporting measurements through IR-MS. This research was conducted within the scope of the Leibniz ScienceCampus Phosphorus Research Rostock.

Funding information Open Access funding provided by Projekt DEAL. Peter Gros acknowledges a PhD grant from the state of Mecklenburg-Western Pommerania.

Compliance with ethical standards

Conflict of interest The authors declare that they have no conflict of interest.

References

Ahmed, A. A., Leinweber, P., & Kühn, O. (2017). Unravelling the nature of glyphosate binding to goethite surfaces by *ab initio* molecular dynamics simulations. *Physical Chemistry Chemical Physics, 20*, 1531.

Ahmed, A. A., Gros, P., Kühn, O., & Leinweber, P. (2018). Molecular level investigation of the role of peptide interactions in the glyphosate analytics. *Chemosphere, 196*, 129–134.

Al-Rajab, A. J., Amellal, S., & Schiavon, M. (2008). Sorption and leaching of ^{14}C-glyphosate in agricultural soils. *Agronomy of Sustainable Development, 28*, 419–428.

Bergström, L., Börjesson, E., & Stenström, J. (2011). Laboratory and lysimeter studies of glyphosate and aminomethylphosphonic acid in a sand and a clay soil. *Journal of Environmental Quality, 40*, 98–108.

Borggaard, O. K., & Gimsing, A. L. (2008). Fate of glyphosate in soil and the possibility of leaching to ground and surface waters: a review. *Pest Management Science, 64*, 441–456.

Bott, S., Tesfamariam, T., Kania, A., Eman, B., Aslan, N., Römheld, V., & Neumann, G. (2011). Phytotoxicity of glyphosate soil residues re-mobilised by phosphate fertilisation. *Plant and Soil, 342*, 249–263.

Coupe, R. H., Kalkhoff, S. J., Capel, P. D., Gregoire (2012). Fate and transport of glyphosate and aminomethylphosphonic acid in surface waters of agricultural basins. *Pest Management Science, 68*, 16–30.

de Jonge, H., de Jonge, L. W., & Jacobsen, O. H. (2000). [14C]glyphosate transport in undisturbed topsoil columns. *Pest Management Science, 56*, 909–915.

Dion, H. M., Harsh, J. B., & Hill Jr., H. H. (2001). Competitive sorption between glyphosate and inorganic phosphate on clay minerals and low organic matter soils. *Journal of Radioanalytical and Nuclear Chemistry, 249*, 385–390.

Dousset, S., Chauvin, C., Durlet, P., & Thévenot, M. (2004). Transfer of hexazinone and glyphosate through undisturbed soil columns in soils under Christmas tree cultivation. *Chemosphere, 57*, 265–272.

Duke, S. O., Lydon, J., Koskinen, W. C., Moorman, T. B., Chaney, R. L., & Hammerschmidt, R. (2012). Glyphosate effects on plant mineral nutrition, crop rhizosphere microbiota, and plant disease in glyphosate resistant crops. *Journal of Agricultural and Food Chemistry, 60*, 10375–10397.

Fomsgaard, I. S., Spliid, N. H., & Fielding, G. (2003). Leaching of pesticides through normal-tillage and low-tillage soil—a lysimeter study: II. Glyphosate. *Journal of Environmental Science and Health. Part. B, 38*, 19–35.

Führ, F., Hance, R. J., Plimmer, J. R., & Nelson, J. O. (1998). *The lysimeter concept: environmental behaviour of pesticides* (Vol. 699). *ACS Symposium Series*, Washington.

Giesy, J. P., Dobson, S., & Solomon, K. R. (2000). Ecotoxicological risk assessment for roundup® herbicide. In G. W. Ware (Ed.), *Reviews of Environmental Contamination and Toxicology* (Vol. 167). New York: Springer.

Gros, P., Ahmed, A. A., Kühn, O., & Leinweber, P. (2017). Glyphosate binding in soil as revealed by sorption experiments and quantum-chemical modelling. *Science of the Total Environment, 586*, 527–535.

Grundmann, S., Dörfler, U., Ruth, B., Loos, C., Wagner, T., Karl, H., Munch, J. C., & Schroll, R. (2008). Mineralization and transfer processes of ^{14}C-labeled pesticides in outdoor lysimeters. *Water, Air, & Soil Pollution: Focus, 8*, 177–185.

Kjær, J., Olsen, P., Ullum, M., & Grant, R. (2005). Leaching of glyphosate and amino-methylphosphonic acid from Danish agricultural field sites. *Journal of Environmental Qualilty, 34*, 608–620.

Klier, C., Grundmann, S., Gayler, S., & Priesack, E. (2008). Modelling the environmental fate of the herbicide glyphosate in soil lysimeters. *Water, Air, & Soil Pollution: Focus, 8*, 187–207.

Laitinen, P., Rämö, S., & Siimes, K. (2007). Glyphosate translocation from plants to soil-does this constitute a significant proportion of residues in soil? *Plant and Soil, 300*(1–2), 51–60.

Malone, R. W., Shipitalo, M. J., Wauchope, R. D., & Sumner, H. (2004). Residual and contact herbicide transport through field lysimeters via preferential flow. *Journal of Environmental Qualilty, 33*, 2141–2148.

Meissner, R., Rupp, H., Seeger, J., Ollesch, G., & Gee, G. W. (2010). A comparison of water flux measurement: passive wick-samplers versus drainage lysimeters. *European Journal of Soil Science, 61*(4), 609–621.

Morillo, E., Undabeytia, T., & Maqueda, C. (1997). Adsorption of glyphosate on the clay mineral montmorillonite: effect of Cu(II) in solution and adsorbed on the mineral. *Environmental Science and Technology, 31*, 3588–3592.

Muskus, A. M., Krauss, M., Miltner, A., Hamer, U., & Nowak, K. M. (2019). Effect of temperature, pH and total organic carbon variations on microbial turnover of $^{13}C_3$ ^{15}N-glyphosate in agricultural soil. *The Science of the Total Environment, 658*, 697–707.

Neumann, G., Kohls, S., Landsberg, E., Stock-Oliveira Souza, K., Yamada, T., & Römheld, V. (2006). Relevance of glyphosate transfer to non-target plants via the rhizosphere. *Journal of Plant Diseases and Protection*, 963–969 ISSN 1861-4051.

Okada, E., Costa, J. L., & Bedmar, F. (2016). Adsorption and mobility of glyphosate in different soils under no-till and conventional tillage. *Geoderma, 263*, 78–85.

Richmond, M. E. (2018). Glyphosate: a review of its global use, environmental impact, and potential health effects on humans and other species. *Journal of Environmental Studies and Sciences, 8*, 416–434.

Rupp, H., Meissner, R., & Leinweber, P. (2018). Plant available phosphorous in soil as predicted for leaching potential: insights from long-term lysimeter studies. *Ambio, 41*(suppl. 1), 103–113.

Skeff, W., Neumann, C., & Schulz-Bull, D. E. (2015). Glyphosate and AMPA in the estauries of the Baltic Sea method optimization and field study. *Marine Pollution Bulletin, 100*(1), 577–585.

Tang, F. H. M., Jeffries, T. C., Vervoort, R. W., Conoley, C., Coleman, N. V., & Maggi, F. (2019). Microcosm experiments and kinetic modelling of glyphosate biodegradation in soils and sediments. *Science of the Total Environment, 658*, 105–115.

Van Stempvoort, D. R., Roy, J. W., Brown, J., & Bickerton, G. (2014). Residues of the herbicide glyphosate in riparian groundwater in urban catchments. *Chemosphere, 95*, 455–463.

Wirth, M. A., Sievers, M., Habedank, F., Kragl, U., Schulz-Bull, D. E., & Kanwischer, M. (2019). Electrodialysis as a sample processing tool for bulk organic matter and target pollutant analysis of seawater. *Marine Chemistry, 217*, 103719. https://doi.org/10.1016/j.marchem.2019.103719.

Publication 5

A Glyphosate Pulse to Brackish Long-Term Microcosms Has a Greater Impact on the Microbial Diversity and Abundance of Planktonic Than of Biofilm Assemblages

by

René Janßen, Wael Skeff, Johannes Werner, **Marisa A. Wirth**, Bernd Kreikemeyer, Detlef E. Schulz-Bull, Matthias Labrenz

Frontiers in Marine Sciences

Year 2019, Volume 6, Article 758

DOI: 10.3389/fmars.2019.00758

frontiers in Marine Science

ORIGINAL RESEARCH
published: 10 December 2019
doi: 10.3389/fmars.2019.00758

A Glyphosate Pulse to Brackish Long-Term Microcosms Has a Greater Impact on the Microbial Diversity and Abundance of Planktonic Than of Biofilm Assemblages

*René Janßen[1], Wael Skeff[2], Johannes Werner[1], Marisa A. Wirth[2], Bernd Kreikemeyer[3], Detlef Schulz-Bull[2] and Matthias Labrenz[1]**

[1] Department of Biological Oceanography, Leibniz Institute for Baltic Sea Research Warnemünde, Rostock, Germany, [2] Department of Marine Chemistry, Leibniz Institute for Baltic Sea Research Warnemünde, Rostock, Germany, [3] Institute of Medical Microbiology, Virology and Hygiene, University of Rostock, Rostock, Germany

OPEN ACCESS

Edited by:
Xiaoshou Liu,
Ocean University of China, China

Reviewed by:
Ying Wang,
Tianjin University of Commerce, China
Wenyan Zhang,
Institute of Oceanology (CAS), China

***Correspondence:**
Matthias Labrenz
matthias.labrenz@io-warnemuende.de

Specialty section:
This article was submitted to Marine Pollution, a section of the journal Frontiers in Marine Science

Received: *26 August 2019*
Accepted: *21 November 2019*
Published: *10 December 2019*

Citation:
Janßen R, Skeff W, Werner J, Wirth MA, Kreikemeyer B, Schulz-Bull D and Labrenz M (2019) A Glyphosate Pulse to Brackish Long-Term Microcosms Has a Greater Impact on the Microbial Diversity and Abundance of Planktonic Than of Biofilm Assemblages. Front. Mar. Sci. 6:758. doi: 10.3389/fmars.2019.00758

The widespread herbicide glyphosate has been detected in aquatic coastal zones of the southern Baltic Sea. We monitored community dynamics in glyphosate-impacted chemostats for 20 weeks to evaluate the potential impact of the herbicide on free-living and biofilm-associated bacterial community assemblages in a brackish ecosystem. A HPLC-MS/MS method was developed to measure glyphosate, aminomethylphosphonic acid and sarcosine concentrations within a brackish matrix. These concentrations were analyzed weekly, together with prokaryotic succession, determined by total cell counts and next generation 16S rRNA (gene) amplicon sequencing. Shotgun metagenomics provided insights into the glyphosate degradation potential of the microbial communities. Temporal increases in total cell counts, bacterial diversity and the abundances of distinct bacterial operational taxonomic units were identified in the water column. Biofilm communities proved to be less affected than pelagic ones, but their responses were of longer duration. The increase of glyphosate oxidoreductase (*gox*) and *thiO* gene as well as the *phn* operon abundance indicated glyphosate degradation by first the aminomethylphosphonic acid pathway and possibly a subsequent cleavage of the C-P bond. However, although glyphosate concentrations were reduced by 99%, 1 μM of the herbicide remained until the end of the experiment. Thus, when present at low concentrations, glyphosate may evade bacterial degradation and persist in Baltic Sea waters.

Keywords: glyphosate, AMPA, Baltic Sea, *phn*, *gox*, next-generation sequencing, *Gallaecimonas*, bacteria

INTRODUCTION

Microorganisms are ubiquitous on Earth and respond rapidly to environmental changes. The majority of microorganisms live within biofilms, which promote high cell abundances and activities (Costerton et al., 1995). In mature biofilms, extracellular polymeric substances produced by resident species give rise to a distinct three dimensional structure. That way microorganisms are protected

from disturbances that for planktonic cells or even higher organisms induce toxicity and other forms of stress (Davey and O'Toole, 2000; Reese et al., 2016). However, biofilms are not completely invulnerable (Qu et al., 2017), as evidenced by changes in their assemblages in response to a wide range of disturbances.

A potential environmental stressor is glyphosate, which has been in use since the 1970s. Following assessments demonstrating its relatively low environmental toxicity, it has become the most widely produced and sold herbicide worldwide. However, as a synthetic combination of glycine and a phosphate residue, coupled to form a stable phosphonate, glyphosate provides carbon (C), nitrogen (N), and phosphorus (P) for bacteria and fungi (Lipok et al., 2007; Duke and Powles, 2008). Two major routes of glyphosate biodegradation have been described according to their first respective intermediate: the sarcosine pathway and the aminomethylphosphonic acid (AMPA) pathway, encoded mainly by the *phn* operon and the glyphosate oxidoreductase (*gox*) gene, respectively. The *phn* operon encodes a C-P lyase, whose activity makes the P component of phosphonate bioavailable. In the AMPA pathway, glyphosate is cleaved at the C-N bond, resulting in AMPA and glyoxylate. An alternative pathway to yield AMPA from glyphosate was discovered with the enzyme glycine oxidase encoded by *thiO*. However, this enzyme possesses an unspecific K_m of 87 mM for glyphosate, compared to 0.6 mM for glycine (Pedotti et al., 2009).

Glyphosate has been detected in marine and freshwater systems (Van Bruggen et al., 2018; Carles et al., 2019), representing a disturbance to microbial communities at concentrations upwards of 5.92 nM (Stachowski-Haberkorn et al., 2008). Moreover, its dissipation is enhanced by biofilms, probably due to their adsorption capacities (Klátyik et al., 2017). The presence of glyphosate in the brackish Baltic Sea from agricultural runoff has been reported (Skeff et al., 2015), but the effects of the herbicide on its ecosystems are as yet unknown. The Baltic Sea is known for elevated contamination levels and monitoring of the environmental state is mandatory (Helcom, 2018). Thus, the aim of this study was to investigate the impact of glyphosate on the state and succession of bacterial community assemblages in a Baltic-Sea-like environment. Potential effects were compared between free-living and biofilm communities, as biofilm communities are expected to be more resilient. Furthermore, the potential for and means of biodegradation, as well as the possibly involved OTUs, were analyzed to evaluate the fate of glyphosate entering the Baltic Sea.

MATERIALS AND METHODS

Experimental Setup

Microcosm Experiment

The experiment was conducted in two 12 L (20 × 30 × 20 cm) microcosms (Rebie Aquaristik, Bielefeld, Germany) made of float glass plates sealed with silicone glue. The microcosms were filled with 2 kg of combusted quartz sand as hard substrate, 8 L artificial brackish water (ABW) amended with casamino acids as liquid medium (modified after Bruns et al., 2002) and combusted GF/F microfiber filters (Ø 47 mm, Whatman, Little Chalfont, United Kingdom) as collectible, inert biofilm substrate. An air pump aerated and mixed the system continuously. The microcosms were incubated with a Baltic Sea-derived inoculum and the 140-day experiment started with an equilibration period from day −69 until day 0 to allow biofilm to form and mature. On day −31 the system switched from batch to continuous cultivation mode with an average efflux rate of 475–489 $mL \cdot d^{-1}$. During the whole period microbial succession in both microcosms was monitored. On day 0, a sterile-filtrated glyphosate solution (final concentration of 82.45 μM; Dr. Ehrenstorfer, Augsburg, Germany) was syringe-injected into the water column of the treatment microcosm and dispersed throughout by manual stirring. Monitoring went on until day +71. For further details on experimental procedures see Janßen et al. (2019).

Prevention of Glyphosate Adsorption to Abiotic Surfaces

Glyphosate can adsorb to glass or sediment surfaces (Bergström et al., 2011; Huang and Zhang, 2011) and might also adhere to biofilms. Adsorption may affect not only glyphosate degradation in the liquid phase but also act as a glyphosate reservoir during incubations. However, a surface adsorption test performed prior to the start of our experiment showed stable glyphosate concentrations in the water column of the glyphosate-containing microcosms (**Supplementary Material 1**).

Sampling Procedure

Five-mL water samples for glyphosate, AMPA, sarcosine/L-alanine and nutrient analyses were stored at −20°C without further treatment. For nucleic acid extraction and subsequent next-generation sequencing (NGS) of planktonic cells, 100 mL of water was filtered through 0.22-μM GVWP filters in three replicates. For the analysis of biofilm communities, three overgrown GF/F filters were selected with sterile tweezers. The total data set consisted of 287 samples, with water samples covering 16 time points (days −25, −7, 0, +3, +7, +10, +14, +17, +22, +29, +36, +43, +50, +57, +64, +71) and biofilm filters eight time points (days −7, 0, +7, +17, +29, +43, +57, +71). Detailed meta-information describing the samples is provided in **Supplementary Material 2**. The filters were shock frozen in liquid nitrogen and stored at −80°C until their use for DNA/RNA extractions. Planktonic cell counts were determined in 1-mL water samples fixed with 1/10 $v \cdot v^{-1}$ formol (37%, sterile filtered, Rotipuran p.a. ACS, Carl Roth GmbH, Karlsruhe, Germany), incubated for at least 2 h at room temperature or overnight at 4°C and processed within 24 h. For C and N analyses, 100 mL of water was collected on day +71.

Determination of Total Cell Counts

Water column cell counts were determined by 4′,6-diamidino-2-phenylindole (DAPI; Applichem GmbH, Darmstadt, Germany) staining according to Porter and Feig (1980). To ensure that cells on the filter surfaces were evenly distributed, the cells on the filter were diluted, if necessary, using sterile ABW. The cells obtained

by filtering 50–500 μL of water on a Cyclopore filter (PC BLK, 25 mm, 0.2 μm, Whatman, Maidstone, United Kingdom) were stained with 10 mg DAPI·L^{-1} for 3 min and embedded using AF1 (Citifluor Ltd, London, United Kingdom) and Vectashield (H 1000, Vector Laboratories, Burlington, CA, United States) at a 7:1 ratio. Total cell counts were determined in triplicate samples using an Axio Lab. A1 equipped with a *N*-Achroplan 100× oil dispersion objective (both Carl Zeiss AG, Göttingen, Germany). Twenty small quadrats were counted in 25 different fields of view per filter.

Significance Testing Applied to Total Cell Counts

To test for a statistically significant change in total cell counts after the addition of glyphosate, the cell counts prior to (days −7 to +3) and after (days +28 to +36) the cell number increase were combined and compared with the counts from days in which cell numbers increased (days +7 to +22). A second comparison was performed between treatment and control microcosms for the cell counts from day +7 to +22 only. Total cell counts were analyzed in triplicate samples using a two tailed *t*-test for two heteroscedastic samples. Significant changes ($p < 0.05$) are marked with * in **Figure 1A**.

Nutrient Analysis

To understand the nutritional relevance of glyphosate, particulate organic nitrogen and carbon (POC/PON) concentrations were analyzed using an vario Micro element analyzer (Elementar Analysensysteme GmbH, Langenselbold, Germany), and dissolved organic carbon and nitrogen (DOC/DON) concentrations using a Shimadzu TOC-V + TNM1 analyzer (Duisburg, Germany). Dissolved inorganic phosphorus (DIP) was measured following the method of Grasshoff et al. (2007).

Glyphosate and AMPA Analysis

Glyphosate and AMPA analyses followed the procedure of Skeff et al. (2015, 2016). Internal standards of glyphosate (1-2-^{13}C2 ^{15}N glyphosate) and AMPA (^{13}C ^{15}N AMPA) were prepared in the same sample matrices and added to the samples. The samples were adjusted to pH 9 by the addition of 100 μL of borate buffer and then derivatized by treatment with 100 μL of 19.8 mM FMOC-Cl in acetonitrile. After 4 h of incubation at 21°C, the derivatized samples were filtered through a 0.45-μm Phenex-RC 15-mm syringe filter and subjected to LC–MS/MS. The target compounds were analyzed using an Accela HPLC system connected to a TSQ Vantage triple quadrupole mass analyzer with a heated electrospray ionization source interface. Chromatographic reversed-phase separation was achieved on a Gemini-NX C18 column coupled to a Gemini-NX Security Guard cartridge. The samples were eluted gradually from the column with (a) a 2 mM ammonium hydrogen carbonate buffer and ammonia solution (32%, v·v^{-1}) at pH 9 and (b) acetonitrile. Before the analysis, the instrument was calibrated for the target substances using the same sample matrices. Each compound, including the internal standard, was scanned for two transitions in selected reaction monitoring mode. The most abundant transition was used for quantification and the other transition for confirmation.

Additional measurements for AMPA and sarcosine were carried out after an initial evaluation of the data. The applied method generally followed the procedure described above, with the following differences: After derivatization of the samples, 1 mL of dichloromethane was added to the mixture to extract the remaining FMOC-Cl. Samples were shaken and then centrifuged for 10 min at 1000 rpm. The supernatant was removed and transferred into a vial for analysis. Chromatographic separation and mass spectrometric detection was carried out as described above, but with a LC-2040C Nexera-I and a triple quadrupole mass spectrometer LCMS-8060 as also described in Wirth et al. (2019). Compounds were detected through SRM events, as described above. Sarcosine has the same MS fragments and retention time as L-alanine, since the two compounds are isomers. Thus, they could not be differentiated with the utilized method. To acquire evidence for the presence or absence of sarcosine in the samples, comparative measurements between samples from both microcosms were conducted, since the L-alanine concentration should be identical.

Nucleic Acid Extraction and Sequencing

The kit-based extraction of nucleic acids from free-living bacteria and subsequent DNAse digestion of the RNA extracts were performed according to Bennke et al. (2018). Biofilm samples were extracted using the phenol-chloroform method described in Weinbauer et al. (2002). cDNA synthesis was performed using 20 ng of DNA-free total RNA as the input for the MultiScribe (Fisher Scientific GmbH, Germany) reverse transcriptase system using the reverse primer 1492r (5′ TACGGYTACCTTGTTACGACTT, Lane, 1991). Illumina amplicon sequencing was prepared as described in Bennke et al. (2018). The V3-V4 region of the 16S rRNA gene was targeted using the primer set 341f-805r (forward: CCTACGGGNGGCWGCAG, reverse: GACTACHVGGGTATCTAATCC, Herlemann et al., 2011). Indexed amplicon libraries were pooled to a concentration of 4 μM. The PhiX control was spiked into the library pools at a concentration of 10%. Each final library pool (4 pM) was subjected to one of three consecutive individual paired-end sequencing runs using 600 cycle V3 chemistry kits on an Illumina MiSeq.

Bioinformatic and Statistical Analysis of the Amplicon Data

Amplicon read processing and annotation were conducted using Mothur v. 1.39.5 (Schloss et al., 2009). Sequences were combined in a pre-cluster step if there were less than 2 mismatches. Chimeras were removed using VSEARCH (Rognes et al., 2016). OTUs were picked based on a 98% similarity threshold. When counting the number of OTUs, singletons were ignored, but not removed from the data set. OTUs were only removed where mentioned and all parameters are deposited in the Github repository listed in the data availability statement.

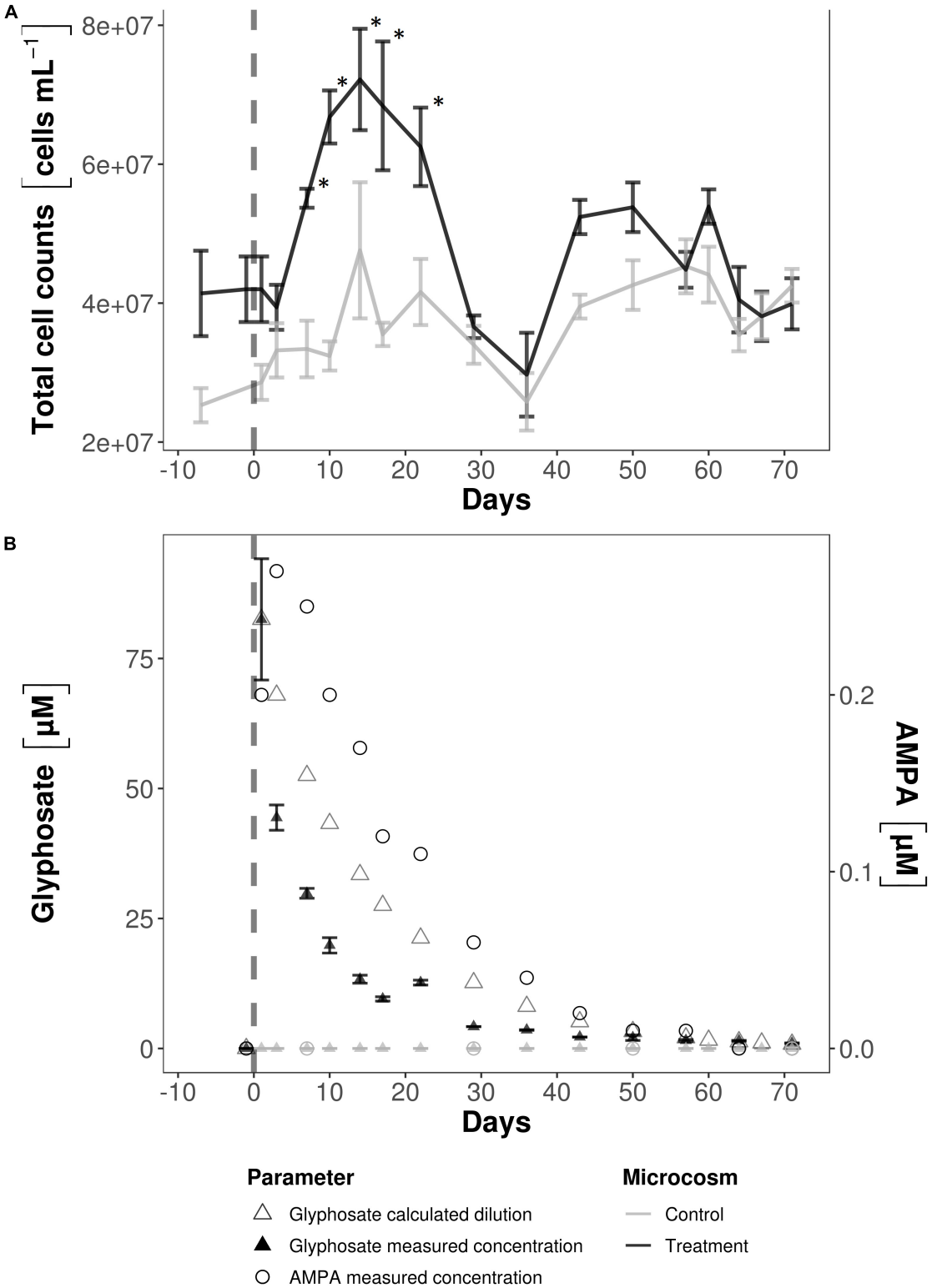

FIGURE 1 | Total cell counts **(A)** and glyphosate and AMPA concentrations **(B)** in the water column of the microcosms. **(A)** Total cell counts after glyphosate addition at day 0 increased significantly (*) compared to cell numbers before and later after herbicide addition ($p < 0.001$) and to the cell counts of the control microcosms during the same time period ($p < 0.001$). **(B)** On day 0, the concentration was measured before and after glyphosate addition. AMPA was already present in the first sample taken 4 h afterward, though not at its highest concentration. The decrease in the calculated glyphosate concentration was slower than the measured values. Note the different scales for glyphosate and AMPA and that at the end of the experiment glyphosate persisted at a concentration > 1 µM.

The operational taxonomic unit (OTU) and taxonomy table were imported into R v. 3.5.1 (R Core Team, 2018) and analyzed using phyloseq v. 1.26.0 (McMurdie and Holmes, 2013), ggplot2 v. 3.1.0 (Wickham, 2009) and DESeq2 v. 1.22.1 (Love et al., 2016). Taxonomic annotation of the data presented herein was accomplished using the Silva release 132 (Yilmaz et al., 2014), including the taxonomic changes proposed by Parks et al. (2018).

Basic information on the amplicon sequencing-based approaches is provided in **Supplementary Material 3**, including the MiSeq run statistics, sequencing depth and average sequence length in the 16S complementary rRNA and 16S rRNA gene libraries.

The composition of the microbial communities was plotted enforcing a relative abundance cut-off value of 0.15% at order level to reduce the legend size. To identify OTUs whose abundance changed after glyphosate addition, unfiltered 16S rRNA gene and 16S rRNA OTU tables were used separately as input for DESeq2, as suggested by McMurdie and Holmes (2014). DESeq2 performed the Wald test on two time points (in three technical replicates) before glyphosate addition versus five time points directly thereafter. For the less-frequent biofilm sampling, the time span was the same, resulting in comparisons of two time points before versus two time points immediately after glyphosate addition. The abundances of selected OTUs were plotted. The relative abundances of the OTUs in treatment and control microcosms were compared manually to identify those OTUs that responded to glyphosate.

The similarity of microbial communities was visualized in non-metric multidimensional scaling (NMDS) analyses based on Bray–Curtis dissimilarities. Relative abundances were used as input, square-root-transformed and Wisconsin double-standardized. The ordination with the lowest stress was determined based on 100 runs. OTUs with at least three reads were included. OTU tables for the Chao1 richness estimate and Shannon index included singletons. A *t*-test was applied to analyze the significance of a change in α-diversity after glyphosate addition and was performed for all sample subsets from day −22 to day 0 vs. day +3 to day +17.

To include the concentration of glyphosate into the ordination, canonical correspondence analysis (CCA) and redundancy analysis (RDA) were performed within phyloseq using its ordinate function. The input data was as described for NMDS and glyphosate concentration was the constraint. The resulting plots are shown in **Supplementary Material 4**.

Metagenomic Analysis

For metagenomic analyses, technical replicates of DNA extracts were pooled. Metagenomic reads of seven treatment and three control microcosm water-column samples were generated by a full run on an Illumina Nextseq500 (LGC Genomics GmbH, Berlin, Germany). Reads were quality checked using FastQC v. 0.11.7[1] and trimmed with Trimmomatic v. 0.38 (Bolger et al., 2014). The individual samples were merged and co-assembled using MEGAHIT v. 1.1.3 (Li et al., 2014) with the k-mer list 21, 25, 29, 33, 37, 41, 45, 49, 53, 57, 61, 65, 69, 73, 77, 81, 85, 89, 93, 97, and 99. The genes were predicted and functionally annotated using Prokka v. 1.13.0 (Seemann, 2014). For gene quantification, the reads of the individual samples were mapped on the assembled contigs using Kallisto v. 0.44.0 (Bray et al., 2016).

[1]https://www.bioinformatics.babraham.ac.uk/projects/fastqc/

Functional Tree Calculation

Correlations between the abundances of OTUs and glyphosate degradation genes were identified. Protein sequences of organisms related to the OTUs identified in this study were downloaded from UniProt (Bateman et al., 2017). The corresponding genes identified in the assembled metagenome were translated and added to this sequence set. After the removal of exact duplicates using CD-Hit auxtools v.4.6.8 (Fu et al., 2012), a multiple sequence alignment was built using Mafft v. 7.407 (Katoh and Standley, 2013). A phylogenetic tree was calculated using RAxML v. 8.2.12 (Stamatakis, 2014), with "PROTCATAUTO" as the amino acid substitution model, and plotted together with the respective abundances using R package ggtree v. 1.8.2 (Yu et al., 2018). This workflow was implemented in Nextflow v. 18.10.1 (Di Tommaso et al., 2017).

No *gox* genes were annotated in the metagenomes. Instead, a sequence-based approach was used: reference sequences of *gox* were downloaded from UniProt and GenBank to create a DIAMOND database (v. 0.9; Buchfink et al., 2014). The metagenomic sequences were blasted against the DIAMOND database (*e*-value of $1E^{-8}$, sequence identity $\geq$ 40%, query coverage $\geq$ 70%) and eventually phylogenetic trees with the corresponding abundance were plotted as described above.

RESULTS

Total Cell Counts, Glyphosate and AMPA Concentrations and Nutrients

Total cell counts in the water column were in the range of 2–4 $\times$ 10^7 cells·mL^{-1} both in the treatment and control water samples (**Figure 1A**). Following glyphosate addition, they increased significantly, up to 7 $\times$ 10^7 cells·mL^{-1}, and remained elevated over the following 14-day period, during which the decrease in glyphosate was the strongest (**Figure 1B**). Based on the chemostat's volume and flow rate, the theoretical glyphosate concentration after approximately 60 days of incubation was close to zero. With a starting glyphosate concentration of 82.45 μM at day 0, the measured glyphosate concentrations, especially within the first two weeks of incubation, were 18–24 μM lower than the theoretical values. The results of the adsorption test (**Supplementary Material 1**) suggested that glyphosate was neither incorporated into biofilms nor adsorbed onto surfaces under our experimental conditions. After 71 days, glyphosate concentrations were reduced by 99%. AMPA was detected as soon as 4 h after addition in the first sample. 3 days later AMPA concentrations ranged from 0.27 μM to below the detection limit (LOD) by day +64 and +71. The highest ratio of AMPA to glyphosate was 1.35% on day +29. Peaks representing the isomers sarcosine and L-alanine could also be detected but were not reliably quantifiable, as their concentration (−0.017 to

0.016 μM) was close to the LOD. The peaks were present in both microcosms, before and after the addition of glyphosate.

The DIP concentration on day −69 was 15 μM, and on day 0 before and after glyphosate addition 23.3 and 24 μM, respectively. On day +71, at the end of the experiment, it declined to 16 μM. DOC and DN concentrations in the microcosms on day +71 were 80,000 and 20,000 μM, respectively. The resulting DOC:DN:DIP ratios were 238:56:1 for 24 μM DIP and 380:90:1 for 15 μM DIP.

16S rRNA and rRNA Gene Based Community Compositions

Among the 12,852 OTUs with more than one read, 10,692 originated from the water column. Two thousand nine hundred and three OTUs stem from the biofilm and 743 OTUs were present in both habitats. Planktonic 16S rRNA was roughly twice as rich in OTUs as either the planktonic 16S rRNA genes or the biofilm communities (**Supplementary Material 2**). Based on the number of reads, free-living (**Figure 2**) and biofilm (**Supplementary Material 5**) microbial community assemblages consisted almost exclusively of *Proteobacteria*, mainly *Alpha- and Gammaproteobacteria.* After the glyphosate pulse *Alphaproteobacteria* eventually comprised > 90% of the bacterial assemblages in the treatment microcosm. Therein, *Rhizobiales* and *Rhodospirillales* represented large and increasing portions thereof. Unclassified *Rhizobiales* OTU 1 was the most abundant OTU, up to 84% in the biofilm 16S rRNA (**Supplementary Material 6**). However, *Pseudomonas* OTU 7 reads (**Supplementary Material 6**) represented up to 25% of the 16S rRNA community in the water column of the treatment microcosm. *Pseudomonas* OTU 7 increased in abundance after the glyphosate pulse together with *Alteromonadales*, which includes the genus *Gallaecimonas*. In total, the OTUs covered > 320 genera, with 280 genera represented by 1–10 OTUs each. Ten very abundant genera, including *Hoeflea*, *Ferrovibrio* and undistinguished taxa (e.g., "unclassified" or "uncultured"), were represented by 100–318 OTUs. Based on a 0.01% relative abundance threshold, the biofilm community consisted of 90 genera and the water column community of 75 genera, with 59 shared genera (**Supplementary Material 2**). The diversity of members of the *Gammaproteobacteria* was evidenced by the finding that 10,088 of the 12,852 OTUs belonged to *Pseudomonas*, although > 98% of them were present at abundances of < 0.01%.

NMDS Ordination

Overall changes in 16S rRNA and 16S rRNA gene OTU composition were visualized via NMDS. Both 16S rRNA genes and 16S rRNA based assemblages were mainly arranged along the NMDS 2 axis, thus correlating with the sampling time (**Figure 3**). Samples from treatment and control microcosms were clearly separated. The PERMANOVA yielded *p*-values of <0.001, with no significant differences in the dispersion of the control vs. the treatment groups for all subsets. In general, the water column samples from the treatment microcosms were more similar along NMDS 2 than were the control microcosms. Water column 16S rRNA gene (stress 0.113) and 16S rRNA (stress 0.102) based community compositions produced similar ordinations. However, the 16S rRNA gene data formed two main clusters that were separated by the glyphosate pulse (day 0 vs. day +3). As long as glyphosate concentrations exceeded 5.92 μM (day +3 to day +22), the free-living community composition in the treatment microcosm formed a subcluster (red polygons in **Figure 3**). These observations also applied to the 16S rRNA data but the differences were less distinctive.

Based on 16S rRNA gene data from the biofilm (stress 0.042), all communities remained stable. Biofilm community succession was generally less pronounced than that of planktonic communities, while control and treatment assemblages spanned a similar distance on NMDS2. In contrast to the control samples, the overall biofilm 16S rRNA (stress 0.072) communities before and after glyphosate addition (days −7 to +7) formed distinguishable clusters.

Alpha Diversity Measures

The Shannon index was statistically assessed to test the impact of glyphosate on community diversity. Samples were grouped before and after day 0. For planktonic samples, the trend in the diversity of control microcosm communities was toward lower indices whereas in the treatment microcosm diversity increased temporarily after glyphosate addition, from a Shannon index of about 2.2 to >2.5 (**Figure 4**). This development was again more pronounced for the 16S rRNA gene data, in which a significantly higher estimated richness (Chao1) after the pulse was also evident.

By contrast, the Shannon index of the biofilm community samples decreased after day 0 regardless of the treatment, from approximately 2.7–2.3 (16S rRNA gene) and from 1.8–1.2 (16S rRNA), hence displaying a uniform mode of succession. A decrease in the diversity of the planktonic control communities was also observed. Shannon indices between sample groups before and after day 0 were significant, ranging from a *p*-value of $1.04{\cdot}10^{-07}$ for changes in the 16S rRNA gene of the treated planktonic samples to 0.03 for changes in the control 16S rRNA of the biofilm (**Supplementary Material 7**).

OTUs Increasing in Abundance After Glyphosate Treatment

The succession in planktonic and biofilm community composition was analyzed based on the relative OTU abundances that increased significantly after glyphosate addition. The analysis identified 24 OTUs, assigned to seventeen genera, that responded to glyphosate in the water column; three more OTUs originated from biofilms (**Table 1**, detailed statistics are provided in **Supplementary Material 8**). Distinctive positive responses were determined for OTUs of three *Gallaecimonas* spp. (**Figure 5** and **Supplementary Material 6**, OTU 109/129), *Methylotenera* spp., *Hyphomonas* spp. and *Parvibaculum* spp., with both 16S rRNA and rRNA gene abundances increasing immediately after glyphosate addition (**Supplementary Material 6**, OTU 44/25/46). In agreement with the results

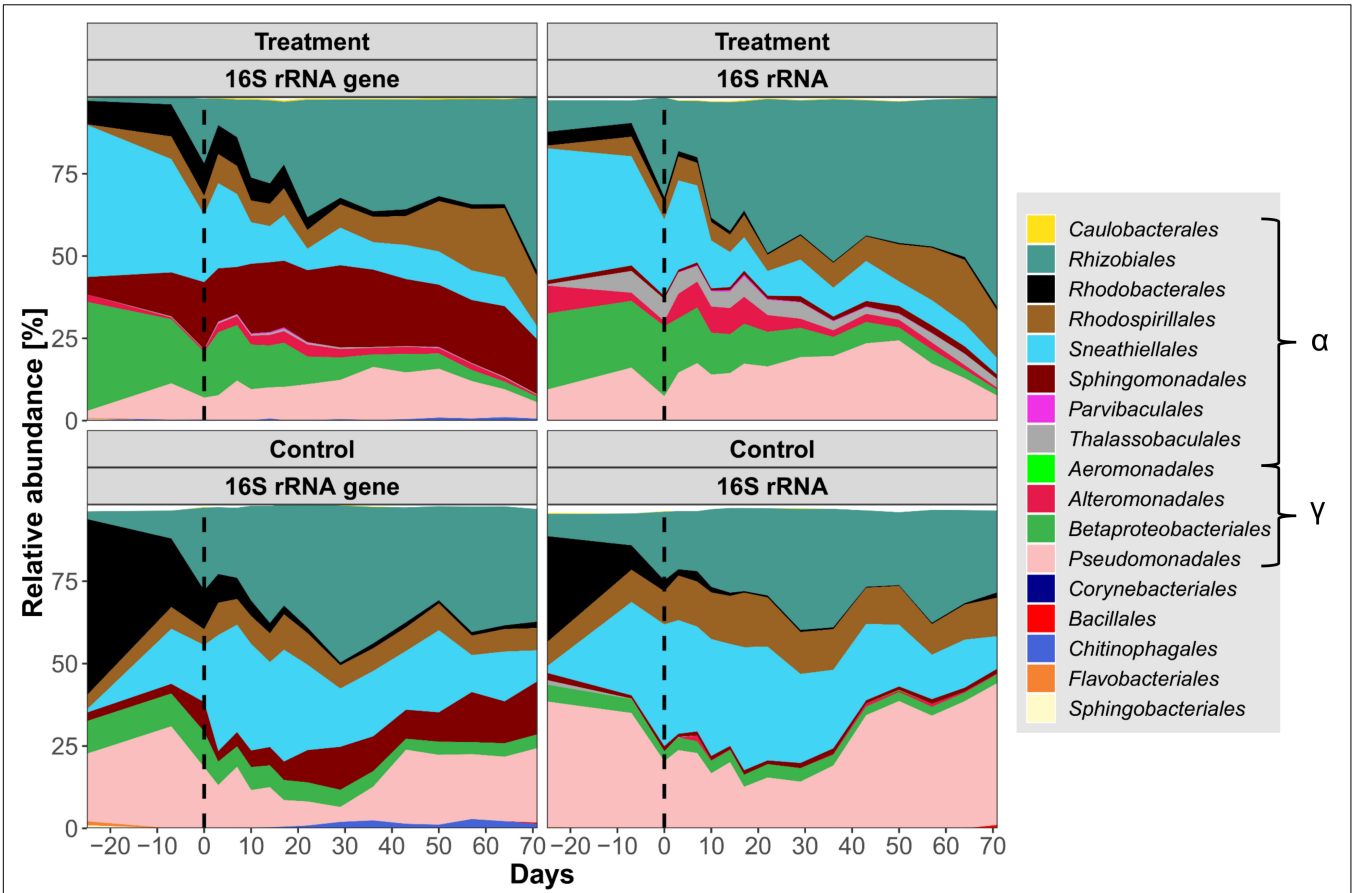

FIGURE 2 | Relative planktonic community composition in the treatment and control microcosms based on 16S rRNA gene and 16S rRNA abundances. Taxa were cumulated on the order level, sorted by class. α = *Alphaproteobacteria*, γ = *Gammaproteobacteria*. All orders with a relative abundance > 0.15% are displayed. Time of glyphosate addition is indicated by a vertical dashed line. Notice the dominance of *Proteobacteria* and the overall increase of planktonic *Alphaproteobacteria*.

reported above, the corresponding biofilm abundances for these OTUs remained stable.

The genus *Pseudomonas* accounted for most of the overall diversity within the microcosms, with variable responses by individual *Pseudomonas* OTUs to glyphosate addition. Thus, while the relative abundances of planktonic OTUs 7, 36 and 78 increased significantly, the abundance of OTU 29 was unaffected (**Supplementary Material 6**).

Duration of the Detected Signals

The detected microbial signals representative of free-living and biofilm communities after the glyphosate pulse differed in length and intensity. Total cell counts in the water column increased significantly from day +7 to day +22, whereupon the glyphosate concentration remained $\leq$ 4.4 μM and AMPA $<$ 0.1 μM. The Shannon index increased significantly from day +3 to day +17 for both the 16S rRNA and 16S rRNA gene based planktonic communities. The clusters in the NMDS of the 16S rRNA gene (except for one technical replicate) and 16S rRNA data from free-living bacteria indicated that the community composition from day +3 to +22 (**Figure 3**; red polygons) was more similar among these samples than in subsequent samples. The relative abundances of the responding planktonic OTUs generally increased from day +3 to day +22. Some of the detected planktonic OTUs retained elevated abundances for a longer period, until day 64, such as several *Pseudomonas* OTUs. However, this behavior was commonly observed for biofilm OTUs, and specifically for *Brevundimonas* OTU 42, *Defluviimonas* OTU 98 and *Pseudolabrys* OTU 38 (**Supplementary Material 6**). The increase in abundance began gradually and was first detected typically after day +7, but it continued until the end of the experiment. For these biofilm OTUs, the continuously high abundances were accompanied by corresponding changes in planktonic abundances. Thus, biofilm reactions were maintained whereas most planktonic reactions ended on day +22, when the glyphosate concentration was 12.7 μM.

Distribution of Glyphosate Degradation Genes in Metagenomic Samples

Metagenomes of free-living microbial communities were analyzed to gain insights into glyphosate-related bacterial functions. All relevant glyphosate-degradation genes *gox*, *thiO*

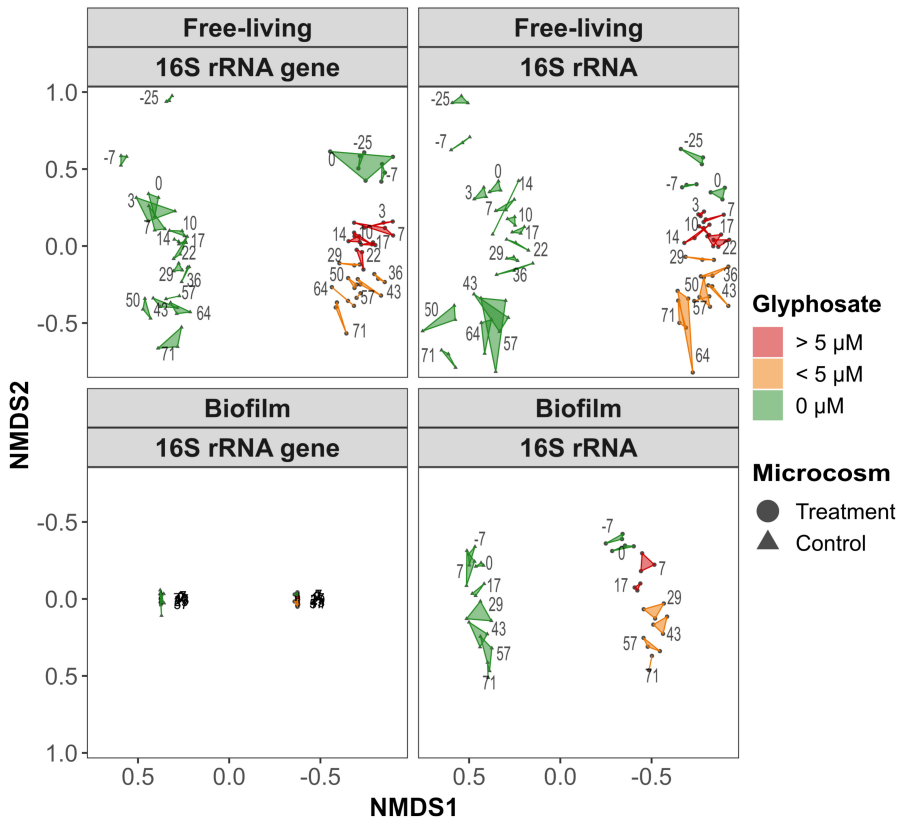

FIGURE 3 | NMDS ordination plots based on the Bray–Curtis dissimilarity of the square-root-transformed and Wisconsin double-standardized 16S rRNA gene and 16S rRNA based community composition in the biofilms and water column. The axis direction for the biofilm ordinations was reversed to correspond to the pelagic orientation. The numbers refer to the sampling day; glyphosate was added before day 3. Technical replicates are connected by a polygon colored according to the measured glyphosate concentration.

and *phnC-P* were detected. The *phn* operon might be involved in metabolization at two steps, either degrading glyphosate to sarcosine or cleaving the C-P bond in AMPA. Identifying the responsible pathway, if not all of them, was required.

For the sarcosine pathway, whether a particular *phn* operon enables glyphosate degradation at all depends on the encoded substrate specificity. Therefore, we screened for sequence clusters that became more abundant after glyphosate addition, as these may also have contained sequence motifs typical of glyphosate degradation. An example is the *phnJ* gene, which codes for an essential protein within the C-P lyase multienzyme core complex. Nonetheless, in samples from the treatment microcosm, the abundance profiles proved to be complex even for closely related sequences of *phnJ* genes (**Figure 6**). Based on phylogenetic analyses, *phnJ* genes similar to that of the alphaproteobacteria *Yoonia vestfoldensis* spp. (formerly *Loktanella vestfoldensis*, UniProtKB: A0A1Y0ECC7) were most abundant on day +14, when the total cell count reached a peak. This development was similar for the *phnJ* sequences of *Ruegeria pomeroyi* strain ATCC 700808 (UniProtKB: Q5LW71), *Rhizobium meliloti* strain 1021 (UniProtKB: Q52987) and *Agrobacterium radiobacter* strain ATCC BAA-868 (UniProtKB: B9J6Q8). Moreover, *phnJ* sequence reads correlated with the abundance of 16S rRNA gene OTUs, such as those of *Yoonia* spp., based on the taxonomy of the reference genes (**Supplementary Material 6**, OTU 59).

From the 29 *phnJ* genes annotated in the treatment microcosm, four main groups could be recognized. Based on the embedded reference genes from known organisms, the largest group consisted solely of the alphaproteobacterial *phnJ* sequences grouping with sixteen genes from the metagenomes. *Alphaproteobacteria* were by far the most abundant class inhabiting the microcosms. The second group solely contained gammaproteobacterial reference genes and six metagenomic genes. For the first two groups, phylogenetic relationships based on the 16S rRNA gene were similar to the clustering of the *phnJ* sequences, as highlighted by the subgroup of sequences from *Enterobacter cloacae* ssp. *cloacae* strain ATCC 13047 (UniProtKB: A0A0H3CFJ4) and *Escherichia coli* K12 (UniProtKB: P16688). Groups 3 and 4 gathered *phnJ* sequences from several less-related organisms. Also in these groups multiple *phnJ* sequences were those of the alphaproteobacteria *Yoonia vestfoldensis* spp. and were encountered in the first, third and fourth group. In the latter two groups, there was a low similarity with their closest relatives, which even included the cyanobacterium *Nostoc* sp. strain PCC 7120. Interestingly, the highly diverse genus *Pseudomonas* was represented by only three sequences; these

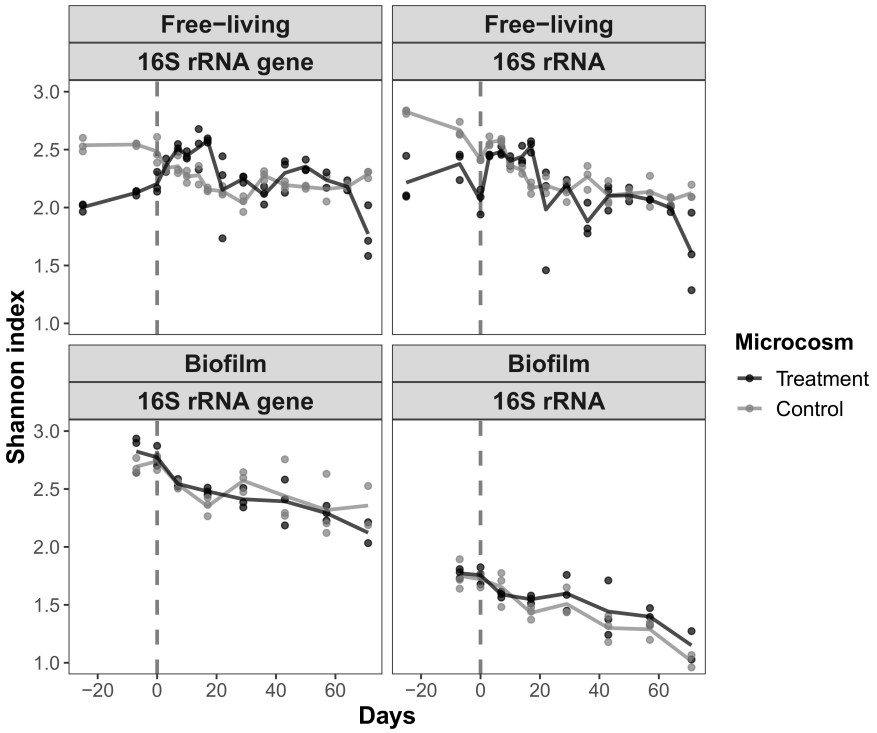

FIGURE 4 | The change in α-diversity (Shannon index) of the free-living and biofilm communities according to the 16S rRNA gene and 16S rRNA data from the treatment and control microcosms. The vertical dashed line indicates the time of glyphosate addition. Samples obtained between the start of the experiment and day 0 (group 1) and from day +3 to day +17 (group 2) were compared in a *t*-test. The increase in the diversity of the free-living communities was significant.

were most closely related to *phnJ* from *P. fluorescens* strain SBW25 (UniProtKB: C3K5L9). Comparable results, i.e., varying numbers of *Pseudomonas*-related genes (data not shown), were achieved for other *phn* and the sarcosine oxidase (*sox*) genes.

The *gox* gene was not identified by Prokka in the metagenomes. A manually conducted comparison, however, detected thirteen closely related sequences which were annotated by Prokka as *dadA* (D-amino acid dehydrogenase), but instead appear to be more closely related to *gox* genes. The reference *gox* genes create a distinct group (UniProtKB: D2KI28, A0A142MF04, D4NZ76, D4NZ75; GenBank: ATE50174.1, ADV58259.1), whereas the metagenomic sequences are distinguished from this group (**Figure 7**). When challenged, the annotation of these sequences, by adding the Prokka-referenced *dadA* sequences (UniProtKB: P0A6J5, Q9HTQ0, A3KEZ1), the metagenomic sequences were indeed more similar to *gox* genes. The abundance of the potential *gox* sequences *gox*_1, 3, 5, 12, and 13 converged with the total cell counts peak. Due to the separate clustering of the reference sequences, the taxonomic inference remains unknown. However, a basic online BLASTp analysis assigned *gox*_10, 11 and 12 (**Figure 7**, purple ellipse) to FAD-binding oxidoreductase from *Hoeflea marina* (UniProtKB: A0A317PMM8) and *Hoeflea* sp. BRH c9 (UniProtKB: A0A0F2P8D1) with a query coverage of 100% and an identity > 88%.

thiO sequences were detected 28 times (**Figure 8**) with no clear taxonomic separation based on the positioning of the reference sequences. Three sequences were most abundant at day +14 in time with the cell counts peak (*thiO*_9, 12, 19) with *thiO*_19 being somewhat related to *Yoonia vestfoldensis* (UniProtKB: A0A1Y0E718). *thiO*_1 to 9 grouped with *Pseudomonas aeruginosa* ATCC 15692 (UniProtKB: G8PX29). *Betaproteobacteria* clustered together (*Cupriavidus*, UniProtKB: Q0KF33, G0ETC1, A0A1K0I947 and *Burkholderia*, UniProtKB: A0A0H3HPX7), although alphabacterial sequences were also similar. Interestingly, *Yoonia vestfoldensis* (UniProtKB: A0A1Y0EFI8, A0A1Y0E718) and *Pseudomonas* (UniProtKB: P33642, G8PX29) harbored dissimilar *thiO* sequences, which might be obtained by horizontal gene transfer.

DISCUSSION

Potential Impacts of Glyphosate on a Brackish Microbial Ecosystem

A glyphosate incubation experiment with a brackish water community was conducted to investigate the impact of glyphosate on free-living and biofilm microbial assemblages. Following the glyphosate pulse, changes in community composition and increases in total cell counts, α-diversity and the abundances of specific 16S rRNA (gene) OTUs were detected in the water column. By contrast, with a few exceptions, the biofilm, which was 69 days old when glyphosate was added, remained undisturbed. Other studies have also shown

TABLE 1 | Differentially abundant OTUs in the treatment microcosm after the addition of glyphosate.

Free-living/Biofilm	16S rRNA gene/16S rRNA	Class	Order	Family	Genus	OTU ID
−/X	X/X	*Alphaproteobacteria*	*Caulobacterales*	*Caulobacteraceae*	*Brevundimonas*	Otu000042
X/−	X/X	*Alphaproteobacteria*	*Caulobacterales*	*Hyphomonadaceae*	*Hyphomonas*	Otu000025
X/−	X/X	*Alphaproteobacteria*	*Parvibaculales*	*Parvibaculaceae*	*Parvibaculum*	Otu000046
X/−	X/−	*Alphaproteobacteria*	*Rhizobiales*	*Rhizobiaceae*	*Aminobacter*	Otu000072
X/−	−/X	*Alphaproteobacteria*	*Rhizobiales*	*Rhizobiaceae*	*Hoeflea*	Otu000320
X/−	X/X	*Alphaproteobacteria*	*Rhizobiales*	*Rhizobiaceae*	*Mesorhizobium*	Otu000056
X/−	X/−	*Alphaproteobacteria*	*Rhizobiales*	*Rhizobiaceae*	*Rhizobiaceae* unclassified	Otu000037
X/−	X/X	*Alphaproteobacteria*	*Rhizobiales*	*Rhizobiaceae*	*Rhizobiaceae* unclassified	Otu000070
X/X	X/X	*Alphaproteobacteria*	*Rhizobiales*	*Xanthobacteraceae*	*Pseudolabrys*	Otu000038
−/X	X/X	*Alphaproteobacteria*	*Rhodobacterales*	*Rhodobacteraceae*	*Defluviimonas*	Otu000098
X/−	X/−	*Alphaproteobacteria*	*Rhodobacterales*	*Rhodobacteraceae*	*Loktanella*	Otu000059
X/−	X/−	*Alphaproteobacteria*	*Rhodobacterales*	*Rhodobacteraceae*	*Seohaeicola*	Otu000094
X/−	X/−	*Alphaproteobacteria*	*Sphingomonadales*	*Sphingomonadaceae*	*Sphingorhabdus*	Otu000032
X/−	X/−	*Alphaproteobacteria*	*Thalassobaculales*	*Thalassobaculaceae*	*Thalassobaculum*	Otu000018
X/−	X/X	*Gammaproteobacteria*	*Alteromonadales*	*Gallaecimonadaceae*	*Gallaecimonas*	OtuOOOOll
X/−	X/X	*Gammaproteobacteria*	*Alteromonadales*	*Gallaecimonadaceae*	*Gallaecimonas*	Otu000109
X/−	X/X	*Gammaproteobacteria*	*Alteromonadales*	*Gallaecimonadaceae*	*Gallaecimonas*	Otu000129
X/−	X/−	*Gammaproteobacteria*	*Alteromonadales*	*Idiomarinaceae*	*Idiomarina*	Otu000049
X/−	X/X	*Gammaproteobacteria*	*Betaproteobacteriales*	*Burkholderiaceae*	*Hydrogenophaga*	Otu000139
X/−	X/X	*Gammaproteobacteria*	*Betaproteobacteriales*	*Methylophilaceae*	*Methylotenera*	Otu000044
X/−	X/X	*Gammaproteobacteria*	*Pseudomonadales*	*Pseudomonadaceae*	*Pseudomonas*	Otu000007
X/−	X/X	*Gammaproteobacteria*	*Pseudomonadales*	*Pseudomonadaceae*	*Pseudomonas*	Otu000036
X/−	X/X	*Gammaproteobacteria*	*Pseudomonadales*	*Pseudomonadaceae*	*Pseudomonas*	Otu000078
X/−	X/X	*Gammaproteobacteria*	*Puniceispirillales*	uncultured	uncultured	Otu000191
X/−	X/X	*Gammaproteobacteria*	*Sphingomonadales*	*Sphingomonadaceae*	*Sphingobium*	Otu000176
X/−	X/−	*Planctomycetacia*	*Planctomycetales*	*Gimesiaceae*	*Gimesia*	Otu000058

OTU abundance before and after glyphosate addition were first tested using the Wald test with Benjamini–Hochberg corrected p-values < 0.01. From this selection, 24 OTUs in the water column and three in the biofilm were then identified as potentially glyphosate-responsive based on a visual comparison with the corresponding abundance of the OTUs in the control microcosm. Taxonomy after Silva release 132 and Parks et al. (2018).

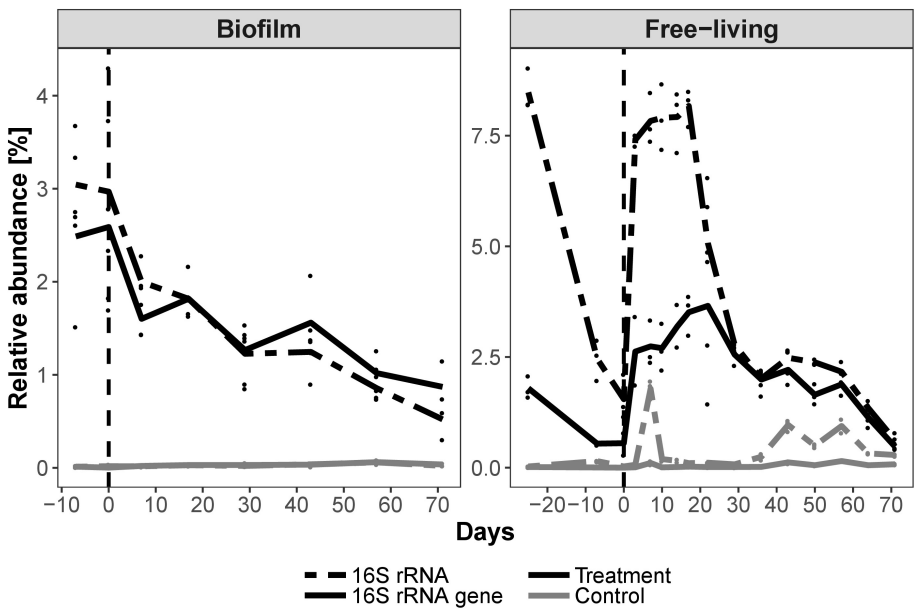

FIGURE 5 | Changes in the relative abundance of *Gallaecimonas* OTU 11 in the treatment and control microcosms over time as determined by 16S rRNA gene and rRNA amplicon analyses. The vertical dashed line indicates the time of glyphosate addition. There was no evidence of an impact of glyphosate on OTU 11 in the biofilm whereas planktonic OTU 11 responded rapidly based on 16S rRNA gene and 16S rRNA abundances.

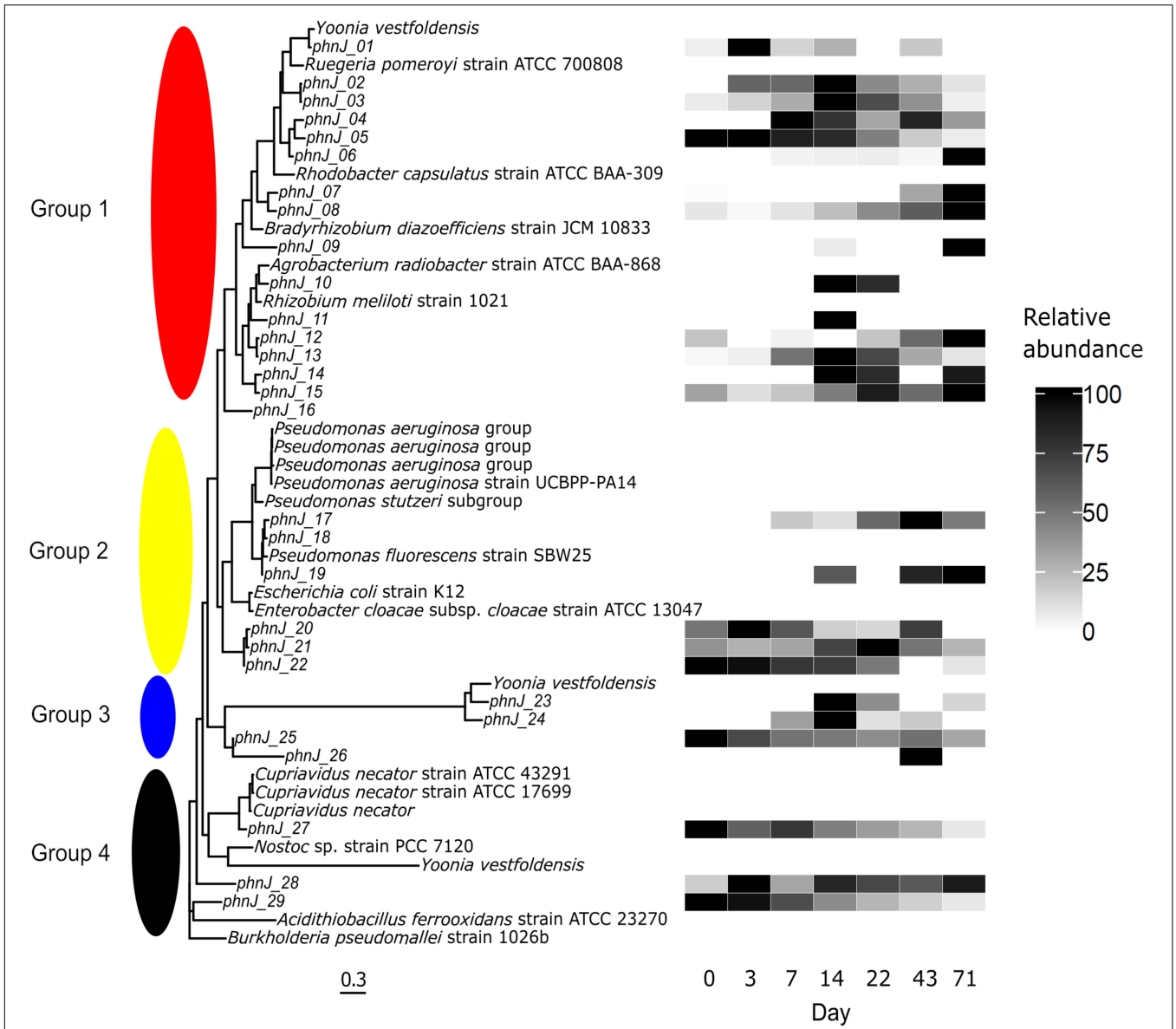

FIGURE 6 | Multiple sequence alignment of protein fasta sequences of the *phnJ* gene from the free-living treatment metagenomes. As a reference, the tree contains sequences from cultivated organisms related to the differentially abundant OTUs detected in this experiment. Taxonomy is presented according to UniProt. The heat map shows the abundance of a given *phnJ* gene relative to the other samples over time. Relative abundances in (%). Four groups are labeled, the first two consisting exclusively of *Alphaproteobacteria* and *Gammaproteobacteria*, respectively.

that organisms embedded in a biofilm are less responsive to disturbances in the surrounding medium (Davey and O'Toole, 2000; Tlili et al., 2011). Similarly, in this study, compared to the water column, fewer OTUs in the biofilm were affected by glyphosate. A smaller impact of glyphosate on freshwater biofilms, and especially on phototrophic organisms, was previously reported. Khadra et al. (2018) investigated periphytic biofilms differing in age (at least 2 months) and exposed to different glyphosate concentrations (35.4, 383.5, and 3540 nM) in a lake. They concluded that glyphosate had no effect on biofilms, a finding also reported by Lozano et al. (2018), who showed that periphyton was more resistant than phytoplankton to 17.7 μM glyphosate. Although the latter study did not find a biomass-based effect on periphyton, the abundance of certain taxa decreased. Vera et al. (2010) noted a delayed increase in the biomass of periphyton exposed to 47.3 μM glyphosate in freshwater mesocosms.

In our study, from the initial 82.45 μM glyphosate added at day 0, 1 μM remained at the end of the experiment. Thus, with the decreasing availability of glyphosate, the cost-benefit ratio of producing proteins for its metabolism seems to become increasingly unfavorable. This is supported by the absence

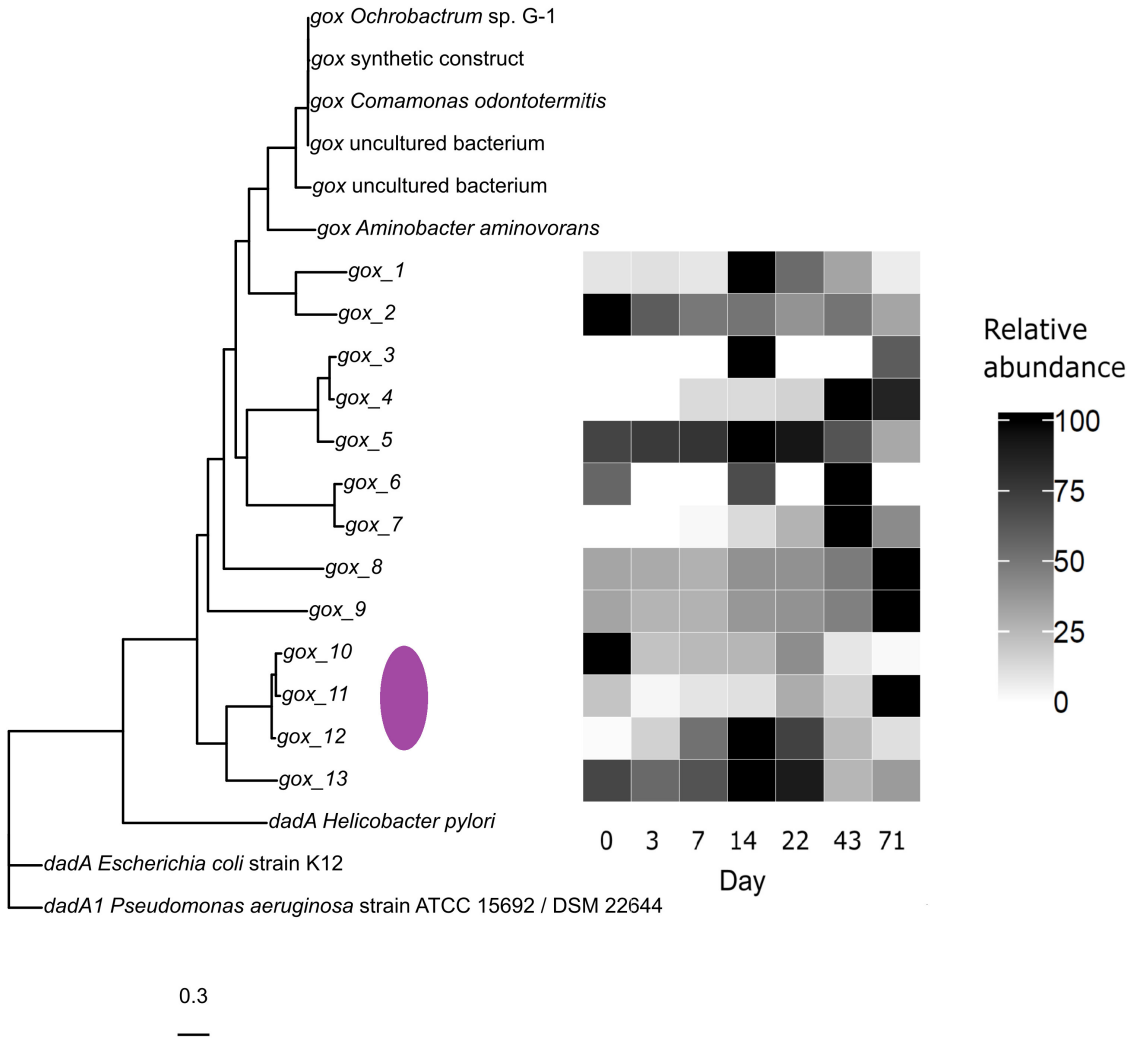

FIGURE 7 | Multiple sequence alignment of protein fasta sequences of the *gox* and *dadA* genes deposited in Uniprot and GenBank. *gox* and *dadA* reference sequences clustered separately with the metagenomic sequences more related to *gox*. The purple ellipse marks sequences similar to those of the genus *Hoeflea*. Relative abundances in (%).

of AMPA as indication of degradation in the later samples. Given that at 4.4 μM glyphosate a response by planktonic communities was no longer detectable, then at the pM to nM concentration ranges measured in estuaries of the Baltic Sea (Skeff et al., 2015) neither biofilms (harboring the majority of microbial cells) nor planktonic bacteria in the Baltic Sea are likely to be disturbed by the herbicide. However, the nutrient regime in Baltic seawater differs from that of the rich medium provided in this study. In addition, the long-term effects of glyphosate on microbial communities are as yet unknown. Mercurio et al. (2014) demonstrated an unexpected glyphosate persistence in seawater in the presence and absence of light. The study of Stachowski-Haberkorn et al. (2008) suggested that even low-nM glyphosate concentrations can affect natural coastal microbial communities in marine environments. According to our results, planktonic bacteria better reflect short-term disturbances, whereas the accompanying biofilm provides a reference for examining overall succession trends occurring as a result of exchange with the water column. A biofilm response would thus indicate that a threshold of disturbance tolerance had been exceeded. Expanding the shotgun sequencing to involve the biofilms could support this idea.

Differences in the Responses of Water Column and Biofilm Communities to Glyphosate Addition

The response of biofilm OTUs to glyphosate addition, as measured by abundance, was minor but detectable until the end of the experiment. One interpretation of this result is that the glyphosate pulse favored these OTUs over others in the biofilm community. Glyphosate has been shown to accumulate in biofilms, including those within a Brazilian river (59.2–1806 nmol·kg^{-1}, AMPA 450.29–6033.89 nmol·kg^{-1};

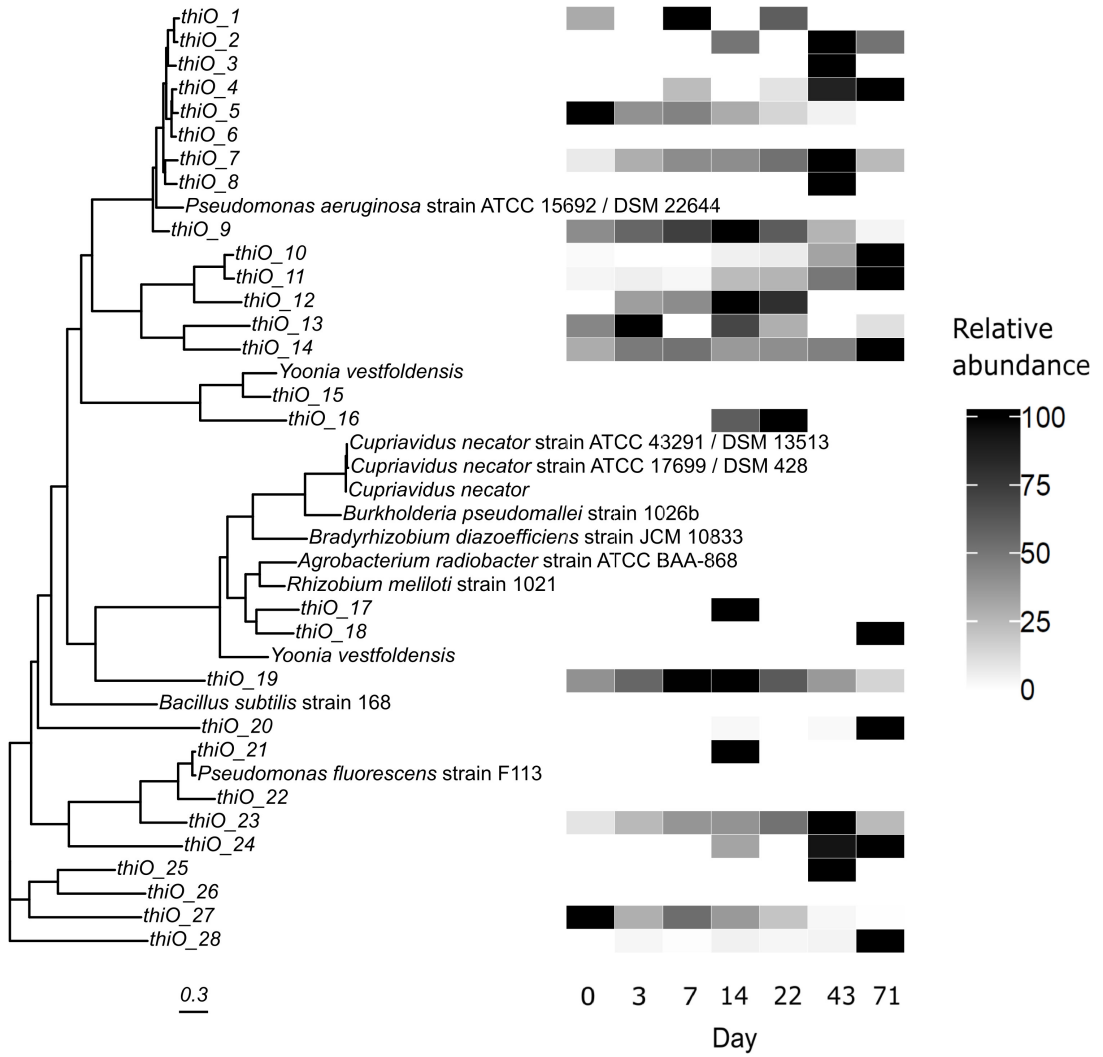

FIGURE 8 | Multiple sequence alignment of protein fasta sequences of the *thiO* gene. Placement of sequences could be different between the same or closely related organisms such as *Yoonia vestfoldensis* or *Pseudomonas*. The presence of *thiO* genes over all sampled time points was less comprehensive compared to *gox* and *phnJ* genes. Relative abundances in (%).

Fernandes et al., 2019), or to persist at a very small percentage of the initial concentration, as demonstrated in a microcosm study of biofilms in a French river (Carles et al., 2019). Either would provide glyphosate-degrading OTUs with a nutritional advantage. Our initial tests conducted prior to the experiment showed that the biofilms did not enrich glyphosate, at least not during the first 3 days after the glyphosate pulse. However, in the few cases in which a response by biofilm OTUs was identified, the respective signal was also detected in the water column, both for a longer time and indicative of a higher abundance. Several of the abundant biofilm OTUs, however, were characterized by a concise albeit constant changes in abundance regardless of the condition, which complicated the detection of glyphosate-responding OTUs (**Figure 5**). It should be noted that the growth substrates for the biofilm were initially sterile and that all colonization occurred via the inoculated water column. This could explain the overall concordance between abundant OTUs in the water column and in the biofilms.

Microbial responses within the water column were in most cases limited to day +22, which coincided with the strongest decrease in the glyphosate concentration to $\leq$4.4 μM, the AMPA concentration fell below 0.1 μM afterward. Transient effects on microbial communities by glyphosate have been previously described. For example, Weaver et al. (2007) found small, brief (<7 days) changes in the levels of fatty acid methyl esters and a reduction in the hydrolytic activity of a soil microbial community exposed to a glyphosate concentration of 277–828 $\mu mol \cdot kg^{-1}$. Using Biolog assays and phospholipid fatty acids analyses, Ratcliff et al. (2006) measured a non-specific, short-term stimulation of bacteria at a high glyphosate concentration. The increased α-diversity determined in this study confirmed the findings of

Lu et al. (2017), who analyzed the rhizosphere of a glyphosate-tolerant soybean line based on 16S rRNA gene amplicon sequencing. The authors also found a higher diversity and varying OTU abundances in the rhizosphere of the treated than of the control cultivar. In a metatranscriptomic analysis, Newman et al. (2016) investigated changes in bacterial gene patterns in response to long-term glyphosate exposure. The results indicated a potential shift in bacterial community composition toward more glyphosate-tolerant bacteria. Wang et al. (2017) described the effects of two glyphosate concentrations on the microbial community associated with the dinoflagellate *Prorocentrum donghaiense* and showed that 36 μM glyphosate caused a decrease and 360 μM an increase in α-diversity. Several OTUs detected in our study belonged to genera whose abundance increased following glyphosate treatment (*Methylotenera, Pseudomonas, Sphingobium, Thalassobaculum*), demonstrating the ability of glyphosate to cause favorable conditions for these genera across various habitats. On a further note, the herein identified *Rhodobacteraceae* and *Rhizobiaceae* OTUs were confirmed in a novel approach using artificial neural networks and Random Forest to detect responding OTUs (Janßen et al., 2019).

Glyphosate-Induced Changes in OTU Abundance

In our study, temporally highly resolved NGS data revealed increased OTU abundances, but the mechanisms of the increases were unclear. While glyphosate can be considered as a source of C, N, or P, the microcosms were supplied with sufficient amounts of C and N (evidenced by the medium composition and end-of-experiment data points) and P from other sources.

Specific reactions to glyphosate have been described in studies of bacterial cultures, especially those of degraders (Wang et al., 2016) and resistant cyanobacteria (López-Rodas et al., 2007). Within the same species, different strains may or may not be capable of degrading glyphosate and several pathways for glyphosate degradation may be present in a single strain. This is the case in *Pseudomonas* (Jacob et al., 1988; White and Metcalf, 2004; Zhao et al., 2015; Lidbury et al., 2016) and would explain why some, but not all of the *Pseudomonas* OTUs detected in our study became abundant after glyphosate addition. Thus, the pronounced diversity of *Pseudomonas* was also expressed by its reactions toward glyphosate.

Probability of Glyphosate Degradation

The responses mainly by free-living bacteria, such as the increase in cell counts and the presence of AMPA indicated that glyphosate was degraded. The amount of AMPA detected in comparison to the corresponding glyphosate concentrations suggests that only a minor fraction was metabolized, a quality associated with the glycine oxidase *thiO*. The increase in total cell counts and the discrepancy between the measured and the calculated glyphosate levels require a more complete degradation of glyphosate. Sarcosine/L-alanine levels do not compensate for this difference and as they did not change after glyphosate addition and were present in both microcosms it was more likely only L-alanine was present due to the inclusion of the casamino acids. This implicates that glyphosate was not metabolized by the sarcosine pathway. It is possible that rapid degradation of the intermediate product could have occurred, thus rendering it hardly detectible. However, it is unlikely that the glycine oxidase would be capable of such a degradation rate due to its low specificity toward glyphosate. A possible explanation is the degradation of glyphosate by *gox* into AMPA with an immediate continuation by C-P lyase. Sviridov et al. (2015) concluded in their review that the majority of described glyphosate-degrading bacteria use the *gox* gene and consequently export AMPA into their environment, but also stated that organisms not being capable of degrading glyphosate might still metabolize AMPA.

Furthermore, the abundances of *gox* genes, *thiO* genes, the *phn* operon, *sox* genes and *aroA* genes correlated with those of the detected OTUs (via multiple sequence alignment and reference sequences; **Figure 6**). It must be noted that *phn* operons encode functions that result in the degradation of a variety of phosphonates, although not necessarily including glyphosate. The respective genes are subject to extensive lateral transfer, which complicates data interpretation (Huang et al., 2005). The results of our metagenomic analysis suggested that *phn* genes have a higher sequence similarity based on phylogeny than on substrate specificity. Sequence abundances of a *phnJ* gene correlated with OTU 59 (classified as *Yoonia/Loktanella* spp.). This suggested that this OTU possesses *phn* genes whose abundances' increase might be in response to the presence of glyphosate or AMPA as a nutrient source. The same reference organism, as well as *Pseudomonas aeruginosa,* correlated with the abundance of *thiO* genes. The phylogenetic comparison of *gox*, *dadA* and our metagenomic sequences (**Figure 7**) underlined the demand of properly described references and the potential of undiscovered *gox* variants. For the *Hoeflea*-related *gox* sequences, no treatment-specific abundance change could be assigned to *Hoeflea* OTUs. In conclusion, a metatranscriptomic analysis that describes the expressed *phn*, *gox,* and *thiO* mRNAs may have provided clearer evidence of the pathways used for glyphosate degradation (Martínez et al., 2013; Wang et al., 2016) as well as the involved organisms.

However, amplicon sequences still proved to be a cost efficient and sensitive method for community analysis, as comparisons of 16S rRNA (gene) and shotgun sequencing data indicated that glyphosate-responsive low-abundance OTUs were not covered in the metagenome. Furthermore, the 16S rRNA gene amplicon counts were a better indicator of community changes than 16S rRNA, indicating that DNA is a better proxy of abundance. Field experiments or laboratory studies involving more than one determinant should further investigate the potential of using detailed community composition data as an indicator of community disturbance.

DATA AVAILABILITY STATEMENT

The datasets generated for this study can be found in the NCBI database under BioProject ID PRJNA434253 and SRA accession SRP151042. OTU and taxonomy table

as well as corresponding code to process and analyze the data are available in the GitHub repo: https://github.com/RJ333/Glyphosate_gene_richness, code for the metagenomic analysis is available under https://github.com/RJ333/calculate-functional-trees.

AUTHOR CONTRIBUTIONS

RJ and ML designed the experiment. RJ conducted the experiment, lab work, amplicon data processing, analysis and statistics and wrote the manuscript. JW processed and analyzed the metagenomic data and contributed to the manuscript. WS performed the glyphosate and AMPA analysis, designed and conducted the adsorption experiment and contributed to the manuscript. MW re-performed the AMPA with more sensitive equipment and developed a method for sarcosine/L-alanine analytics. ML, DS-B, and BK provided invaluable comments and intellectual input. ML, BK, and DS-B provided laboratory equipment and measurement of data. ML revised the manuscript. All authors have read and approved the final version of the manuscript.

FUNDING

This work was funded partially by the German national BMBF project "Sektorale Verwertung" (01IO1448) and from the BONUS Blueprint project supported by BONUS (Art 185), funded jointly by the EU and the Swedish Research Council FORMAS and The Federal Ministry of Education and Research (BMBF). RJ and JW personally acknowledge the use of de.NBI cloud and the support by the High Performance and Cloud Computing Group at the Zentrum für Datenverarbeitung of the University of Tübingen and the Federal Ministry of Education and Research (BMBF) through grant no 031 A535A. Purchase of the Illumina MiSeq was kindly supported by the EU-EFRE (European Funds for Regional Development) program and funds from the University Medicine Rostock awarded to BK.

ACKNOWLEDGMENTS

We would like to thank Mercè Berga Quintana for the introduction to R, Christin Laudan and Jenny Jeschek for measuring nutrient concentrations, Stephanie Mothes for extracting nucleic acids from biofilm and Jana Bull for running the MiSeq. RJ would like to thank Anders Andersson, Johannes Alneberg and Luisa Hugerth for the introduction into bioinformatics and metagenomic analysis. We would also like to thank the two reviewers for their helpful critics, which improved the quality of this manuscript and Alexander S. Tagg for proofreading the revised version.

SUPPLEMENTARY MATERIAL

The Supplementary Material for this article can be found online at: https://www.frontiersin.org/articles/10.3389/fmars.2019.00758/full#supplementary-material

REFERENCES

Bateman, A., Martin, M. J., O'Donovan, C., Magrane, M., Alpi, E., Antunes, R., et al. (2017). UniProt: the universal protein knowledgebase. *Nucleic Acids Res.* 45, D158–D169. doi: 10.1093/nar/gkw1099

Bennke, C. M., Pollehne, F., Müller, A., Hansen, R., Kreikemeyer, B., and Labrenz, M. (2018). The distribution of phytoplankton in the Baltic Sea assessed by a prokaryotic 16S rRNA gene primer system. *J. Plankton Res.* 40, 244–254. doi: 10.1093/plankt/fby008

Bergström, L., Börjesson, E., and Stenström, J. (2011). Laboratory and lysimeter studies of glyphosate and aminomethylphosphonic acid in a sand and a clay soil. *J. Environ. Qual.* 40, 98–108. doi: 10.2134/jeq2010.0179

Bolger, A. M., Lohse, M., and Usadel, B. (2014). Trimmomatic: a flexible trimmer for Illumina sequence data. *Bioinformatics* 30, 2114–2120. doi: 10.1093/bioinformatics/btu170

Bray, N. L., Pimentel, H., Melsted, P., and Pachter, L. (2016). Near-optimal probabilistic RNA-Seq quantification. *Nat. Biotechnol.* 34, 525–527. doi: 10.1038/nbt.3519

Bruns, A., Cypionka, H., and Overmann, J. (2002). Cyclic AMP and acyl homoserine lactones increase the cultivation efficiency of heterotrophic bacteria from the central Baltic Sea. *Appl. Environ. Microbiol.* 68, 3978–3987. doi: 10.1128/AEM.68.8.3978

Buchfink, B., Xie, C., and Huson, D. H. (2014). Fast and sensitive protein alignment using DIAMOND. *Nat. Methods* 12, 7–9. doi: 10.1038/nmeth.3176

Carles, L., Gardon, H., Joseph, L., Sanchís, J., Farré, M., and Artigas, J. (2019). Meta-analysis of glyphosate contamination in surface waters and dissipation by biofilms. *Environ. Int.* 124, 284–293. doi: 10.1016/j.envint.2018.12.064

Costerton, J. W., Lewandowski, Z., Caldwell, D. E., Korber, D. R., and Lappin-Scott, H. M. (1995). Microbial biofilms. *Annu. Rev. Microbiol.* 49, 711–745.

Davey, M. E., and O'Toole, G. A. (2000). Microbial biofilms: from ecology to molecular genetics. *Microbiol. Mol. Biol. Rev.* 64, 847–867. doi: 10.1128/MMBR.64.4.847-867.2000

Di Tommaso, P., Chatzou, M., Floden, E. W., Barja, P. P., Palumbo, E., and Notredame, C. (2017). Nextflow enables reproducible computational workflows. *Nat. Biotechnol.* 35, 316–319. doi: 10.1038/nbt.3820

Duke, S. O., and Powles, S. B. (2008). Glyphosate: a once-in-a-century herbicide. *Pest Manag. Sci.* 64, 319–325. doi: 10.1002/ps.1518

Fernandes, G., Aparicio, V. C., Bastos, M. C., De Gerónimo, E., Labanowski, J., Damian, P. O., et al. (2019). Indiscriminate use of glyphosate impregnates river epilithic biofilms in southern Brazil. *Sci. Total Environ.* 651, 1377–1387. doi: 10.1016/j.scitotenv.2018.09.292

Fu, L., Niu, B., Zhu, Z., Wu, S., and Li, W. (2012). CD-HIT: accelerated for clustering the next-generation sequencing data. *Bioinformatics* 28, 3150–3152. doi: 10.1093/bioinformatics/bts565

Grasshoff, K., Kremling, K., and Ehrhardt, M. (eds) (2007). *Methods of Seawater Analysis. Third*. Weinheim: Wiley-VCH, doi: 10.1002/9783527613984

Helcom. (2018). State of the Baltic Sea - Second HELCOM holistic assessment 2011-2016. *Balt. Sea Environ. Proc.* 155, 1–155.

Herlemann, D. P. R., Labrenz, M., Jürgens, K., Bertilsson, S., Waniek, J. J., and Andersson, A. F. (2011). Transitions in bacterial communities along the 2000 km salinity gradient of the Baltic Sea. *ISME J.* 5, 1571–1579. doi: 10.1038/ismej.2011.41

Huang, J., Su, Z., and Xu, Y. (2005). The evolution of microbial phosphonate degradative pathways. *J. Mol. Evol.* 61, 682–690. doi: 10.1007/s00239-004-0349-4

Huang, X. L., and Zhang, J. Z. (2011). Phosphorus sorption on marine carbonate sediment: phosphonate as model organic compounds. *Chemosphere* 85, 1227–1232. doi: 10.1016/j.chemosphere.2011.07.016

Jacob, G. S., Garbow, J. R., Hallas, L. E., Kimack, N. M., Kishore, G. M., and Schaefer, J. (1988). Metabolism of glyphosate in *Pseudomonas* sp. strain LBr. *Appl. Environ. Microbiol.* 54, 2953–2958.

Janßen, R., Zabel, J., von Lukas, U., and Labrenz, M. (2019). An artificial neural network and Random Forest identify glyphosate-impacted brackish communities based on 16S rRNA amplicon MiSeq read counts. *Mar. Pollut. Bull.* 149:110530. doi: 10.1016/j.marpolbul.2019.110530

Katoh, K., and Standley, D. M. (2013). MAFFT multiple sequence alignment software version 7: improvements in performance and usability. *Mol. Biol. Evol.* 30, 772–780. doi: 10.1093/molbev/mst010

Khadra, M., Planas, D., Girard, C., and Amyot, M. (2018). Age matters: submersion period shapes community composition of lake biofilms under glyphosate stress. *Facets* 3, 934–951. doi: 10.1139/facets-2018-9

Klátyik, S., Takács, E., Mörtl, M., Földi, A., Trábert, Z., Ács, É, et al. (2017). Dissipation of the herbicide active ingredient glyphosate in natural water samples in the presence of biofilms. *Int. J. Environ. Anal. Chem.* 97, 901–921. doi: 10.1080/03067319.2017.1373770

Lane, D. (1991). "16/23S rRNA sequencing," in *Nucleic Acid Techniques in Bacterial Systematics*, eds E. Stackebrandt, and M. Goodfellow, (New York, NY: John Wiley & Sons).

Li, D., Liu, C. M., Luo, R., Sadakane, K., and Lam, T. W. (2014). MEGAHIT: an ultra-fast single-node solution for large and complex metagenomics assembly via succinct de Bruijn graph. *Bioinformatics* 31, 1674–1676. doi: 10.1093/bioinformatics/btv033

Lidbury, I. D. E. A., Murphy, A. R. J., Scanlan, D. J., Bending, G. D., Jones, A. M. E., Moore, J. D., et al. (2016). Comparative genomic, proteomic and exoproteomic analyses of three *Pseudomonas* strains reveals novel insights into the phosphorus scavenging capabilities of soil bacteria. *Environ. Microbiol.* 18, 3535–3549. doi: 10.1111/1462-2920.13390

Lipok, J., Owsiak, T., Młynarz, P., Forlani, G., and Kafarski, P. (2007). Phosphorus NMR as a tool to study mineralization of organophosphonates — The ability of *Spirulina* spp. to degrade glyphosate. *Enzyme Microb. Technol.* 41, 286–291. doi: 10.1016/j.enzmictec.2007.02.004

Lópes-Rodas, V., Flores-Moya, A., Maneiro, E., Perdigones, N., Marva, F., García, M. E., et al. (2007). Resistance to glyphosate in the cyanobacterium *Microcystis aeruginosa* as result of pre-selective mutations. *Evol. Ecol.* 21, 535–547. doi: 10.1007/s10682-006-9134-8

Love, M. I., Anders, S., and Huber, W. (2016). Differential analysis of count data – the DESeq2 package. *Genome Biol.* 15:550.

Lozano, V. L., Vinocur, A., Sabio y García, C. A., Allende, L., Cristos, D. S., Rojas, D., et al. (2018). Effects of glyphosate and 2,4-D mixture on freshwater phytoplankton and periphyton communities: a microcosms approach. *Ecotoxicol. Environ. Saf.* 148, 1010–1019. doi: 10.1016/j.ecoenv.2017.12.006

Lu, G. H., Zhu, Y. L., Kong, L. R., Cheng, J., Tang, C. Y., Hua, X. M., et al. (2017). Impact of a glyphosate-tolerant soybean line on the rhizobacteria, revealed by illumina Miseq. *J. Microbiol. Biotechnol.* 27, 561–572. doi: 10.4014/jmb.1609.09008

Martínez, A., Ventouras, L. A., Wilson, S. T., Karl, D. M., and DeLong, E. F. (2013). Metatranscriptomic and functional metagenomic analysis of methylphosphonate utilization by marine bacteria. *Front. Microbiol.* 4:1–18. doi: 10.3389/fmicb.2013.00340

McMurdie, P. J., and Holmes, S. (2013). Phyloseq: an R package for reproducible interactive analysis and graphics of microbiome census data. *PLoS One* 8:e61217. doi: 10.1371/journal.pone.0061217

McMurdie, P. J., and Holmes, S. (2014). Waste not, want not: why rarefying microbiome data is inadmissible. *PLoS Comput. Biol.* 10:e1003531. doi: 10.1371/journal.pcbi.1003531

Mercurio, P., Flores, F., Mueller, J. F., Carter, S., and Negri, A. P. (2014). Glyphosate persistence in seawater. *Mar. Pollut. Bull.* 85, 385–390. doi: 10.1016/j.marpolbul.2014.01.021

Newman, M. M., Lorenz, N., Hoilett, N., Lee, N. R., Dick, R. P., Liles, M. R., et al. (2016). Changes in rhizosphere bacterial gene expression following glyphosate treatment. *Sci. Total Environ.* 553, 32–41. doi: 10.1016/j.scitotenv.2016.02.078

Parks, D. H., Chuvochina, M., Waite, D. W., Rinke, C., Skarshewski, A., Chaumeil, P. A., et al. (2018). A standardized bacterial taxonomy based on genome phylogeny substantially revises the tree of life. *Nat. Biotechnol.* 36, 996–1004. doi: 10.1038/nbt.4229

Pedotti, M., Rosini, E., Molla, G., Moschetti, T., Savino, C., Vallone, B., et al. (2009). Glyphosate resistance by engineering the flavoenzyme glycine oxidase. *J. Biol. Chem.* 284, 36415–36423. doi: 10.1074/jbc.M109.051631

Porter, K. G., and Feig, Y. S. (1980). The use of DAPI for identifying and counting aquatic microflora. *Limnol. Ocean.* 25, 943–948. doi: 10.4319/lo.1980.25.5.0943

Qu, X., Ren, Z., Zhang, H., Zhang, M., Zhang, Y., Liu, X., et al. (2017). Influences of anthropogenic land use on microbial community structure and functional potentials of stream benthic biofilms. *Sci. Rep.* 7, 1–12. doi: 10.1038/s41598-017-15624-x

R Core Team, (2018). *R: A Language and Environment for Statistical Computing*. Available at: http://www.R-project.org/ (accessed May, 2019).

Ratcliff, A. W., Busse, M. D., and Shestak, C. J. (2006). Changes in microbial community structure following herbicide (glyphosate) additions to forest soils. *Appl. Soil Ecol.* 34, 114–124. doi: 10.1016/j.apsoil.2006.03.002

Reese, A. T., Savage, A., Youngsteadt, E., McGuire, K. L., Koling, A., Watkins, O., et al. (2016). Urban stress is associated with variation in microbial species composition—but not richness—in Manhattan. *ISME J.* 10, 751–760. doi: 10.1038/ismej.2015.152

Rognes, T., Flouri, T., Nichols, B., Quince, C., and Mahé, F. (2016). VSEARCH: a versatile open source tool for metagenomics. *PeerJ* 4, 1–22. doi: 10.7717/peerj.2584

Schloss, P. D., Westcott, S. L., Ryabin, T., Hall, J. R., Hartmann, M., Hollister, E. B., et al. (2009). Introducing mothur: open-source, platform-independent, community-supported software for describing and comparing microbial communities. *Appl. Environ. Microbiol.* 75, 7537–7541. doi: 10.1128/AEM.01541-9

Seemann, T. (2014). Prokka: rapid prokaryotic genome annotation. *Bioinformatics* 30, 2068–2069. doi: 10.1093/bioinformatics/btu153

Skeff, W., Neumann, C., and Schulz-Bull, D. E. (2015). Glyphosate and AMPA in the estuaries of the Baltic Sea method optimization and field study. *Mar. Pollut. Bull.* 100, 577–585. doi: 10.1016/j.marpolbul.2015.08.015

Skeff, W., Recknagel, C., and Schulz-Bull, D. E. (2016). The influence of salt matrices on the reversed-phase liquid chromatography behavior and electrospray ionization tandem mass spectrometry detection of glyphosate, glufosinate, aminomethylphosphonic acid and 2-aminoethylphosphonic acid in water. *J. Chromatogr. A* 1475, 64–73. doi: 10.1016/j.chroma.2016.11.007

Stachowski-Haberkorn, S., Becker, B., Marie, D., Haberkorn, H., Coroller, L., and de la Broise, D. (2008). Impact of Roundup on the marine microbial community, as shown by an in situ microcosm experiment. *Aquat. Toxicol.* 89, 232–241. doi: 10.1016/j.aquatox.2008.07.004

Stamatakis, A. (2014). RAxML version 8: a tool for phylogenetic analysis and post-analysis of large phylogenies. *Bioinformatics* 30, 1312–1313. doi: 10.1093/bioinformatics/btu033

Sviridov, A. V., Shushkova, T. V., Ermakova, I. T., Ivanova, E. V., Epiktetov, D. O., and Leontievsky, A. A. (2015). Microbial degradation of glyphosate herbicides (Review). *Appl. Biochem. Microbiol.* 51, 188–195. doi: 10.1134/S0003683815020209

Tlili, A., Corcoll, N., Bonet, B., Morin, S., Montuelle, B., Bérard, A., et al. (2011). In situ spatio-temporal changes in pollution-induced community tolerance to zinc in autotrophic and heterotrophic biofilm communities. *Ecotoxicology* 20, 1823–1839. doi: 10.1007/s10646-011-0721-2

Van Bruggen, A. H. C., He, M. M., Shin, K., Mai, V., Jeong, K. C., Finckh, M. R., et al. (2018). Environmental and health effects of the herbicide glyphosate. *Sci. Total Environ.* 616–617, 255–268. doi: 10.1016/j.scitotenv.2017.10.309

Vera, M. S., Lagomarsino, L., Sylvester, M., Pérez, G. L., Rodríguez, P., Mugni, H., et al. (2010). New evidences of Roundup® (glyphosate formulation) impact on the periphyton community and the water quality of freshwater ecosystems. *Ecotoxicology* 19, 710–721. doi: 10.1007/s10646-009-0446-7

Wang, C., Lin, X., Li, L., Lin, L. X., and Lin, S. (2017). Glyphosate shapes a dinoflagellate-associated bacterial community while supporting algal growth as sole phosphorus source. *Front. Microbiol.* 8:2530. doi: 10.3389/fmicb.2017.02530

Wang, C., Lin, X., Li, L., and Lin, S. (2016). Differential growth responses of marine phytoplankton to herbicide glyphosate. *PLoS One* 11:1–20. doi: 10.1371/journal.pone.0151633

Weaver, M. A., Krutz, L. J., Zablotowicz, R. M., Reddy, K. N., Zablatowicz, R. M., and Reddy, K. N. (2007). Effects of glyphosate on soil microbial communities

and its mineralization in a Mississippi soil. *Pest Manag. Sci.* 63, 388–393. doi: 10.1002/ps.1351

Weinbauer, M. G., Fritz, I., Wenderoth, D. F., and Höfle, M. G. (2002). Simultaneous extraction from bacterioplankton of total RNA and DNA suitable for quantitative structure and function analyses simultaneous extraction from bacterioplankton of total RNA and DNA suitable for quantitative structure and function analyses. *Appl. Environ. Microbiol.* 68, 1082–1087. doi: 10.1128/AEM.68.3.1082

White, A. K., and Metcalf, W. W. (2004). Two C-P lyase operons in *Pseudomonas stutzeri* and their roles in the oxidation of phosphonates, phosphite, and hypophosphite. *J. Bacteriol.* 186, 4730–4739. doi: 10.1128/JB.186.14.4730-4739.2004

Wickham, H. (2009). *ggplot2: Elegant Graphics for Data Analysis*. New York, NY: Springer-Verlag.

Wirth, M. A., Sievers, M., Habedank, F., Kragl, U., et al. (2019). Electrodialysis as a sample processing tool for bulk organic matter and target pollutant analysis of seawater. *Mar. Chem.* 217:103719. doi: 10.1016/j.marchem.2019.103719

Yilmaz, P., Parfrey, L. W., Yarza, P., Gerken, J., Pruesse, E., Quast, C., et al. (2014). The SILVA and "all-species Living Tree Project (LTP)" taxonomic frameworks. *Nucleic Acids Res.* 42, 643–648. doi: 10.1093/nar/gkt1209

Yu, G., Lam, T. T.-Y., Zhu, H., and Guan, Y. (2018). Two methods for mapping and visualizing associated data on phylogeny using ggtree. *Mol. Biol. Evol.* 35, 3041–3043. doi: 10.1093/molbev/msy194

Zhao, H., Tao, K., Zhu, J., Liu, S., Gao, H., and Zhou, X. (2015). Bioremediation potential of glyphosate-degrading *Pseudomonas* spp. strains isolated from contaminated soil. *J. Gen. Appl. Microbiol.* 61, 165–170. doi: 10.2323/jgam.61.165

Conflict of Interest: The authors declare that the research was conducted in the absence of any commercial or financial relationships that could be construed as a potential conflict of interest.

Scientific CV

PERSONAL INFORMATION

Marisa A. Wirth, M. Sc.

Date of Birth: 1st August 1992

Place of Birth: Hamburg

Nationality: German

WORK EXPERIENCE

since 11/2017	**Leibniz Institute for Baltic Sea Research Warnemünde** Working Group Organic Trace Substances, Prof. Dr. Detlef Schulz-Bull PhD Student
03/2017 – 08/2017	**Leibniz Institute for Baltic Sea Research Warnemünde** Working Group Organic Trace Substances, Prof. Dr. Detlef Schulz-Bull Student Lab Assistant
04/2016 – 08/2016 and 10/2015 – 12/2015	**University of Rostock** Working Group Analytical Chemistry, Prof. Dr. Ralf Zimmermann Student Lab Assistant

RESEARCH STAYS

01/2018 – 03/2018	**University of California, Santa Barbara** Working Group of Dr. Uta Passow Topic: "Partitioning of oil compounds into marine oil snow: Insights into prevailing mechanisms and dispersant effects"

10/2016 – 01/2017 **Alfred Wegener Institute, Biologische Anstalt Helgoland**

Working Group of Dr. Gunnar Gerdts

Topic: "Database design for the automated analysis of microplastic samples with μFTIR and imaging"

EDUCATION

10/2015 – 09/2017 **Master of Science, Chemistry, University of Rostock**

Degree: Master of Science (1.0, ECTS grade A)

Master Thesis: "Interactions between Marine Snow and Macondo Oil spilled during the Deepwater Horizon Accident"

10/2012 – 10/2015 **Bachelor of Science, Chemistry, University of Rostock**

Degree: Bachelor of Science (1.2, ECTS grade A)

Bachelor Thesis: "Proton Sponges as Dopants for Electrospray- Ionization"

09/2002 – 06/2011 **High School Education, Kopernikus Gymnasium Bargteheide**

Degree: Abitur (1.4)

AWARDS

2017 **"Faculty Award"** from the Faculty of Mathematics and Natural Sciences of the University of Rostock (valedictorian)

PUBLICATIONS (PEER REVIEWED)

Wirth, M. A., Schulz-Bull, D.E., Kanwischer, M. (2021). The challenge of detecting the herbicide glyphosate and its metabolite AMPA in seawater - Method development and application in the Baltic Sea. Chemosphere 262: 128327, doi: 10.1016/j.chemosphere.2020.128327

Gros, P., Meissner, R., **Wirth, M.A.**, Kanwischer, M. Rupp, H., Schulz-Bull, D.E., Leinweber, P. (2020). Leaching and degradation of 13C2-15N-glyphosate in field lysimeters. Environ. Monit. Assess. 192: 1-10, https://doi.org/10.1007/s10661-019-8045-4

Lohrer, C., Cwierz, P.P., **Wirth, M.A.**, Schulz-Bull, D.E., Kanwischer, M. (2020). Methodological aspects of methylphosphonic acid analysis: Determination in river and coastal water samples. Talanta 211: 120724, doi: 10.1016/j.talanta.2020.120724

Wirth, M. A., Sievers, M., Habedank, F., Kragl, U., Schulz-Bull, D.E.,Kanwischer, M. (2019). Electrodialysis as a sample processing tool for bulk organic matter and target pollutant analysis of seawater. Mar. Chem. 217: 103719, doi: 10.1016/j.marchem.2019.103719

Janßen, R., Skeff, W., Werner, J., **Wirth, M.A.**, Kreikemeyer, B., Schulz-Bull, D., Labrenz, M. (2019). A glyphosate pulse to brackish long-term microcosms has a greater impact on the microbial diversity and abundance of planktonic than of biofilm assemblages. Front. Mar. Sci. 6: 758, doi: 10.3389/fmars.2019.00758

Primpke, S., **Wirth, M.**, Lorenz, C., Gerdts, G. (2018). Reference database design for the automated analysis of microplastic samples based on Fourier transform infrared (FTIR) spectroscopy. Anal. Bioanal. Chem. 410, 21: 5131-5141, doi: 10.1007/s00216-018-1156-x

Wirth, M. A., Passow, U., Jeschek, J., Hand, I., D. E. Schulz-Bull (2018). Partitioning of oil compounds into marine oil snow: Insights into prevailing mechanisms and dispersant effects. Mar. Chem. 206: 62-73, doi: 10.1016/j.marchem.2018.09.007

Wirth, M.A., Rüger, C.P., Sklorz, M., Zimmermann, R. (2017). Using aromatic polyamines with high proton affinity as “proton sponge” dopants for electrospray ionization mass spectrometry. Eur. J. Mass. Spectrom. 23, 2: 49-54, doi: 10.1177/1469066717697985

PUBLICATIONS (NON-PEER REVIEWED)

Kanwischer, M., **Wirth, M.A.**, Schulz-Bull, D.E. (2019). Analyse von organischen Spurenstoffen in der Ostsee. WasserFORUM 11: 54-56.

SCIENTIFIC PRESENTATIONS

Wirth, M.A.; Schulz-Bull, D.E.; Kanwischer, M.; Detection of the herbicide Glyphosate and its metabolite Aminomethylphosphonic acid in the Marine Environment; *SETAC Europe SciCon*, Virtual Conference, 2020 (oral presentation)

Wirth, M.A.; Schulz-Bull, D.E.; Kanwischer, M.; Desalting of Marine Water through Electrodialysis - Application for the Analysis of Glyphosate and AMPA in Seawater; *International Symposium of the Leibniz ScienceCampus Phosphorus Research Rostock*, Warnemünde, Germany, 2019 (oral presentation)

Wirth, M.A.; Sievers, M.; Habedank, F.; Kragl, U.; Schulz-Bull, D.E.; Kanwischer, M. How Phosphorus Analysis can benefit from Electrodialysis; *International Phosphorus Workshop 9*, Zürich, Schweiz, 2019 (poster presentation)

Wirth, M.A.; Sievers, M; Abraham, M.; Kragl, U.; Schulz-Bull, D.E.; Electrodialysis of Marine Water for the Measurement of Organophosphorus Compounds; *International Symposium of the Leibniz ScienceCampus Phosphorus Research Rostock*, Dummerstorf, Germany, 2018 (oral presentation)

Wirth, M.A.; Passow, U.; Jeschek, J.; Hand, I.; Schulz-Bull, D.E.; Formation Mechanisms and Sedimentation of Marine Oil Snow: New Insights Through an Oil Compound-Specific Approach; *Gulf of Mexico Oil Spill and Ecosystem Science Conference*, New Orleans, USA, 2018 (oral presentation)

Wirth, M.A.; Abraham, M.; Kragl, U.; Schulz-Bull, D.E.; Desalting of Marine Water through Electrodialysis; *International* S*ymposium of the Leibniz ScienceCampus Phosphorus Research Rostock*, Warnemünde, Germany, 2017 (oral presentation)